ROLES OF THE PROTEINS PUHB, PUHC, PUHE, PUFQ, AND PUFX IN PHOTOSYNTHESIS BY *RHODOBACTER CAPSULATUS*.

by

Muktak Ashok Aklujkar

B.Sc. (Hon.), The University of British Columbia, 1998

A THESIS SUBMITTED IN PARTIAL FULFILMENT OF
THE REQUIREMENTS FOR THE DEGREE OF

DOCTOR OF PHILOSOPHY

IN THE FACULTY OF GRADUATE STUDIES
Department of Microbiology and Immunology

We accept this thesis as conforming

to the required standard

THE UNIVERSITY OF BRITISH COLUMBIA

May 2004

ABSTRACT

The photosynthetic apparatus of anoxygenic purple bacteria such as *Rhodobacter capsulatus* is a remarkable example of membrane protein organization. Much remains to be understood about the factors that govern the proportionate synthesis of pigments and proteins, the assembly and maintenance of pigment-protein complexes in the membrane, and the long-range organization of these complexes through protein-protein interactions.

The *puh* operon of *R. capsulatus* contains four genes, the first encoding a polypeptide of the photosynthetic reaction centre (RC). The remaining genes: *puhB*, *puhC*, and *puhE*, are found in all purple phototrophic bacteria examined to date. This study examines the roles of the three proteins PuhB, PuhC, and PuhE in assembly and decay of the RC and of the associated antenna called light harvesting complex 1 (LH1), in phototrophic growth, and in interactions with other proteins. Serendipitously, each protein was found to have a different functional relationship to PufQ, a protein implicated in many aspects of photosynthetic apparatus biogenesis, and new roles were discovered for PufX, a polypeptide of the RC-LH1 complex. Overall, the results emphasize the interrelatedness of assembly processes of the RC and LH1.

All three predicted transmembrane (TM) segments of PuhB were found to span a bacterial inner membrane, and the second TM segment was capable of self-association. In the absence of PuhB, the amount of RC was as little as 12% of the wild type level, and it did not bind bacteriochlorophyll (BChl) properly. There was an RC-dependent near-total loss of LH1, the PufX protein was almost completely absent, and cells required at least 12 hours to adapt to anaerobic phototrophic growth. A tag at the N-terminus of PuhB prevented complementation in *trans*, but co-translation with PufQ eliminated the lag and restored the specific growth rate to 84% of wild type. A plausible model for the function of PuhB is that a PuhB dimer co-operates with PufQ to assist in RC assembly.

Without PuhC in the membrane, phototrophic growth was sustained with difficulty, and benefited from 48 hours, compared to 24 hours, of semiaerobic pre-incubation. PuhC of *R. capsulatus* could be substituted perfectly with PuhC of *Rhodobacter sphaeroides*, but distantly

related PuhC proteins improved the specific growth rate from 14% of wild type to between 19% and 24%. The *puhC*⁻ growth defect depended on *pufQ* and *puhE*, genes that regulate BChl biosynthesis, and was mitigated by downregulation or loss of light harvesting complex 2 (LH2). When PufX was transcribed separately from the RC-LH1 proteins, its level was reduced when *puhC* was deleted. Because PuhC was required for optimum levels of the RC-LH1 complex, but proved to be at most a minor determinant of RC assembly and LH1 assembly, the role of PuhC may be to expand and reorganize the RC-LH1 core complex as a whole.

A *puhE* deletion created a minor obstacle to the transition from aerobic respiratory growth to active phototrophy that could not be complemented in *trans*. PuhE, an integral membrane protein with seven predicted TM segments, was found to inhibit BChl production by 49%, counterbalancing PufQ, and reduced the individual rates of RC and LH1 assembly by about 30% and 26%, respectively, without affecting expression of the polypeptides. However, the *puhE* deletion reduced the steady-state level of RC-LH1 by as much as 53% under high light intensity. Therefore, PuhE may perform two functions: to modulate BChl biosynthesis and/or degradation in response to light intensity; and to direct BChl into RC-specific and LH1-specific pathways.

When the *puf* operon encoding the RC and LH1 (as well as PufX) was deleted and portions of the *puf* operon were restored on a plasmid, the final amount of RC-specific absorption was increased by 74% by leaving the chromosomal *pufX* gene intact, only in the presence of PufB, the outer polypeptide of LH1, and only in the absence of the inner LH1 polypeptide, PufA. PufX was not immunodetected at stoichiometric levels in the absence of any RC-LH1 polypeptide or PuhB. The *pufX* merodiploid strains expressed more PufX protein than strains that contained a single *pufX* gene, and the extra protein reduced the level of LH1 by 14% only in the presence of the RC. The chromosomal *pufX* gene produced more protein but it affected LH1 absorption less (25% reduction) than PufX produced from the co-transcribed gene (43% reduction). The single TM segments of PufX from both *R. capsulatus* and *R. sphaeroides* were capable of homodimerization. Therefore, PufX could be the axis of twofold symmetry in dimers of RC-LH1, and may form an oligomer when overexpressed, by interacting with PufB, to enhance RC assembly.

In short, this work has furthered our understanding of five important photosynthesis proteins.

Table of Contents

LIST OF TABLES

LIST OF FIGURES

ABBREVIATIONS

A_{760}, A_{800}	Absorbance at 760 nm, absorbance at 800 nm
ATP	adenosine triphosphate
BChl, BPhe	bacteriochlorophyll, bacteriopheophytin
BSA	bovine serum albumin
cAMP	cyclic adenosine monophosphate
CAT	chloramphenicol acetyltransferase
cyt *b/c1*	cytochrome *b/c1* complex
cyt *c2*, cyt *cy*	cytochromes *c2* and *cy*
DHPC	diheptanoylphosphatidylcholine
DMSO	dimethylsulfoxide
DNA	deoxyribonucleic acid
dNTPs	deoxyribonucleotide triphosphates (e.g. dATP, dTTP)
EDTA	disodium ethylenediaminetetraacetate
GTA	gene transfer agent
IPTG	isopropylthio-β-D-galactopyranoside
KLH	keyhole limpet hemocyanin
LDAO	lauryldimethylamine oxide
LH1, LH2	light harvesting complexes 1 and 2
PAGE	polyacrylamide gel electrophoresis
RC	photosynthetic reaction centre
RNA, mRNA	ribonucleic acid, messenger ribonucleic acid
SDS	sodium dodecyl sulfate
TM	transmembrane
Tris HCl	*tris*-hydroxymethylmethylamine hydrochloride

Standard codes have been used for DNA and protein sequences.

ACKNOWLEDGEMENTS

॥ श्रीविघ्नहर्त्रे नमः ॥ श्रीकुलदेवताभ्यो नमः ॥

I am forever indebted to my supervisor, Dr. J. Thomas Beatty, for his enthusiasm and expert advice, for his timely hesitation and caution, encouragement, guidance, and pride. I thank my committee members: Drs. Robert Hancock, William Mohn, Michael Murphy, and formerly George Spiegelman, as well as Dr. Michael Gold, for their guidance. My experience was enriched also by the Microbiology Journal Club and many others within the Department of Microbiology and Immunology at U.B.C., and I thank the Media Room staff and the "ladies upstairs" for their gracious support of my endeavours.

I owe thanks to my students and stepstudents: Yu-Ching Cheng, Kevin Lin, Greg Gill, Lisa Dreolini, Jeannie Chui, Y.-W. Maria Wang, Chantal Mutanda, and Janny Lau who worked with the TOXCAT and CyaA systems, Shannon Foster, Joy Hong, Hanna Boehmer, and Pooya Kazemi who worked with PuhE, and Emily Pang, Allison Louie, and Nicole Jabali who worked with PufX. And I am grateful to other members of the Beatty lab, past and present, especially Jeanette Johnson for her maternal kindness.

I remember with gratitude the contribution of rabbits that produced antibodies against PuhC and PufX. Thanks are due to the staff who immunized them and kept them happy.

I gratefully acknowledge funding in the form of a National Sciences and Engineering Research Council Postgraduate Scholarship and a University Graduate Fellowship from U.B.C.

To Dr. Roger Prince, my collaborator on many, many chromatophore experiments, a very humble thank you.

There are many who deserve mention for gifts of materials: Drs. Kenji Nagashima, Samuel Kaplan, Mary Lynne Perille Collins, Gerhart Drews, James Smart and William Richards, William Russ and Donald Engelman, Jennifer Leeds and Jonathan Beckwith, Daniel Ladant, Roger Parton and John Coote, and others whose projects I inherited: Danny Wong, Bill Collins, Andrea Harmer, and Tim Lilburn. Thank you all.

I share credit for this work with my parents and my sister, whose constant prodding and broadcasting made every day worthwhile.

सामुद्रो हि तरङ्गः क्वचन समुद्रो न तारङ्गः ।

I dedicate this thesis to the memory of my cat Manuram, who never ceded his seat to my laptop. And to Sonubai, who was, as always, on the wrong side of a door!

1. INTRODUCTION

1.1. General properties of *Rhodobacter capsulatus*

Rhodobacter capsulatus is a purple phototrophic bacterium, a member of the α group of Proteobacteria (62). The purple phototrophic bacteria are a phylogenetically diverse subset of the α- and β-Proteobacteria (the so-called purple nonsulfur bacteria), and of the γ-Proteobacteria (purple sulfur bacteria), their members being interspersed among various chemotrophic bacteria (62). The purple bacteria carry out anoxygenic photosynthesis under anaerobic conditions; that is, they do not produce oxygen gas when employing light as their source of energy (62).

R. capsulatus is capable of growth by aerobic respiration, anaerobic respiration with a variety of electron donors and acceptors, and metabolism of organic compounds such as malate under anaerobic conditions with light as the source of energy (62). Under semiaerobic conditions (low levels of oxygen) in the dark, the photosynthetic apparatus is assembled gratuitously (33).

The gene transfer agent (GTA) is a phage-like particle of *R. capsulatus* that packages ~4.5 kbp linear dsDNA fragments from the donor strain non-specifically. It can be used to generate chromosomal gene knockouts by transduction.

1.2. The photosynthetic apparatus of *R. capsulatus*

The photosynthetic apparatus of *R. capsulatus* has a Photosystem II-type reaction centre: excited electrons are transferred from bacteriochlorophyll (BChl) pigments via bacteriopheophytins (BPhe) to quinones rather than to iron-sulfur clusters (106). Such reaction centres are found in all purple phototrophic bacteria, in filamentous anoxygenic phototrophic bacteria (e.g. the *Chloroflexaceae*), and as Photosystem II of cyanobacteria and plastids in algae and plants. The known components of the apparatus in *R. capsulatus* comprise a reaction centre (RC) and two light-harvesting complexes: LH1 and LH2 (110), a complex including cytochromes *b* and *c1* and a

Rieske iron-sulfur protein (cyt *b/c1*), a periplasmic soluble cytochrome *c2* (cyt *c2*) and membrane-anchored alternative cytochrome *cy* (98), and a proton-translocating ATP synthase (Figure 1.1).

All of these components are located in the intracytoplasmic membrane system, which in *R. capsulatus* consists of invaginations of the inner cell membrane (25). Upon lysis of cells, the intracytoplasmic membrane spontaneously forms vesicles called chromatophores.

The RC consists of three polypeptides: RC H, RC M, and RC L, also known as PuhA, PufM, and PufL, respectively (168). PuhA possesses a short periplasmic N-terminus, a single transmembrane (TM) segment, and a large cytoplasmic domain. PufL and PufM are larger, each with five TM segments and short cytoplasmic and periplasmic segments; together, they hold a symmetrical system of pigments within the RC. Near the periplasmic side of the membrane are two molecules of BChl *a* known as the special pair and a carotenoid pigment, followed by two more BChl *a* molecules called the voyeur pair, a pair of BPhe *a* pigments, a ferrous iron cofactor, and a pair of quinone molecules known as Q_A and Q_B that are close to the cytoplasmic side. The special pair BChl absorption peak is at 865 nm, the voyeur BChls absorb light at 804 nm and the BPhes absorb light at 760 nm (36). A typical absorption spectrum of the RC is shown in Figure 1.2.

An electron from the special pair is excited either by direct incident light or by energy transferred from LH1 and LH2. This electron travels down the active branch of pigments held mostly by PufL, reaching Q_A near the cytoplasmic side of PufM, and is transferred rapidly to Q_B (168). The special pair is quickly reduced by cyt *c2* or cyt *cy* and a second excitation event follows. Shortly after each electron reaches Q_B, a proton is transferred from the cytoplasm to Q_B through the cytoplasmic domain of PuhA. Q_B, reduced to a quinol, is replaced by another quinone molecule in the oxidized state. The quinol reaches cyt *b/c1* and is oxidized in a complicated cycle of single-electron transfers that allows one more proton to be taken up by a quinone for each electron passed on to cyt *c2* (100), two such cycles being coupled in a dimeric cyt *b/c1* complex (53). Both protons from each electron transfer are released into the periplasm, and the electrons return to the RC via cyt *c2* (107). The electrochemical gradient of protons is a source of energy for many cellular processes. It is exploited by the ATP synthase, which couples translocation of protons from the periplasm to the cytoplasm to the synthesis of adenosine triphosphate (ATP) (54).

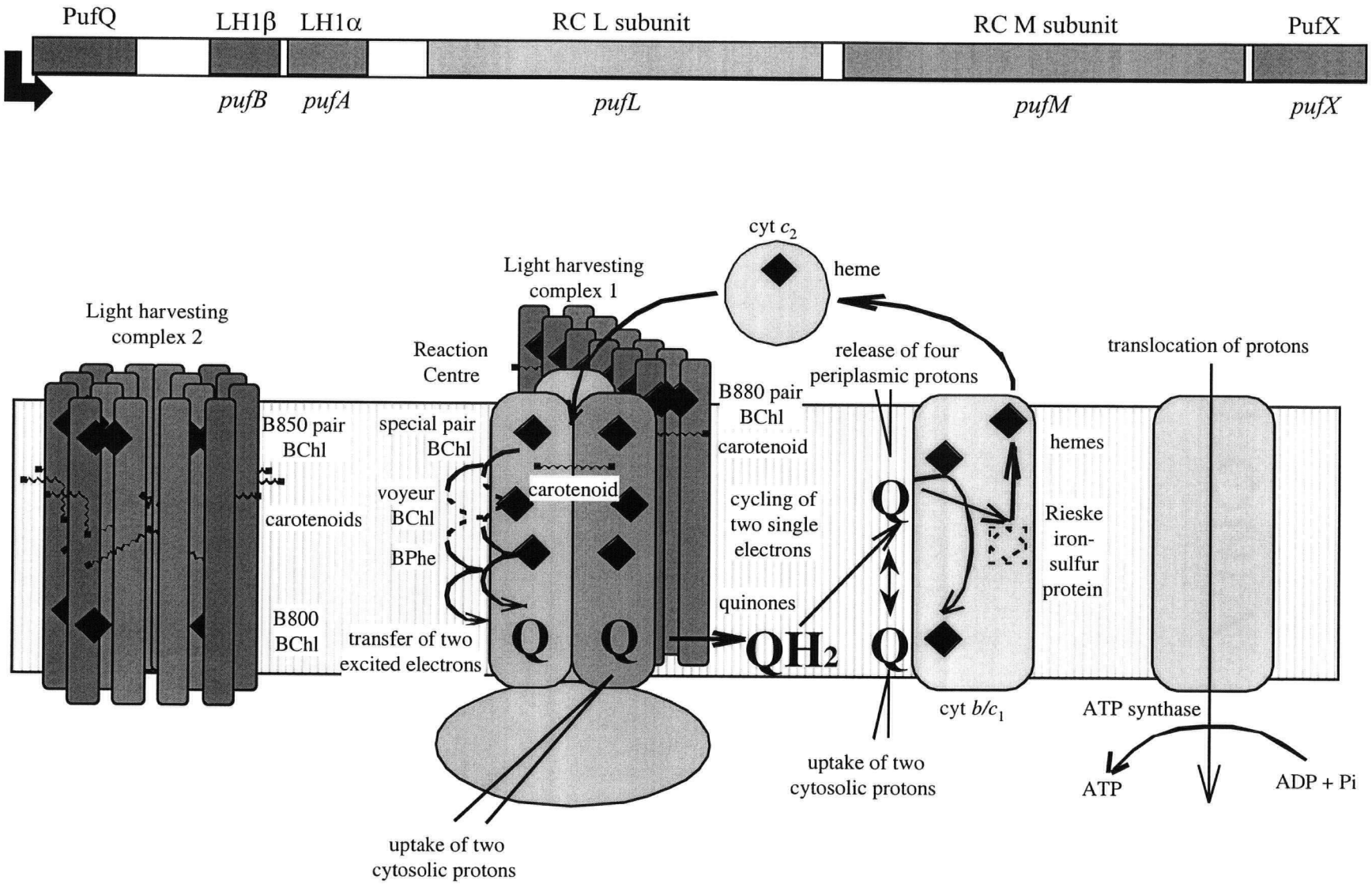

Figure 1.1. The *puf* operon and the core photosynthetic apparatus of *R. capsulatus*. All of the pigment-binding integral membrane proteins of the core photosynthetic apparatus are encoded by *puf* genes, along with PufQ, an enigmatic factor in the biogenesis of the apparatus. Light energy can be captured by the RC directly, or transferred from LH1 or LH2. Electrons excited in the RC must be carried past LH1 by quinones. PufX facilitates this process.

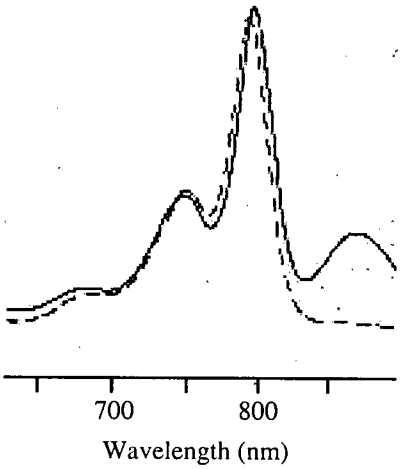

Figure 1.2. Spectrum of the *R. capsulatus* RC in membranes isolated from a mutant unable to produce LH1 and LH2 (solid line). Addition of ferricyanide resulted in complete bleaching of the special pair BChl peak at 865 nm (dashed line). Reproduced from Stiehle *et al.* (147).

LH1 is made up of two small polypeptides called LH1α and LH1β, also known as PufA and PufB, respectively, which have cytoplasmic N-termini and a single TM segment each (174) (see Figure 3.6.15). A pair of BChl *a* molecules, absorbing light at 870 nm (36), and a carotenoid are thought to be held at the level of the RC special pair BChls near the periplasmic side of the inner membrane between each PufA-PufB dimer, and twelve to sixteen such dimers associate (42, 67, 70, 129, 136, 139, 158) such that the carotenoids may mediate contact between adjacent BChls (89). This LH1 structure surrounds the RC, with PufA on the inside and PufB on the outside, the N-terminus of PufB potentially contacting the RC polypeptide PuhA (27).

There is debate as to the shape of LH1, which must include a means to allow quinols to escape from the RC to reach cyt *b/c1*. Evidence from other purple phototrophic bacteria suggests a circular or elliptical LH1 structure that may flex (42, 67, 129, 139, 158). In *Rhodopseudomonas palustris*, one position within the inner PufA ring, near the Q_B pocket of the RC, is occupied by a protein designated "W," which has a single TM helix and could conceivably bind a pigment cofactor (129). It is very likely that quinols exit through an aperture near W. There is speculation that a small LH1-associated protein called Ω could perform the same function in *Rhodospirillum rubrum* (50).

The best-known such protein, however, is PufX of *R. capsulatus* and the closely related species *Rhodobacter sphaeroides*. Very recently, *pufX* genes have also been discovered in three other

Rhodobacter species (153). PufX, which improves the efficiency of quinol transfer to cyt *b/c1* (8, 34, 87), is a small protein with a single TM segment, resembling the LH1 and LH2 polypeptides (see Section 3.6.5), and tightly associated with PufA during purification of LH1 (125). Association of PufA and PufX *in vitro* requires BChl, and interaction of PufX with BChl has also been demonstrated *in vitro* (82). The requirement for PufX for phototrophic growth can be compensated by mutation of the Ser2 amino acid residue of PufA to Pro or Phe in *R. capsulatus* (86, 88), and by various mutations of PufA and PufB in *pufBA* merodiploid *R. sphaeroides* (7).

Although the original hypothesis was that PufX itself forms a gate in LH1, as it is no longer required for phototrophic growth of *R. sphaeroides* when LH1 is absent or at an abnormally low level relative to the RC (94, 95), recent structural and biochemical studies suggest that LH1 is an arc and that a role of PufX in *R. sphaeroides* is to convert the "core complex" of RC-LH1 into a dimeric "supramolecular complex" (43, 44, 70, 136, 143) or even a paracrystalline helical array with long-range interactions orienting every RC-LH1 dimer in the same direction in tubular photosynthetic membranes packed with RC-LH1 core complexes (45, 143). In both *R. capsulatus* and *R. sphaeroides*, PufX has two GxxxG sequence motifs (see Figure 3.6.16), which have been identified as a signature of homodimerizing TM segments (130). However, monomeric core complexes containing PufX have recently been isolated from *R. sphaeroides* (143). Intriguingly, the LH1 ring in these complexes is closed; however, the fact that this particular strain synthesizes the carotenoid pigment neurosporene rather than the usual sphaeroidene may affect the shape of the LH1 structure in the presence of PufX (94).

PufX was detected in the core complex at a ratio of 1 per RC (43). When isolated from *R. capsulatus*, it lacked the initial Met and final 9 residues; from *R. sphaeroides*, it lacked the initial Met and final 12 residues (112). A large part of the N-terminal (predicted cytoplasmic) and C-terminal (predicted periplasmic) domains of PufX were required for formation of the RC-LH1 dimer in *R. sphaeroides* (44). When 7, 11, and 15 amino acid residues were removed from the C-terminus of PufX, the protein did not co-purify with the RC-LH1 monomer, perhaps because it could not insert into the core complex. When 29 amino acid residues were removed from the C-terminus, PufX was found associated with the RC-LH1 monomer and with a structure intermediate

between the monomer and dimer. Therefore, the C-terminal processing of PufX likely takes place after it inserts into the RC-LH1 structure.

The polypeptide components of LH2 are LH2α and LH2β, known as PucA and PucB, respectively (174) (see Figure 3.6.15), which form dimers that oligomerize to form a ring with ninefold symmetry – eightfold symmetry in *Phaeospirillum molischianum*, in which the PucA and PucB sequences have characteristics typical of LH1 polypeptides (75, 93, 111, 121, 134, 137, 138, 159). In *R. capsulatus*, a non-BChl-binding peripheral membrane protein, LH2γ or PucE, co-purifies with LH2, and other γ polypeptides have been observed in other species (174). The crystal structures of LH2 in other purple bacterial species reveal that in addition to the BChl pair near the periplasmic side (absorbing light at 850 nm), there is a single BChl pigment (absorbing light at 800 nm) near the cytoplasmic side of LH2, a carotenoid molecule connecting each B800 to the next B850 pair, and another, hairpin-bent carotenoid that protrudes from the ring (75, 111). A speculative model situates eight LH2 rings symmetrically around each monomeric RC-LH1 in the membrane (110). In some purple bacteria, there are multiple *puc* operons that encode LH2 structural polypeptides, and LH2 complexes with different spectroscopic properties are expressed depending on light intensity (49, 79, 133, 172, 174).

1.3. The photosynthesis gene cluster and the roles of PufQ

Most of the genes involved in phototrophy are grouped together in *R. capsulatus* and related bacteria to form the photosynthesis gene cluster (3). This cluster was first identified in *R. capsulatus*, as 46 kbp of DNA encoding the biosynthetic enzymes for BChl pigments and isoprenoid molecules (BChl tails, carotenoid pigments, and quinones), as well as the structural polypeptides of the RC and LH1 (Figure 1.3). A few open reading frames regulate transcription (*ppsR*), encode LH1/LH2 assembly factors (*lhaA*), or have uncertain functions (*pufQ*, *orf428*). In other purple phototrophic bacteria, the operons within the cluster may be arranged differently, and the cluster may be interrupted or include other phototrophy-related genes such as the *puc* operon that encodes the structural polypeptides of LH2 (13, 24, 61, 76, 79).

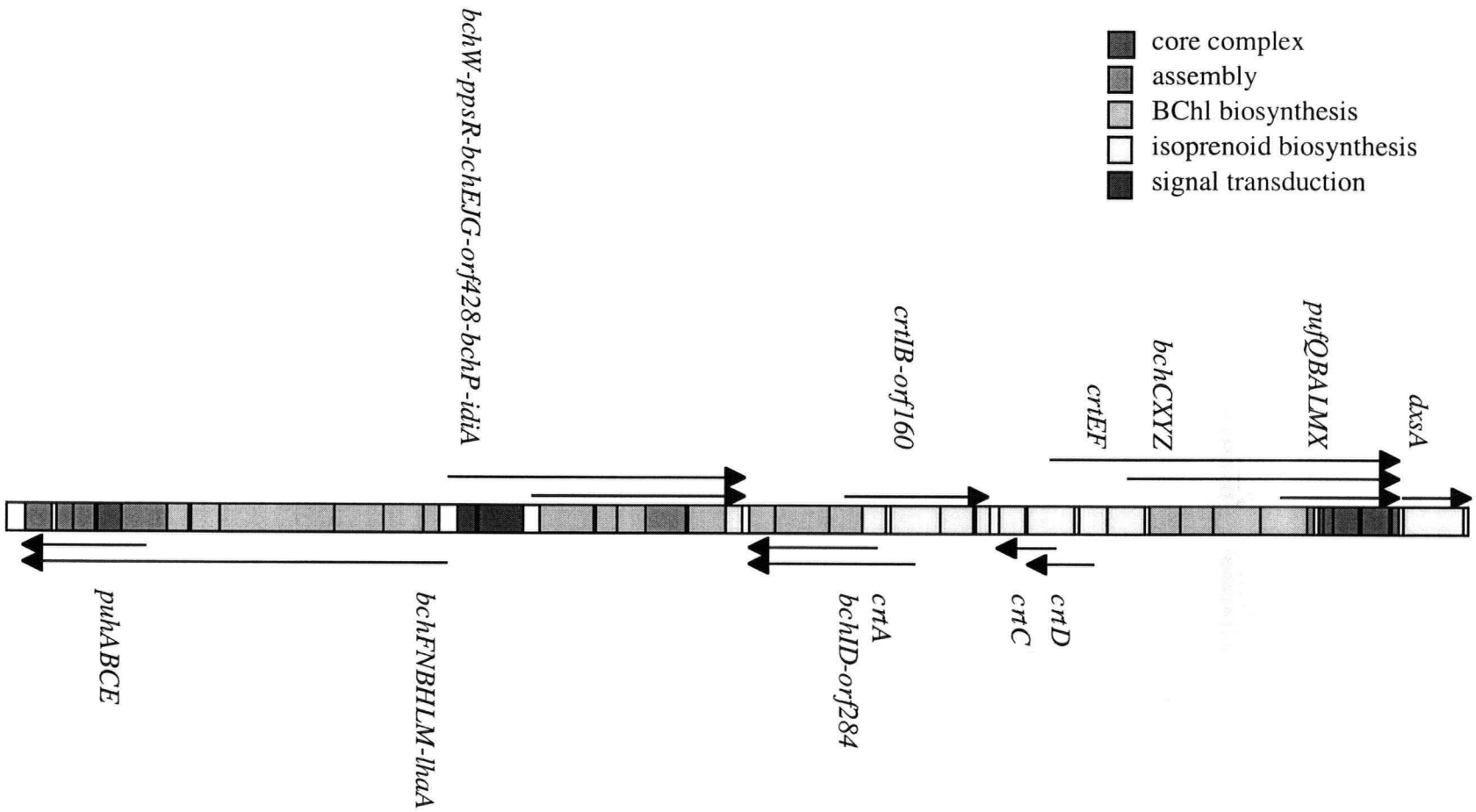

Figure 1.3. The photosynthesis gene cluster of *R. capsulatus*. Transcription of the *puh* operon is increased by readthrough from the *bchF* promoter (9, 11). Transcription of the *puf* operon includes readthrough from the *crtE* and *bchC* promoters (11, 162, 163). The cluster encodes many enzymes required for the biosynthesis of BChl and isoprenoids (quinones, carotenoids, and the hydrophobic tail of BChl), as well as a transcriptional regulator and assembly factors for the RC and LH1.

Near one end of the *R. capsulatus* cluster is the *puf* operon consisting of the genes *pufQBALMX*. As mentioned above, the gene products PufB and PufA are the β and α polypeptides of LH1, PufL and PufM are the L and M polypeptides of the RC, and PufX is closely associated with both the RC and LH1 (Figure 1.1). In other purple bacteria, there may be more than one set of PufB and PufA (59), and the *pufBA* genes may be found after *pufLM* (13), and even with one copy before and two after (103). The *pufX* gene is found only in the *Rhodobacter* genus of freshwater bacteria and not in closely related marine genera such as *Rhodovulum* and *Roseobacter* (153). These genera and others have *pufC* instead, encoding a tetraheme cytochrome *c* polypeptide of the RC that transfers electrons from cyt *c2* to the special pair (165). There are two kinds of PufC proteins: one possesses an N-terminal signal peptide that is removed with the addition of a cysteine-linked lipid anchor, while the other has a TM segment distantly related to that of PufX (60). There are also species that have neither *pufX* nor *pufC* (13, 79).

The first gene of the *puf* operon, *pufQ*, has been found only in the α-3 group of Proteobacteria: *R. capsulatus*, *R. sphaeroides*, *Rhodovulum sulfidophilum*, and uncultured marine Proteobacterium BAC 60D04. It encodes a small protein with a single TM segment and numerous lysyl/arginyl residues (see Section 3.6.5), required for high levels of BChl biosynthesis and for phototrophy (10). The exact function of PufQ is unknown although numerous roles have been proposed.

PufQ exhibits slight sequence similarity to the portions of RC L and RC M that bind BChl and quinone (1, 10), which has led to speculation that PufQ allows purple bacteria to respond to sudden exposure to oxygen and light by instantaneously downregulating pigment biosynthesis (10). Such a regulatory factor was postulated to explain the tight control of pigment biosynthesis (25). PufQ can bind protochlorophyllide, a BChl precursor, substoichiometrically (40), and its lipophilic character and predicted molecular mass of 8549 Da are consistent with the major protein species of ~9 kDa released by detergent treatment of a protein complex together with which excess BChl precursors were excreted in mutant strains of *R. sphaeroides* (126). A carrier polypeptide for BChl precursors was postulated to exist long ago (80, 81). However, excreted BChl precursors in *R. capsulatus* were associated instead with the 32 kDa major porin of the outer membrane, and PufQ was not detected (16). The evidence at present is inconclusive.

PufQ stimulates the synthesis of coproporphyrinogen, an early step shared by the biosynthesis pathways of BChl and heme (39). PufQ may also affect the expression of HemB (the second enzyme of both pathways, which makes porphobilinogen), HemZ (an enzyme for which coproporphyrinogen is a substrate), and HemH (an enzyme exclusive to the heme pathway) (J. Smart and C. E. Bauer, manuscript in revision).

Different point mutations in PufQ of *R. sphaeroides* (see Figure 3.6.13) had both positive and negative effects on the levels of LH1 and LH2 (52): (1) G58P decreased the amount of LH1 and increased that of LH2; (2) A63S increased LH1 and decreased LH2; (3) A69S abolished LH1 and increased LH2 drastically; (4) deletion of the termination codon and 3' loop sequence, such that PufQ was extended through a loop (underlined) with the sequence RHAIRRLPLGRRINREG and fused to PufK, an open reading frame that includes the ribosome-binding site of PufB in *R. sphaeroides*, increased LH1 and abolished LH2; and (5) mutation of the 3' end of the *pufQ* mRNA decreased LH1 and increased LH2 drastically. These effects were thought to be mostly post-transcriptional (52).

Taken together, these observations suggested that the involvement of PufQ extends from regulation of the earliest steps of porphyrin biosynthesis to modulation of one or more BChl-specific biosynthetic enzymes to proportional assembly of specific LH complexes. PufQ may achieve this range of involvement by associating with protochlorophyllide and other biosynthetic precursors of BChl, moving from enzyme to enzyme until LH complexes are assembled. Control of porphyrin biosynthesis may be sensitive to the availability of PufQ to bind BChl precursors.

1.4. The *puh* operon in phototrophic bacteria

Near the end of the *R. capsulatus* photosynthesis gene cluster opposite the *puf* operon is the *puhA* gene that encodes the RC H polypeptide. My research focusses on the genes co-transcribed with *puhA* and their roles in the processes of phototrophy. Following the identification of multiple roles for these proteins in phototrophy of *R. capsulatus* and the discovery of similar sequences in other species, the genes of this operon are hereby designated *puhB*, *puhC*, and *puhE*.

The first open reading frame 3' of *puhA* in *R.capsulatus* is *puhB* (formerly *orf214*) and the second is *puhC* (formerly *orf162b*). Mutational analysis showed that these sequences are in fact genes involved in phototrophy (2, 167). Subsequently, the *puhABC* arrangement of genes was discovered in all other purple phototrophic bacteria examined thus far, as enumerated below. The next open reading frame in *R. capsulatus*, *orf55*, has a GTG initiation codon and no obvious ribosome-binding site. It is not found in this position in other phototrophic bacteria, which may have instead the genes *puhD* and *acsF*, or just *acsF*. The *puhE* gene (formerly *orf274*) follows *orf55* in *R. capsulatus* and is found in all bacteria with Photosystem II-type reaction centres examined thus far.

In *R. sphaeroides*, *puhB*, *puhC*, *acsF*, and *puhE* are termed *orf213*, *orf128*, *orf277*, and *orf292*, respectively, and the presence of *puhD* was overlooked (24). (Confusingly, the name "*orf128*" was given to two dissimilar genes in the *R. sphaeroides* cluster, of which *puhC* would have been called *orf153* if the putative ribosome-binding site and initiation codon had not been missed due to sequencing errors.)

In *Rhodospirillum rubrum*, *puhBCE* are called *orf12372*, *orf13087*, and *orf295*, respectively (www.jgi.doe.gov). In the *Rhodopseudomonas palustris* genome, the *puhBCD-acsF-puhE* open reading frames are numbered or2138 through or2142 (79). Curiously, the *puhE* open reading frame of *R. palustris* is 41 to 105 codons longer than in other species. The *puhCD-acsF* genes, flanked by partial *puhB* and *puhE* sequences, are found in the genome of *Magnetospirillum magnetotacticum* (www.jgi.doe.gov), although I was unable to observe phototrophic growth or BChl synthesis in this organism (unpublished observations).

In the marine bacterium *R. sulfidophilum*, only *puhE* has been sequenced along with a short 3' end of *acsF* (sequence made available by M. Yoshida, S. Masuda, K. V. P. Nagashima, A. Verméglio, K. Shimada, and K. Matsuura). In *Roseobacter denitrificans*, a so-called aerobic phototrophic bacterium, only *puhB* has been sequenced, incompletely (sequence made available by S. Herter, O. Hucke, A. Labahn, C. Kortlueke, and G. Drews). However, two uncultured species of marine proteobacteria, designated BAC 29C02 and BAC 65D09, have *puhBCE*, and the third, BAC 60D04, has *puhBCD-acsF-puhE* (13).

In *Rubrivivax gelatinosus*, which belongs to the β group of Proteobacteria, the *puhBC-acsF-puhE* genes are called *orf227*, *orf154*, *orf358*, and *orf276* (61). *R. gelatinosus* is unique in that it has *acsF* without *puhD*. AcsF in *R. gelatinosus* is responsible for cyclization of the fifth ring of BChl under aerobic conditions, and similar sequences have been found in cyanobacteria and plastids (109, 118).

In the purple sulfur γ-proteobacterium *Thiocapsa roseopersicina*, the *puhBCE* genes are *orf218*, *orf138* (which should be *orf150* by my assignment of a putative ribosome-binding site and start codon) and *orf312* (76). Although *puhA* and 1.6 kbp of the 3' region have been sequenced in the thermophilic purple sulfur bacterium, *Thermochromatium tepidum* (35), requests for this sequence met with no response. In the green filamentous anoxygenic phototrophic bacterium *Chloroflexus aurantiacus*, which is believed to have a Photosystem II-type RC without a PuhA polypeptide (37), an incomplete *puhE* sequence has been reported (www.jgi.doe.gov).

The operon that begins with *puhA* may extend no farther than *puhE*, which is followed by different sequences in different bacteria: a hypothetical exported protein in *R. capsulatus* (*orf162a*), a cytochrome *c2* apoprotein in *R. sphaeroides* and *R. sulfidophilum*, a 5-aminolevulinate synthase in *R. palustris*, a BChl biosynthesis enzyme (*bchE*) in *R. rubrum* and *T. roseopersicina*, several isoprenoid biosynthesis enzymes in *R. gelatinosus*, and enzymes for acetyl-CoA metabolism in *C. aurantiacus*. It is not known whether the superoperonal organization of these other genes with the *puh* operon exists.

1.5. Thesis objectives

The primary goal of my research was to characterize the proteins PuhB, PuhC, PuhE, and, incidentally, PufX of *R. capsulatus* as assembly or stability factors either for the RC or for LH1, using strains in which either the RC or LH1 could be observed independently. Secondary goals were (1) to elicit antibody responses against these proteins in order to locate them in *R. capsulatus*; (2) to search for interactions among these proteins; (3) to discover functional relationships among these proteins and the photosynthetic apparatus as well as, incidentally, PufQ; and (4) to determine

whether the PuhC proteins of different species, despite differences in primary structure, could substitute for the native protein in *R. capsulatus*.

1.6. Tests of RC function and protein-protein interactions

A few of the methods used in this work require a brief introduction here. The carotenoid bandshifts reflect electron and proton transfer reactions in chromatophores flashed with light (63). In the first phase, electron transfer within the RC to reduce Q_B results in a large nanosecond-scale shift in absorption by carotenoids (mostly associated with LH2). The second phase, reduction of the special pair BChl by cyt *c*2 and oxidation of Q_B by cyt *b*/*c*1, occurs on a microsecond timescale. The third phase, a further bandshift due to the generation of a proton gradient, is more gradual due to the "quinone cycle" of single electron transfer reactions that result in the pumping of two protons for every electron returned to the RC (100). The second and third phases are sensitive to antimycin, an inhibitor of cyt *b*/*c*1 (154). Carotenoid bandshifts from successive flashes are additive until a saturating proton gradient is reached.

The TOXCAT system (Figure 1.4) can detect interactions between TM segments in the inner membrane of *E. coli* (131). It was used to answer two questions: (1) whether the predicted TM segments of PuhB, PuhC, and PufX are real in the sense that they insert into and span the inner membrane of *E. coli* (indicated by growth on maltose minimal medium) and (2) whether these TM segments are sufficient to mediate homodimerization of a protein (indicated by chloramphenicol acetyltransferase (CAT) activity.

The CyaA bacterial two-hybrid system (Figure 1.5) detects interactions between protein domains in *E. coli*; interaction results in the production of cyclic adenosine monophosphate (cAMP), an inducer of several catabolic operons (71). Although this system, in theory, can work with integral membrane proteins, because cAMP can diffuse through the cell, it was used only to determine whether the predicted cytoplasmic and periplasmic domains of PuhB and PuhC interact either with themselves or with each other.

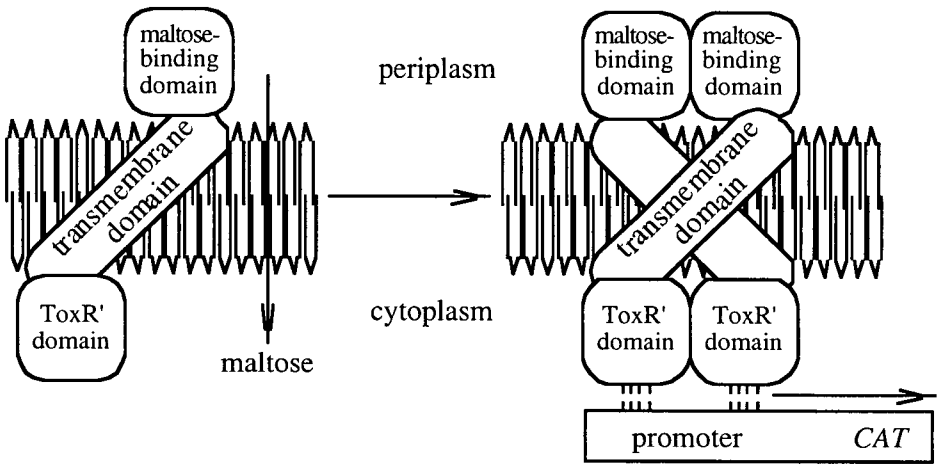

Figure 1.4. The TOXCAT system (131). A putative TM segment is fused between the cytoplasmic ToxR' transcription factor (from *Vibrio cholerae*) and a periplasmic maltose-binding domain. If the TM segment inserts correctly, the *E. coli* cell will grow on maltose minimal medium. If the TM segment homodimerizes, the chloramphenicol acetyltransferase (CAT) reporter gene is transcribed and its activity can be detected in cell lysates by addition of fluorescently labelled 1-deoxychloramphenicol as a substrate, followed by thin layer chromatography.

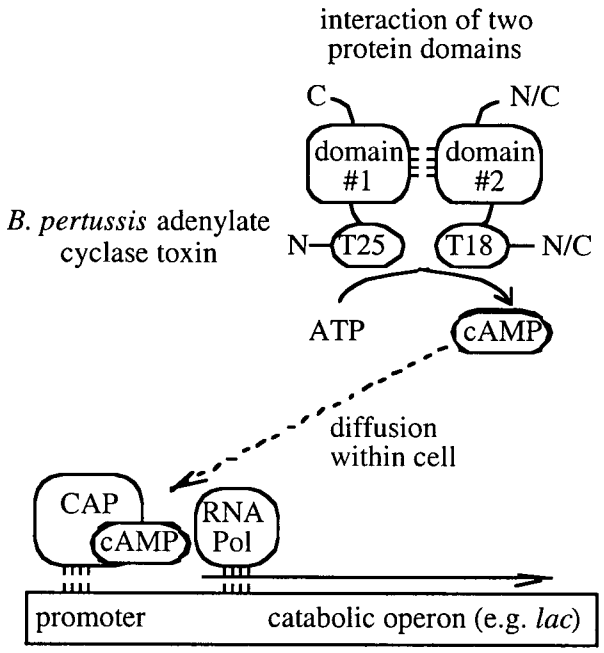

Figure 1.5. The CyaA bacterial two-hybrid system (71). Two fragments of the catalytic domain of adenylate cyclase toxin (CyaA) from *Bordetella pertussis*, designated T25 and T18, are fused to two domains of interest. (Fusion to T18 is possible at either terminus.) If the two domains interact, cAMP is produced and diffuses through the *E. coli* cell. Upon binding to the catabolite activator protein (CAP), cAMP triggers recruitment of RNA polymerase to the promoters of catabolic operons for lactose, maltose, etc.

2. MATERIALS AND METHODS

2.1. Bacterial strains and plasmids

E. coli strains are listed in Table 2.1 and *R. capsulatus* strains in Table 2.2. Most plasmids are listed in Table 2.3; *R. capsulatus* expression plasmids of the IncP and IncQ incompatibility groups are listed in Tables 2.4 and 2.5. When I made IncQ incompatibility group complementation plasmids for various *puh* genes by replacing the *puhC* gene of pAH8 (2), I was unaware that this plasmid carries the *pufQ* gene along with the *puf* promoter (17) until I observed the effects of *pufQ* merodiploidy with the supposed empty vector pRR5C (170). Consequently, the *pufQ* gene had to be deleted from every plasmid, and so the IncQ incompatibility group plasmids are listed pairwise as *pufQ*$^-$ and *pufQ*$^+$.

Numerous plasmids constructed for the purpose of chromosomal gene deletions, for overexpression of recombinant proteins, and for use in the TOXCAT and CyaA systems are not listed here in the interest of brevity, but are described in Sections 2.4-2.9.

Table 2.1. *E. coli* strains used in this study.

E. coli strain	Relevant genotypes and phenotypes	Source
DH5α	no DNA restriction, DNA is *dam* methylated	GIBCO BRL
C600	no DNA restriction, DNA is *dam* methylated	(14)
RB404	DNA is not *dam* methylated	(19)
TEC5	recombination and conjugative transfer of pUC plasmids to *R. capsulatus*	(148)
S17-1	conjugative transfer of IncP and IncQ plasmids to *R. capsulatus*	(144)
HB101(pRK2013)	helper strain to mobilize plasmids from C600 to *R. capsulatus*	(30)
MM39	*malE*$^-$ strain for TOXCAT system	J. Beckwith
BTH101, DHM1	adenylate cyclase deficient strains (DHM1 is *recA*$^-$) for CyaA system	Hybrigenics
M15(pREP4)	*lacI*^{q}-T5 RNAP-controlled overexpression of 6xHis-tagged proteins	QIAGEN

Table 2.2. *R. capsulatus* strains constructed in this study, grouped with their parent strains. There are three groups: (1) $LH2^+$ strains, used to evaluate the effects of *puh* gene deletions on phototrophic growth and abundance and function of the photosynthetic apparatus, (2) $LH2^-$ strains, tested for growth phenotypes similar to those of group 1, (3) RC^-LH1^- (all $LH2^-$ except MA15) background strains in which the assembly, decay, and structural variations of the photosynthetic apparatus were studied with attention to the *puh* gene deletions and *pufX* merodiploidy. Abbreviations: km^r, kanamycin resistance, sp^r, spectinomycin resistance, gm^r, gentamicin resistance.

Strain	Relevant genotypes and phenotypes	Markers	Source
Group 1			
DE442	GTA overproducer for GTA transductions (Sections 2.4-2.5)		(169)
SB1003	wild type *R. capsulatus* strain (RC^+, $LH1^+$, $LH2^+$, *puhBCE*$^+$)		(145)
DW1	polar *puhA*$^-$ derivative of SB1003	sp^r	(167)
MA05	nonpolar *puhB*$^-$ derivative of SB1003	km^r	this work
SBK1	nonpolar *puhC*$^-$ derivative of SB1003	km^r	(2)
SBK18	spontaneous secondary mutant of SBK1 with LH2 downregulation	km^r	this work
SBSpec	polar *puhC*$^-$ derivative of SB1003	sp^r	(56)
MA06	nonpolar *puhE*$^-$ derivative of SB1003	km^r	this work
MA07	polar *puhE*$^-$ derivative of SB1003	sp^r	this work
MA12	nonpolar *puhB*$^-$ derivative of MA07	$km^r sp^r$	this work
Group 2			
MW442	(*pucC* missense mutation) $LH2^-$ derivative of SB1003		(141)
DW23	nonpolar, noninsertional *puhB*$^-$ derivative of MW442		(167)
MWK1	nonpolar *puhC*$^-$ derivative of MW442	km^r	(56)
MWSpec	polar *puhC*$^-$ derivative of MW442	sp^r	(56)
MA08	nonpolar *puhE*$^-$ derivative of MW442	km^r	this work
MA10	polar *puhE*$^-$ derivative of MW442	sp^r	this work
MA09	nonpolar *puhE*$^-$ derivative of DW23	km^r	this work
MA11	polar *puhE*$^-$ derivative of DW23	sp^r	this work
Group 3			
MA15	RC^-LH1^- derivative of SB1003	km^r	this work
MA01	RC^-LH1^- derivative of MW442	km^r	this work
MA03	RC^-LH1^- derivative of DW23	km^r	this work
MA02	RC^-LH1^- derivative of MWK1	$km^r gm^r$	this work
MA04	polar *puhE*$^-$ derivative of MA01	$km^r sp^r$	this work
MA13	*puhE*$^-$ derivative of MA03	$km^r sp^r$	this work
MA14	*puhE*$^-$ derivative of MA02	$km^r gm^r sp^r$	this work
U43	RC^-LH1^-*pufX*$^-$ derivative of MW442	sp^r	(171)

Table 2.3. Plasmids used to make gene deletions and to express tagged and hybrid proteins in this study.

Plasmid	Purpose	Source
pUC12	gene deletions	(156)
pUC18, pUC19	gene cloning and sequencing	(105)
pUC4::KIXX	source of kanamycin resistance cartridge	(5)
pUC18::Ω	source of spectinomycin resistance cartridge	(119)
pWKR440	source of gentamicin resistance cartridge	W. Klipp
pccKAN	pUC family vector (km^r) for expression of TOXCAT hybrids	(131)
pccTNM	negative control for membrane insertion of TM segment hybrids	(131)
pccGpAwt, pccGpA83I	positive and negative controls for TM segment homodimerization	(131)
pUT18, pUT18C	pUC family vectors for expression of CyaA T18 fragment hybrids	Hybrigenics
pKT25	pSU40 vector for expression of CyaA T25 fragment hybrids	Hybrigenics
pQE40, pQE60, pQE70	pUC family vectors for expression of 6xHis-tagged proteins	QIAGEN
pUI8711, pUI8714	source of *R. sphaeroides puhC* DNA	(24)
pH3.6-	source of *R. rubrum puhC* DNA	(23)
pPGC#6-207	source of *R. gelatinosus puhC* DNA	(61)
pRPS404	source of *R. capsulatus puhE* DNA	(148)

Table 2.4. IncP incompatibility group plasmids (tetracycline resistance) for *R. capsulatus* gene expression.

Plasmid	Genes carried by plasmid	Source
pRK767	empty vector	(72)
pTB999	*pufQBALMX*	(173)
pTPR9	*pufQALMX* with in-frame deletion of all but 4 codons of *pufB*	(128)
pTPR8	*pufQBLMX* with in-frame deletion of all but 7 codons of *pufA*	(128)
pMA10	*pufQLMX* with combined *pufB* and *pufA* in-frame deletions	this work
p*Stu* I	*pufQBAX* with *Stu* I-*Tth*111 I deletion of *pufLM* and putative ribosome-binding site of *pufX*	(74)
pTL2	*pufQBALM* with *Tth*111 I-*Fsp* I deletion of *pufX*	(87)
pXCA601	*lacZ* gene preceded by multiple cloning site	(1)
pXCA6::935	*puf* promoter, *pufQ*, and *pufB::lacZ* gene	(1)

Table 2.5. IncQ incompatibility group plasmids (gentamicin resistance) for *R. capsulatus* gene expression.

(*pufQ*$^-$)	(*pufQ*$^+$)	***puh* gene carried**
pMA20	**pRR5C**	none (170)
pMA22	none	*puhB*
pMA17	**pMA7**	*puhB* with 6xHis tag immediately after initiation codon
pMA18	**pMA8**	*puhB* with 6xHis tag immediately before termination codon
none	**pAH8**	*puhC* (2)
pMA12	**pMA1**	*puhC* with 6xHis tag immediately after initiation codon
pMA13	**pMA3**	final 111 codons of *puhC* with 6xHis tag immediately after initiation codon
none	**pMA9**	*puhC* with 6xHis tag immediately before termination codon
pMA14	**pMA4**	*puhC* of *R. sphæroides*
pMA16	**pMA6**	*puhC* of *R. rubrum*
pMA15	**pMA5**	*puhC* of *R. gelatinosus*
pMA19	**pMA11**	*puhE*

2.2. Growth conditions

E. coli strains were grown at 37°C in Luria-Bertani (LB) medium (132). To optimize expression of 6xHis-tagged proteins, 2xYT broth, Super Broth, and Terrific Broth (132) were also used, and cells were grown at 30°C and 25°C. For TOXCAT analysis, *E. coli* MM39 strains were grown on M9 minimal medium with 0.4% maltose (132); for the CyaA system, *E. coli* BTH101 strains were grown on M63 medium (99) with 1% maltose. *R. capsulatus* strains were grown in RCV, a minimal medium containing malate as the sole carbon source (12), for analysis of phototrophic growth and absorption spectra; in YPS, a rich medium containing yeast extract and peptone (160), for GTA production; and in a mixture of equal volumes of RCV and YPS for other purposes such as conjugation. Plates contained 1.5 % agar.

Antibiotics (Fisher, Invitrogen, Sigma) were used at the following concentrations for *R. capsulatus* cultures (only during strain construction and plating): gentamicin sulfate 2 μg/ml, kanamycin sulfate 10 μg/ml, spectinomycin 10 μg/ml (50 μg/ml for initial selection), and tetracycline hydrochloride 0.5 μg/ml; and for *E. coli* cultures: ampicillin 100 μg/ml, carbenicillin 50

μg/ml, chloramphenicol 30 μg/ml, gentamicin sulfate 10 μg/ml, kanamycin sulfate 25 μg/ml, spectinomycin 50 μg/ml, and tetracycline hydrochloride 10 μg/ml. Isopropylthio-β-D-galactopyranoside (IPTG) was used for overexpression of 6xHis-tagged proteins at 1 mM. For the CyaA system, IPTG was used at 0.5 mM, and X-gal was used at 400 μg/ml.

Aerobic and semiaerobic *R. capsulatus* cultures were grown at 30°C without illumination, in Erlenmeyer flasks filled to 20% and 80% of their nominal capacity, respectively, and shaken at 300 rpm and 150 rpm, respectively. Phototrophic cultures were grown anaerobically in screw-cap tubes (20 ml) or Roux bottles (800 ml) inoculated from semiaerobic cultures (unless specified as aerobic, in the case of the *puhE* deletion study) and filled with RCV medium; or on RCV agar plates placed in BBL GasPak anaerobic jars (Becton Dickinson & Co.). Phototrophic cultures were incubated at 30°C in an aquarium filled with water and illuminated by halogen flood lamp bulbs at non-uniform high light intensity (between 100 $\mu E/m^2/s$ and 400 $\mu E/m^2/s$); the positions of the culture tubes were switched after every timepoint. To observe the growth of strains carrying pTL2, and to obtain chromatophores from the *puhB* and *puhE* deletion strains, however, tungsten filament incandescent lamp tubes were used for uniform high light intensity (150 $\mu E/m^2/s$) or low light intensity (30 $\mu E/m^2/s$). Light intensity was measured with a photometer (LI-COR Inc.) equipped with the LI-190SB quantum sensor. Culture density was monitored with a Klett-Summerson photometer equipped with a red (No. 66) filter (100 Klett units = 3.3×10^8 CFU/ml). The mean culture density of triplicate (occasionally duplicate) cultures was plotted, with the standard deviation as a measure of error.

2.3. Recombinant DNA techniques

Chromosomal DNA was isolated from 10 ml of an *R. capsulatus* culture by resuspension in 1 ml of SSC (132) and lysis by adding 4 μl of 100 mg/ml lysozyme, 10 μl of 10 mg/ml ribonuclease A, 50 μl of 10% SDS, and incubating at 37°C for 30 minutes. Ten microlitres of 20 mg/ml proteinase K were added, and after 60 minutes at 65°C, the lysates were extracted four times with 1 ml of a 1:1 mixture of phenol-chloroform. The DNA was precipitated with 100 μl of 3 M sodium

acetate, pH 5.5, and 2.5 ml of 95% ethanol, washed with 1 ml of 70% ethanol, and resuspended in 100 μl of TE buffer (10 mM Tris, 1 mM EDTA, pH 8.0).

Standard methods were used for isolation of plasmid DNA, agarose gel electrophoresis of DNA and transformation of *E. coli* (132). DNA was purified from agarose gels with silica beads from QIAGEN. Restriction endonucleases, T4 DNA ligase, the thermostable DNA polymerases *Taq* and *Pfu*, T4 DNA polymerase, and the Klenow fragment of DNA Polymerase I (henceforth simply "Klenow") were used as recommended by the suppliers.

The polymerase chain reaction (PCR) was done as recommended by the suppliers of *Taq* and *Pfu* polymerases, usually in the presence of 10% v/v dimethylsulfoxide (DMSO), 0.2 mM of each dNTP, 3 ng of template and 1 pM concentration of each primer. Reactions were done in a Perkin-Elmer GeneAmp 2400 instrument. The touchdown PCR method included 4 minutes at 96°C, 4 minutes at 80°C during which the enzyme was added, and 30 to 50 cycles of denaturation at 94°C for 30 seconds, annealing at temperatures from 60°C to 50°C (decreasing in increments of 0.4°C over the first 26 cycles and remaining at 50°C thereafter) for 30 seconds, and extension at 72°C for 3 minutes.

For conjugations, 100 μl of donor, 100 μl of helper (if required), and 500 μl of recipient cultures, densely grown, were mixed, centrifuged at 13,000 x g for 30 seconds, and resuspended in about 50 μl of RCV medium. Aliquots of 10 μl adsorbed onto an RCV agar plate were incubated overnight at 30°C. Donor cells were absent from the negative controls. Cells from each spot were resuspended in 2 ml of RCV medium and 100 μl and 500 μl were spread on RCV agar plates containing the appropriate antibiotics. Transconjugant colonies were streaked on YPS agar plates to test for the absence of *E. coli* donors.

Chromosomal gene deletions were made by transformation of pUC family plasmids carrying the deletions into *E. coli* TEC5, which contains a conjugative plasmid that recombines with pUC family plasmids (148), and selection of the antibiotic resistance marker (kanamycin, spectinomycin, or gentamicin) inserted into each deletion. This was followed by conjugative transfer to the *R. capsulatus* GTA overproducer DE442, selection on RCV agar plates, GTA transduction of linear DNA fragments into *R. capsulatus* recipients, and selection of recombinants for a double crossover.

DE442 strains carrying deletions of *pufQBALM* or *puhB* or *puhE* were grown phototrophically in YPS medium into stationary phase (> 300 KU) and filtered (pore size 0.45 μm) to obtain cell-free GTA. Recipient cells were grown aerobically or semiaerobically in RCV medium, pelleted, resuspended in half the initial volume, and mixed: 100 μl of cells with 400 μl G buffer (10 mM Tris-HCl pH 7.8, 1 mM $CaCl_2$, 1 ml NaCl, 500 μg/ml BSA) and 100 μl GTA filtrate. Negative controls received 500 μl G buffer without GTA filtrate. These mixtures were incubated for 1 hour at 30°C in a shaking water bath, followed by addition of 0.9 ml of RCV medium and further incubation for 4 hours to allow the transductants to express antibiotic resistance. Transductants were selected on RCV agar plates.

Conjugative transfer of IncP and IncQ plasmids from *E. coli* to *R. capsulatus* used *E. coli* S17-1 as the donor strain (144), or C600 as donor with HB101(pRK2013) as helper (30).

2.4. Construction of LH2$^-$ *pufQBALM* deletion background strains and *pufQLMX* complementation plasmids

To evaluate the direct effects of *puhB*, *puhC*, and *puhE* deletions on assembly and decay of the RC and LH1, I chose to delete the *puf* operon from the chromosome in an LH2$^-$ background and to restore the RC-specific and LH1-specific parts of it on plasmids (Figure 2.1). Due to the ready availability of p*Stu* I for LH1 restoration, and an awareness that the important *pufX* gene lacks its putative ribosome-binding site on this plasmid (74), I decided not to delete *pufX* from the chromosome. To determine the consequences of this choice, background strain U43, which has a chromosomal *pufQBALMX* deletion (171), was included as a control in every experiment.

For the chromosomal *pufQBALM* deletion, a *Bam*H I-*Xba* I fragment containing the *puf* operon of *R. capsulatus* was excised from a pBluescript-derived plasmid (S. Braatsch, personal communication) and ligated into pUC12 cut with *Bam*H I and *Xba* I. The resultant plasmid, pUC*puf*, was cut with *Hind* III and *Xba* I, the ends filled in with Klenow and religated to remove the *Sal* I site from the multiple cloning site. This modified pUC*puf* was cut with *Sal* I to delete the *pufQBALM* coding sequence, which was replaced with the gentamicin resistance cartridge from

plasmid pWKR440 as an *Xho* I fragment. The parallel orientation of the cartridge's promoter with the *puf* promoter was confirmed with an *Sph* I digest. This plasmid, called pUCΔ*puf*, was conjugatively transferred to DE442 and the deletion was transduced into the LH2$^-$ *puhC* deletion strain MWK1 to produce strain MA02.

In my hands, the gentamicin resistance cartridge appeared to be too large (2676 bp) for efficient GTA transduction. Therefore, a kanamycin resistance cartridge from plasmid pUC4::KIXX was inserted into the *Sal* I deletion of *pufQBALM* in the modified pUC*puf* plasmid as an *Xho* I fragment, producing plasmid pUCΔ*puf*K+. Verification of the promoter's orientation and transduction of this deletion into the LH2$^-$ strain MW442, the LH2$^-$ *puhB* deletion strain DW23, and the LH2$^+$ wild type strain SB1003 were carried out as above, producing strains MA01, MA03, and MA15, respectively. This approach was not taken with MWK1, which is already resistant to kanamycin (56).

Strains MA04, MA13, and MA14 are *puhE*$^-$ derivatives of MA01, MA03, and MA02, respectively. Their construction is detailed in Section 2.5.

Plasmids pTPR9 and pTPR8 contain *puf* operons with near-total in-frame deletion mutations of *pufB* and *pufA* respectively (128). To create a plasmid-borne *puf* operon lacking *pufB* and *pufA* that would restore RC expression to MA01, MA03, MA02, MA04, and U43 in the absence of LH1, the *puf* operons from these plasmids were excised as *Kpn* I-*Xba* I fragments and ligated into pUC18. An *Xho* I-*Bse*R I fragment of 1097 bp containing *pufQB* was removed from pUC18::*pufQB(ΔA)LMX* and replaced with the corresponding *pufQΔB* fragment of 992 bp from pUC18::*pufQ(ΔB)ALMX*. The resultant *pufQ(ΔBΔA)LMX* operon was excised as a *Kpn* I-*Xba* I fragment and ligated into pRK767 cut with *Kpn* I and *Xba* I, producing plasmid pMA10.

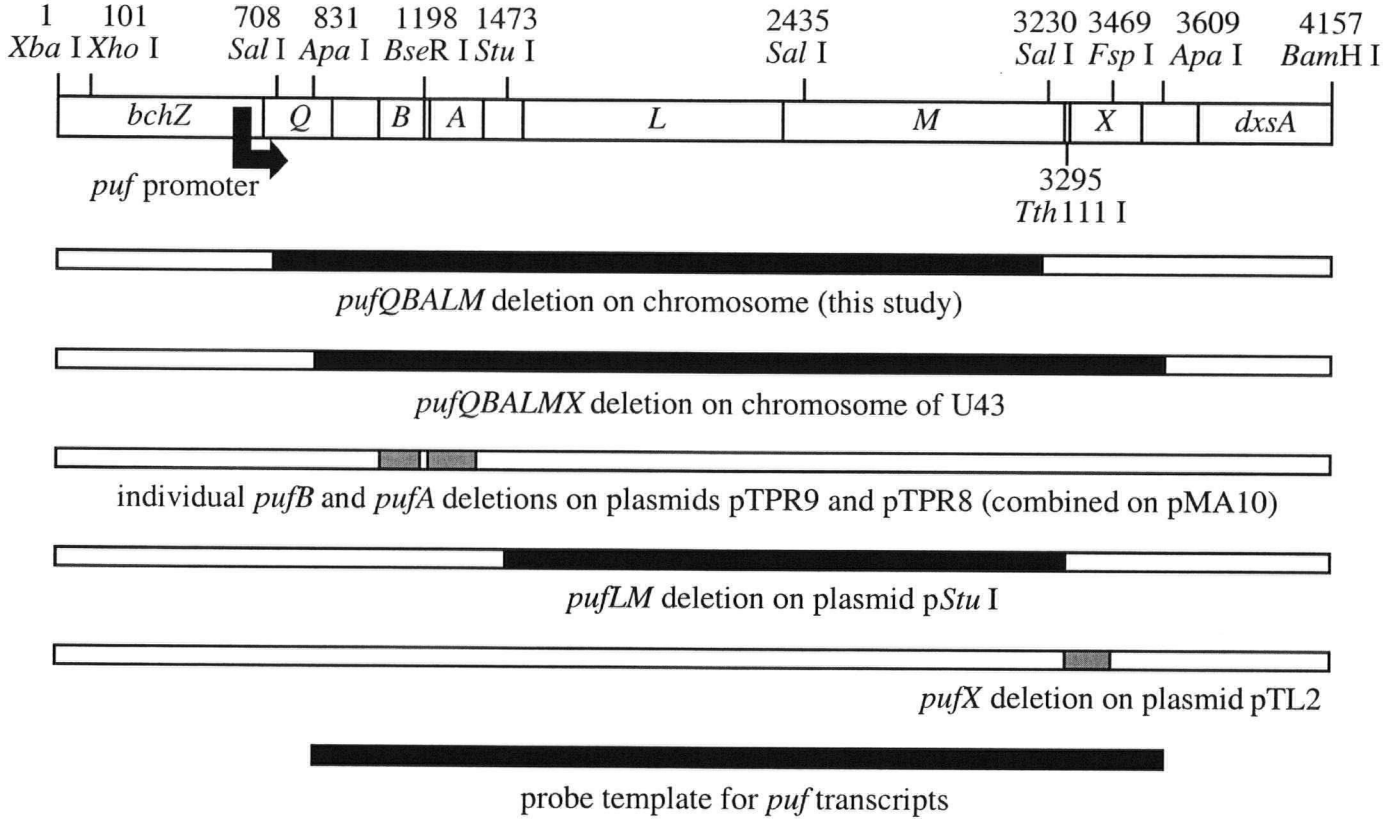

Figure 2.1. Deletions of *puf* genes. At the top is a representation of the chromosomal *puf* region. The shaded regions of bars underneath indicate the positions of deletions. Background strains MA01, MA03, MA04, and MA15 have a *Sal* I-*Sal* I deletion of *pufQBALM* substituted by a kanamycin resistance cartridge; in MA02, the gentamicin resistance cartridge is present instead. The promoters of both cartridges appeared to drive transcription of *pufX* (results in Section 3.5.3). The background strain U43 has an *Apa* I-*Apa* I deletion that encompasses *pufQBALMX* with a spectinomycin resistance cartridge inserted (171). This same *Apa* I-*Apa* I fragment was used to generate radiolabelled probes for RNA blots (results in Sections 3.1.2 and 3.4.3). Plasmid p*Stu* I has a *Stu* I-*Tth*111 I deletion of *pufLM* and the putative ribosome-binding site of *pufX* (74). The non-enzymatic deletions of all but four codons of *pufB* on pTPR9 and all but seven codons of *pufA* on pTPR8 (128) were combined by exchange of *Xho* I-*Bse*R I fragments to produce pMA10. The *Tth*111 I-*Fsp* I deletion of *pufX* on pTL2 contains a spectinomycin resistance cartridge (87).

2.5. Construction and genotyping of *puhB* and *puhE* mutant strains

An *Eco*R I-*Hin*d III fragment of 2734 bp containing *puhB* (Figure 2.2) was excised from plasmid pUC13::EcoF (166) and ligated into pUC19, producing plasmid pEH214. *Bst*B I and *Cla* I were used to excise a 359 bp fragment of *puhB* (56% of the coding sequence) from pEH214, and to excise the kanamycin resistance cartridge from pUC4::KIXX. The cartridge was ligated into the deletion, and the parallel orientation of the cartridge promoter with the *puhA* promoter was confirmed by digestion with *Bst*BI and *Cla* I. This plasmid was transferred to DE442 and the deletion was transduced into SB1003 to produce strain MA05.

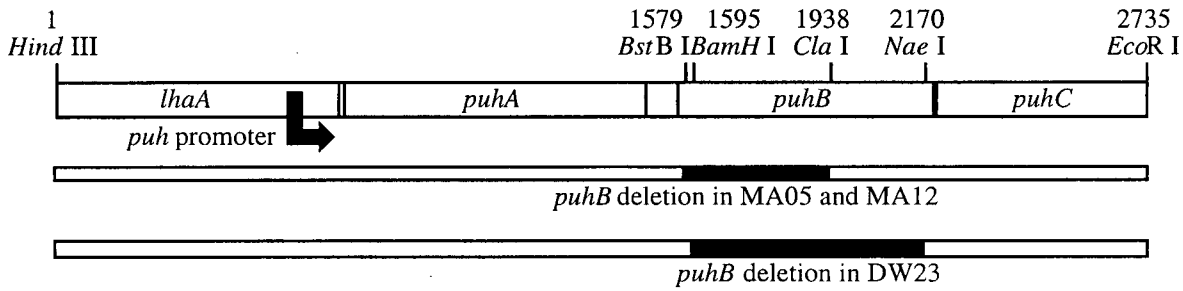

Figure 2.2. The *Hind* III-*Eco*R I fragment used to delete *puhB* and as template for PCR amplification. The arrow represents the *puh* promoter within *lhaA*, and the *puhB* deletions' extents are indicated by the black bars underneath.

The method used to delete 63% of the coding region of *puhC* (Figure 2.3) to make strains SBK1, SBSpec, MWK1, and MWSpec, with insertion of KIXX and Ω cartridges, has been described previously (2, 56).

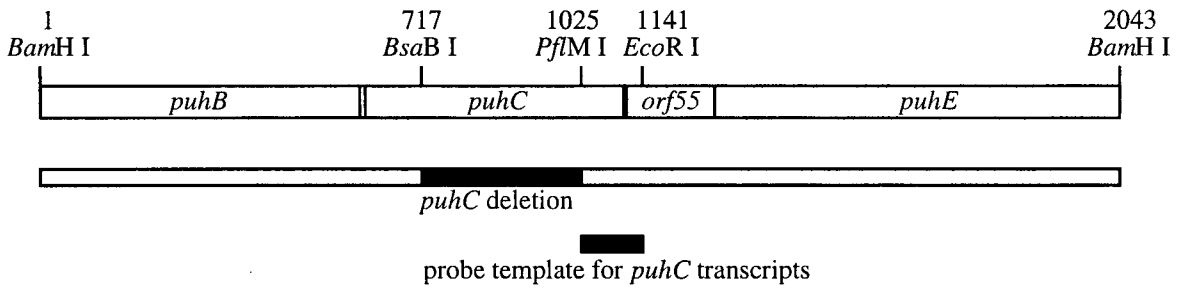

Figure 2.3. The *Bam*H I-*Bam*H I fragment earlier used to delete *puhC* (56) and used here as template for PCR amplification. The extents of the *puhC* deletion and the probe for *puhC-orf55* mRNA in an RNA blot (results in Section 3.3.1) are indicated by the black bars underneath.

Plasmid pRPS404, which contains the *R. capsulatus* photosynthesis gene cluster as an insert of 46 kbp (148), was digested with *Bgl* II and *Kpn* I. A fragment of about 4 kbp containing *puhE* was ligated into pUC18, and an *Eco*R I-*Hind* III fragment of 1330 bp containing *puhE* (Figure 2.4) was subcloned into pUC18 to produce plasmid pEH274. The two *Msc* I sites in *puhE* were used to make a deletion of a 369 bp (45% of the coding sequence), into which were ligated *Sma* I-cut cartridges for kanamycin resistance from pUC4::KIXX and for spectinomycin resistance from pUC18::Ω. The Ω cartridge contains transcription termination signals; the KIXX cartridge does not. The parallel orientation of the KIXX cartridge promoter with the *puhA* promoter was confirmed. These two plasmids were transferred to DE442 and the deletions with KIXX and Ω insertions were transduced into SB1003, MW442, and DW23 to create strains MA06 and MA07, MA08 and MA10, MA09 and MA11, respectively (for genotypes, refer to Table 2.2). The Ω cartridge mutation was also transduced into MA05 to create strain MA12, into MA01 to create MA04, into MA03 to create MA13, and into MA02 to create MA14.

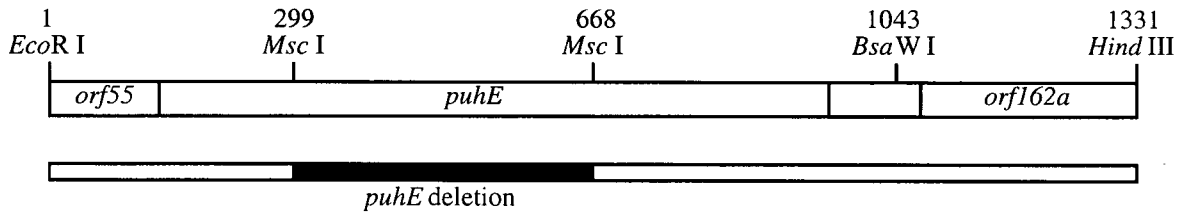

Figure 2.4. The *Eco*R I-*Hind* III fragment used to delete *puhE*. The complementation plasmid pMA19 carries the *Eco*R I-*Bsa*W I fragment. The extent of the *puhE* deletion is indicated by the black bar underneath.

The presence of a KIXX insert of the expected size in the deleted *puhB* gene was confirmed by PCR of chromosomal DNA from SB1003 and MA05, using primers that add an N-terminal 6xHis tag to *puhB* (see Section 2.6). PCR was also used to confirm the deletion of *puhB* in strain DW23, and the insertions of KIXX and Ω cartridges into the deletion of *puhE* in MA04, MA06, MA07, MA08, MA09, MA10, MA11, and MA12, compared to the parent strains, using primers 5'-GGTGCCGCTCATGAACAATCC-3' and 5'-ACGAAGTCGAAGCTTACTCGCCCAC-3', which consist of DNA sequences at the 5' and 3' ends of *puhE*.

2.6. Construction of plasmids to express 6xHis-tagged PuhC in *E. coli*

Six histidine codons were added by PCR to the N-termini and C-termini of *puhB*, *puhC*, and *puhE* for the purposes of purification using a chelated nickel resin in column chromatography. Overexpression of the tagged proteins in *E. coli* was attempted with the intent to raise rabbit antisera against each protein. To evaluate the importance of the predicted TM segment of PuhC, a truncated form of PuhC without this segment (PuhC-NS) was made with the C-terminal 111 amino acid residues of PuhC preceded by an N-terminal 6xHis tag.

The templates for PCR were fragments of *R. capsulatus* DNA excised from pUC vectors (see Section 2.5): EcoF (166) and BamK (148). The forward and reverse primers for each tagged construct are listed in Table 2.6. For PuhC-NS, the reverse primer was the same as for PuhC-N.

Table 2.6. Primers used to add 6xHis tags to PuhB and PuhC. Relevant restriction sites and the 6xHis tags are underlined.

PuhB-N	5'-CCGCGCCTTGAATTCTCGGAGGTCTGCATGCATCATCATCATCATCATAGCGACCATG-ACTTCGACTTC-3'
reverse	5'-CCATCGGGGTAAGCTTATTCCGCCACGGCCAGAG-3'
PuhB-C	5'-CCGCACTACTGAATTCCGGAGGTCTTCATGAGCGACCATGACTTCGACTTC-3'
reverse	5'-GGGAAAGCAGAAGCTTAGTGATGGTGGTGATGATGTTCCGCCACGGCCAGAG-3'.
PuhC-N	5'-TTTATATATTAGAATTCAGGAATAAGGGGACCCGCATGCATCATCATCACCACCACGC-ACAGCTTCCGCTTT-3'
reverse	5'-GTGTTAGGGACCCGGGAAAGCTTACTTCATGTCGAGAATACGC-3'
PuhC-NS	5'-TTGCTGGTACGCATGCATCACCATCACCACCATGGGCGCCCGCACGAA-3'
PuhC-C	5'-ATAATAATAAGAATTCAGGAATAAGGGGACCCCCATGGCACAGCTTCC-3'
reverse	5'-AATAATTAATCCCGGGTAAGCTTAGTGGTGGTGATGATGATGCTTCATGTCGAGAATA-3'

Four of these amplicons: *puhB-N*, *puhB-C*, *puhC-N*, and *puhC-C*, were cut with *Eco*R I (on the 5' side of the ribosome-binding sites of *puhB* and *puhC* predicted for *R. capsulatus*) and *Hin*d III (overlapping the termination codons) and inserted into pUC19 for sequencing. The fifth amplicon, *puhC-NS*, was cut with *Sph* I (overlapping the initiation codon) and *Hin*d III and inserted into a pUC19 plasmid from which the full-length *puhC* gene with an N-terminal 6xHis tag had been cut out with *Sph* I (overlapping the initiation codon) and *Hin*d III.

For overexpression in *E. coli*, the tagged *puhC* genes without their ribosome-binding sites were subcloned into the vectors pQE70 and pQE60 (QIAGEN), using restriction sites that overlap the initiation codon (*Sph* I/*Nsi* I and *Nco* I) and termination codon (*Hind* III). In the pQE vectors, these sites are located 3' to a unique promoter recognized by T5 RNA polymerase and a ribosome-binding site. The *puhC-N* and *puhC-NS* genes were subcloned into pQE70 with *Sph* I and *Hind* III, *puhC-C* was subcloned into pQE60 with *Nco* I and *Hind* III. The pQE plasmids were transformed into M15 cells. Table 2.7 gives the characteristics expected of all these 6xHis-tagged proteins.

Table 2.7. Characteristics expected of 6xHis-tagged PuhB and PuhC.

Name	His tag location	Length (amino acid residues)	Size (kDa)	TM segments
PuhB-N	N-terminus	219	24.4	3
PuhB-C	C-terminus	219	24.4	3
PuhC-N	N-terminus	168	18.2	1
PuhC-C	C-terminus	168	18.2	1
PuhC-NS	N-terminus	117	13.0	0

2.7. Construction of plasmids to express Puh proteins in *R. capsulatus*

Plasmids of the IncQ incompatibility group had been used before to complement deletions of *lhaA* (170) and *puhC* (56), with the gene of interest being inserted at an *Eco*R I site 3' of the *puf* promoter (Figure 2.5). These and other recent records failed to state that the *pufQ* gene was present on these plasmids and on the "empty vector" pRR5C, a derivative of pPUFP1 (17). Consequently, whenever I constructed *puh* gene restoration plasmids to express the 6xHis-tagged proteins PuhB-N, PuhB-C, PuhC-N, PuhC-C, and PuhC-NS, or to express PuhE, or to express the PuhC proteins of three other purple bacterial species, I unwittingly created an unnatural situation of *pufQ* merodiploidy and *pufQ-puh* gene co-transcription. After performing many complementation experiments with *pufQ*$^+$ plasmids, I discovered the basis of the variable growth defect due to the *puhC* deletion and was able to establish that pRR5C complements this defect under certain conditions. Thereafter, I rectified my complementation plasmids by deleting *pufQ*, and repeated my experiments, which allowed me to study how *pufQ* merodiploidy affects each *puh* gene deletion.

The details of construction for these plasmids (listed in Table 2.5) are as follows. The four 6xHis-tagged constructs *puhB-N*, *puhB-C*, *puhC-N*, and *puhC-NS* (see Section 2.6) were excised from pUC19 together with their natural *R. capsulatus* ribosome-binding sites, using *Hind* III (filled in with Klenow) and *Eco*R I, and ligated into the pRR5C derivative pAH8 (2), from which the untagged *puhC* gene had been excised as three fragments with *Eco*R I and *Sma* I. The resultant plasmids were named pMA7, pMA8, pMA1, and pMA3, respectively.

The *puhC* genes of *R. sphaeroides*, *R. rubrum*, and *R. gelatinosus* were amplified by PCR from their respective templates (see Table 2.3), using the primers listed in Table 2.8, which added the ribosome-binding site of *R. capsulatus puhC* to each homologous gene. The *R. sphaeroides puhC* gene was cut with *Eco*R I and *Xma* I and inserted into pUC19 for sequencing. The *R. rubrum puhC* gene was cut with *Bsp*E I (filled in with Klenow) and *Eco*R I and inserted into pUC19 cut with *Hind* III (filled in with Klenow) and *Eco*R I. The *Bsp*E I site following the termination codon of the gene was regenerated in this plasmid. Then the *R. rubrum* gene was excised and the *R. gelatinosus* gene cut with *Eco*R I and *Bsp*E I was inserted in its place. All three genes were excised with *Eco*R I and *Xma* I/*Bsp*E I and inserted into pAH8, from which *R. capsulatus puhC* had been excised with *Eco*R I and *Xma* I, resulting in plasmids pMA4, pMA6, and pMA5, which contain the *R. sphaeroides*, *R. rubrum*, and *R. gelatinosus puhC* genes respectively.

The 6xHis-tagged *puhC-C* gene (see Section 2.6) was excised from pUC19 as an *Eco*R I-*Bsa*W I fragment and ligated into pMA4, from which *R. sphaeroides puhC* had been excised with *Eco*R I and *Xma* I, resulting in plasmid pMA9.

The *puhE* gene was excised from plasmid pEH274 (see Section 2.5) with *Eco*R I and *Bsa*W I and ligated into pMA4 cut with *Eco*R I and *Xma* I to produce plasmid pMA11.

Table 2.8. Primers used to amplify the *puhC* genes from *R. sphaeroides*, *R. rubrum*, and *R. gelatinosus*.

R. sphaeroides	5'-AAAAAAAAAAGAATTCAAGGGGACCCCGATGAGCGCACAGAA-CTCCCG-3'
reverse	5'-AAAAAAAAATCCCGGGTCATTCGGACAGCATCCGCTCG-3'
R. rubrum	5'-AAAAAAAAAAGAATTCAAGGGGACCCCGATGAGCGCCGGCCA-CCG-3'
reverse	5'-AAAAAAAACCTCCGGATTAGCGGCCGTCCCGGGC-3'
R. gelatinosus	5'-AAAAAAAAAAGAATTCAAGGGGACCCCGATGAGCGACAACGC-GTCCC-3'
reverse	5'-AAAAAAAAAATCCGGATCAGCGGGCCGGGGCCTGCTGG-3'

When the *pufQ* gene on plasmid pRR5C and its derivatives was suspected to interfere with analysis of complementation by various *puhC* genes and by *puhE*, deletion of *pufQ* from the plasmids became imperative. A *Hind* III-*Eco*R I fragment of 872 bp from pRR5C, carrying the *puf* promoter and *pufQ* (Figure 2.5), was inserted into pUC18, and the sequence between the *Acc* I site at the 3' end of the *puf* promoter (1) and the *Eco*R I site 3' of *pufQ* was removed as two fragments. A multiple cloning site for *Xba* I, *Nsi* I, *Cla* I, and *Bsp*E I was inserted with the oligonucleotides 5'-CTAGATGCATCGATCCGG-3' and 5'-AATTCCGGATCGATGCATCT-3'. The modified *Hind* III-*Eco*R I fragment of 344 bp was returned to pRR5C, pMA1, pMA3, pMA4, pMA5, pMA6, pMA7, pMA8, and pMA11. The resulting *pufQ*-free plasmids were named pMA20, pMA12, pMA13, pMA14, pMA15, pMA16, pMA17, pMA18, and pMA19, respectively.

Plasmid pMA22, carrying the untagged *puhB* gene, was constructed by excision of a *Hind* III-*Mlu* I fragment from pMA17, encompassing the 6xHis-tagged N-terminus, and replacement with the corresponding fragment of pMA18.

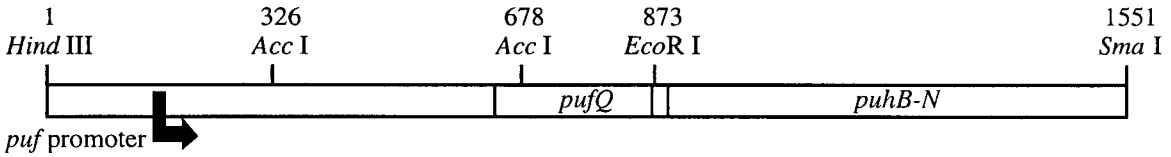

Figure 2.5. The unnatural *pufQ-puh* gene transcriptional fusion in pRR5C-type plasmids, from which *pufQ* was removed with the restriction sites indicated to make pMA20-type plasmids. All *puhB*, *puhC*, and *puhE* genes, including tagged constructs and homologues from other species, such as *puhB-N* in this example, were inserted on one side of the *Hind* III-*Eco*R I fragment of the *puf* operon, between the *Eco*R I and *Sma* I sites.

2.8. Construction of TOXCAT hybrids; the TOXCAT test method

DNA fragments encoding amino acid residues 38-65 ("TM1"), 70-95 ("TM2"), and 101-126 ("TM3") of PuhB and residues 23-50 of PuhC were amplified by PCR from the BamK fragment of the *R. capsulatus* photosynthesis gene cluster (see Figure 2.3). Initially, the Arg96 residue of PuhB was included in TM2 ("TM2R") - this PCR used a different reverse primer. Following the discovery of homodimerization of TM2, a library of 256 mutated TM2 segments was generated

with a pair of primers with twofold degeneracy at six positions and fourfold degeneracy at one position. The mutations introduced were T72A, F76L, M79L, Y84F/S/C, M87L, F92L, and Q94E. Residues 29-51 of *R. capsulatus* PufX were amplified from the pUC*puf* plasmid (see Section 2.4). Residues 30-52 of *R. sphaeroides* PufX were amplified from a plasmid called pQE*pufX-12*, which contains a 6xHis-tagged *pufX* gene from which twelve codons at the C-terminus have been deleted (unpublished). All of the primers are listed in Table 2.9.

The amplicons were ligated into pccKAN as *Nhe* I-*Bam*H I fragments, transformed into DH5α, isolated, sequenced, and transformed into MM39. The primer for sequencing, 5'-TGTAGTGAACACACCGCAG-3', is called TMSEQ4 (W. Russ, personal communication).

Table 2.9. Primers used to amplify the TM segments of PuhB, PuhC, and PufX from *R. capsulatus* and PufX from *R. sphaeroides*. The *Nhe* I and *Bam*H I sites and the positions of degeneracy are underlined.

PuhB-TM1	5'-GTGGATGCTGGCTAGCGACGCGTTCAAG-3'
reverse	5'-AATAATGCCTGGATCCCGCCTTCCTCGTGCCAG-3'
PuhB-TM2	5'-TTGCACCCGAGCTAGCCTGCCCA-3'
reverse	5'-GTGTAGATCGGGATCCCGGCCTGCGCGAA-3'
TM2R reverse	5'-ATGGTGTAGAGGATCCCACGGGCCTGCGCGAA-3'
PuhB-TM2M	5'-AGGCGCCCGGGCTAGCCTGCCCRCCGCCGTCCTGYTCCTTCTGMTGGCC-3'
reverse	5'-GTGTAGATCGGGATCCCGGCCTSCGCGARGGCGAGCAGAAGCAKCAGCCCGNAG-ACG-3'
PuhB-TM3	5'-CCGTGCCGCGGCTAGCACCATCACCTC-3'
reverse	5'-GCCAGCGACAGGATCCCGATCACGGTGAAG-3'
PuhC-TM	5'-CCCTTGCAATGCTAGCGCCGAGCTGATCCCGAAA-3'
reverse	5'-TCGAGCGAGTGGATCCCCAGGACCGCATAGGTGG-3'
PufXcaps-TM	5'-TCGTCAGATGGCTAGCGGTGCCTTCC-3'
reverse	5'-TCGGGCAGCAGGATCCCGAGGCCATAGG-3'
PufXsphæ-TM	5'-TTTCCAGATGGCTAGCGGTGCGGGCTG-3'
reverse	5'-ATCGGAAGCAGGATCCCGACCACC-3'

The insertion of each TM segment hybrid protein into the inner membrane of *E. coli* was tested by streaking MM39 cells expressing each hybrid on plates of M9-maltose minimal medium, with pccGpAwt as the positive control and pccTNM as the negative control (131).

For the CAT assay, 8 ml LB medium cultures of isolated colonies were grown either for a few hours or overnight at 37°C, and a volume of culture equivalent to 100 μl at 160 Klett units (~6 x 10^7 cells) was harvested in an Eppendorf tube. Cells were sometimes frozen at -80°C. The duration of growth or freezing did not affect the outcome. Cells were resuspended in 500 μl of 100 mM Tris HCl pH 8.0, to which was added 20 μl of a solution of 50 mM Tris HCl pH 8.0, 100 mM EDTA and 100 mM DTT, followed by 20 μl of toluene. After permeabilization of the cell membranes by incubation at 30°C for 30 min and pelleting of cell debris in a microcentrifuge for 5 min, the cell extract supernatants were incubated on ice. Then, 60 μl of cell extract were mixed with 10 μl of substrate (BODIPY FL 1-deoxychloramphenicol from Sigma in methanol) and incubated at 37°C for 5 minutes. Ten μl of 9 mM acetyl-CoA (Sigma) were added, and samples taken at 15 minute intervals were spotted on a silica gel plate (Sigma) for thin layer chromatography. The solvent for chromatography was a mixture of 85 ml dichloromethane and 15 ml methanol.

2.9. Construction of CyaA hybrids

DNA fragments encoding the N-terminal 43 amino acid residues of PuhB ("N43"), the C-terminal 84 amino acid residues of PuhB ("C84"), and the C-terminal 118 amino acid residues of PuhC ("C118") were amplified by PCR. The templates were the *Eco*R I-*Hind* III fragment carrying *puhB* and the BamK fragment carrying *puhC* and most of *puhB* (see Section 2.5). The primers are listed in Table 2.10.

Table 2.10. Primers used to amplify the predicted cytoplasmic and periplasmic domains of PuhB and PuhC. The relevant restriction sites are underlined: *Rsa* I in the N43 forward primer, *Bam*H I in the C84 and C118 forward primers, and *Kpn* I in all reverse primers.

PuhB-N43	5'-TGGAATACAGCGTACGCCATGTCAGACCATGACT-3'
reverse	5'-GATGCTCGTTGGTACCCGGATCTTGAACGCG-3'
PuhB-C84	5'-CCGTGATCGAGGATCCGTCGCTGGCCAA-3'
reverse	5'-ATCAGGGTCTGGTACCTCCGCCACGGCCAG-3'
PuhC-C118	5'-TTCTGTTACTGGATCCGACCACCTATGC-3'
reverse	5'-GGCATGGGTTGGTACCTTCATGTCGAGAAT-3'

The amplicons were cut with *Kpn* I and, in the case of C84 and C118, with *Bam*H I. They were ligated into pRASIKA, a plasmid constructed by ligation of the annealed oligonucleotides 5'-GCT-AGCGAAGACCGTACGATCGATGGTCGACCGTTCGAAGGATCCGTCCCG-3' and 5'-GTA-CCGGGACGGATCCTTCGAACGGTCGACCATCGATCGTACGGTCTTCGCTAGCTGCA-3' into pUC19 cut with *Kpn* I and *Pst* I, regenerating both sites. The N43 amplicon was ligated into pRASIKA cut with *Kpn* I and *Hinc* II (underlined with small dashes in the oligonucleotide sequences above), and the C84 and C118 amplicons were ligated into pRASIKA cut with *Kpn* I and *Bam*H I (underlined with large dashes). After sequencing, N43 was excised by digestion with *Kpn* I followed by *Rsa* I (underlined), while C84 and C118 were excised with *Kpn* I and *Bam*H I. All three fragments were inserted into the CyaA hybrid expression plasmids pUT18, pUT18C, and pKT25, which were cut with *Sma* I followed by *Kpn* I for insertion of N43, and with *Kpn* I and *Bam*H I for insertion of C84 or C118. BTH101 *E. coli* cells were transformed with the nine different plasmids singly and in all combinations of T25 hybrids with T18 hybrids. The pUT18 derivatives have the domains of interest fused to the N-terminus of T18; the pUT18C derivatives have them fused to the C-terminus of T18, and the pKT25 derivatives have them fused to the C-terminus of T25.

Due to doubts regarding the transmembrane nature of the second and third TM segments of PuhB, a larger segment of PuhB called C147 (the last 147 amino acid residues) was obtained by digesting pUT18C::C84 with *Bam*H I and *Sph* I, filling in the *Bam*H I end with Klenow, and ligating in an *Sma* I-*Sph* I fragment of the *puhB* gene from plasmid pEH214 (see Section 2.5). This T18-C147 hybrid was tested against all T25 hybrids.

The CyaA test was carried out by plating transformed cells on selective M63-maltose minimal medium, and by screening on LB agar containing IPTG and X-gal, although IPTG is not strictly required to induce expression of CyaA hybrids.

2.10. β-galactosidase assay of *R. capsulatus* strains

The effects of *puh* gene deletions on transcription from the *puf* promoter and translation of PufB were evaluated by β-galactosidase assays of cells carrying plasmid pXCA6::935. This plasmid expresses PufQ and a PufB-LacZ fusion protein from the *puf* promoter (1).

Cells from semiaerobic *R. capsulatus* cultures, and from phototrophic cultures grown with high and low light intensity, were harvested by centrifugation. Pellets from 10 ml of culture were resuspended in 1 ml of RCV medium and stored at -80°C before assay as previously described (90). Samples were diluted tenfold in RCV medium to estimate the number of cells by spectroscopy (~4.5 x 10^8 cells per A_{650} unit) and 20 μl of this dilution were mixed with 500 μl of Z buffer (100 mM sodium phosphate, 10 mM potassium chloride, 1 mM magnesium sulfate, 50 mM β-mercaptoethanol, pH 7.0), 50 μl of 0.1% SDS, and 50 μl of chloroform, and vortexed vigorously for 10 seconds. The reaction was started with 200 μl of 4 mg/ml *o*-nitrophenyl-β-D-galactopyranoside and stopped after 15 minutes (at which time a yellow colour had developed) with 500 μl of 1 M sodium carbonate. The absorbance at 420 nm and the extinction coefficient of 6.032 x 10^{-3} nmol/ml/A_{420} were used to calculate activity (nmol per minute per 10^8 cells). The mean activity from three independently grown cultures was calculated for each experiment, with the standard deviation as a measure of error.

2.11. RNA blots

To compare the levels of *puhC* mRNA in SB1003, DW1, and SBK1, aerobic and semiaerobic cultures were grown to a density of 100 Klett units, and RNA was isolated from 25 ml of each culture using the RNeasy Midi kit (QIAGEN). Samples were treated with 30 units of deoxyribonuclease I in 100 mM sodium acetate, 5 mM magnesium sulfate (pH 5.0) for 30 minutes at room temperature, followed by phenol-chloroform extraction and ethanol precipitation. Seven μg of each RNA sample were used for formaldehyde gel electrophoresis (84) and electro-blotted onto a nylon membrane (ICN) for 2 hours at 80 V in 0.5X TBE (132). The membrane was baked at

80°C for 2 hours and pre-hybridized in 10 ml of 50% formamide, 10% dextran sulfate, 5.8% sodium chloride, 1% SDS, 0.2% BSA, 0.2% ficoll, 0.2% polyvinylpyrrolidone, 0.1 sodium pyrophosphate, and 50 mM Tris HCl (pH 7.5) with 0.1 mg/ml sheared salmon sperm DNA (Sigma) at 42°C for 3 hours with rotation in an oven (BIO/CAN Scientific). The probe was a gel-purified DNA fragment extending from the *Bsa*B I site in *puhC* to the *Eco*R I site in *orf55* (Figure 2.3), labelled with ^{32}P using the Redi-Prime kit (Amersham Pharmacia Biotech) for 2 hours. After 16 hours of hybridization, the membrane was washed with agitation twice in 100 ml 2X SSC (132) for 10 minutes at room temperature, twice in 100 ml 2X SSC containing 1% SDS for 15 minutes at 60°C, and once in 100 ml 0.1X SSC for 15 minutes at room temperature. Hybridization signals were detected with BioMax MS film (Kodak).

To compare levels of *puf(BA)LM* and *pufBA* mRNA in MA01(pTB999), MA01(pTPR9), MA01(pTPR8), and MA01(pMA10), cultures of 40 ml were grown aerobically to about 70 Klett units and then semiaerobically for 4 hours to 100 Klett units. Cells were pelleted in ice-packed tubes for 10 minutes at 6,000 rpm in a Beckman JA-20 rotor. The cell pellets were frozen at -80°C and RNA was isolated using the RNeasy Midi kit. Ten μg of each RNA sample were used for analysis as above; however, the membrane was crosslinked in a UV Stratalinker oven (Stratagene) in lieu of baking, and the probe was an *Apa* I fragment of pUC*puf* extending from the middle of *pufQ* to the 3' region of *pufX*. This method was also used to compare levels of *pufLM* mRNA in MA01(pMA10) and MA04(pMA10), and levels of *pufBA* mRNA in MA01(p*Stu* I) and MA04(p*Stu* I).

2.12. Isolation of chromatophores; electrophoresis and blotting of proteins

To isolate vesicularized intracytoplasmic membranes (chromatophores), cell pellets from *R. capsulatus* cultures grown in 800 ml to 1600 ml of RCV medium were resuspended in chromatophore buffer (20 mM 3-(N-morpholino)propanesulfonate pH 7.2, 100 mM potassium chloride, 1 mM magnesium chloride), homogenized with a hand-held mortar and pestle, and passed through a chilled French press cell three times to break the cells. Cell debris was pelleted in a JA-20

rotor at 15,000 rpm for 8 minutes. Chromatophores were pelleted from the supernatant by ultracentrifugation in a TLA100.3 rotor at 100,000 rpm for 14 minutes, and resuspended in chromatophore buffer. Samples for flash spectroscopy were stored on ice or cold packs until use; samples for SDSPAGE and immunoblotting were stored at -80°C.

The amount of protein in each chromatophore preparation was determined by a modified Lowry method, with BSA as the standard (116). Samples containing 50 μg of protein were mixed with loading buffer, heated at 50°C for 10 min, and used in a tricine-SDS-polyacrylamide gel (SDSPAGE) system (135). Gels were stained in a solution of 0.025% Coomassie Brilliant Blue G-250 or R-250 (Fisher) in 40% methanol and 10% acetic acid, and destained in the same solution lacking the dye.

Samples of unfractionated cells (50 μg of protein) or of protein were run on 12% polyacrylamide gels by the Laemmli method, and either stained as above or blotted. For blots, Towbin Transfer Buffer (25 mM Tris HCl, 192 mM glycine, 20% methanol) was used to transfer proteins at 80 V for 2 hours to nitrocellulose membranes. For amino acid analysis and N-terminal sequencing, CAPS buffer (10 mM 3-cyclohexylamino-1-propanesulfonate pH 11.0, 10% methanol) was used instead, and the polyvinyledene difluoride membranes were stained with 0.025% Coomassie Brilliant Blue R-250 in 40% methanol. The bands of interest were outlined by perforations with a syringe needle. N-terminal sequencing was done at the Nucleic Acid and Protein Services Unit, U.B.C. Amino acid analysis was done at the Victoria Protein Microchemistry Centre, Department of Biochemistry and Microbiology, University of Victoria, B.C., Canada.

The primary antibodies against CyaA, PuhC, and PufX were used at 1:1000, 1:2000, or 1:5000 dilution in 20 ml of TBS-T containing 5% Nestle Carnation skim milk powder. (TBS-T is 20 mM Tris HCl pH 7.6, 0.8% NaCl, 0.1% Tween-20.) Following an overnight incubation shaking at 7°C with the primary antibody, the membranes were washed three times in 20 ml of TBS-T for 20 minutes at room temperature. The secondary antibody, horseradish peroxidase-linked donkey anti-rabbit IgG (Amersham), was used at 1:2000 and 1:5000 dilution in TBS-T containing 5% skim milk powder for 1 hour at room temperature, followed by three more washes. Chemiluminescence was produced with the ECL kit (Amersham) and detected with BioMax MS film (Kodak).

2.13. Expression, nickel resin affinity purification, and concentration of 6xHis-tagged proteins; generation of antibodies against PuhC and PufX

Expression studies on 6xHis-tagged proteins were done using various media (see Section 2.2). For large-scale purification, starter cultures of *E. coli* cells containing pQE-derived expression plasmids were grown overnight in 2xYT medium and used to inoculate 1000 ml cultures. Expression of the 6xHis-tagged protein was induced at a culture density of 70 Klett units by adding IPTG to 1 mM, and the culture was harvested at 6,000 rpm in a JA-14 rotor. Cells from each 1000 ml culture expressing PuhC-N were resuspended in 15 ml of Purification Buffer (10 mM Tris HCl pH 8.0, 300 mM sodium chloride) containing 10 mM imidazole, and incubated on ice with 1 mg/ml lysozyme for 30 minutes followed by the addition of ribonuclease A to 10 μg/ml and deoxyribonuclease I to 5 μg/ml and an additional incubation for 15 minutes. Five ml of Purification Buffer containing 10 mM imidazole and 4% lauryldimethylamine oxide (LDAO) were added, and the lysate was centrifuged at 10,000 rpm in a JA-20 rotor for 10 minutes. Cells expressing PuhC-NS were similarly treated except that the Purification Buffer contained 50 mM sodium phosphate instead of 10 mM Tris HCl, and LDAO was not used.

One ml of nickel agarose resin (QIAGEN) in a plastic column was mixed with 4 ml of lysate supernatant for one hour at 4°C, then drained, washed twice with 4 ml of Purification Buffer containing 25 mM imidazole (+ 0.1% LDAO for PuhC-N), and eluted four times in 500 μl of Purification Buffer containing 250 mM imidazole (+ 0.1% LDAO for PuhC-N). Centriplus X-10 columns (Amicon) were used to concentrate PuhC-N and PuhC-NS.

Two female New Zealand White rabbits were immunized with a mixture of purified PuhC-N and PuhC-NS in 0.5 ml PBS mixed with 0.5 ml Freund's Adjuvant (Difco). Complete Freund's Adjuvant was used for the primary immunization and Incomplete Freund's Adjuvant was used for all eight boosts. The first injection and the first boost were done with 1 mg each of PuhC-N and PuhC-NS. To improve the affinity of antibodies, the second boost was done with only 125 μg each of PuhC-N and PuhC-NS. At this point, trace impurities were detected in concentrate PuhC-N by SDSPAGE, and so the third boost was done with 250 μg of PuhC-NS. The remaining five boosts

were done with only 100 μg of PuhC-NS. Blood samples of 10 ml were taken seven to fourteen days after each boost. The rabbits were exsanguinated thirteen days after the eighth boost.

The following timeline shows injections (diamonds) and bleeds (squares) over 166 days from primary immunization to exsanguination.

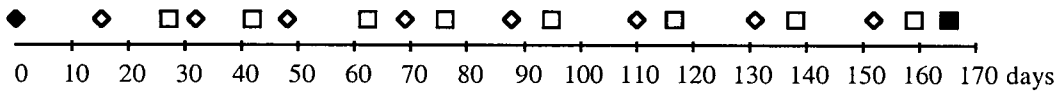

Antibodies were raised against peptides corresponding to the N-terminal and C-terminal regions of "mature" PufX: (NH_3^+)-SMFDKPFDYENGSKFC(NH_2)-(KLH) and (KLH)-LPERAHQAPSPYTTEV-(COO^-). Two rabbits were injected with a combination of both peptides conjugated to keyhole limpet hemocyanin (KLH). The procedure was performed by Genemed Synthesis by the following timeline.

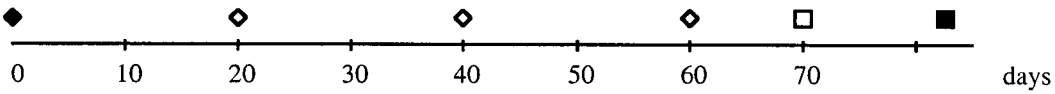

Solubilization of the RC-LH1 complex was performed by adding aliquots of 200 mM diheptanoylphosphatidylcholine (DHPC) dropwise to rapidly stirring suspensions of chromatophores from strain MWK1(pMA1), an LH2$^-$ *puhC*$^-$ strain complemented with 6xHis-tagged *puhC* on a plasmid, in Buffer TNM (10 mM Tris HCl pH 7.5, 150 mM sodium chloride, 2 mM magnesium chloride), on ice. After each aliquot was added, a sample of 3 ml was subjected to ultracentrifugation in a TLA100.3 rotor at 100,000 rpm for 14 minutes, and the uppermost 1 ml portion of the supernatant was collected. Equal volumes of each fraction were immunoblotted for PuhC and analyzed by absorption spectroscopy. Ten ml of the remaining suspension containing 20 mM DHPC were incubated with 1 ml nickel agarose resin at 4°C for one hour, followed by washing with 20 ml of Buffer TNM and elution in Buffer TNM containing 250 mM imidazole. The flowthrough and eluates were also immunoblotted for PuhC.

2.14. Spectral analysis of light harvesting and reaction centre complexes

Semiaerobic and phototrophic *R. capsulatus* cultures were grown to 150 Klett units (KU), which is in early stationary phase of semiaerobic growth and mid-exponential phase of wild type phototrophic growth. A 1.5 ml sample of each culture (about 7.4 x 10^8 CFU) was harvested in a microcentrifuge, frozen at -20°C, resuspended in 0.25 ml of RCV medium and mixed with 0.75 ml of a 30% BSA solution containing 0.85% sodium chloride and 0.1% sodium azide (to reduce light scattering by cells). Samples were scanned from 200 to 1000 nm in a J&M Tidas II spectrophotometer, and data were collected and analyzed with Spectralys software. In the case of early data (e.g. for strain SBK18), samples were scanned from 350 to 1000 nm using a Hitachi U-2000 spectrophotometer, data were collected using SpectraCalc software, and spectra were analyzed with the Grams 386 software package (Galactic Industries Corporation). Because pigments do not absorb light of 650 nm, the spectra were normalized by multiplication to yield a light scattering A_{650} of 1.0. In the case of the pTB999/pTL2 strains, 200 μg of protein were used, spectra were not normalized, and a baseline was drawn from 700 nm to 930 nm.

Low temperature absorption spectroscopy of chromatophores used a Hitachi 557 double beam spectrophotometer. Chromatophores in chromatophore buffer (see Section 2.12) were mixed with an equal volume of anhydrous glycerol and frozen in liquid nitrogen. Spectra were obtained with the samples chilled by, but not immersed in, liquid nitrogen. Flash spectroscopy was carried out as previously described (87). Samples were normalized for BChl absorbance to A_{858} = 2.0. Photobleaching of the RC was measured at 605 nm in the presence of ascorbate, antimycin to eliminate cyt *b*/*c*1 activity (154), and valinomycin to prevent the formation of a proton gradient.

Carotenoid bandshifts were measured as the change in A_{510} - A_{540} difference for semiaerobically grown cultures (A_{540}-A_{510} in Figures 3.3.10 and 3.3.11 only), and A_{490} - A_{475} for phototrophically grown cultures, in the presence of ascorbate, with and without antimycin.

2.15. Kinetic analysis of assembly and decay of the reaction centre and light harvesting complex 1

To evaluate the effects of deletion of *puhB*, *puhC*, or *puhE* upon assembly and decay of the RC and LH1, samples of intact cells capable of assembling only one protein complex were scanned in the spectrophotometer as they adapted from aerobic to semiaerobic growth, and then after transfer to aerobic growth.

Triplicate seed cultures of 50 ml RCV medium in 250 ml flasks were inoculated with strains of the MA01, MA02, MA03, MA04, and U43 series from fresh YPS agar plates containing tetracycline to select for plasmids p*Stu* I, pTPR9, pTPR8, and pMA10. After about 28 hours of high-aeration growth at 300 rpm in a 30°C room, the fifteen well-grown cultures (> 150 Klett units) were diluted to a density of approximately 15 Klett units in 450 ml of RCV medium and grown in 2 L flasks with high aeration for 8 hours until a density of approximately 60 Klett units was reached. These starter cultures were diluted into a final volume of 1650 ml RCV medium in 2 L flasks and grown with low aeration at 150 rpm.

Samples of 20 ml were collected immediately and samples of 10 ml were collected at intervals of 1.5 hours thereafter to monitor assembly over 19.5 hours. The culture density of each sample was determined with the Klett-Summerson photometer.

After 9 and 15 hours of semiaerobic growth, 35 ml of each culture were transferred to sterile 250 ml flasks and grown with high aeration at 30°C. Three samples of 10 ml were collected from each of these cultures at intervals of 1.5 hours to monitor decay.

Cells from each sample were pelleted, resuspended in 250 μl of RCV medium, and mixed with 500 μl of 30% BSA containing 0.85% sodium chloride and 0.1% sodium azide. Intact cell absorption spectra were collected on 600 μl of each sample. The spectra were normalized to A_{650} = 1.0. For observations of LH1, a baseline was drawn from the absorbance value at 700 nm to that at 820 nm to that at 930 nm; for the RC, the baseline was drawn from the absorbance value at 700 nm to that at 830 nm to that at 930 nm. The absorbance values along the baseline were considered background due to light scattering and were subtracted from the values of the normalized spectrum

(measured at 1 nm intervals) before measurement of peak heights and areas. The area of the LH1 peak was determined from 820 nm to 920 nm, and the mean area for each set of triplicate cultures was plotted as a measure of LH1 production, with the standard deviation as a measure of error. The area of the RC voyeur BChl peak was determined from 780 nm to 830 nm, and the area of about half the peak, from 800 nm to 830 nm, was also determined to eliminate the contributions of the BPhe peak of the RC and unbound BChl. The absorption values at 760 nm and at 800 nm were taken as measures of BPhe and voyeur BChl, respectively, to assess overall RC "structural order" - the proper assembly of pigment cofactors into stable folds of the RC polypeptides, resulting in distinct peaks at characteristic wavelengths. Negative and zero absorption values were adjusted to 0.001 to allow determination of the A_{800}/A_{760} ratio. For each set of triplicate cultures, the mean 800-to-830-nm area was plotted as a measure of RC production, and both the A_{800}/A_{760} ratio as well as the ratio of 800-to-830-nm area to 780-to-830-nm area were plotted as measures of RC structural order, with the standard deviation as a measure of error.

Kinetic analysis of unbound BChl production in the absence of the RC and LH1 differed from the above method in that only the MA01 and MA04 backgrounds were used, the plasmids pMA20 and pRR5C were selected with gentamicin in the plates, and pXCA6::935 was selected with tetracycline. The experiment was stopped after 13.5 hours and decay was not studied. The spectra were normalized to $A_{650} = 1.0$. The baseline was drawn from 700 nm to 830 nm, absorbance values along the baseline were subtracted, and the unbound BChl peak area was determined from 740 nm to 815 nm.

For each culture, a second-order polynomial approximation of production was made over the first 10.5 hr for LH1, over the first 7.5 hours for the RC in the presence of either PufA or PufB, and over the first 9 hours for the RC alone. A second-order polynomial approximation of exponential decay was made for each culture using the natural logarithm of the area from 800 nm to 830 nm over 4.5 hours after mid-assembly and post-assembly induction of decay (initiated after 9 and 15 hours, respectively, of semiaerobic growth). Tangent line slopes were computed by taking the first derivative at the following times after induction: 4.5 hours for production of LH1 and of the RC alone; 6 hours for production of the RC in the presence of either PufA or PufB; and 0 hours

for production of unbound BChl and for decay of LH1, the RC, and unbound BChl. The mean production rates and decay rate constants were tabulated with their standard deviations.

The kinetic analysis experiments were performed many times to optimize the methods and to find suitable measures of assembly and decay. Results were similar to those presented here. For convenience and due to graphical constraints, early data points with high noise or subzero values have been omitted from some of the graphs.

2.16. Alignments, phylogenetic trees, and hydropathy plots

Searches for predicted protein sequences with significant similarity to PuhB, PuhC, PuhD, PuhE, and PufQ were carried out by BLAST of translated nucleotide sequences in the GenBank database at www.ncbi.nih.gov and of microbial genomes published by the Joint Genome Institute at www.jgi.doe.gov. PufX sequences were copied from Tsukatani *et al.* (153).

Alignments were done manually. Phylogenetic trees with the protein sequences were constructed with ClustalW software (http://www.es.embnet.org), using 1000 bootstraps. Hydropathy plots were done with DNA Strider software (91), using the Kyte-Doolittle algorithm (78).

3. RESULTS

3.1. Observations on the structure of the photosynthetic apparatus

3.1.1. Effects of *pufB* and *pufA* deletions upon RC assembly

In this first subchapter of results, I will briefly present my observations on the genes and protein complexes of the photosynthetic apparatus in strains that bear no mutations of the *puh* operon. To elucidate the process by which each of the *puh* gene deletions resulted in low levels of the RC-LH1 core complex and poor phototrophic growth, I decided to delete the *puf* operon and restore portions of it on a series of plasmids, resulting in strains that expressed (1) only LH1 in the absence of the RC and LH2 and (2) only the RC in the absence of all light-harvesting antenna complexes. My purpose was to study the effects of Puh proteins on the RC in the absence of LH1, and *vice versa*. In these control experiments, I discovered that deletions of the LH1 polypeptide genes *pufB* and *pufA* had significant effects of their own on the absorption spectrum of the RC, on the transcription of RC proteins, and on phototrophic growth.

Earlier observations on such *puf* deletion-restoration strains by Klug and Cohen (74) indicated that the level of LH1 in *R. capsulatus* is reduced due to deletion of two RC polypeptide genes, *pufL* and *pufM*, and the putative ribosome-binding site of the *pufX* gene from the *puf* operon on plasmid p*Stu* I (see Figure 2.1); however, the remaining LH1 is sufficient to evaluate the pleiotropic effects of other gene deletions on the LH1 absorption spectrum. Similarly, single deletions of the LH1 polypeptide genes, *pufB* and *pufA*, from the *puf* operon on plasmids pTPR9 and pTPR8, respectively (see Figure 2.1), were reported by Richter and Drews not to abolish the characteristic RC absorption peaks of a *puf* deletion-restoration strain but only to reduce their amplitudes (128). However, during the course of my work with these plasmids, I consistently observed that my LH2$^-$ *pufQBALM* deletion strain MA01, complemented with a *pufQALMX* operon on plasmid pTPR9, produced an absorption spectrum that began to resemble the RC spectrum only after many hours of semiaerobic growth (Figure 3.1.1), whereas complementation with a *pufQBLMX* operon on plasmid

pTPR8 resulted in smaller and less distinct peaks, and a *pufQLMX* operon on plasmid pMA10 resulted in a very small and poorly differentiated RC spectrum. I also observed significant absorption at 780 nm, an unusual observation that may indicate the presence of unbound BChl.

My original plan was to study the direct effects of *puh* gene deletions on assembly and decay of the RC in the total absence of LH1 polypeptide genes, using MA01(pMA10) as the control strain. Due to the aberrant RC spectrum of MA01(pMA10), however, I chose to study the RC also in the presence of either PufA or PufB, with MA01(pTPR9) and MA01(pTPR8) as controls. Thus, any effect of a *puh* gene deletion on the RC that I could observe in the absence of either LH1 polypeptide might be considered a direct effect on the RC. These observations are presented in the next three subchapters of Results, which deal with PuhB, PuhC, and PuhE, respectively. Serendipitously, my threefold investigation allowed me to identify an LH1 polypeptide-specific difference in RC assembly when partial *puf* operons were restored to my *pufQBALM* deletion strain MA01 and the *pufQBALMX* deletion strain U43 (171), as described in the fifth subchapter.

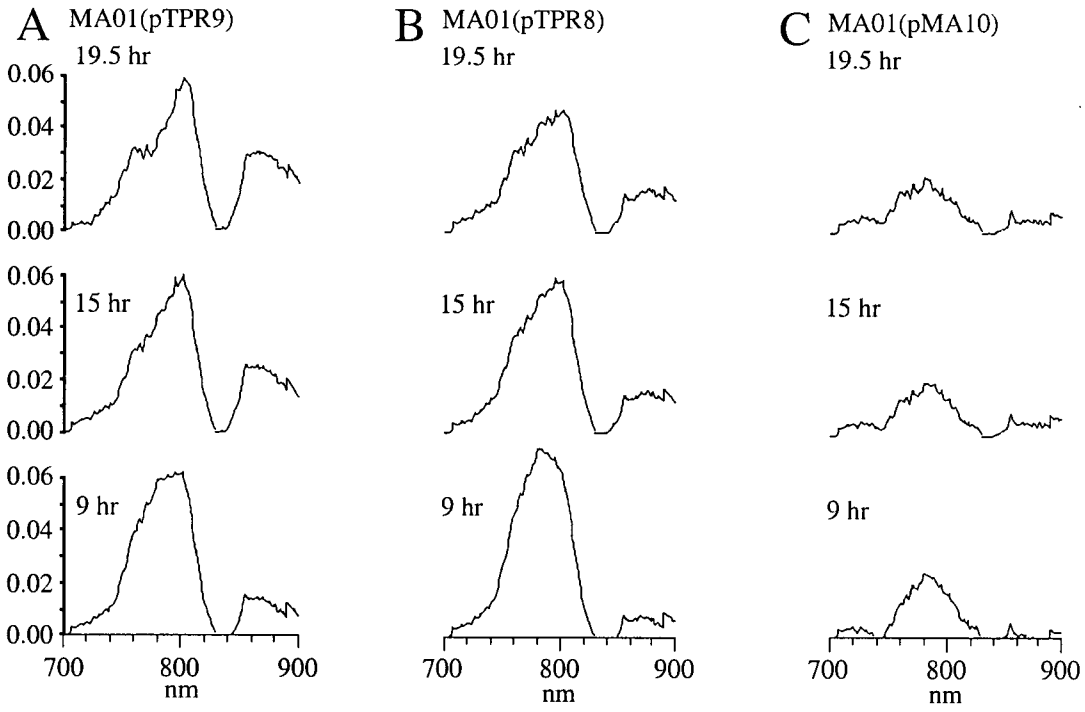

Figure 3.1.1. Absorption spectra (room temperature, pathlength 1 cm) of the nascent RC in the MA01 background, in the absence of the LH1 polypeptides PufB - plasmid pTPR9 (**A**), PufA - plasmid pTPR8 (**B**), or both - plasmid pMA10 (**C**), after 9 hours, 15 hours, and 19.5 hours of semiaerobic growth. Spectra were normalized and a baseline was drawn as described in Section 2.15. The RC absorbs at 760 nm, 800 nm, and 865 nm. Additional absorption at 780 nm is attributed to unbound BChl.

3.1.2. Effects of *pufB* and *pufA* deletions upon *puf* transcript levels

The aberrant absorption spectra of the *puf* deletion-restoration strains MA01(pTPR8) and MA01(pMA10), which lack PufA and both PufB and PufA, respectively, suggested that the PufA and PufB proteins have distinct roles in RC assembly, PufA being somewhat more important perhaps because it forms the inner side of the LH1 structure around the RC. However, it was conceivable that deletion of either *pufB* or *pufA* might affect the level of the *pufLMX* mRNA segment encoding the RC as well as PufX. (The *puf* operon produces a *pufBALMX* message encoding all five RC-LH1 proteins.) Therefore, I evaluated the levels of *puf* mRNA in MA01(pTB999), a strain with an intact *puf* operon on a plasmid, and the three strains with deletions of either *pufB* or *pufA* or both: MA01(pTPR9), MA01(pTPR8), and MA01(pMA10), respectively.

An RNA blot showed that the amount of *pufALMX* mRNA in strain MA01(pTPR9) was slightly more than that of *pufBALMX* mRNA in MA01(pTB999), whereas the amount of *pufBLMX* mRNA in MA01(pTPR8) was slightly less (Figure 3.1.2). The amount of *pufLMX* mRNA in MA01(pMA10) was significantly less, indicating that the combination of the *pufB* and *pufA* deletions greatly reduced either synthesis of *pufLMX* or the stability of this transcript.

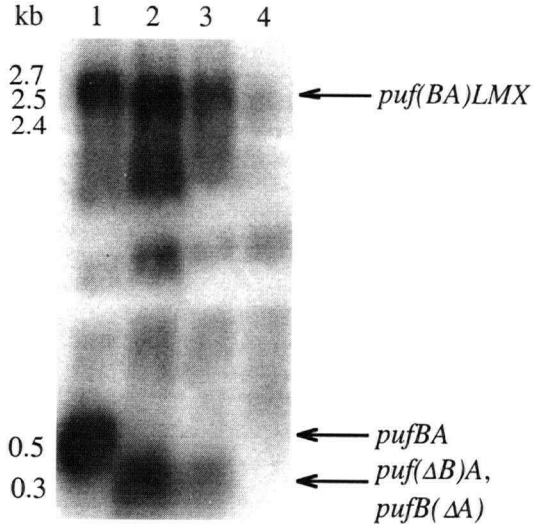

Figure 3.1.2. RNA blot showing effects of *pufB* and *pufA* deletions on the levels of *pufLM* transcripts. The lanes represent RNA isolated from (1) MA01(pTB999), (2) MA01(pTPR9), (3) MA01(pTPR8), and (4) MA01(pMA10). The probe was an *Apa* I fragment extending from the middle of *pufQ* to the 3' region of *pufX*

This RNA blot is evidence that the reduced RC peak amplitudes of strain MA01(pMA10) were due to reduced amounts of RC mRNA. However, the fact that the BPhe peak at 760 nm and the voyeur BChl peak at 800 nm did not become distinct from unbound BChl absorbing at 780 nm in MA01(pTPR8) as well as MA01(pMA10) (see Figure 3.1.1) suggested that RC assembly was also less efficient in the absence of PufA and even less efficient without both LH1 polypeptides.

3.1.3. Phototrophic growth of RC-only, RC-LH1 and RC-LH2 strains

To determine whether the RC was functional in the strains with aberrant RC absorption spectra, I examined the phototrophic growth properties of MA01 and similar strains in which whole and partial *puf* operons were restored on plasmids pTB999, pTPR9, pTPR8, and pMA10. Along with my *puh* gene deletion strains, I included U43, in which the entire chromosomal *pufQBALMX* operon was deleted, and MA15, an $LH2^+$ strain isogenic to MA01.

R. capsulatus strains MA01(pMA10) and U43(pMA10), which lacked LH2 and both polypeptides of LH1, were capable of phototrophic growth (Figure 3.1.3, Table 3.1.1), as were MA01(pTPR9) and U43(pTPR9), expressing the RC together with PufA, and MA01(pTPR8) and U43(pTPR8), expressing the RC with PufB. The strains of the MA01 series, which are *pufX* merodiploid, occasionally grew more slowly than their U43 counterparts, which carry *pufX* only on a plasmid; for example, MA01(pMA10) compared to U43(pMA10) in this experiment.

When the growth of MA01(pTB999) and U43(pTB999), in which the entire *puf* operon is restored, was compared to that of their $RC^+LH1^+LH2^-$ parent MW442, both grew a little more slowly (Figure 3.1.3, Table 3.1.1), which may be because the *puf* genes on the plasmid are no longer part of the superoperon that has evolved on the chromosome (11, 162, 163).

Earlier studies concluded that *R. capsulatus* is unable to grow with LH2 as the sole antenna complex (64, 66, 120). To examine this hypothesis, I compared the growth of four strains, all of which were *pufX* merodiploid: the $RC^+LH1^+LH2^-$ strain MA01(pTB999) and the $RC^+LH1^-LH2^+$ strains MA15(pTPR9), MA15(pTPR8), and MA15(pMA10). MA15(pTPR9) grew as well as MA01(pTB999) (Figure 3.1.3, Table 3.1.1), suggesting that LH2 is an effective antenna.

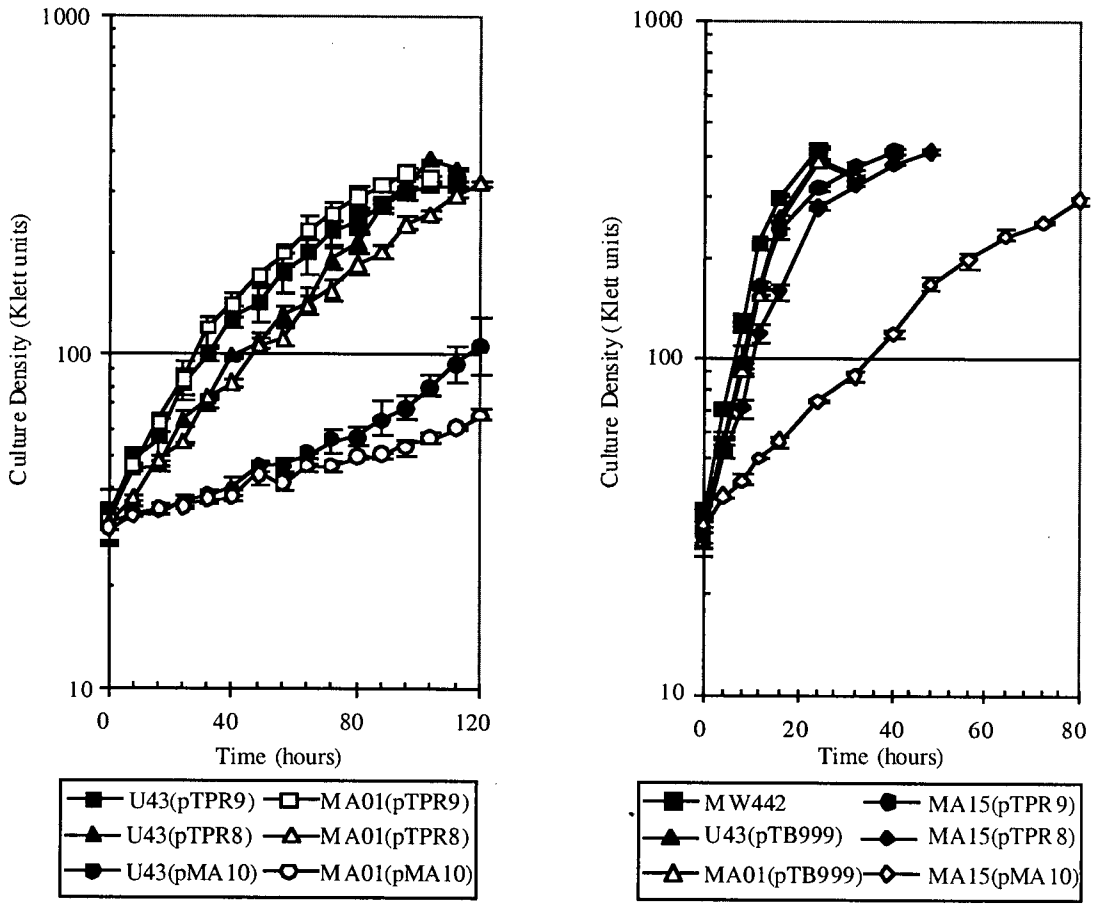

Figure 3.1.3. Phototrophic growth of *R. capsulatus* containing either the RC only (left) or the RC plus either LH1 or LH2 (right) as the photosynthetic apparatus. The genotypes and phenotypes are listed in Table 3.1.1.

Table 3.1.1. Phototrophic growth of *R. capsulatus* with RC-LH1, with RC-LH2, and with the RC alone.

Strain and antenna phenotype	Genotype chromosome (plasmid)	Relative specific growth rate ± standard deviation of 3 cultures
MW442 $LH1^+LH2^-$	*pucC⁻pufQBALMX⁺*	100% ± 2%
U43(pTB999) $LH1^+LH2^-$	*pucC⁻pufQBALMX⁻(pufQBALMX)*	86% ± 5%
MA01(pTB999) $LH1^+LH2^-$	*pucC⁻pufQBALM⁻X⁺(pufQBALMX)*	88% ± 3%
MA15(pTPR9) $LH1^-LH2^+$	*pucC⁺pufQBALM⁻X⁺(pufQALMX)*	87% ± 2%
MA15(pTPR8) $LH1^-LH2^+$	*pucC⁺pufQBALM⁻X⁺(pufQBLMX)*	68% ± 5%
MA15(pMA10) $LH1^-LH2^+$	*pucC⁺pufQBALM⁻X⁺(pufQLMX)*	20% ± 1%
U43(pTPR9) $LH1^-LH2^-$	*pucC⁻pufQBALMX⁻(pufQALMX)*	22% ± 3%
U43(pTPR8) $LH1^-LH2^-$	*pucC⁻pufQBALMX⁻(pufQBLMX)*	15% ± 0%
U43(pMA10) $LH1^-LH2^-$	*pucC⁻pufQBALMX⁻(pufQLMX)*	6% ± 1%
MA01(pTPR9) $LH1^-LH2^-$	*pucC⁻pufQBALM⁻X⁺(pufQALMX)*	27% ± 4%
MA01(pTPR8) $LH1^-LH2^-$	*pucC⁻pufQBALM⁻X⁺(pufQBLMX)*	14% ± 1%
MA01(pMA10) $LH1^-LH2^-$	*pucC⁻pufQBALM⁻X⁺(pufQLMX)*	4% ± 0%

Transcripts of the RC genes *pufLMX* were abundant from plasmids pTB999 and pTPR9 (see Figure 3.1.2), and RC assembly could proceed with either PufB and PufA from pTB999 or only PufA from pTPR9 (see Figure 3.1.1). Therefore, the major difference between MA15(pTPR9) and MA01(pTB999) was that the former had LH2 and the latter had LH1. Their similar growth suggested that abundant LH2 may be as good an antenna as a more modest amount of LH1. MA15(pTPR8), which had only PufB, grew more slowly, and MA15(pMA10), in which neither LH1 polypeptide was available to support RC assembly, grew even more slowly (Figure 3.1.3, Table 3.1.1). However, MA15(pMA10) grew better than any $RC^{+}LH1^{-}LH2^{-}$ strain, which probably means that LH2 was transferring energy directly to the RC as in *R. sphaeroides* (57).

Having established that *pufBA* gene deletions affect the RC in ways that were not anticipated, I will outline how I organized my observations of the further effects of four other mutations on the RC and LH1. These mutations are: deletions of *puhB*, *puhC*, and *puhE*, and *pufX* merodiploidy.

The next three subchapters of results have a parallel structure. In the first section of each, I describe the phototrophic growth defect associated with a particular *puh* gene deletion, and how it may be mitigated or exacerbated. Examples of factors that affect the growth defects are: (1) deletion or attenuated expression of a 3' *puh* gene (i.e., *puhE*); (2) complementation with native *puh* genes, 6xHis-tagged constructs, and homologous genes from other species; (3) *pufQ* merodiploidy and co-transcription of a *puh* gene with *pufQ*; and (4) the duration of semiaerobic growth prior to phototrophic growth.

In the second section of each subchapter, I explore the basis of the growth defects, using SDSPAGE and flash spectroscopy to compare the amounts of RC and LH1 polypeptides and functional RC-LH1 complexes. Again, I investigate how the RC-LH1 deficiencies may be mitigated and exacerbated. In the third sections, I use a β-galactosidase gene fusion reporter to establish that each deletion results in an RC-LH1 deficiency without reduced transcription and translation of RC-LH1 genes.

In the fourth sections, I evaluate the effect of each deletion on RC assembly and decay by measuring the sizes and ratios of characteristic peaks in the absorption spectra of nascent RCs. Similar studies of LH1 assembly and decay are presented in the fifth sections.

The fifth subchapter, concerning PufX, opens with a section in which I study the effect of *pufX* merodiploidy on the assembly and decay of the RC, followed by a similar investigation of assembly and decay of LH1 in the second section.

Each of the following four subchapters concludes with one or two unique sections. At the end of the subchapter on PuhB, I present analyses of interactions of the predicted TM segments and cytoplasmic and periplasmic regions of PuhB in the TOXCAT and CyaA systems. The final two sections of the subchapter on PuhC include immunoblots that detected the subcellular location of PuhC, evaluations of the importance of the PuhC TM segment, and an attempt to purify 6xHis-tagged PuhC from *R. capsulatus*. The subchapter on PuhE ends with a study of the effects of PuhE and PufQ on the production of unbound BChl. In the penultimate section of the subchapter on PufX, I use immunoblots to evaluate the levels of PufX in strains with a *pufX* gene separated from the remaining *puf* genes, and in *pufX* merodiploid, *puhC*$^-$, and *puhB*$^-$ strains. I show that the two *pufX* genes have distinct effects on the RC-LH1 absorption spectrum, and on phototrophic growth in the absence of PuhC. I conclude with a TOXCAT analysis of the PufX TM segment.

In the sixth and final subchapter, I present alignments, phylogenetic trees, and hydropathy plots of predicted PuhB, PuhC, PuhE, PufQ, and PufX sequences.

3.2. Characterization of PuhB as an RC assembly factor

3.2.1. The growth defect of the *puhB* deletion strain MA05; complementation and the effect of *pufQ* in *cis*

Phototrophic growth of the *puhB* deletion strain MA05 began with a lag of at least 12 hours, and thereafter was slower than the growth of the wild type strain SB1003 (Figure 3.2.1, Table 3.2.1). The lag cannot be attributed to a secondary mutation because when semiaerobically grown MA05 cells were plated on RCV agar containing kanamycin, the number of colonies that appeared within three days was the same (106% ± 18%) under anaerobic phototrophic incubation conditions as under aerobic dark conditions. Therefore, the PuhB protein is not essential for phototrophic growth, refuting the conclusion of an earlier report on the $LH2^-$ *puhB* deletion strain DW23, which also grew after a lag (167). Rather, the deletion mutant phenotype is a delayed transition from semiaerobic respiratory growth to anaerobic phototrophic growth.

Restoration of the *puhB* gene in *trans* on plasmid pMA22 eliminated the phototrophic growth lag phase of the *puhB* deletion strains MA05 ($LH2^+$) and DW23 ($LH2^-$) and resulted in growth rates only slightly less than those of the parental strains SB1003 and MW442, respectively (Table 3.2.1). Introduction of an extra copy of *puhB* into SB1003 via pMA22 did not affect phototrophic growth.

Plasmid pMA18, which carries *puhB* with a C-terminal 6xHis tag (*puhB-C*), restored growth of MA05 to that of the parental strain SB1003 (Figure 3.2.1, Table 3.2.2), as did pMA8, in which *puhB-C* is preceded by an extra copy of *pufQ* (not shown). However, plasmid pMA17, carrying *puhB* with an N-terminal 6xHis tag (*puhB-N*), only minimized the lag phase and barely improved growth (Figure 3.2.1, Tables 3.2.2 and 3.2.3). Serendipitously, introduction of a *pufQ-puhB-N* transcriptional fusion on plasmid pMA7 was found to improve the growth of MA05 to a rate slightly lower than that of SB1003, with no lag phase (Figure 3.2.1, Table 3.2.3). An extra copy of *pufQ* did not improve growth of MA05 when introduced on pRR5C (not shown), or significantly improve growth of MA05(pMA17) when introduced on pXCA6::935 (Figure 3.2.1, Table 3.2.3).

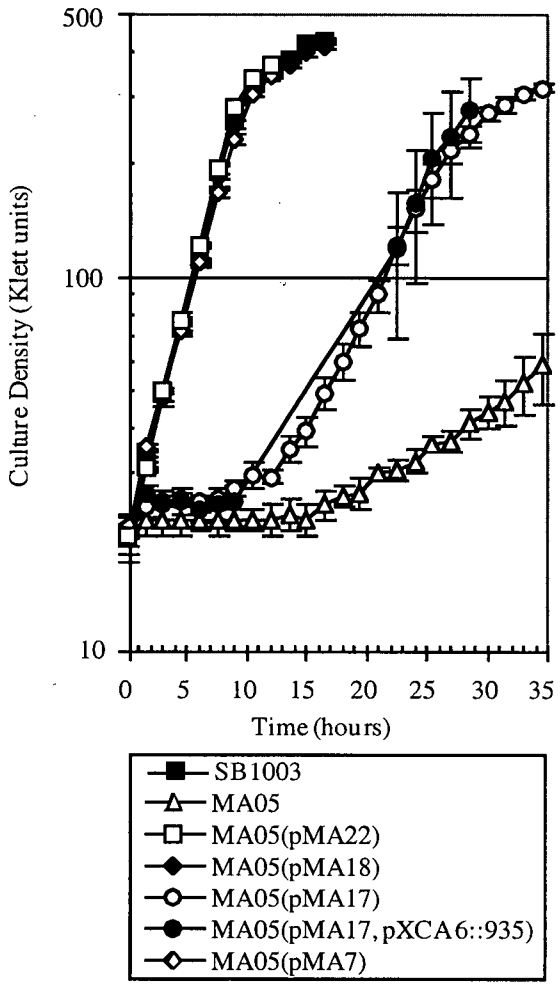

Figure 3.2.1. Phototrophic growth of the *puhB*⁻ strain MA05 *trans*-complemented with native and 6xHis-tagged PuhB proteins, compared to its *puhB*⁺ parent SB1003. The data in this figure were compiled from three experiments; reproducible growth patterns were observed for the controls. Both native *puhB* (pMA22) and the C-terminally 6xHis-tagged gene *puhB-C* (pMA18) complemented the deletion perfectly, whereas the N-terminally 6xHis-tagged gene *puhB-N* (pMA17) had a minimal effect. Although an extra copy of *pufQ* in *trans* (pXCA6::935) did not co-operate with *puhB-N*, co-transcription of *pufQ* and *puhB-N* (pMA7) eliminated the lag phase of MA05 and allowed growth at a rate slightly lower than that of the parental strain SB1003.

It is possible that the unnatural co-transcription of *pufQ* and *puhB* from pMA7 results in a productive co-operation of PufQ and PuhB-N.

Strain MA12, in which both *puhB* and *puhE* have been deleted, grew phototrophically as poorly as the *puhB* deletion strain MA05 (not shown). The *puhE*⁻ derivatives of the LH2⁻ *puhB*⁻ strain DW23, namely MA09 and MA11, resembled DW23 (not shown). There was no consistent difference in growth rate or in the length of the lag phase between *puhB*⁻*E*⁺ and *puhB*⁻*E*⁻ strains.

Table 3.2.1. *Trans*-complementation of the phototrophic growth defect due to the *puhB* deletion. SB1003 and MW442 are parental strains, MA05 and DW23 are *puhB*$^-$ strains, and plasmid pMA22 carries *puhB*.

LH2$^+$ strains	Genotype chromosome (plasmid)	Relative specific growth rate ± standard deviation of 3 cultures
SB1003	*pucC*$^+$*puhB*$^+$	100% ± 1%
SB1003(pMA22)	*pucC*$^+$*puhB*$^+$(*puhB*)	95% ± 2%
MA05	*pucC*$^+$*puhB*$^-$	48% ± 17%
MA05(pMA22)	*pucC*$^+$*puhB*$^-$(*puhB*)	92% ± 3%
LH2$^-$ strains		
MW442	*pucC*$^-$*puhB*$^+$	100% ± 3%
DW23	*pucC*$^-$*puhB*$^-$	57% ± 13%
DW23(pMA22)	*pucC*$^-$*puhB*$^-$(*puhB*)	85% ± 2%

Table 3.2.2. *Trans*-complementation of the *puhB* deletion strains' phototrophic growth defect by 6xHis-tagged *puhB* constructs: *puhB-N* (pMA17) and *puhB-C* (pMA18). pMA20 is the empty vector.

LH2$^+$ strains	Genotype chromosome (plasmid)	Relative specific growth rate ± standard deviation of 3 cultures
SB1003	*pucC*$^+$*puhB*$^+$	100% ± 7%
MA05	*pucC*$^+$*puhB*$^-$	45% ± 7%
MA05(pMA20)	*pucC*$^+$*puhB*$^-$(empty)	34% ± 4%
MA05(pMA17)	*pucC*$^+$*puhB*$^-$(*puhB-N*)	59% ± 3%
MA05(pMA18)	*pucC*$^+$*puhB*$^-$(*puhB-C*)	88% ± 11%
LH2$^-$ strains		
MW442	*pucC*$^-$*puhB*$^+$	100% ± 6%
DW23	*pucC*$^-$*puhB*$^-$	47% ± 10%
DW23(pMA17)	*pucC*$^-$*puhB*$^-$(*puhB-N*)	57% ± 9%
DW23(pMA18)	*pucC*$^-$*puhB*$^-$(*puhB-C*)	98% ± 8%

Table 3.2.3. Effect of co-transcription with *pufQ* (pMA7) upon *trans*-complementation of a *puhB* deletion with PuhB with an N-terminal 6xHis tag (pMA17). pXCA6::935 expresses *pufQ*; pXCA601 is the empty vector.

Strain	Genotype chromosome (plasmid)	Relative specific growth rate ± standard deviation of 3 cultures
SB1003	*pufQ*$^+$*pucC*$^+$*puhB*$^+$	100% ± 3%
MA05	*pufQ*$^+$*pucC*$^+$*puhB*$^-$	43% ± 6%
MA05(pMA17)	*pufQ*$^+$*pucC*$^+$*puhB*$^-$(*puhB-N*)	53% ± 12%
MA05(pMA17, pXCA601)	*pufQ*$^+$*pucC*$^+$*puhB*$^-$(*puhB-N*, empty)	51% ± 8%
MA05(pMA17, pXCA6::935)	*pufQ*$^+$*pucC*$^+$*puhB*$^-$(*puhB-N*, *pufQ*)	68% ± 5%
MA05(pMA7)	*pufQ*$^+$*pucC*$^+$*puhB*$^-$(*pufQpuhB-N*)	84% ± 2%

3.2.2. The RC-LH1 deficiency of the *puhB* deletion strain MA05

SDSPAGE of chromatophores from MA05 revealed that the amounts of all the RC and LH1 polypeptides per total protein were reduced due to the *puhB* deletion (Figure 3.2.2). The LH1 deficiency was confirmed by low temperature absorption spectroscopy (Figure 3.2.3), and the RC deficiency was confirmed by measurements of RC photobleaching with a train of eight flashes of light (Figure 3.2.4, Table 3.2.4). The carotenoid bandshift (explained in Section 2.14), was observed after a single flash of light. In MA05, as in the *puhB*$^+$ parent SB1003, it consisted of a rapid initial shift, attributed to the reduction of quinones in the RC, followed by a more gradual further shift due to the generation of a sustained proton gradient coupled to oxidation of quinols by cyt *b*/*c*1, indicating that these reactions are not abolished by deletion of *puhB* (Figure 3.2.5). However, the much smaller carotenoid bandshift demonstrated that MA05 forms a lesser proton gradient, consistent with a lower RC content than SB1003 (Table 3.2.4). The carotenoid bandshift of MA05 accumulated over successive flashes, indicating that the RC is properly connected to cyt *b*/*c*1 (Figure 3.2.6). This is surprising because the PufX protein, which is known to be important for this connection, was hardly detectable in intact cells of MA05 (see Section 3.5.3).

The *puhB*$^-$*E*$^-$ strain MA12 had a phenotype similar to that of MA05, with a lesser LH1 deficiency under phototrophic conditions (Figures 3.2.2 to 3.2.6, Table 3.2.4).

Although an earlier study reported that the LH2$^-$ *puhB* deletion strain DW23 was almost totally deficient in LH1 (167), the deficiency of DW23 was never so severe in my SDSPAGE (not shown) and absorption spectroscopy experiments (Figure 3.2.7).

Table 3.2.4. Flash spectroscopic measurements (room temperature, pathlength 1 cm) of the effect of *puhB* (MA05) and *puhBE* (MA12) deletions on RC content and function in isolated chromatophores. Data collected by R. C. Prince.

Chromatophore sample	Amount of RC (RC photobleaching, relative to SB1003)	Proton gradient (single-flash carotenoid bandshift, relative to SB1003)
MA05 semiaerobic	12%	21%
MA12 semiaerobic	10%	14%
MA05 phototrophic	25%	33%
MA12 phototrophic	17%	30%

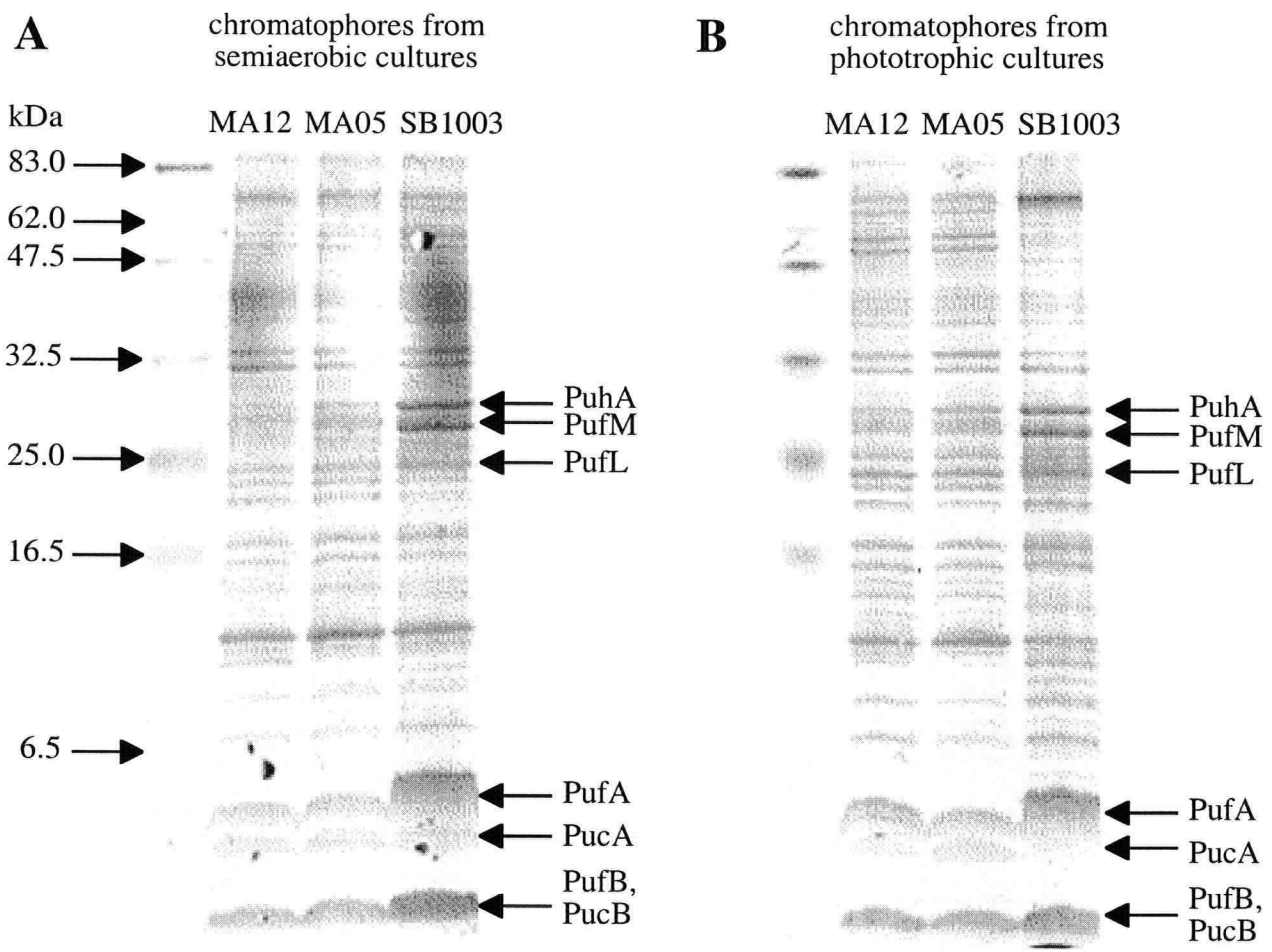

Figure 3.2.2. SDSPAGE of 50 μg of chromatophore protein from the *puhB*$^{+}$*E*$^{+}$ strain SB1003, the *puhB*$^{-}$*E*$^{+}$ strain MA05, and the *puhB*$^{-}$*E*$^{-}$ strain MA12. Under both semiaerobic conditions (**A**) and phototrophic conditions (**B**), all three RC polypeptides (PuhA, PufM, PufL) and both LH1 polypeptides (PufA, PufB) were much less abundant in MA05 and MA12; the amounts of LH2 polypeptides (PucA, PucB) were unaffected. Under phototrophic conditions, MA12 had more LH1 than MA05.

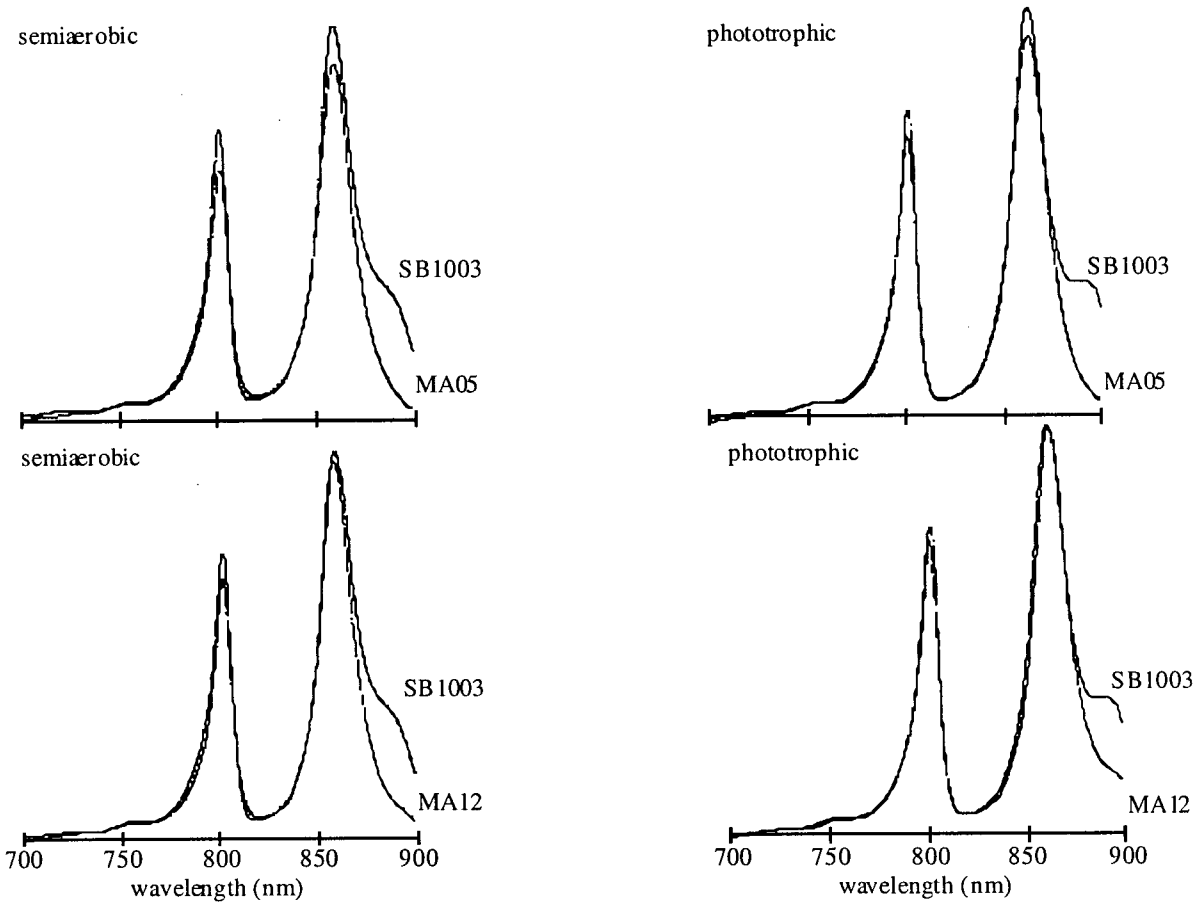

Figure 3.2.3. Low-temperature absorption spectra (77 K, pathlength 1 cm) of chromatophores from strains SB1003, MA05, and MA12. MA05 had little LH1 absorption at 880 nm; MA12, grown phototrophically, was less LH1-deficient than MA05. Data collected by R. C. Prince.

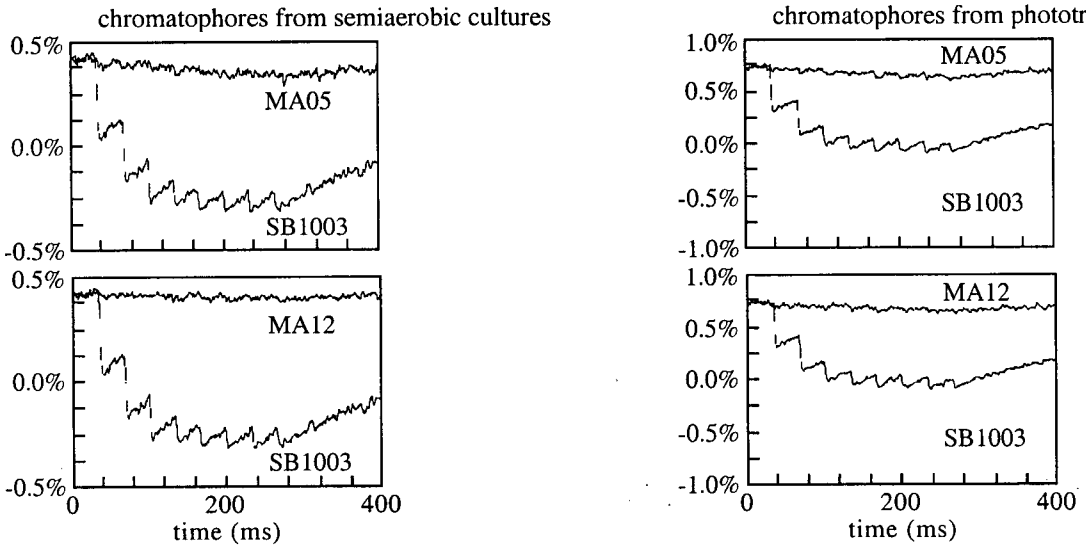

Figure 3.2.4. Photobleaching of the RC (room temperature, pathlength 1 cm) in chromatophores from SB1003, MA05, and MA12. The downward deflection with each flash indicates a decrease in absorption at 605 nm due to photooxidation of the RC special pair. Data collected by R. C. Prince.

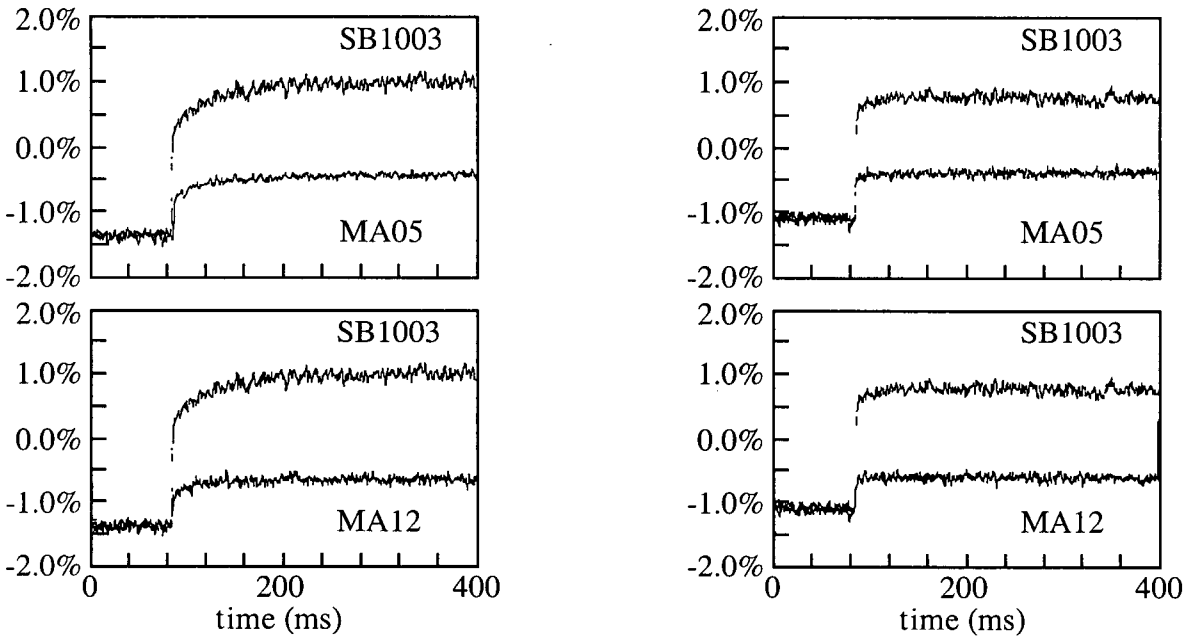

Figure 3.2.5. Single-flash carotenoid bandshifts (room temperature, pathlength 1 cm) in chromatophores from phototrophically grown SB1003, MA05, and MA12. A smaller bandshift was observed for MA05 and MA12, indicating that a smaller proton gradient was produced (left), and the production of this proton gradient was sensitive to antimycin (right). Data collected by R. C. Prince.

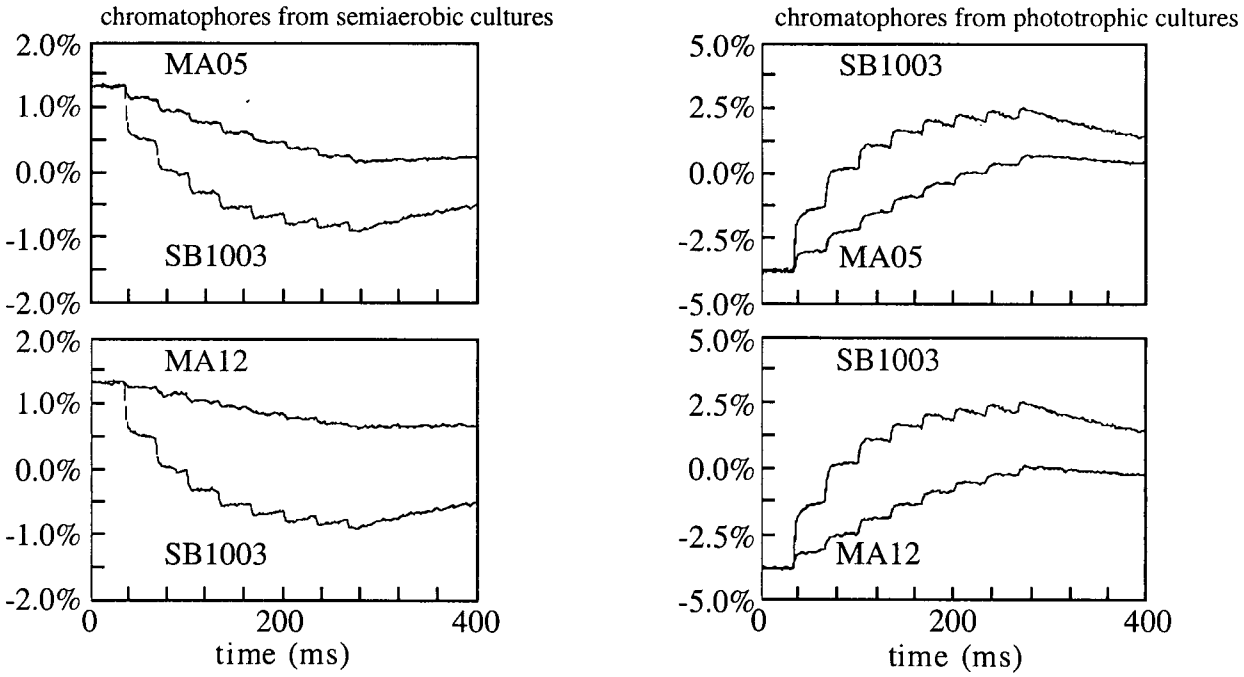

Figure 3.2.6. Eight-flash carotenoid bandshifts (room temperature, pathlength 1 cm) in chromatophores from SB1003, MA05, and MA12. The *puhB*⁻ and *puhB*⁻*E*⁻ mutations did not prevent the formation of a cumulative proton gradient, but reduced its magnitude. A shift to the red was observed for both semiaerobic conditions (decreased absorption at 510 nm vs. 540 nm) and phototrophic conditions (increased absorption at 490 nm vs. 475 nm). Data collected by R. C. Prince.

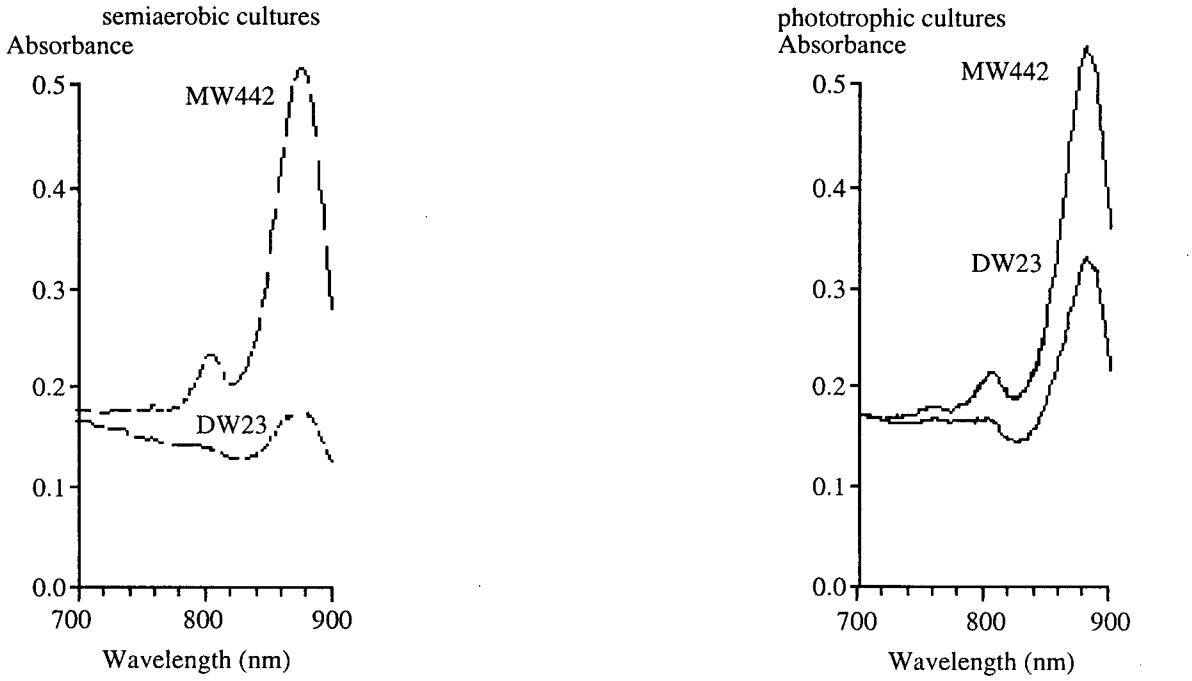

Figure 3.2.7. Absorption spectra (room temperature, pathlength 1 cm) of intact cells of the LH2⁻ strains MW442 (*puhB*⁺) and DW23 (*puhB*⁻).

3.2.3. RC-LH1 gene transcription and translation in the *puhB* deletion strain MA05

The cause of the RC-LH1 deficiency of the *puhB* deletion strain MA05 was studied initially by evaluating transcription of the *puf* operon, which encodes all of the RC-LH1 polypeptides except PuhA. The results of a β-galactosidase assay of MA05 and its *puhB*⁺ parent SB1003, in which a PufB::LacZ fusion protein was expressed from the *puf* promoter on plasmid pXCA6::935, indicate that transcription and translation of the *puf* genes are normal in the absence of PuhB (Table 3.2.5). Therefore, I assumed that the effects of a *puhB* deletion on the levels of the RC-LH1 core complex were due to impairment of a post-translational process such as assembly of either the RC or LH1.

Table 3.2.5. Similar β-galactosidase activity (nmol of *o*-nitrophenol per minute per 10^8 cells) was expressed from the *puf* promoter in *puhB*⁺ (SB1003) and *puhB*⁻ (MA05) backgrounds.

semiaerobic cultures	Mean activity ± standard deviation of 3 samples
SB1003(pXCA6::935)	5.0 ± 1.6
MA05(pXCA6::935)	5.0 ± 0.2
phototrophic cultures	
SB1003(pXCA6::935)	7.3 ± 0.9
MA05(pXCA6::935)	7.0 ± 1.0

3.2.4. Effect of PuhB on assembly of the RC

The kinetics of assembly and decay of the RC, in the absence of one or both LH1 polypeptides, PufB and PufA, were measured in *puhB*$^+$ (MA01) and *puhB*$^-$ (MA03) backgrounds, which contained a deletion of the chromosomal *pufQBALM* genes and were complemented with plasmids carrying partial *puf* operons with deletions of either *pufB* or *pufA*, or both. The absence of LH1 was necessary in order to evaluate the amplitudes of RC peaks in absorption spectra, which are normally obscured by the LH1 peak at 880 nm. For a typical spectrum of a pure RC, see Figure 1.2.

The *puhB*$^+$ and *puhB*$^-$ strains were at similar culture densities throughout the experiments (Figure 3.2.8) and should have progressed similarly into semiaerobic growth conditions. A comparison of their absorption spectra over time (Figure 3.2.9) showed better RC assembly in the *puhB*$^+$ strains MA01(pTPR9) (lacking PufB), MA01(pTPR8) (lacking PufA), and even MA01(pMA10) (lacking both LH1 polypeptides) than in the corresponding *puhB*$^-$ strains MA03(pTPR9), MA03(pTPR8), and MA03(pMA10). After 9 hours of semiaerobic growth, the spectra of all six strains were dominated by absorption at 780 nm, perhaps due to unbound BChl. After 15 hours, this absorption decreased and the RC voyeur BChl peaks at 800 nm began to appear distinct from the BPhe peaks at 760 nm in MA01(pTPR9) and MA01(pTPR8), but not in MA01(pMA10), which appeared not to assemble the RC well due to the absence of both PufB and PufA. In the MA03 strains, the RC peaks were smaller and the absorption at 780 nm was still relatively high. After 19.5 hours, the spectrum of MA01(pTPR9) had begun to resolve into the three peaks at 760 nm, 800 nm, and 865 nm characteristic of the RC. These features were less apparent in MA01(pTPR8) and were weakest in MA01(pMA10). Without PuhB, the BPhe and voyeur BChl peaks were smaller and less well-resolved in MA03(pTPR9) and MA03(pTPR8), whereas the spectrum of MA03(pMA10) indicated very little RC assembly.

Quantitative analysis showed that the *puhB* deletion reduced production of the RC, measured as the RC voyeur BChl peak area between 800 nm and 830 nm (Figure 3.2.10). The mean rates of production computed from these data (Table 3.2.6) also suggested that PuhB is an RC production factor; however, the standard deviations are large. As a measure of the "structural order" of the RC

(defined in Section 2.15), I calculated the height ratio of the voyeur BChl peak at 800 nm and the BPhe peak at 760 nm (Figure 3.2.11), as well as the ratio of RC voyeur BChl peak-specific area (800 nm to 830 nm) to the total RC voyeur BChl peak area, which was inflated by BPhe and unbound BChl absorption (780 nm to 830 nm) (Figure 3.2.12). By both measures, RC structural order was significantly reduced by the *puhB* deletion (unless RC structural order was already poor, as in MA01(pMA10), which lacked both LH1 polypeptides). Measurements of RC decay were not of sufficient quality to implicate or exclude the involvement of PuhB (Figure 3.2.13, Table 3.2.6).

RC production in these experiments was near the limit of detection, and the changes in absorbance over time were small and varied depending on which LH1 polypeptide was present. Nevertheless, it is apparent that the *puhB* deletion interferes with RC assembly, as is most clearly shown by the differences between MA01(pTPR9) and MA03(pTPR9), which are the PufA-containing *puhB*$^+$ and *puhB*$^-$ strains, respectively. The *puhB*$^-$ strains MA03(pTPR9), MA03(pTPR8), and MA03(pMA10), which lack both LH1 and LH2, grew phototrophically after lags of about two hundred hours, or not at all (not shown), indicating that the requirement of *R. capsulatus* for PuhB becomes more stringent in the absence of light-harvesting antenna complexes. This may be explained as the cumulative effect of the loss of three RC assembly factors: PuhB, PufA, and PufB.

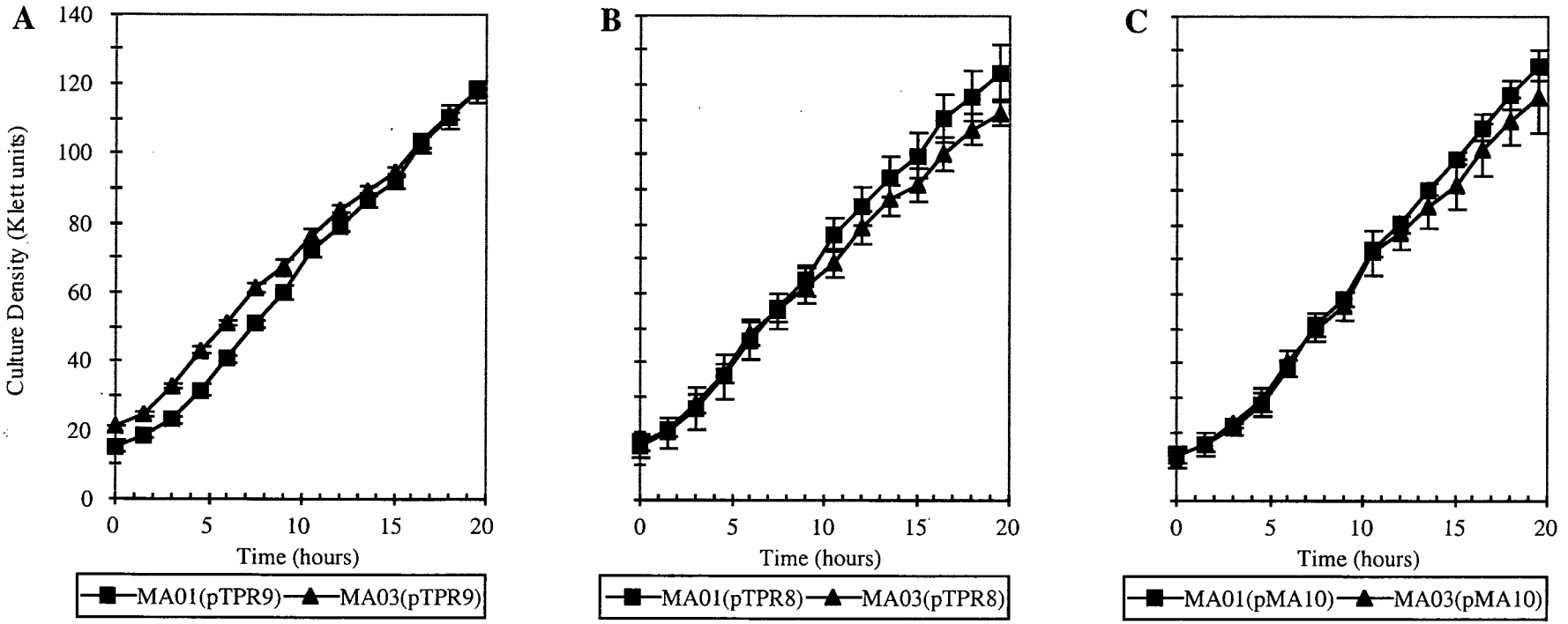

Figure 3.2.8. Semiaerobic growth of *puhB*$^+$ (MA01) and *puhB*$^-$ (MA03) strains expressing the RC (**A**) in the absence of PufB - plasmid pTPR9, (**B**) in the absence of PufA - plasmid pTPR8, and (**C**) in the absence of both LH1 polypeptides - plasmid pMA10.

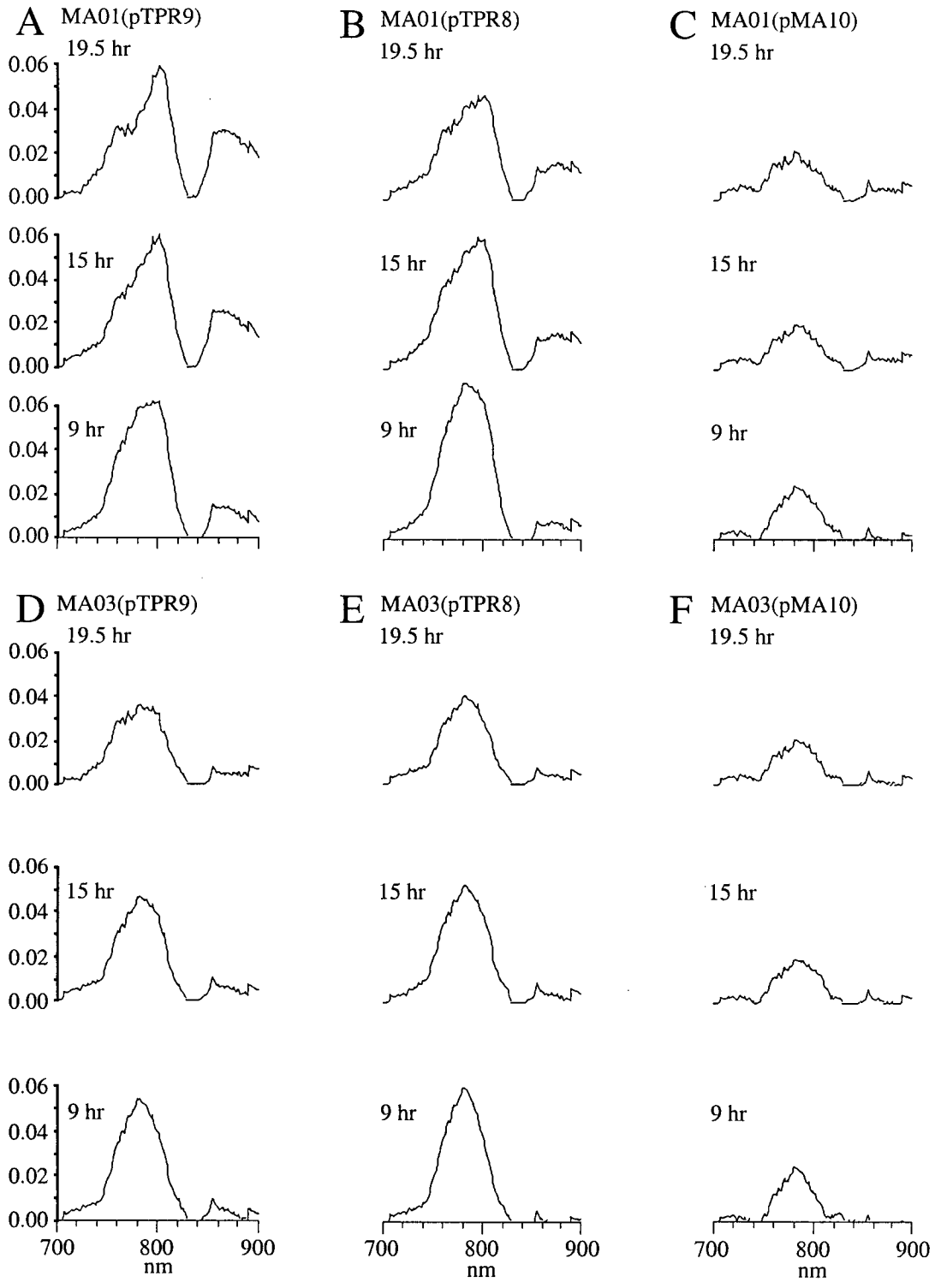

Figure 3.2.9. Absorption spectra (room temperature, pathlength 1 cm) of the nascent RC in the *puhB*$^+$ (MA01) and *puhB*$^-$ (MA03) backgrounds, in the absence of the LH1 polypeptides PufB - plasmid pTPR9 (**A**, **D**), PufA - plasmid pTPR8 (**B**, **E**), or both - plasmid pMA10 (**C**, **F**), after 9 hours, 15 hours, and 19.5 hours of semiaerobic growth. Spectra were normalized and a baseline was drawn as described in Section 2.15. In addition to RC absorption at 760 nm, 800 nm, and 865 nm, there is a peak at 780 nm, attributed to unbound BChl.

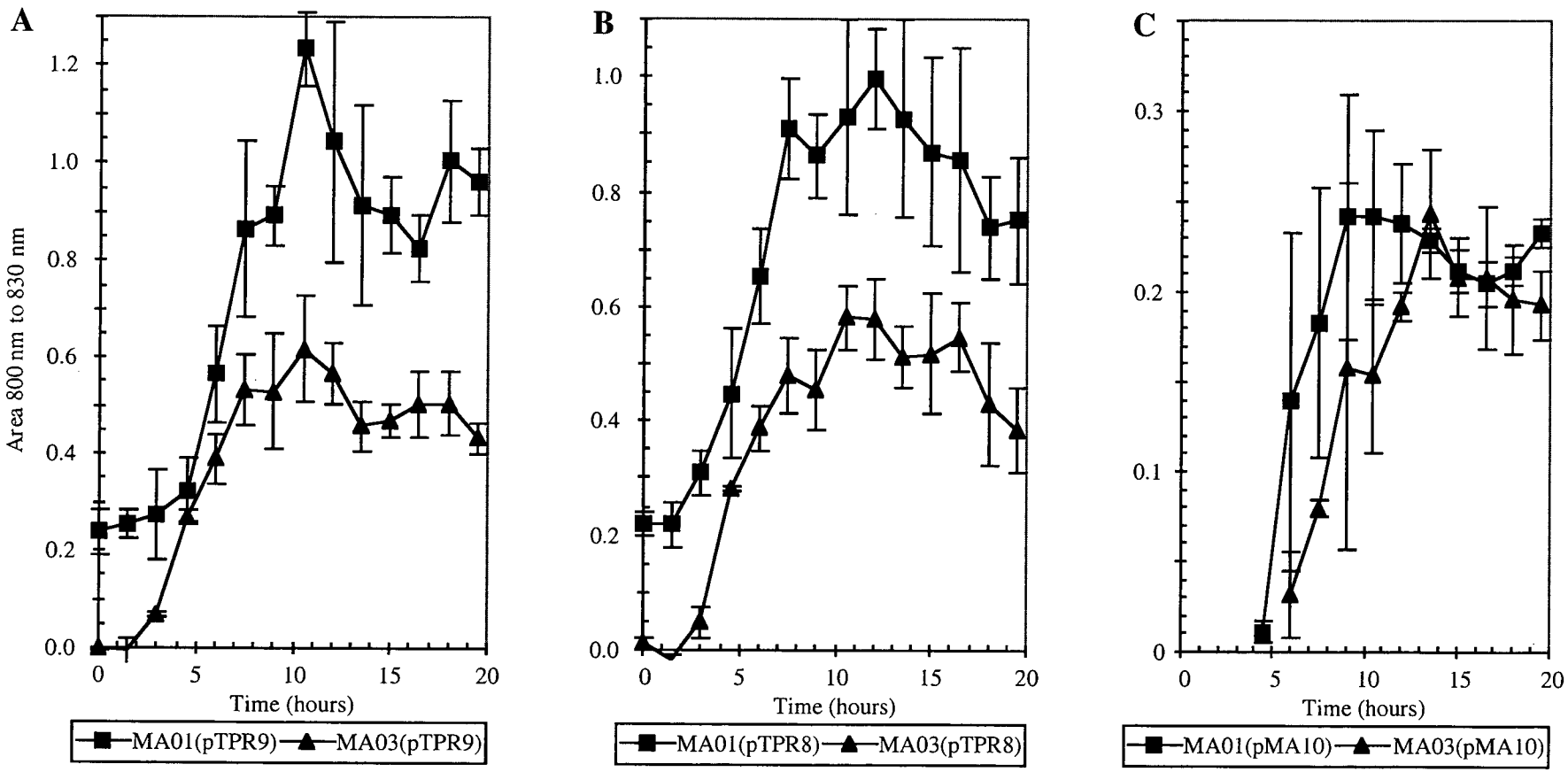

Figure 3.2.10. Production of the RC (**A**) in the absence of PufB - plasmid pTPR9, (**B**) in the absence of PufA - plasmid pTPR8, and (**C**) in the absence of both LH1 polypeptides - plasmid pMA10, in the *puhB*$^+$ (MA01) and *puhB*$^-$ (MA03) backgrounds. A portion of the RC voyeur BChl peak area was measured from 800 nm to 830 nm to minimize the contribution of absorption by BPhe and unbound BChl. In the presence of either PufA or PufB, the *puhB* deletion clearly reduced RC production. In the absence of both LH1 polypeptides, RC production was compromised regardless of PuhB.

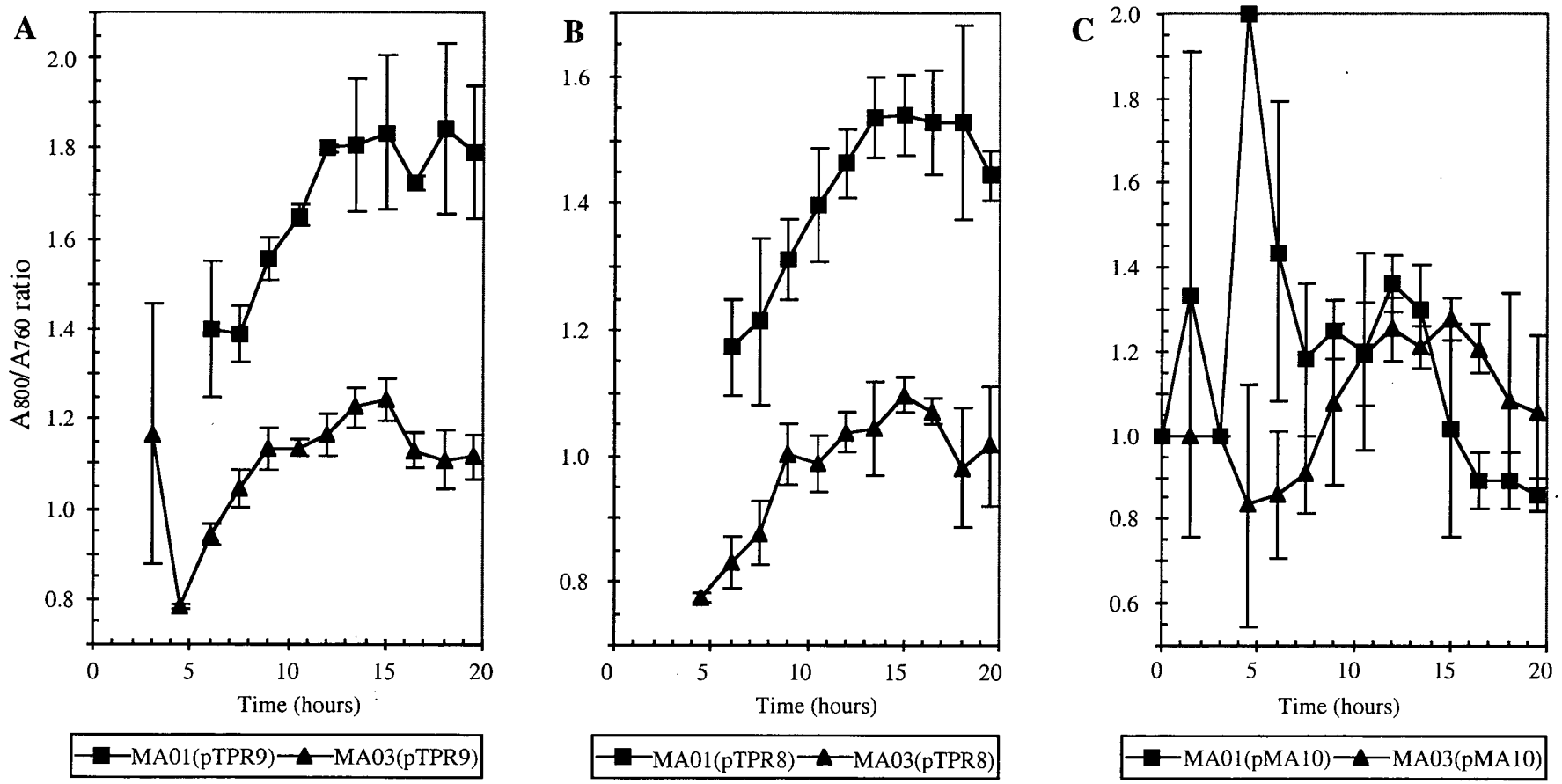

Figure 3.2.11. Peak height ratio of the RC (**A**) in the absence of PufB - plasmid pTPR9, (**B**) in the absence of PufA - plasmid pTPR8, and (**C**) in the absence of both LH1 polypeptides - plasmid pMA10, in the *puhB*$^+$ (MA01) and *puhB*$^-$ (MA03) backgrounds. The height of the voyeur BChl peak at 800 nm was divided by that of the BPhe peak at 760 nm, as a measure of RC "structural order," the proper binding of pigments to polypeptides. In the presence of either PufA or PufB, the *puhB* deletion clearly reduced RC structural order. In the absence of both LH1 polypeptides, RC structural order was compromised regardless of PuhB.

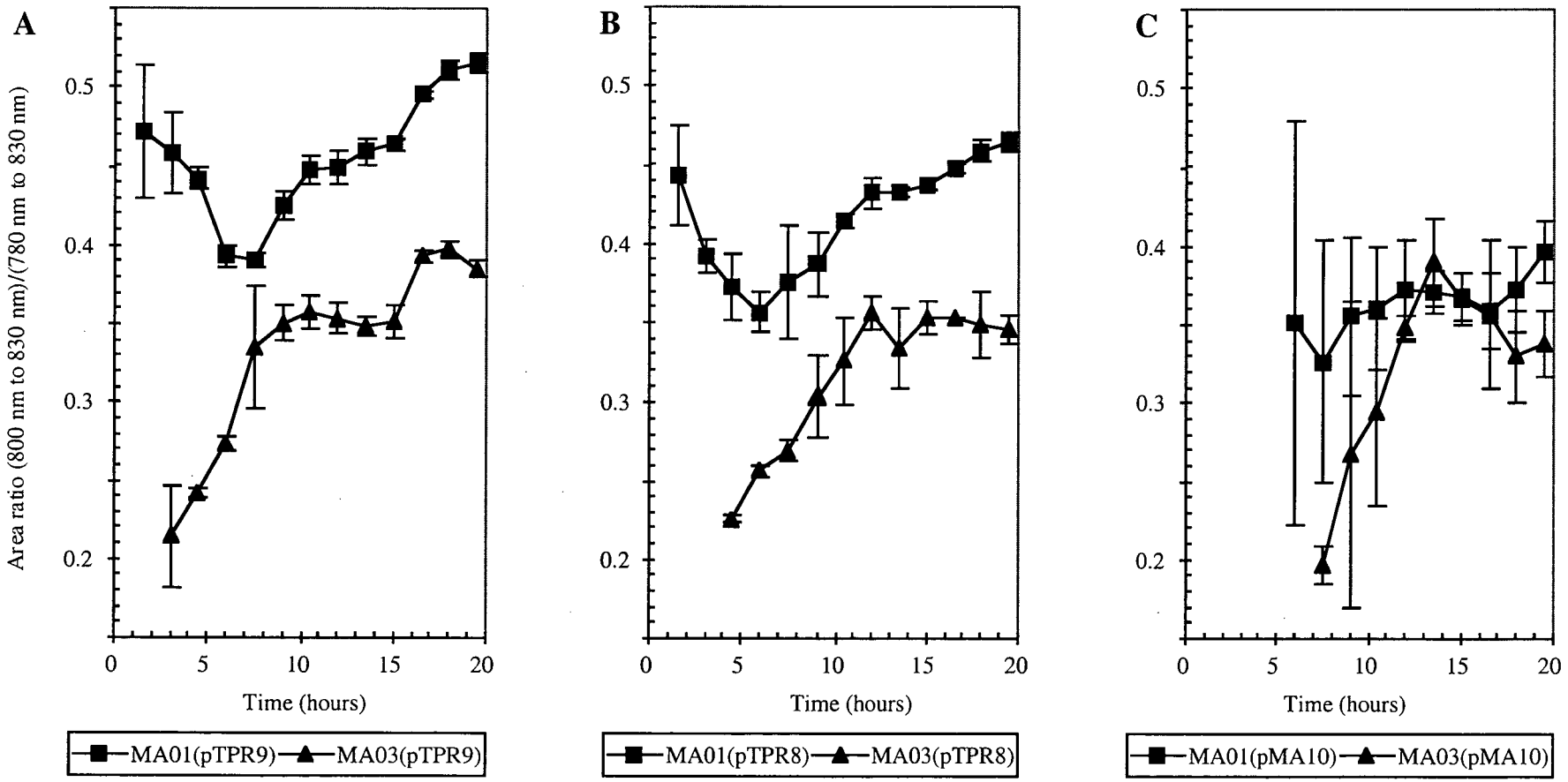

Figure 3.2.12. Voyeur BChl-specific peak area ratio of the RC (**A**) in the absence of PufB - plasmid pTPR9, (**B**) in the absence of PufA - plasmid pTPR8, and (**C**) in the absence of both LH1 polypeptides - plasmid pMA10, in the *puhB*$^+$ (MA01) and *puhB*$^-$ (MA03) backgrounds. The area of a portion of the voyeur BChl peak from 800 nm to 830 nm was divided by the area from 780 nm to 830 nm (which was inflated by absorption from the BPhe peak at 760 nm and the unbound BChl peak at 780 nm), as a measure of RC "structural order," the proper binding of pigments to polypeptides. In the presence of either PufA or PufB, the *puhB* deletion clearly reduced RC structural order. In the absence of both LH1 polypeptides, RC structural order was compromised regardless of PuhB.

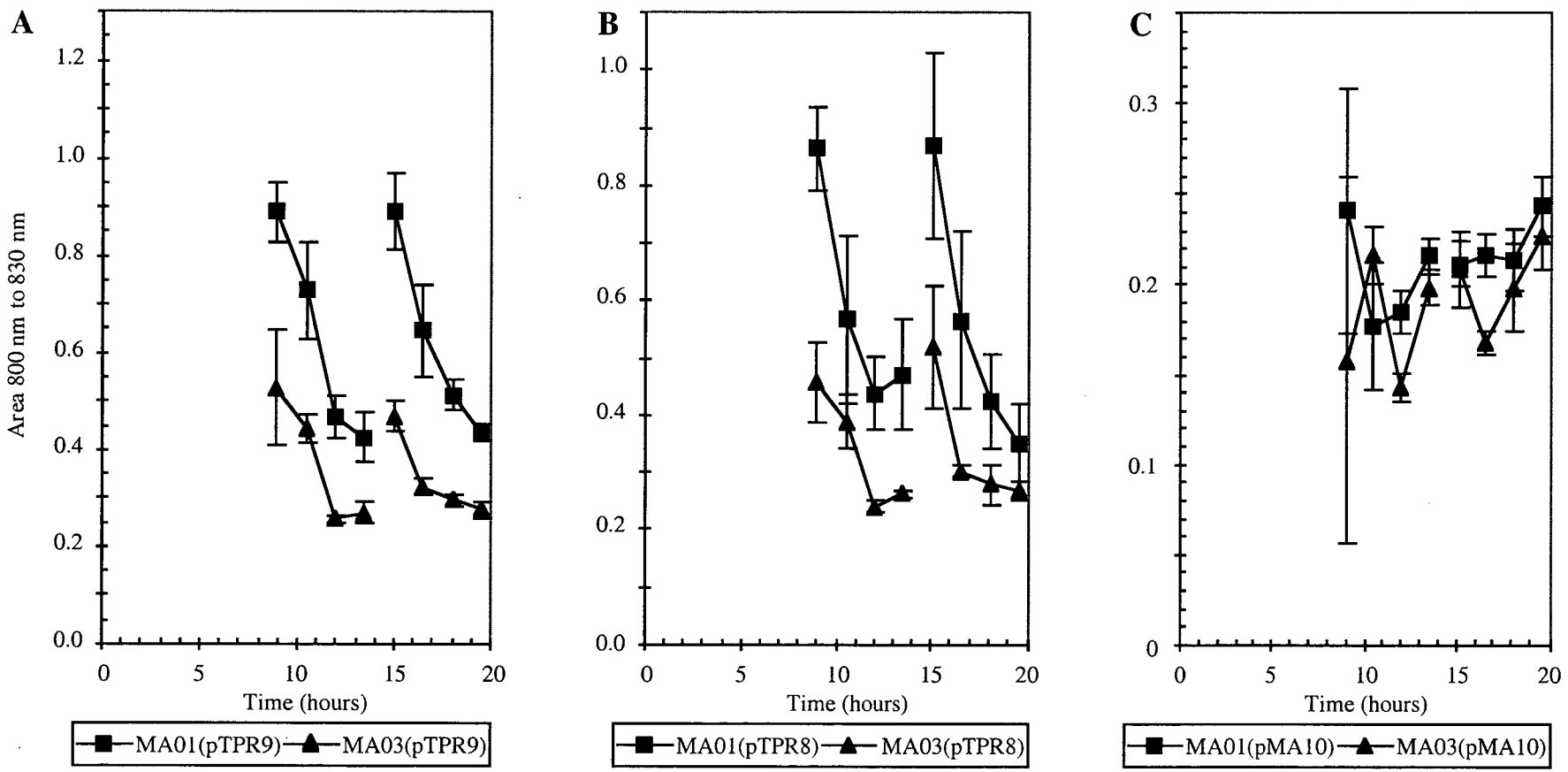

Figure 3.2.13. Decay of the RC (**A**) in the absence of PufB - plasmid pTPR9, (**B**) in the absence of PufA - plasmid pTPR8, and (**C**) in the absence of both LH1 polypeptides - plasmid pMA10, in the *puhB*$^{+}$ (MA01) and *puhB*$^{-}$ (MA03) backgrounds. Decay was initiated at 9 hr and at 15 hr by switching cultures to aerobic conditions. A portion of the RC voyeur BChl peak area was measured from 800 nm to 830 nm to minimize the contribution of absorption by BPhe and unbound BChl.

Table 3.2.6. Linear production rates (area units per hour) and exponential decay rate constants (per hour) for the RC in *puhB*$^+$ (MA01) and *puhB*$^-$ (MA03) backgrounds, determined from triplicate cultures. A portion of the RC voyeur BChl peak area was measured from 800 nm to 830 nm. Note: post-assembly RC decay in pMA10 strains (after 15 hours of semiaerobic growth) was a transient and insignificant phenomenon. When MA03(pMA10) was switched to aerobic conditions mid-assembly (after 9 hours), the average trend was an increase in RC voyeur BChl peak amplitude, hence the negative value of the decay rate constant.

Strain	Genotype chromosome (plasmid)	RC production	Mid-assembly RC decay	Post-assembly RC decay
MA01(pTPR9)	*pufQBALM*$^-$*X*$^+$*puhB*$^+$(*pufQALMX*)	161 ± 32	234 ± 89	239 ± 91
MA03(pTPR9)	*pufQBALM*$^-$*X*$^+$*puhB*$^-$(*pufQALMX*)	110 ± 18	270 ± 192	262 ± 96
MA01(pTPR8)	*pufQBALM*$^-$*X*$^+$*puhB*$^+$(*pufQBLMX*)	156 ± 35	396 ± 192	327 ± 268
MA03(pTPR8)	*pufQBALM*$^-$*X*$^+$*puhB*$^-$(*pufQBLMX*)	100 ± 16	266 ± 121	379 ± 230
MA01(pMA10)	*pufQBALM*$^-$*X*$^+$*puhB*$^+$(*pufQLMX*)	35 ± 7	235 ± 139	28 ± 22
MA03(pMA10)	*pufQBALM*$^-$*X*$^+$*puhB*$^-$(*pufQLMX*)	29 ± 7	-100 ± 443	146 ± 18

3.2.5. PuhB does not directly affect LH1 assembly

Kinetics of assembly and decay of LH1 were measured in *puhB*$^+$ (MA01) and *puhB*$^-$ (MA03) backgrounds, which contained a deletion of the chromosomal *pufQBALM* genes and were complemented with only the *pufQBAX* genes on plasmid p*Stu* I. Such removal of genes encoding two RC polypeptides, PufL and PufM, leaving only PuhA, allowed the evaluation of LH1-specific absorption at 880 nm without the minor contribution of the RC special pair BChl peak at 865 nm. The strains MA01(p*Stu* I) (*puhB*$^+$) and MA03(p*Stu* I) (*puhB*$^-$) were at similar culture densities throughout the experiments (Figure 3.2.14) and should have progressed similarly into semiaerobic growth conditions. Assembly of LH1 in the two strains was similar, and measurements of decay were not of sufficient quality to implicate or exclude the involvement of PuhB (Figure 3.2.14, Table 3.2.7). In the spectra of both MA01(p*Stu* I) and MA03(p*Stu* I), absorption at 780 nm was observed, perhaps due to unbound BChl (Figure 3.2.15).

These results indicate that the reduced level of LH1 in *puhB* deletion strains such as MA05 was probably an indirect effect due to the dependence of LH1 on the RC, PuhB being an RC assembly factor. In Section 3.5.3, I show that PufX, another RC-LH1 polypeptide, depends even more on PuhB.

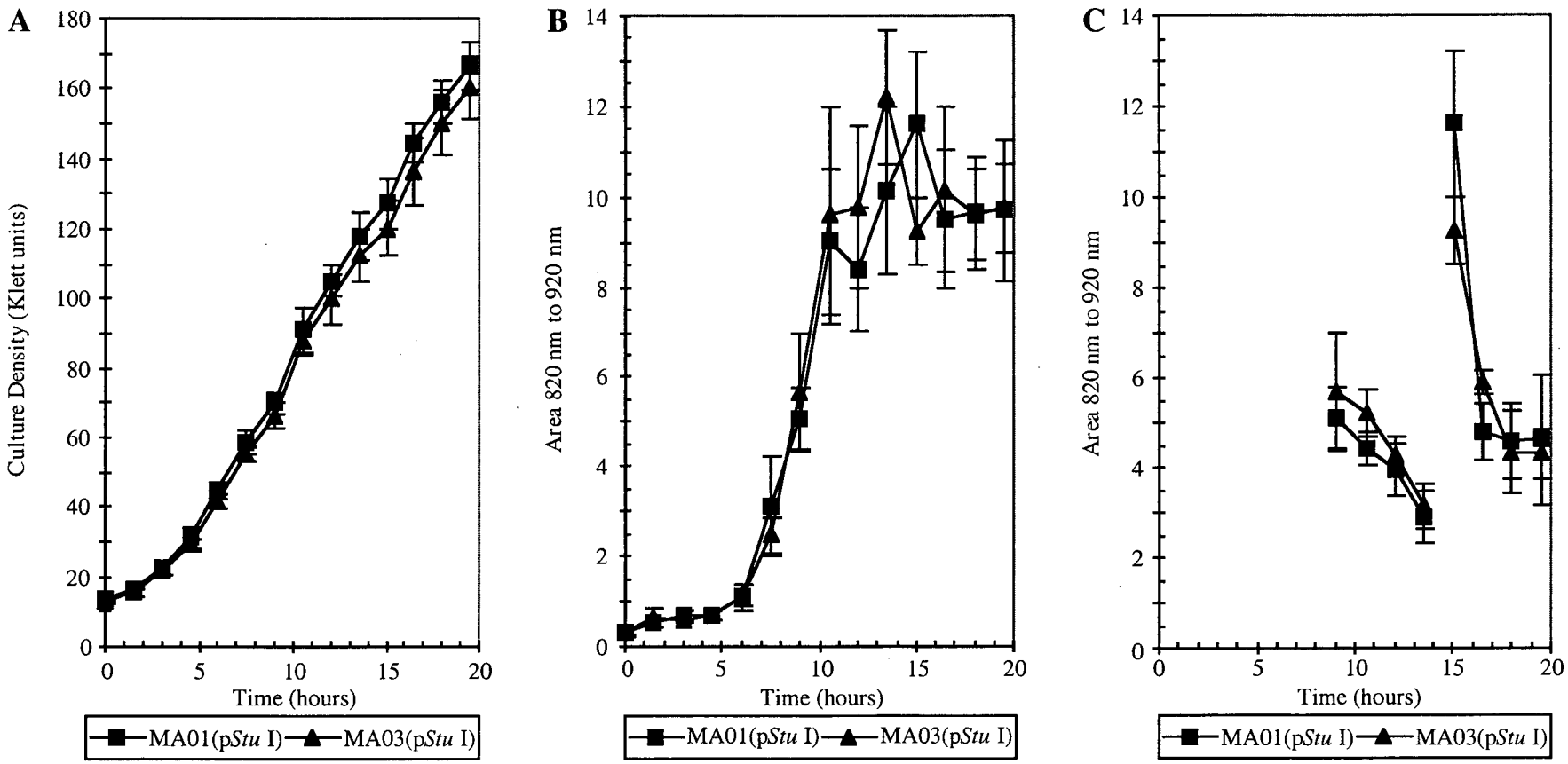

Figure 3.2.14. Assembly and decay of LH1 in the absence of PufL and PufM - plasmid p*Stu* I, in the *puhB*$^+$ (MA01) and *puhB*$^-$ (MA03) backgrounds. (**A**) Semiaerobic growth. (**B**) Production of LH1, measured as the peak area from 820 nm to 920 nm. (**C**) Decay of LH1, initiated at 9 hr and at 15 hr by switching cultures to aerobic conditions.

Table 3.2.7. Linear production rates (area units per hour) and exponential decay rate constants (per hour) for LH1 in *puhB*$^+$ (MA01) and *puhB*$^-$ (MA03) backgrounds, determined from triplicate cultures. The LH1 peak area was measured from 820 nm to 920 nm.

Strain	Genotype chromosome (plasmid)	LH1 production	Mid-assembly LH1 decay	Post-assembly LH1 decay
MA01(p*Stu* I)	*pufQBALM*$^-$*X*$^+$*puhB*$^+$(*pufQBA...X?*)	525 ± 12	37 ± 185	628 ± 35
MA03(p*Stu* I)	*pufQBALM*$^-$*X*$^+$*puhB*$^-$(*pufQBA...X?*)	533 ± 109	11 ± 73	402 ± 84

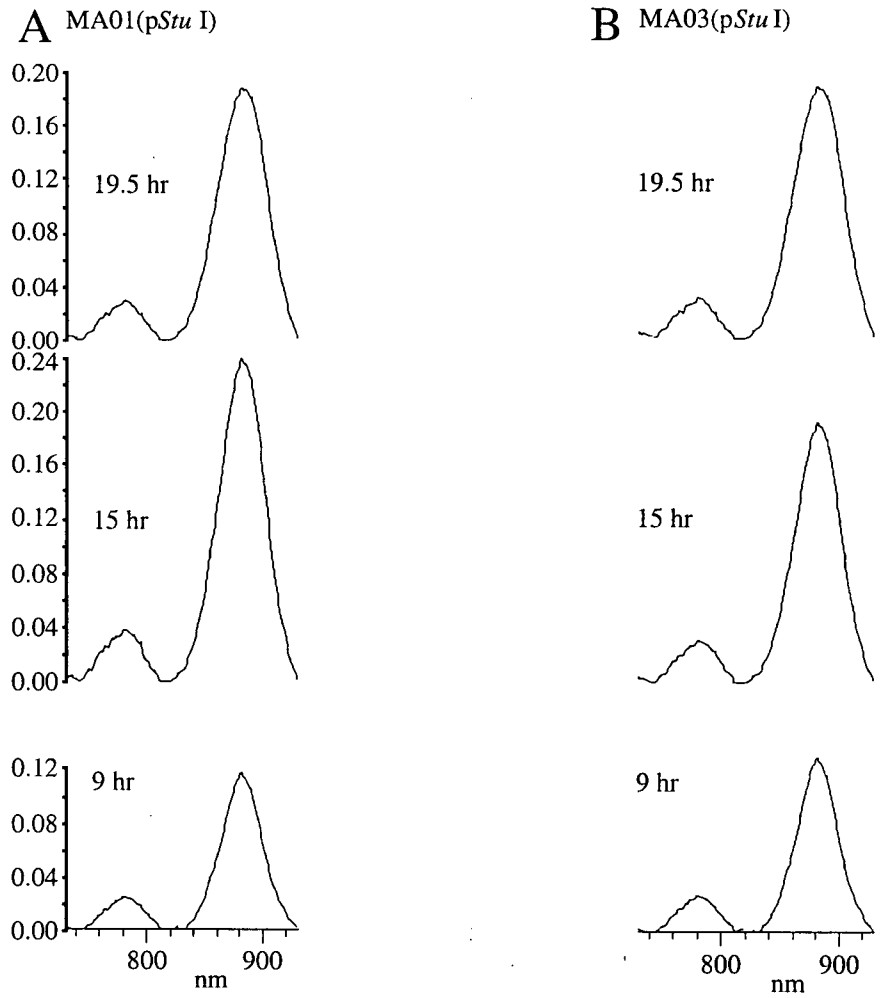

Figure 3.2.15. Absorption spectra (room temperature, pathlength 1 cm) of nascent LH1 in (**A**) *puhB*$^+$ (MA01) and (**B**) *puhB*$^-$ (MA03) backgrounds, in the absence of the RC polypeptides PufL and PufM - plasmid p*Stu* I, after 9 hours, 15 hours, and 19.5 hours of semiaerobic growth. Spectra were normalized and a baseline was drawn as described in Section 2.15. In addition to LH1 absorption at 880 nm, there is a small peak at 780 nm, attributed to unbound BChl.

3.2.4. TOXCAT and CyaA analyses of PuhB

TOXCAT hybrids (see Sections 1.6 and 2.8) with each of the three predicted TM segments of PuhB (Figure 3.2.16) supported growth on maltose minimal medium, indicating that each segment spans a bacterial inner membrane. However, the hybrid of the second TM segment, TM2, which is the only one among the six tested in this study that is predicted to run (N-terminus to C-terminus) from periplasm to cytoplasm, gave rise to smaller colonies than other TM segments. When the arginyl residue that naturally follows this segment was included in the hybrid (TM2R), no growth on maltose minimal medium was observed. The latter observation is consistent with the positive inside rule (157), whereby this arginyl residue would be expected to favour a cytoplasmic location, preventing the adjacent MalE domain from reaching the periplasm to function in maltose transport. The small colonies could indicate that the TM2 segment is in an unnatural orientation and is poorly inserted, unstable, or unable to present MalE properly.

Significant chloramphenicol acetyltransferase (CAT) activity in cells expressing the TM2 hybrid was evident from a thin layer chromatogram of a CAT assay (Figure 3.2.17), and indicated that the TM2 segment could mediate homodimerization of PuhB. Mutagenesis of TM2 indicates that simultaneous missense mutations such as M79L, Y84C, M87L, F92L abolish CAT expression (Figure 3.2.17), however, rare single missense mutants have not yet been identified due to the bias of the degenerate primer method of mutagenesis. It is worthwhile to mention that the cells for the CAT assay were never subjected to selective pressure on maltose minimal medium, which might have caused overproducers of the hybrid protein to create an artifact of self-association.

When CyaA hybrids of the predicted cytoplasmic and periplasmic protein segments N43, C84, and C147 from PuhB and C118 from PuhC (see Sections 1.6 and 2.9) were co-transformed into BTH101 cells, none of the combinations conferred the ability to grow on maltose minimal medium, and none of the transformant colonies that appeared on LB agar plates containing ampicillin, kanamycin, IPTG and X-gal developed a blue colour, indicating that PuhB and PuhC do not interact with themselves or with each other through their predicted cytoplasmic/periplasmic regions.

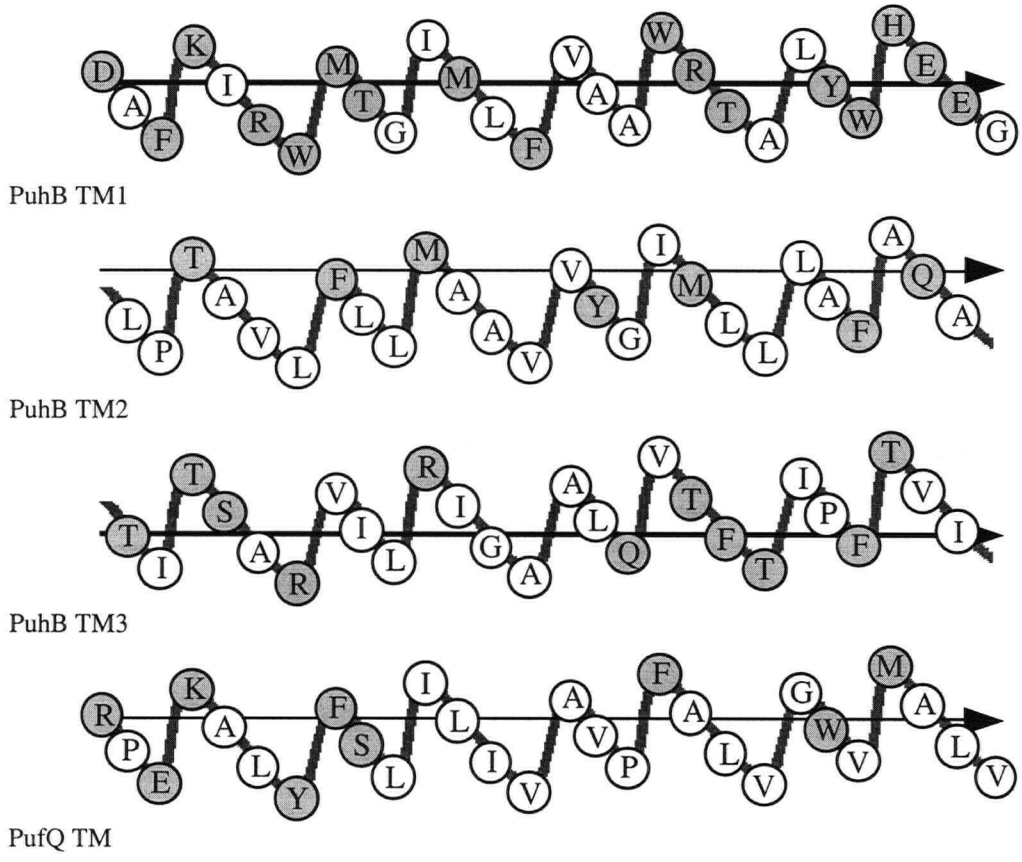

Figure 3.2.16. The putative TM segments of PuhB and PufQ. Grey circles mark potential electrostatic, hydrogen bonding, dipole-dipole, and aromatic ring stacking interactions. In the case of PuhB-TM2, each such residue is being mutated to discover the basis of homodimerization. The arrows, pointing toward the C-terminus of each protein, indicate a face of each helix where I propose that it may interact with another helix based on the locations of residues capable of participation in interactions. PufQ has been included because the possibility of a PuhB-PufQ interaction is being investigated.

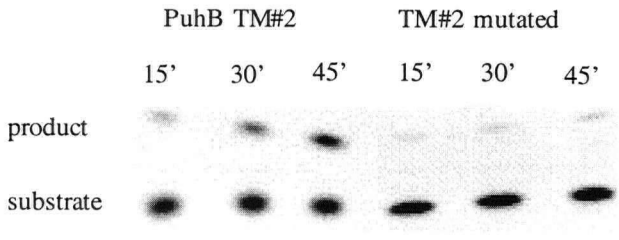

Figure 3.2.17. Thin layer chromatogram showing CAT activity in lysates of *E. coli* MM39 expressing a TOXCAT hybrid of the second TM segment of PuhB (left) and the same hybrid with four simultaneous mutations: M79L, Y84C, M87L, and F92L (right): acetylation of fluorescently labelled 1-deoxychloramphenicol over time. Assay performed by J. Lau.

An immunoblot with antiserum against full-length CyaA (58), a kind gift of J. Coote, failed to detect any upregulation of bands of the size expected for CyaA hybrids in the presence of IPTG. It

appears that the antiserum recognizes only the regulatory domain of CyaA, not the catalytic domain from which the hybrids were made.

To summarize the results of this subchapter, the phototrophic growth defect of *puhB*⁻ strains can be attributed to PuhB's important role in RC assembly. This role is direct, being observed regardless of the presence of one or the other LH1 polypeptide. However, the *puhB* deletion also has an indirect, RC-dependent impact on LH1, suggesting that the RC is not merely less abundant but structurally abnormal, disruptive of LH1. Because RC-driven electron transport is sustained in chromatophores of a *puhB* deletion strain grown semiaerobically, the long lag that precedes phototrophic growth cannot be explained satisfactorily by the RC-LH1 deficiency alone. In Section 3.5.3, I show that the level of PufX, a protein located in the RC-LH1 core complex and required for sustained electron transport (8, 34, 87), is drastically reduced under semiaerobic conditions by the *puhB* deletion. The effect of a PufX deficiency on electron transport could be more significant in intact cells than in chromatophores. To understand the exact role of PuhB, one may find it useful to consider that it is sensitive to co-translation with PufQ and may homodimerize through its second TM segment.

3.3. Characterization of PuhC as an RC-LH1 organization factor

3.3.1. The growth defect of the *puhC* deletion strains SBK1 and MWK1; complementation and the effects of *puhE* and extra *pufQ*

A blot of RNA from highly aerated and semiaerobic cultures, probed with random ^{32}P-labelled fragments of the *puhC* gene, confirmed an earlier observation that *puhC* is co-transcribed with *puhA* from an oxygen-repressed promoter or promoters (56). In my RNA blot (Figure 3.3.1), the *puhC* deletion strain SBK1 was included along with DW1, in which transcription is terminated within *puhA*. Unfortunately, the probe hybridized with ribosomal RNA; however, there is clearly a band corresponding to an mRNA species of about 2.7 kb in the wild type parent SB1003 grown semiaerobically, which is not seen in DW1 or in SBK1. That is, transcription of *puhC* depends on the promoter 5' of *puhA*, and probably on the *bchF* promoter where the superoperon begins (9, 11). Interestingly, a transcript of about 1.5 kb was present in SBK1, and was more abundant under high aeration. This transcript was attributed to the promoter of the KIXX cartridge, which in SBK1 is oriented parallel to the *puh* promoter (56) and may transcribe the 3' end of the disrupted *puhC* gene and the *orf55* and *puhE* sequences that follow *puhC*.

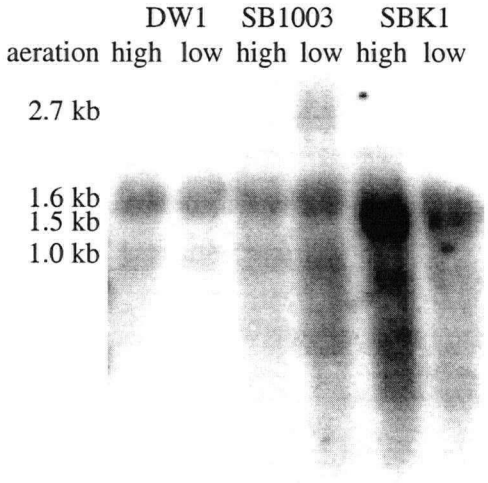

Figure 3.3.1. RNA blot of *puhC* transcripts in cultures grown with high and low aeration. The probe was a *Bsa*B I-*Eco*R I fragment extending from the middle of *puhC* to the middle of *orf55*.

Although the phototrophic growth defect due to the *puhC* deletion in strain SBK1 was originally described as causing premature cessation of growth (2), further experimentation revealed that when a semiaerobic culture incubated for roughly 24 hours was used as inoculum, phototrophic growth was very poor. When the remainder of the same semiaerobic culture was topped up with sterile RCV medium and incubated for an additional 24 hours, phototrophic cultures inoculated with it grew initially at half the wild type rate or more, but entered stationary phase prematurely (Figure 3.3.2, Table 3.3.1).

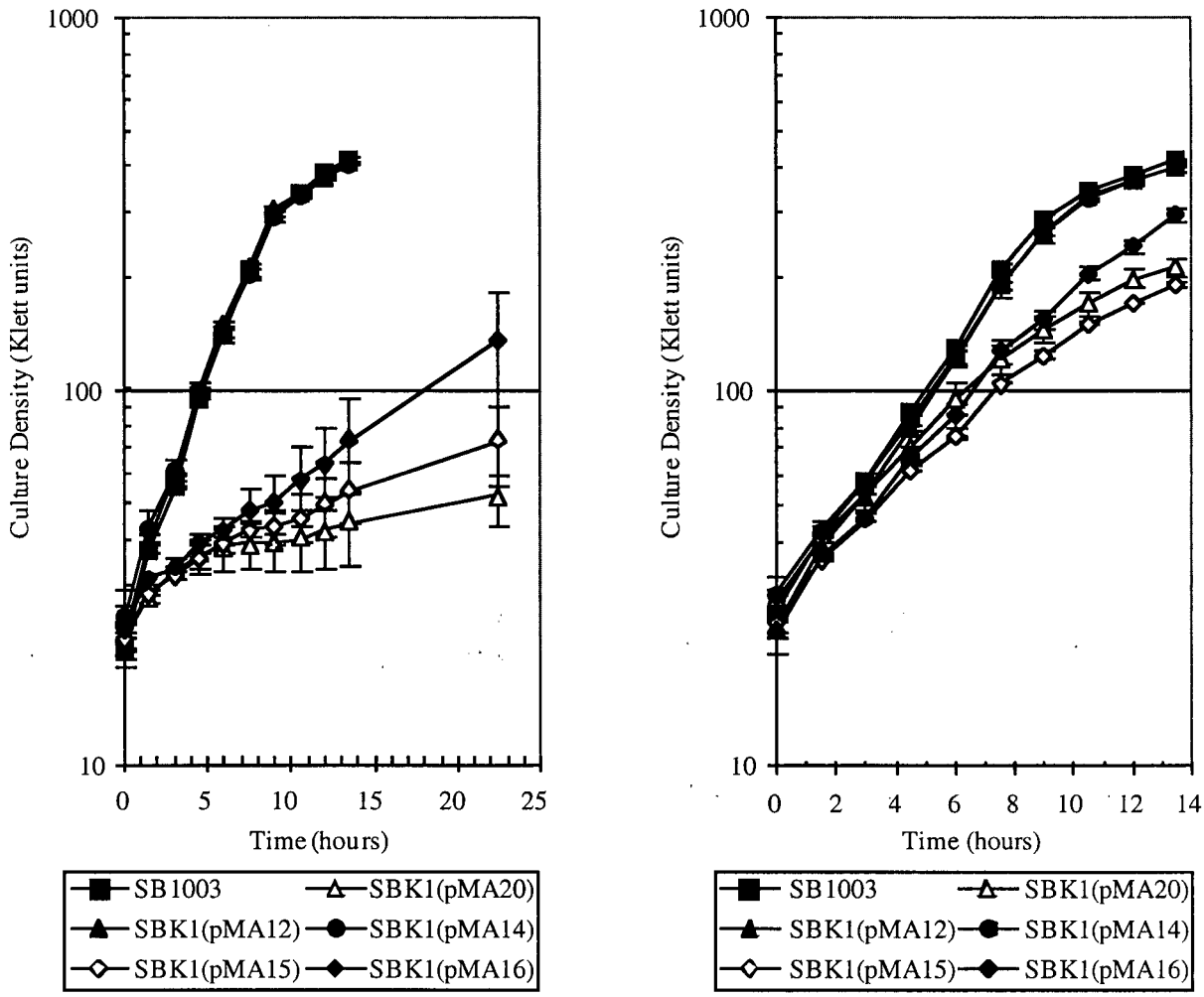

Figure 3.3.2. Phototrophic growth of SBK1 (*puhC*⁻) either with the empty vector pMA20 or complemented in *trans* with 6xHis-tagged *puhC* (pMA12) and *puhC* gene homologues from *R. sphaeroides*, *R. rubrum*, and *R. gelatinosus* (pMA14, pMA16, pMA15), after 24 hours (left) and 48 hours (right) of semiaerobic growth.

The *puhC* deletion strain SBK1, complemented in *trans* with the 6xHis-tagged *puhC* gene of *R. capsulatus* (plasmid pMA12) exhibited the same phototrophic growth rate as the *puhC*$^+$ parent SB1003, and the similar *puhC* gene of *R. sphaeroides* (plasmid pMA14) resulted in growth similar to that of SB1003. The dissimilar *puhC* gene of *R. rubrum* (pMA16) (see Figure 3.6.5) had a minor restorative effect, while that of *R. gelatinosus puhC* (pMA15) was minimal. The empty vector pMA20 had no effect. These observations were made with inocula that had been incubated semiaerobically for 24 hours and for 48 hours (Figure 3.3.2, Table 3.3.1).

Table 3.3.1. *Trans*-complementation of the LH2$^+$ *puhC* deletion strain's phototrophic growth defect by 6xHis-tagged *puhC* (pMA12) and *puhC* gene homologues (pMA14, pMA16, pMA15) after semiaerobic growth for 24 hours and 48 hours. pMA20 is the empty vector.

Strain **24 hours**	Genotype chromosome (plasmid)	Relative specific growth rate ± standard deviation of 3 cultures
SB1003	*puhC*$^+$	100% ± 4%
SBK1	*puhC*$^-$	14% ± 1%
SBK1(pMA20)	*puhC*$^-$(empty)	13% ± 5%
SBK1(pMA12)	*puhC*$^-$(*capsulatus puhC-N*)	99% ± 3%
SBK1(pMA14)	*puhC*$^-$(*sphaeroides puhC*)	91% ± 5%
SBK1(pMA16)	*puhC*$^-$(*rubrum puhC*)	24% ± 7%
SBK1(pMA15)	*puhC*$^-$(*gelatinosus puhC*)	19% ± 4%
48 hours		
SB1003	*puhC*$^+$	100% ± 1%
SBK1	*puhC*$^-$	53% ± 1%
SBK1(pMA20)	*puhC*$^-$(empty)	55% ± 2%
SBK1(pMA12)	*puhC*$^-$(*capsulatus puhC-N*)	98% ± 2%
SBK1(pMA14)	*puhC*$^-$(*sphaeroides puhC*)	91% ± 3%
SBK1(pMA16)	*puhC*$^-$(*rubrum puhC*)	72% ± 2%
SBK1(pMA15)	*puhC*$^-$(*gelatinosus puhC*)	56% ± 1%

A truncated PuhC protein (PuhC-NS) consisting of the predicted periplasmic domain without any TM segment, was expressed from plasmid pMA13. It had no effect on the growth of SBK1 (Table 3.3.2), indicating that the predicted TM segment of *puhC* is required for its function. This protein was also expressed in SB1003 to see if it would interfere with the function of natural PuhC. It did not inhibit growth of SB1003 any more than the empty vector pMA20 did.

Table 3.3.2. Phototrophic growth of *puhC*$^+$ (SB1003) and *puhC*$^-$ (SBK1) strains expressing a truncated, 6xHis-tagged PuhC protein (pMA13). pMA20 is the empty vector.

Strain **24 hours**	Genotype chromosome (plasmid)	Relative specific growth rate ± standard deviation of 3 cultures
SB1003	*puhC*$^+$	100% ± 4%
SB1003(pMA20)	*puhC*$^+$(empty)	88% ± 4%
SB1003(pMA13)	*puhC*$^+$(*capsulatus puhC-NS*)	87% ± 6%
SBK1	*puhC*$^-$	14% ± 1%
SBK1(pMA20)	*puhC*$^-$(empty)	13% ± 5%
SBK1(pMA13)	*puhC*$^-$(*capsulatus puhC-NS*)	13% ± 2%
48 hours		
SB1003	*puhC*$^+$	100% ± 1%
SB1003(pMA20)	*puhC*$^+$(empty)	90% ± 2%
SB1003(pMA13)	*puhC*$^+$(*capsulatus puhC-NS*)	99% ± 3%
SBK1	*puhC*$^-$	53% ± 1%
SBK1(pMA20)	*puhC*$^-$(empty)	55% ± 2%
SBK1(pMA13)	*puhC*$^-$(*capsulatus puhC-NS*)	52% ± 2%

The observation that the LH2$^-$ *puhC* deletion strain MWK1 had a less severe defect relative to its parent MW442 than that of the LH2$^+$ *puhC* deletion strain SBK1 compared to SB1003 (56) was confirmed. Growth of MWK1 may have been improved by the *puhC* gene of *R. sphaeroides*, while those of *R. rubrum* and *R. gelatinosus* had no effect (Table 3.3.3). I speculate that during 24 hours of semiaerobic growth, MWK1 had a smaller burden of pigment and antenna protein synthesis compared to SBK1; MWK1 grew more quickly, resulting in a longer period of oxygen deprivation, synthesized more of the photosynthetic apparatus, and was more prepared for phototrophic growth.

Table 3.3.3. *Trans*-complementation of the LH2$^-$ *puhC* deletion strain's phototrophic growth defect by 6xHis-tagged *puhC* and *puhC* gene homologues after semiaerobic growth for 24 hours.

Strain	Genotype chromosome (plasmid)	Relative specific growth rate ± standard deviation of 3 cultures
MW442	*puhC*$^+$	100% ± 3%
MWK1	*puhC*$^-$	87% ± 3%
MWK1(pMA12)	*puhC*$^-$(*capsulatus puhC-N*)	99% ± 5%
MWK1(pMA14)	*puhC*$^-$(*sphaeroides puhC*)	94% ± 8%
MWK1(pMA16)	*puhC*$^-$(*rubrum puhC*)	88% ± 2%
MWK1(pMA15)	*puhC*$^-$(*gelatinosus puhC*)	84% ± 6%

However, my data may suggest a different explanation for the LH2-dependent *puhC*⁻ mutant phenotypes. After SBK1 ceased to grow at a low culture density, eventual growth was sometimes observed (56). To determine whether the growing cells resulted from secondary mutations, I diluted an SBK1 culture in premature stationary phase, plated the cells, and grew them anaerobically with high light intensity. About 150 colonies appeared within 2 to 4 days for every 10^6 cells plated. Eleven large colonies were streaked on RCV-kanamycin agar to confirm their origin from SBK1, which has a KIXX cartridge in a *puhC* deletion. The pure cultures were designated SBK14 through SBK24. These strains' improved phototrophic growth was mostly similar to that of strain SBSpec, which is identical to SBK1 except that disruption of *puhC* blocks transcription of *puhE* in SBSpec (Figure 3.3.3), and during active growth, they typically had less LH2 per cell than SBK1 and the wild type strain SB1003, as evidenced by the smaller peaks at 800 and 850 nm in their absorption spectra (Figure 3.3.4). Thus, it appears that secondary mutations that reduced the amount of LH2 benefited cells lacking PuhC, consistent with the different growth phenotypes of SBK1 ($LH2^+$) and MWK1 ($LH2^-$) (56). Therefore, PuhC may prevent LH2 from interfering in energy transduction.

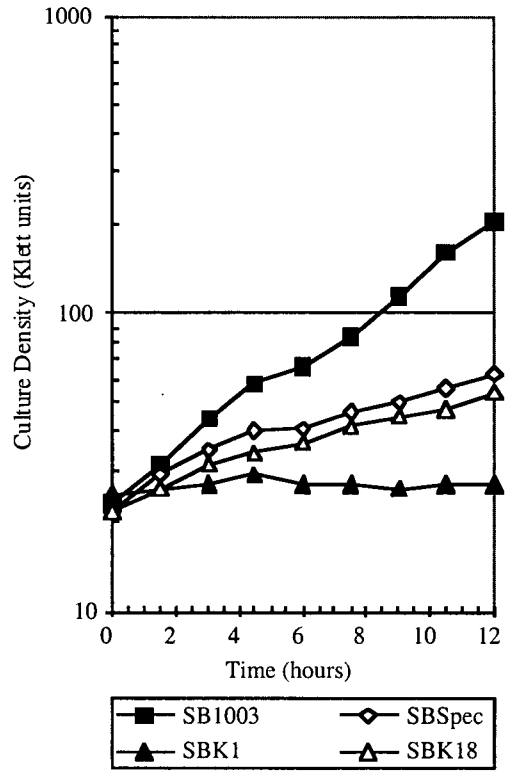

Figure 3.3.3. Comparison of phototrophic growth of SB1003, the *puhC* deletion strain SBK1, a secondary mutant strain called SBK18, and the polar *puhC*⁻ mutant strain SBSpec.

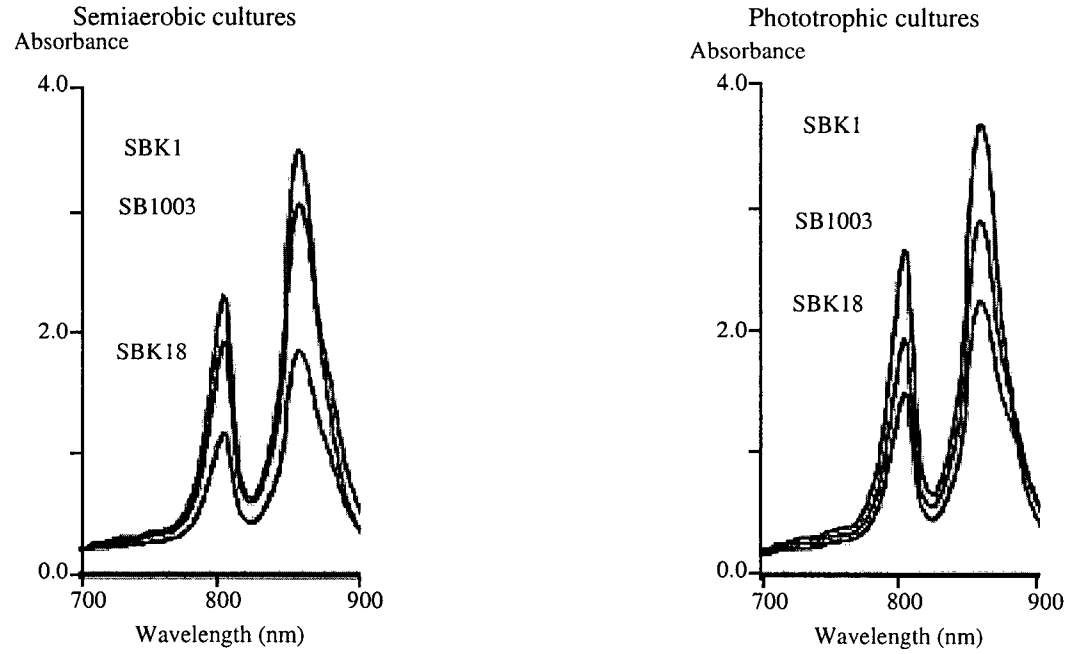

Figure 3.3.4. Normalized absorption spectra (room temperature, pathlength 1 cm) of intact cells of SB1003, SBK1, and SBK18. The two predominant peaks at 800 nm and 850 nm are due to LH2, which is downregulated in SBK18.

As observed previously (56), termination of transcription within the *puhC* deletion, so that the strain (SBSpec) had a PuhC$^-$PuhE$^-$ phenotype, resulted in better growth than that of the nonpolar *puhC* mutant SBK1 (Figure 3.3.5, Table 3.3.4). An extra copy of *puhE* on plasmid pMA19, by contrast, resulted in almost zero growth for SBK1(pMA19) and very poor growth for SBSpec(pMA19). Phototrophic growth of SBK1 was greatly improved by introduction of an extra copy of *pufQ* on a plasmid - either pXCA6::935 or pRR5C. Thus, PufQ and PuhE had opposite effects on phototrophic growth without PuhC. As I show in Section 3.4.6, PufQ promotes BChl production and PuhE inhibits it. Plasmid pMA11, which carries both *pufQ* and *puhE*, improved the growth of SBK1 but inhibited the growth of SBSpec (Figure 3.3.5, Table 3.3.4). This result is counterintuitive according to a simple model in which PufQ and PuhE are antagonists: *pufQ* merodiploidy should counteract the single active *puhE* gene of SBSpec(pMA11) more easily than the two active *puhE* genes of SBK1(pMA11). Therefore, a more complex model may be warranted, in which the extra PuhE protein forms a higher-order structure that either is overcome more easily by the extra PufQ or is self-interfering. Differences in PuhE processing due to ectopic expression (separately from the remaining Puh proteins) are also a possibility.

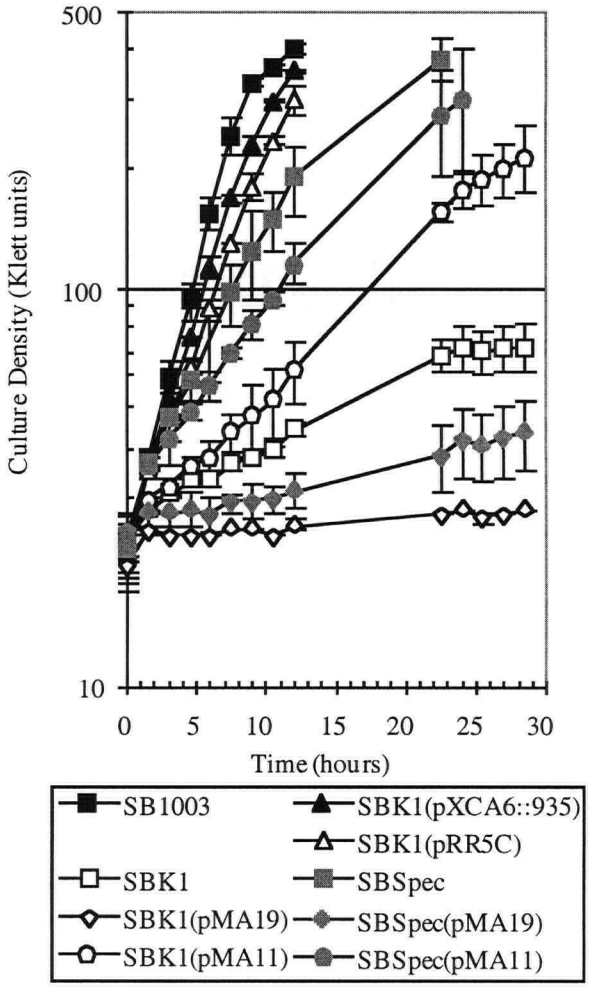

Figure 3.3.5. PufQ and PuhE affect the phototrophic growth of *puhC* deletion mutant strains. The genotypes are listed in Table 3.3.4.

Table 3.3.4. Effects of *pufQ* merodiploidy, *puhE* non-expression, and *puhE* copy number on phototrophic growth of *puhC* deletion strains (SBK1, SBSpec) from 24-hour semiaerobic inocula. The IncP plasmid pXCA6::935 may differ from the other (IncQ) plasmids in terms of copy number, which is unknown in *R. capsulatus*.

Strain	Genotype chromosome (plasmid)	Relative specific growth rate ± standard deviation of 2 cultures
SB1003	*pufQ*$^+$*puhC*$^+$*E*$^+$	100% ± 1%
SBK1(pXCA6::935)	*pufQ*$^+$*puhC*$^-$*E*$^+$(*pufQB::lacZ*)	82% ± 2%
SBK1(pRR5C)	*pufQ*$^+$*puhC*$^-$*E*$^+$(*pufQ*)	70% ± 3%
SBK1	*pufQ*$^+$*puhC*$^-$*E*$^+$	14% ± 0%
SBK1(pMA19)	*pufQ*$^+$*puhC*$^-$*E*$^+$(*puhE*)	2% ± 0%
SBK1(pMA11)	*pufQ*$^+$*puhC*$^-$*E*$^+$(*pufQpuhE*)	25% ± 3%
SBSpec	*pufQ*$^+$*puhC*$^-$Ω*E*$^-$	53% ± 2%
SBSpec(pMA19)	*pufQ*$^+$*puhC*$^-$Ω*E*$^-$(*puhE*)	6% ± 2%
SBSpec(pMA11)	*pufQ*$^+$*puhC*$^-$Ω*E*$^-$(*pufQpuhE*)	38% ± 1%

Merodiploidy for *pufQ* and/or *puhE* (due to plasmids pRR5C, pMA19, and pMA11) did not significantly affect the growth of the *puhC*$^+$ strain SB1003 (not shown).

3.3.2. The RC-LH1 deficiency of the *puhC* deletion strain SBK1

SDSPAGE of chromatophores from SBK1 revealed that the amounts of all the RC and LH1 polypeptides per total protein were reduced due to the *puhC* deletion (Figure 3.3.6). The LH1 deficiency was confirmed by low temperature absorption spectroscopy (Figure 3.3.7), and the RC deficiency was confirmed by measurements of RC photobleaching with a train of eight flashes of light (Figure 3.3.8, Table 3.3.5). The carotenoid bandshift (explained in Section 2.14), was observed after a single flash of light. In SBK1, as in the *puhC*$^+$ parent SB1003, it consisted of a rapid initial shift, attributed to the reduction of quinones in the RC, followed by a more gradual further shift due to the generation of a sustained proton gradient coupled to oxidation of quinols by cyt *b*/*c*1, indicating that these reactions are not abolished by deletion of *puhC* (Figure 3.3.9). However, the much smaller carotenoid bandshift demonstrated that SBK1 forms a lesser proton gradient, consistent with a lower RC content than SB1003, especially when cultures are grown phototrophically (Table 3.3.5). The carotenoid bandshift of SBK1 accumulated over successive flashes, indicating that the RC is properly connected to cyt *b*/*c*1 (Figure 3.3.10).

The RC-LH1 deficiency of SBK1 was complemented perfectly by the 6xHis-tagged *puhC-N* gene (pMA12) and by *R. sphaeroides puhC* (pMA14). The effect of *R. rubrum puhC* (pMA16) was moderate, and that of *R. gelatinosus puhC* (pMA15) insignificant (Figures 3.3.6 and 3.3.10, Table 3.3.5).

Merodiploidy for *pufQ* partially restored the levels of RC-LH1 and the formation of a proton gradient in response to light (Figures 3.3.11 and 3.3.12, Table 3.3.6). Termination of transcription within the *puhC* deletion 5' of *puhE* in strain SBSpec did not significantly increase the amount of RC-LH1 relative to SBK1, but restoration of *puhE* to SBSpec on plasmid pMA19 resulted in RC-LH1 levels even lower than in SBK1, as determined by SDSPAGE and flash spectroscopy (Figure 3.3.12, Table 3.3.6).

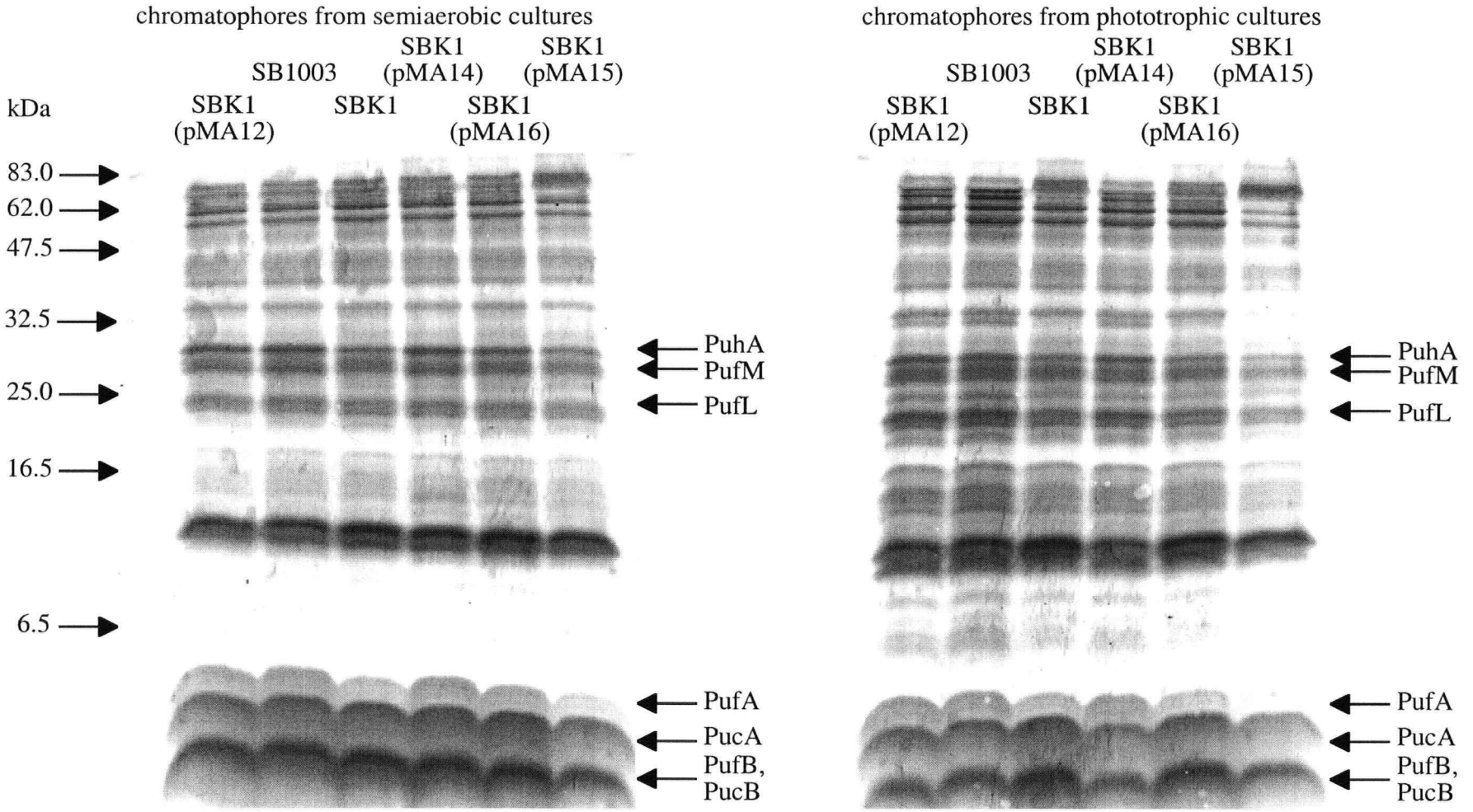

Figure 3.3.6. SDSPAGE of 50 μg of chromatophore protein from *R. capsulatus* SBK1 (*puhC* deletion) strains expressing 6xHis-tagged PuhC (pMA12) and PuhC proteins from different species: *R. sphaeroides* (pMA14), *R. rubrum* (pMA16), and *R. gelatinosus* (pMA15). Only the first two fully restored the polypeptides of the RC (PuhA, PufM, PufL) and LH1 (PufA and PufB) to the levels of the wild type SB1003. *R. rubrum* PuhC had a moderate effect, and *R. gelatinosus* PuhC had none. Differences were most apparent in the intensities of the PuhA and PufA bands; stronger proofs of complementation are the growth and carotenoid bandshift data.

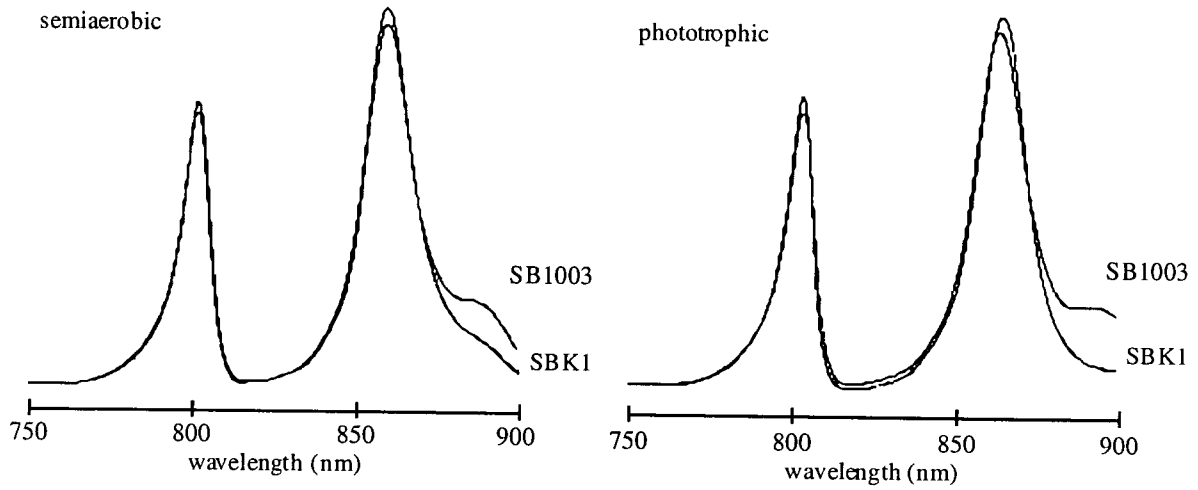

Figure 3.3.7. Low-temperature absorption spectra (77 K, pathlength 1 cm) of chromatophores from strains SB1003 and SBK1. SB1003 had more LH1 absorption at 880 nm. The LH1 deficiency of SBK1 was more pronounced under phototrophic conditions. Data collected by R. C. Prince.

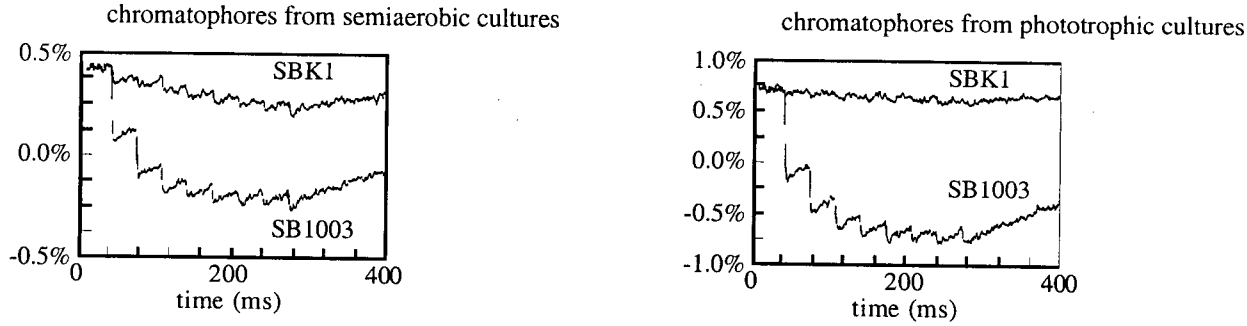

Figure 3.3.8. Photobleaching of the RC (room temperature, pathlength 1 cm) in chromatophores from SB1003 and SBK1. The downward deflection with each flash indicates a decrease in absorption at 605 nm due to photooxidation of the RC special pair. Data collected by R. C. Prince.

Figure 3.3.9. Single-flash carotenoid bandshifts (room temperature, pathlength 1 cm) in chromatophores from phototrophically grown SB1003 and SBK1. A smaller bandshift was observed for SBK1, indicating that a smaller proton gradient was produced (left), and the production of this proton gradient was sensitive to antimycin (right), although it was small to begin with. Data collected by R. C. Prince.

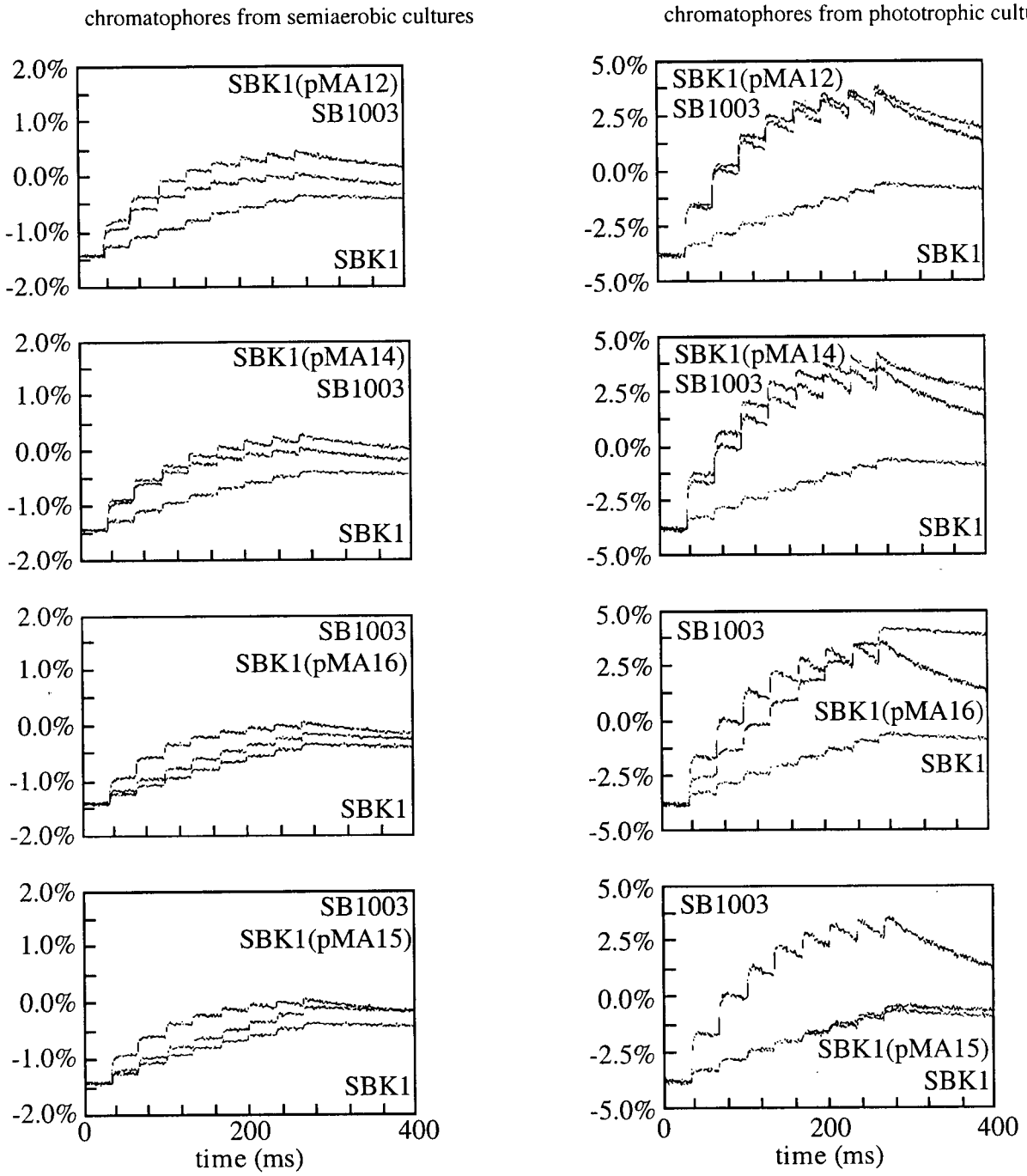

Figure 3.3.10. Eight-flash carotenoid bandshifts (room temperature, pathlength 1 cm) in chromatophores from the *puhC*$^+$ strain SB1003, the *puhC*$^-$ strain SBK1, and SBK1 complemented with 6xHis-tagged PuhC from *R. capsulatus* (pMA12) and with PuhC proteins from different species: *R. sphaeroides* (pMA14), *R. rubrum* (pMA16), and *R. gelatinosus* (pMA15). The *puhC*$^-$ mutation did not prevent the formation of a cumulative proton gradient, but reduced its magnitude. A shift to the red was observed for both semiaerobic conditions (increased absorption at 540 nm vs. 510 nm) and phototrophic conditions (increased absorption at 490 nm vs. 475 nm). Data collected by R. C. Prince.

Table 3.3.5. Flash spectroscopic measurements (room temperature, pathlength 1 cm) of the effects of PuhC proteins from different species (*R. capsulatus* pMA12; *R. sphaeroides* pMA14; *R. rubrum* pMA16, *R. gelatinosus* pMA15) on RC content and function in isolated chromatophores. Data collected by R. C. Prince.

Strain	Amount of RC (RC photobleaching, relative to SB1003)	Proton gradient (single-flash carotenoid bandshift, relative to SB1003)
semiaerobic cultures		
SBK1	26%	41%
SBK1(pMA12)	96%	135%
SBK1(pMA14)	85%	118%
SBK1(pMA16)	44%	53%
SBK1(pMA15)	24%	59%
phototrophic cultures		
SBK1	6%	23%
SBK1(pMA12)	125%	107%
SBK1(pMA14)	137%	123%
SBK1(pMA16)	50%	57%
SBK1(pMA15)	17%	27%

Table 3.3.6. Flash spectroscopic measurements (room temperature, pathlength 1 cm) of the effects of *puhE* non-transcription (SBSpec), *puhE* restoration (pMA19), and *pufQ* merodiploidy (pRR5C) in a *puhC* deletion background. Data collected by R. C. Prince.

Strain	Amount of RC (RC photobleaching, relative to SB1003)	Proton gradient (single-flash carotenoid bandshift, relative to SB1003)
semiaerobic cultures		
SBSpec	37%	59%
SBSpec(pMA19)	11%	35%
SBK1	26%	41%
SBK1(pRR5C)	44%	71%
phototrophic cultures		
SBK1	6%	23%
SBK1(pRR5C)	25%	57%

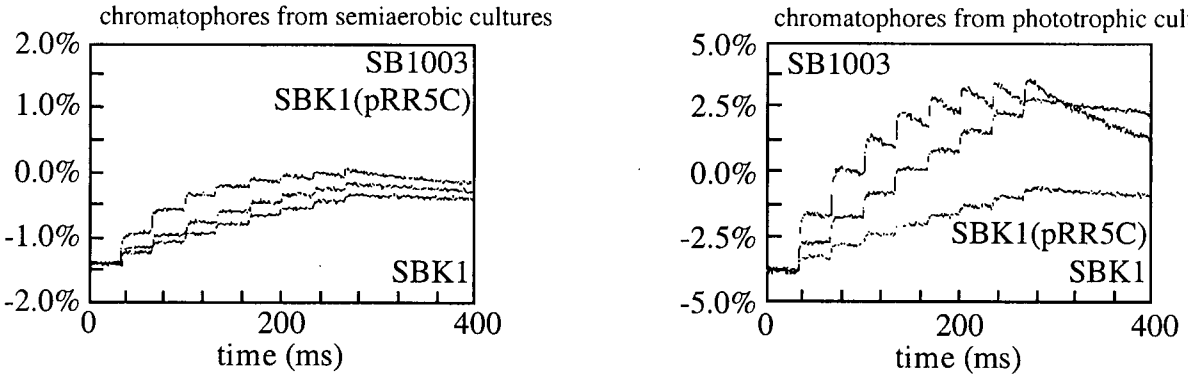

Figure 3.3.11. Extra PufQ improved the carotenoid bandshifts (room temperature, pathlength 1 cm) of chromatophores from semiaerobic (left) and phototrophic (right) cultures of the *puhC* deletion strain SBK1. Data collected by R. C. Prince.

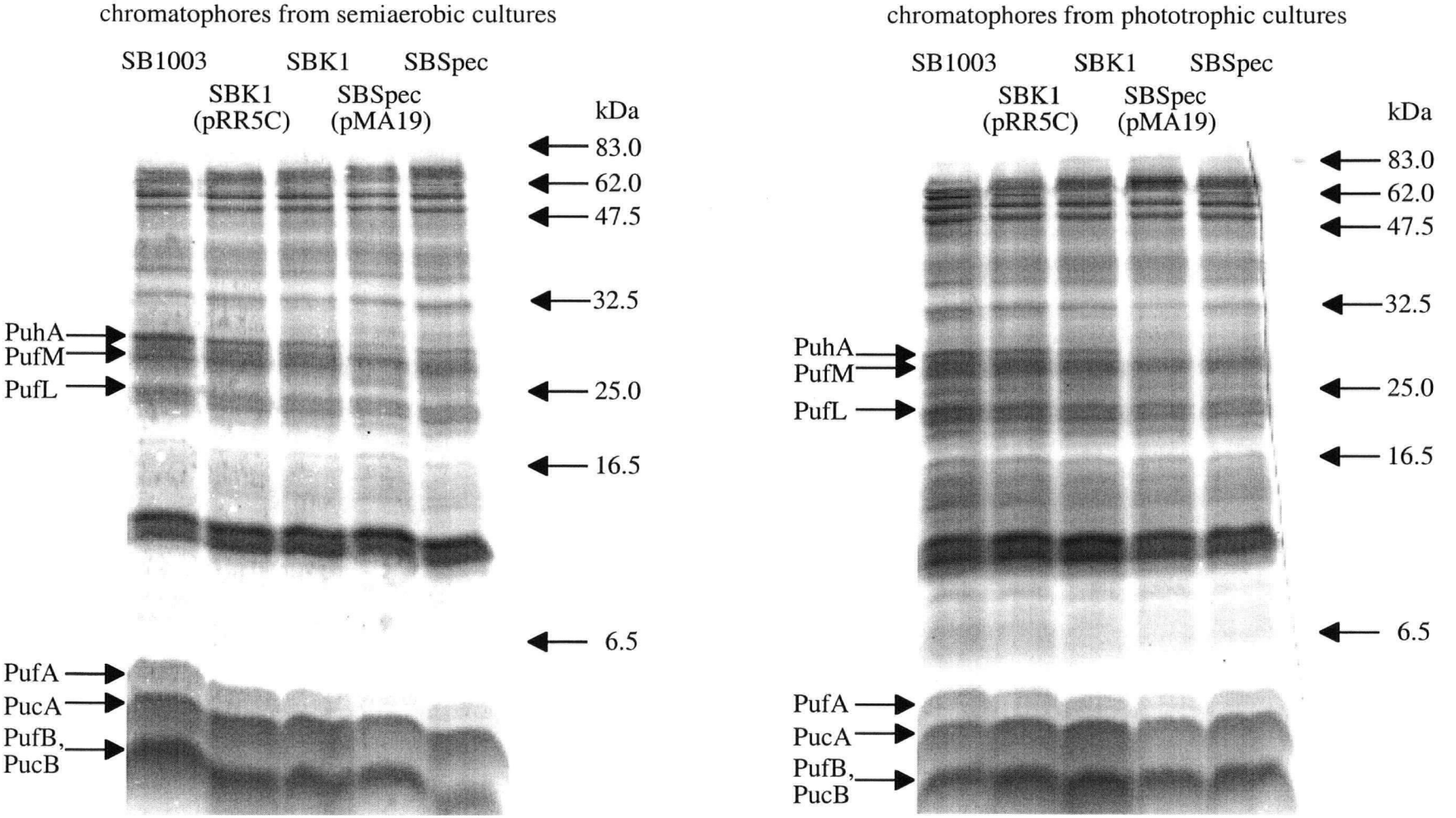

Figure 3.3.12. SDSPAGE of 50 μg of chromatophore protein: loss of PuhE (SBSpec), *puhE* restoration (pMA19), and extra PufQ (pRR5C) in the *puhC* deletion background (SBK1) affected the levels of polypeptides of the RC (PuhA, PufM, and PufL), and LH1 (PufA and PufB). Differences were most apparent in the intensities of the PuhA and PufA bands.

3.3.3. RC-LH1 gene transcription and translation in the *puhC* deletion strain SBK1

The cause of the RC-LH1 deficiency of the *puhC* deletion strain SBK1 was studied initially by evaluating transcription of the *puf* operon, which encodes all of the RC-LH1 polypeptides except PuhA. The results of a β-galactosidase assay of SBK1 and its *puhC*$^+$ parent SB1003, in which a PufB::LacZ fusion protein was expressed from the *puf* promoter on plasmid pXCA6::935, indicate that transcription and translation of the *puf* genes are normal in the absence of PuhC (Table 3.3.7). However, as reported in Sections 3.3.1 and 3.3.2, the plasmid used for this assay, pXCA6::935, carries an extra copy of *pufQ*, and *pufQ* merodiploidy mitigates the RC-LH1 deficiency and phototrophic growth defect of SBK1. The effects of *pufQ* mutations on transcription and translation of the remaining *puf* genes are complex (J. Smart, personal communication). Therefore, the possibility that deletion of *puhC* reduces *puf* operon transcription and *pufQ* merodiploidy counteracts this effect cannot be ruled out. Nevertheless, I assumed that the effects of a *puhC* deletion on the levels of the RC-LH1 core complex were predominantly due to impairment of a post-translational process such as assembly of either the RC or LH1.

Table 3.3.7. Similar β-galactosidase activity (nmol of *o*-nitrophenol per minute per 10^8 cells) was expressed from the *puf* promoter in *puhC*$^+$ (SB1003) and *puhC*$^-$ (SBK1) backgrounds.

semiaerobic cultures	Mean activity ± standard deviation of 3 samples
SB1003(pXCA6::935)	5.0 ± 1.6
SBK1(pXCA6::935)	4.4 ± 1.5
phototrophic cultures	
SB1003(pXCA6::935)	7.3 ± 0.9
SBK1(pXCA6::935)	6.0 ± 1.7

3.3.4. Minimal effect of PuhC on assembly of the RC

The kinetics of assembly and decay of the RC, in the absence of one or both LH1 polypeptides, PufB and PufA, were measured in *puhC*$^+$ (MA01) and *puhC*$^-$ (MA02) backgrounds, which contained a deletion of the chromosomal *pufQBALM* genes and were complemented with plasmids

carrying partial *puf* operons with deletions of either *pufB* or *pufA*, or both. The absence of LH1 was necessary in order to evaluate the amplitudes of RC peaks in absorption spectra, which are normally obscured by the LH1 peak at 880 nm. For a typical spectrum of a pure RC, see Figure 1.2.

The *puhC*$^+$ and *puhC*$^-$ strains were at similar culture densities throughout the experiments (Figure 3.3.13) and should have progressed similarly into semiaerobic growth conditions. A comparison of their absorption spectra over time (Figure 3.3.14) showed that the nascent RCs in the *puhC*$^-$ strains MA02(pTPR9) (lacking PufB), MA02(pTPR8) (lacking PufA), and MA02(pMA10) (lacking both LH1 polypeptides) were fairly similar to those in the *puhC*$^+$ strains MA01(pTPR9), MA01(pTPR8), and MA01(pMA10), respectively. Absorption at 780 nm, perhaps due to unbound BChl, dominated the spectra of all six strains after 9 hours of semiaerobic growth. After 15 hours, this absorption decreased and the RC voyeur BChl peaks at 800 nm began to appear distinct from the BPhe peaks at 760 nm in MA01(pTPR9) and MA01(pTPR8). The *puhC*$^-$ strains MA02(pTPR9) and MA02(pTPR8) had slightly more obscure RC peaks due to absorption at 780 nm. Both MA01(pMA10) (*puhC*$^+$) and MA02(pMA10) (*puhC*$^-$) appeared not to assemble the RC well due to the absence of both PufB and PufA. After 19.5 hours, the spectrum of MA01(pTPR9) had begun to resolve into the three peaks at 760 nm, 800 nm, and 865 nm characteristic of the RC. These features were less apparent in MA01(pTPR8) and were weakest in MA01(pMA10). Without PuhC, the BPhe and voyeur BChl peaks were of similar amplitude but slightly less well-resolved in MA02(pTPR9) and MA02(pTPR8), whereas the spectrum of MA02(pMA10) indicated very little RC assembly.

Quantitative analysis showed that the *puhC* deletion did not affect production of the RC, measured as the RC voyeur BChl peak area between 800 nm and 830 nm (Figure 3.3.15). The rates of production computed from these data (Table 3.3.8) confirmed that PuhC is not an RC production factor. As a measure of the "structural order" of the RC (defined in Section 2.15), I calculated the height ratio of the voyeur BChl peak at 800 nm and the BPhe peak at 760 nm (Figure 3.3.16), as well as the ratio of RC voyeur BChl peak-specific area (800 nm to 830 nm) to the total RC voyeur BChl peak area, which was inflated by BPhe and unbound BChl absorption (780 nm to 830 nm) (Figure 3.3.17). By both measures, the decrease in RC structural order due to the *puhC*

deletion appeared to be slight (and insignificant in MA02(pMA10) compared to MA01(pMA10), which lacked both LH1 polypeptides). Measurements of RC decay were not of sufficient quality to implicate or exclude the involvement of PuhC (Figure 3.3.18, Table 3.3.8). The rates of production computed from these data (Table 3.3.8) confirmed that PuhC is not an RC production factor.

RC production in these experiments was near the limit of detection, and the changes in absorbance over time were small and varied depending on which LH1 polypeptide was present. Nevertheless, I suggest that the *puhC* deletion does not interfere with RC production at all, and at most has a slight effect on RC structural order.

The *puhC*⁻ strains MA02(pTPR9), MA02(pTPR8), and MA02(pMA10), which lack both LH1 and LH2, grew phototrophically only after 48 hours of semiaerobic incubation (not shown), indicating that although the amount of RC produced in 19.5 hours was comparable to that in the MA01 background (Figures 3.3.14-3.3.15), another requirement for phototrophic growth had not been met. Therefore, either the slight effect of PuhC on RC structural order (see Figures 3.3.16 and 3.3.17) or another role of PuhC may be critical for the transition from semiaerobic respiratory growth to anaerobic phototrophy. In Section 3.5.3, I present evidence of such a role by showing that the negative effect of a *puhC* deletion on phototrophic growth is correlated with a low level of PufX, a protein associated with the RC-LH1 core complex.

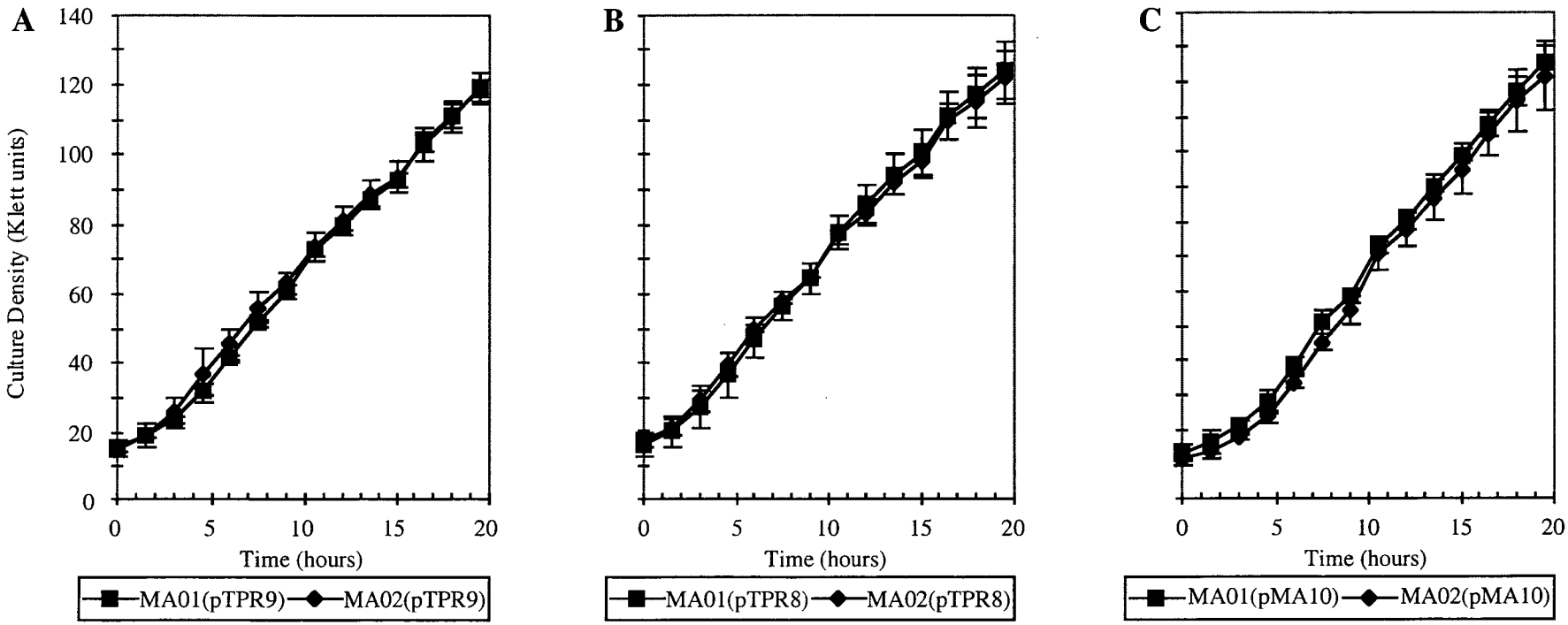

Figure 3.3.13. Semiaerobic growth of *puhC*$^+$ (MA01) and *puhC*$^-$ (MA02) strains expressing the RC (**A**) in the absence of PufB - plasmid pTPR9, (**B**) in the absence of PufA - plasmid pTPR8, and (**C**) in the absence of both LH1 polypeptides - plasmid pMA10.

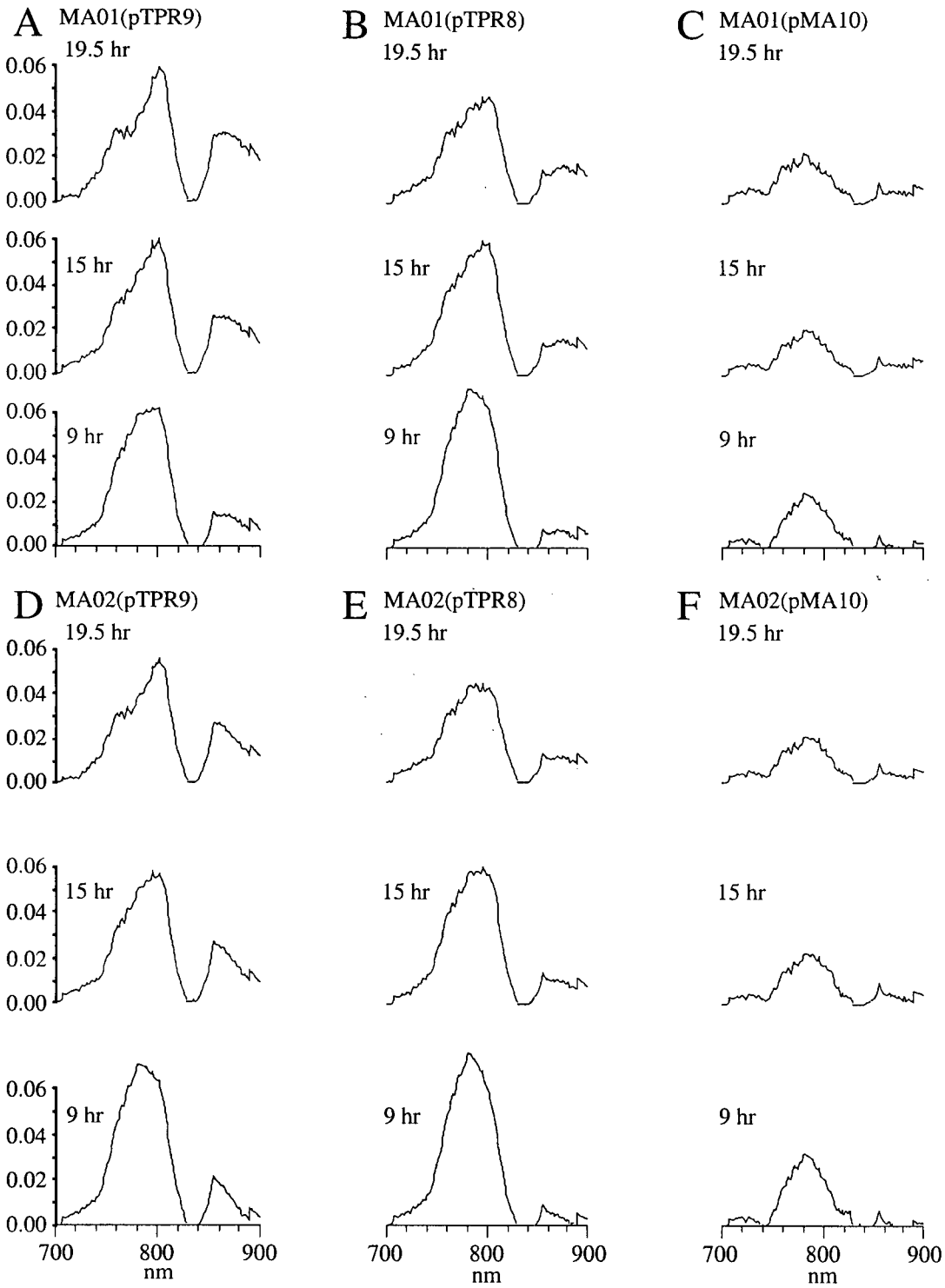

Figure 3.3.14. Absorption spectra (room temperature, pathlength 1 cm) of the nascent RC in the *puhC*$^+$ (MA01) and *puhC*$^-$ (MA02) backgrounds, in the absence of the LH1 polypeptides PufB - plasmid pTPR9 (**A**, **D**), PufA - plasmid pTPR8 (**B**, **E**), or both - plasmid pMA10 (**C**, **F**), after 9 hours, 15 hours, and 19.5 hours of semiaerobic growth. Spectra were normalized and a baseline was drawn as described in Section 2.15. In addition to RC absorption at 760 nm, 800 nm, and 865 nm, there is a peak at 780 nm, attributed to unbound BChl.

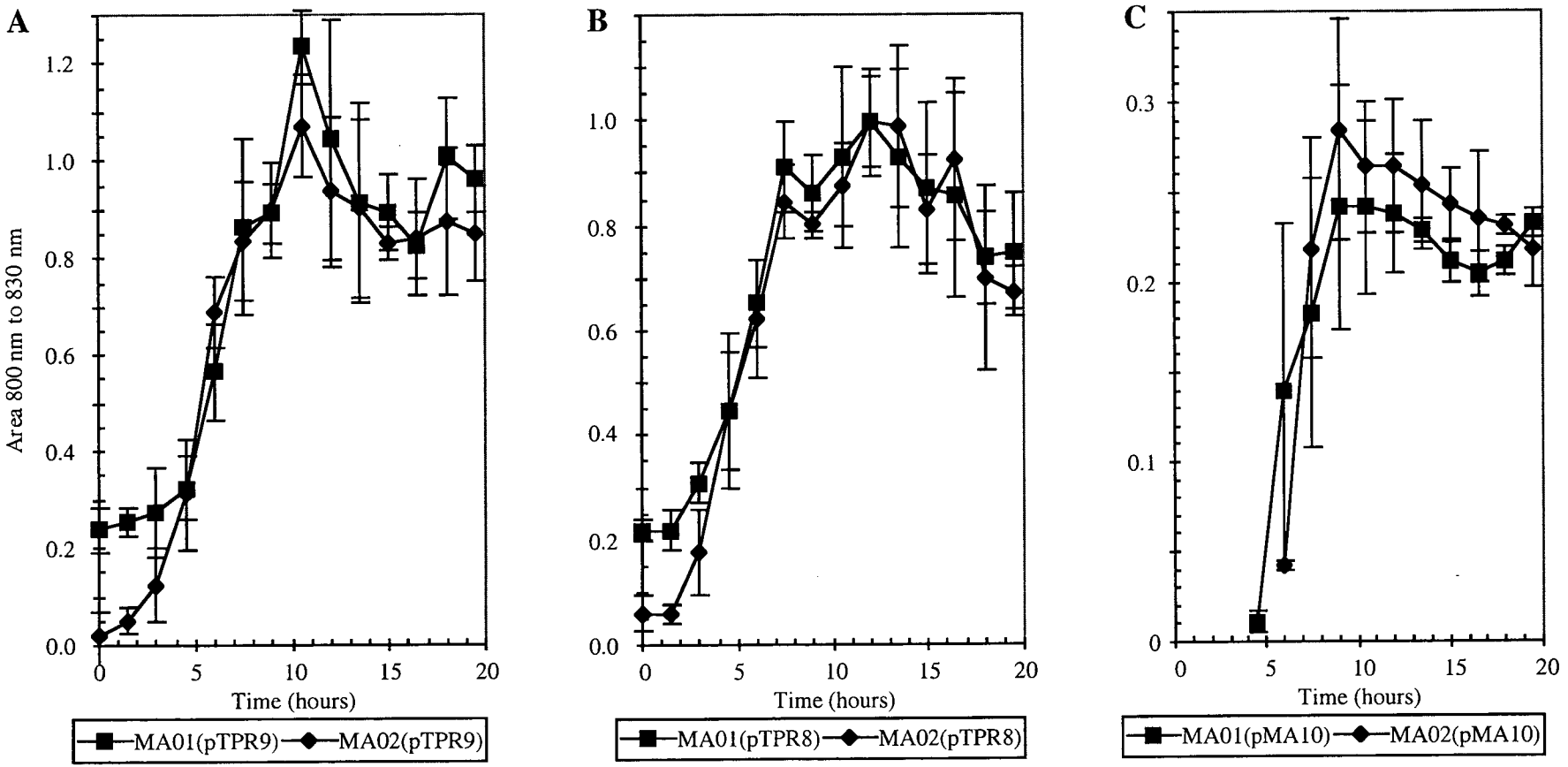

Figure 3.3.15. Production of the RC (**A**) in the absence of PufB - plasmid pTPR9, (**B**) in the absence of PufA - plasmid pTPR8, and (**C**) in the absence of both LH1 polypeptides - plasmid pMA10, in the *puhC*$^{+}$ (MA01) and *puhC*$^{-}$ (MA02) backgrounds. A portion of the RC voyeur BChl peak area was measured from 800 nm to 830 nm to minimize the contribution of absorption by BPhe and unbound BChl. The *puhC* deletion did not affect RC production.

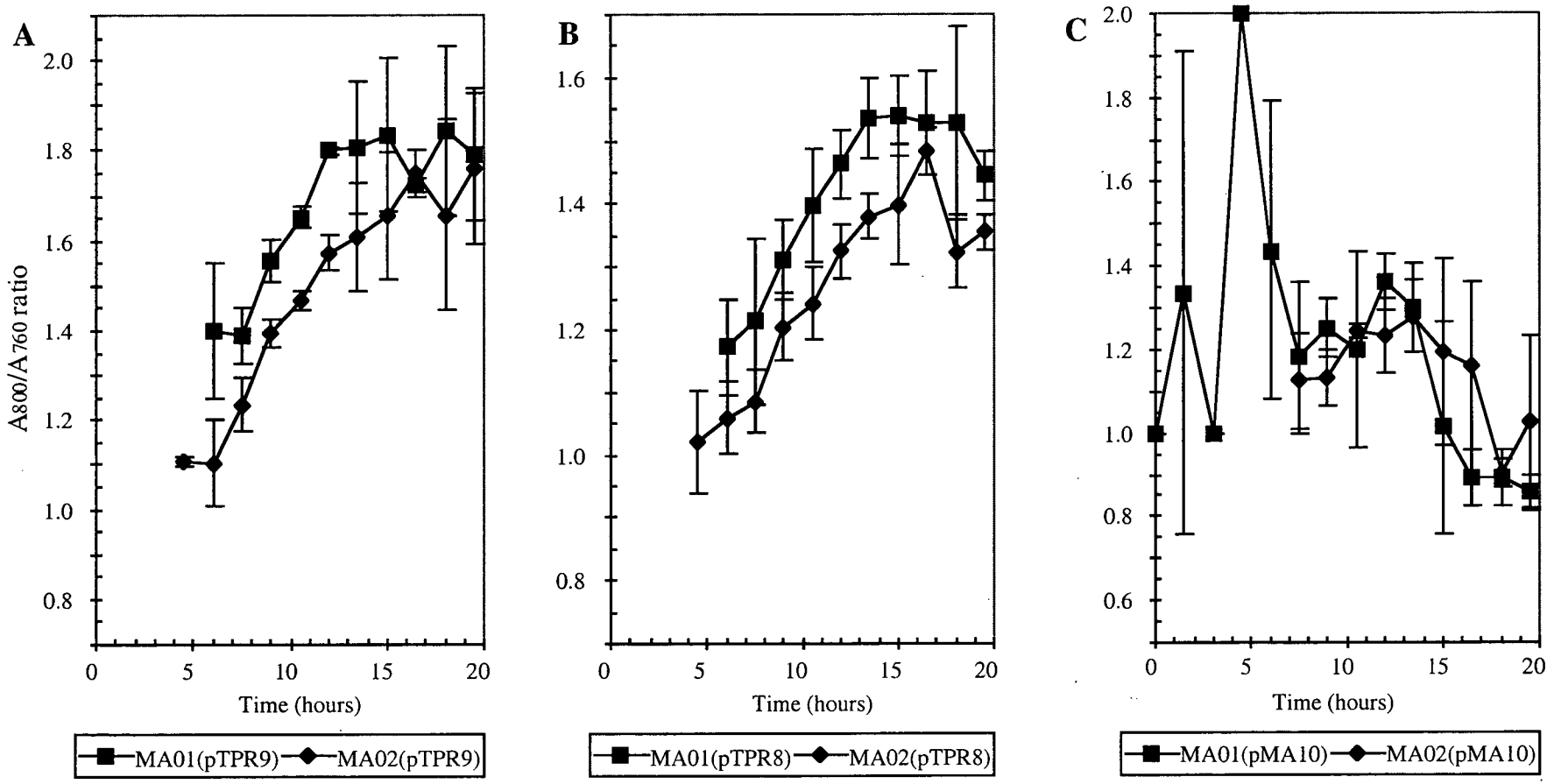

Figure 3.3.16. Peak height ratio of the RC (**A**) in the absence of PufB - plasmid pTPR9, (**B**) in the absence of PufA - plasmid pTPR8, and (**C**) in the absence of both LH1 polypeptides - plasmid pMA10, in the *puhC*$^+$ (MA01) and *puhC*$^-$ (MA02) backgrounds. The height of the voyeur BChl peak at 800 nm was divided by that of the BPhe peak at 760 nm, as a measure of RC "structural order," the proper binding of pigments to polypeptides. In the presence of either PufA or PufB, the *puhC* deletion reduced RC structural order slightly but significantly. In the absence of both LH1 polypeptides, RC structural order was compromised regardless of PuhC.

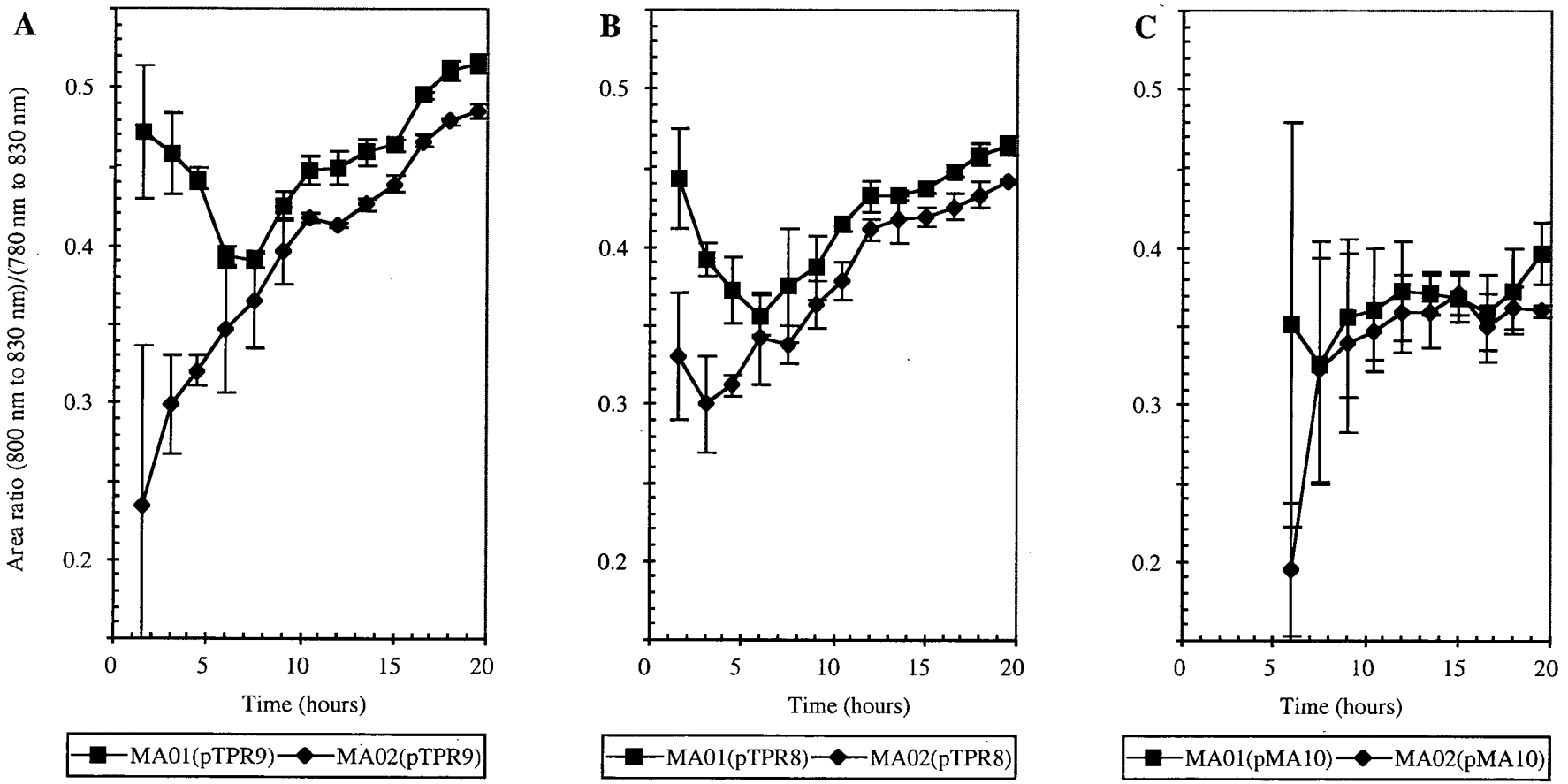

Figure 3.3.17. Voyeur BChl-specific peak area ratio of the RC (**A**) in the absence of PufB - plasmid pTPR9, (**B**) in the absence of PufA - plasmid pTPR8, and (**C**) in the absence of both LH1 polypeptides - plasmid pMA10, in the *puhC*$^{+}$ (MA01) and *puhC*$^{-}$ (MA02) backgrounds. The area of a portion of the voyeur BChl peak from 800 nm to 830 nm was divided by the area from 780 nm to 830 nm (which was inflated by absorption from the BPhe peak at 760 nm and the unbound BChl peak at 780 nm), as a measure of RC "structural order," the proper binding of pigments to polypeptides. In the presence of either PufA or PufB, the *puhC* deletion reduced RC structural order slightly but significantly. In the absence of both LH1 polypeptides, RC structural order was compromised regardless of PuhC.

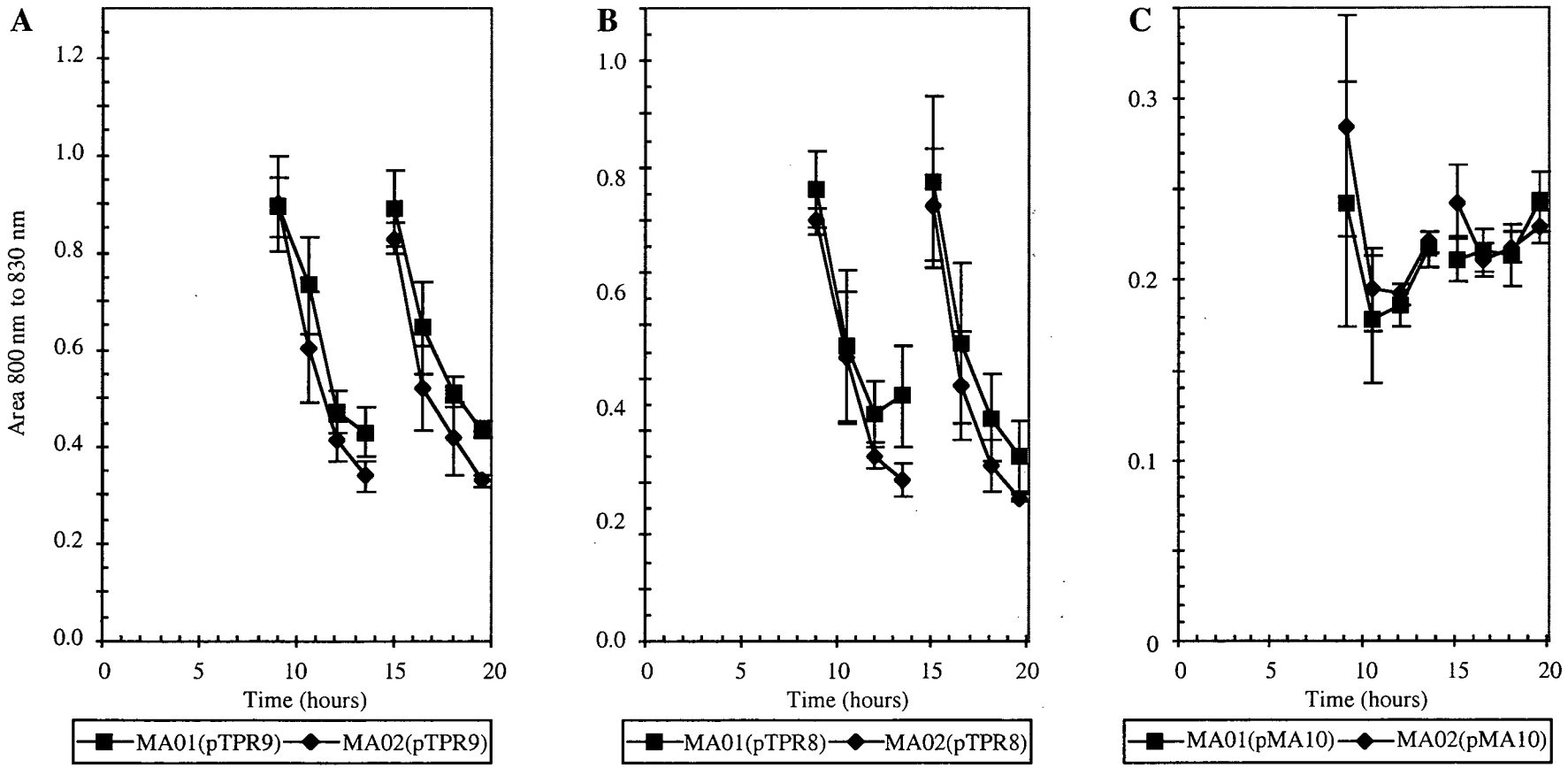

Figure 3.3.18. Decay of the RC (**A**) in the absence of PufB - plasmid pTPR9, (**B**) in the absence of PufA - plasmid pTPR8, and (**C**) in the absence of both LH1 polypeptides - plasmid pMA10, in the *puhC*$^{+}$ (MA01) and *puhC*$^{-}$ (MA02) backgrounds. Decay was initiated at 9 hr and at 15 hr by switching cultures to aerobic conditions. A portion of the RC voyeur BChl peak area was measured from 800 nm to 830 nm to minimize the contribution of absorption by BPhe and unbound BChl.

Table 3.3.8. Linear production rates (area units per hour) and exponential decay rate constants (per hour) for the RC in *puhC*$^+$ (MA01) and *puhC*$^-$ (MA02) backgrounds, determined from triplicate cultures. A portion of the RC voyeur BChl peak area was measured from 800 nm to 830 nm. Note: post-assembly RC decay in pMA10 strains (after 15 hours of semiaerobic growth) was a transient and insignificant phenomenon.

Strain	Genotype chromosome (plasmid)	RC production	Mid-assembly RC decay	Post-assembly RC decay
MA01(pTPR9)	*pufQBALM*$^-$*X*$^+$*puhC*$^+$(*pufQALMX*)	161 ± 32	234 ± 89	239 ± 91
MA02(pTPR9)	*pufQBALM*$^-$*X*$^+$*puhC*$^-$(*pufQALMX*)	182 ± 30	329 ± 163	324 ± 159
MA01(pTPR8)	*pufQBALM*$^-$*X*$^+$*puhC*$^+$(*pufQBLMX*)	156 ± 35	396 ± 192	327 ± 268
MA02(pTPR8)	*pufQBALM*$^-$*X*$^+$*puhC*$^-$(*pufQBLMX*)	161 ± 45	356 ± 139	457 ± 62
MA01(pMA10)	*pufQBALM*$^-$*X*$^+$*puhC*$^+$(*pufQLMX*)	35 ± 7	235 ± 139	28 ± 22
MA02(pMA10)	*pufQBALM*$^-$*X*$^+$*puhC*$^-$(*pufQLMX*)	43 ± 5	303 ± 126	103 ± 46

3.3.5. Minimal effect of PuhC on assembly of LH1

Kinetics of assembly and decay of LH1 were measured in *puhC*$^+$ (MA01) and *puhC*$^-$ (MA02) backgrounds, which contained a deletion of the chromosomal *pufQBALM* genes and were complemented with only the *pufQBAX* genes on plasmid p*Stu* I. Such removal of genes encoding two RC polypeptides, PufL and PufM, leaving only PuhA, allowed the evaluation of LH1-specific absorption at 880 nm without the minor contribution of the RC special pair BChl peak at 865 nm. The strains MA01(p*Stu* I) (*puhC*$^+$) and MA02(p*Stu* I) (*puhC*$^-$) were at similar culture densities throughout the experiments (Figure 3.3.19) and should have progressed similarly into semiaerobic growth conditions. The amounts of LH1 after 9, 15, and 19.5 hours of semiaerobic growth remained the same in MA02(p*Stu* I), whereas a higher steady-state level was reached in MA01(p*Stu* I) (Figure 3.3.19). The production rates computed from these data, shown in Table 3.3.9, suggested that the *puhC* deletion strain exhibits somewhat more rapid LH1 assembly; however, the large standard deviation indicates that the difference, if real, may not be reproducible using this approach. Measurements of LH1 decay (Figure 3.3.19, Table 3.3.9) were not of sufficient quality to implicate or exclude the involvement of PuhC. In the spectra of both MA01(p*Stu* I) and MA02(p*Stu* I), absorption at 780 nm was observed, perhaps due to unbound BChl (Figure 3.3.20).

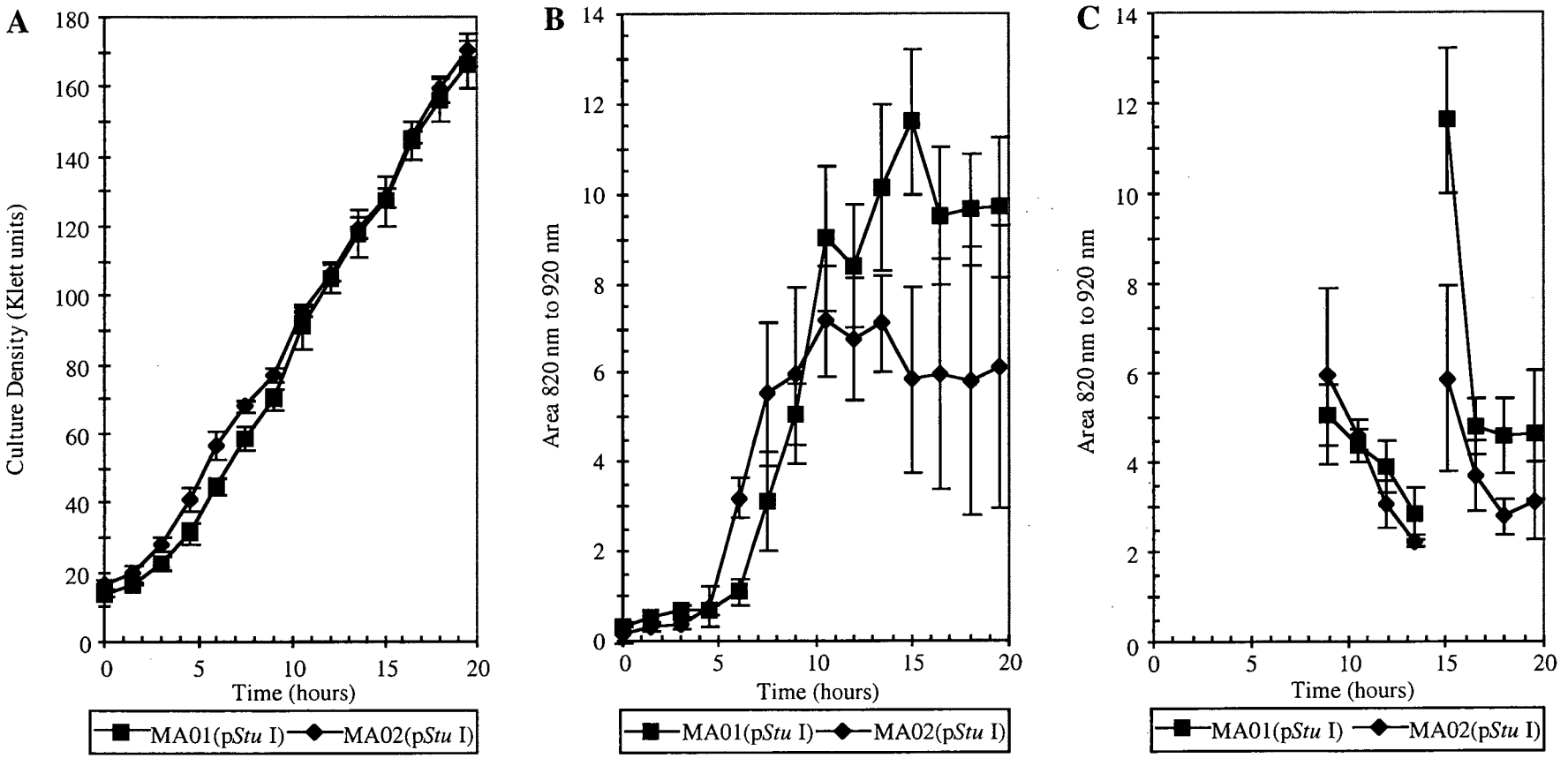

Figure 3.3.19. Assembly and decay of LH1 in the absence of PufL and PufM - plasmid p*Stu* I, in the *puhC*$^+$ (MA01) and *puhC*$^-$ (MA02) backgrounds. (**A**) Semiaerobic growth. (**B**) Production of LH1, measured as the peak area from 820 nm to 920 nm. (**C**) Decay of LH1, initiated at 9 hr and at 15 hr by switching cultures to aerobic conditions.

Table 3.3.9. Linear production rates (area units per hour) and exponential decay rate constants (per hour) for LH1 in *puhC*$^+$ (MA01) and *puhC*$^-$ (MA02) backgrounds, determined from triplicate cultures. The LH1 peak area was measured from 820 nm to 920 nm.

	Genotype chromosome (plasmid)	LH1 production	Mid-assembly LH1 decay	Post-assembly LH1 decay
MA01(p*Stu* I)	*pufQBALM*$^-$*X*$^+$*puhC*$^+$(*pufQBA...X?*)	525 ± 12	37 ± 185	628 ± 35
MA02(p*Stu* I)	*pufQBALM*$^-$*X*$^+$*puhC*$^-$(*pufQBA...X?*)	677 ± 141	176 ± 119	408 ± 147

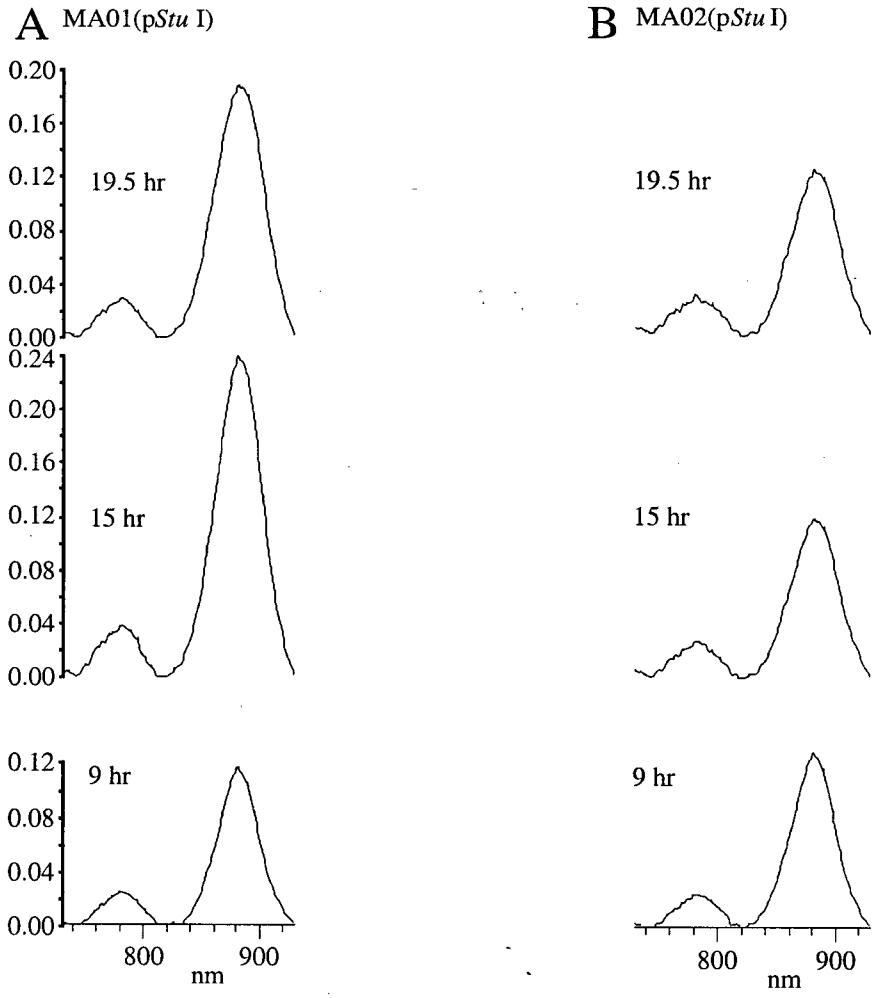

Figure 3.3.20. Absorption spectra (room temperature, pathlength 1 cm) of nascent LH1 in (**A**) *puhC*$^+$ (MA01) and (**B**) *puhC*$^-$ (MA02) backgrounds, in the absence of the RC polypeptides PufL and PufM - plasmid p*Stu* I, after 9 hours, 15 hours, and 19.5 hours of semiaerobic growth. Spectra were normalized and a baseline was drawn as described in Section 2.15. In addition to LH1 absorption at 880 nm, there is a small peak at 780 nm, attributed to unbound BChl.

It is clear from Section 3.3.4 that the amount of RC is not directly reduced by the *puhC* deletion, and the results of this section suggest that the direct effect of PuhC on LH1 alone is also small. Another possibility, that PuhC is required for the organization of the RC-LH1 core complex

as a whole, is suggested by the effect of PuhC on the level of PufX, a protein that does not accumulate in the absence of an intact core complex. I present this result in Section 3.5.3.

3.3.6. Immunodetection and TOXCAT analysis of PuhC

The 6xHis-tagged proteins PuhC-N and PuhC-NS (see Table 2.7) were overexpressed in *E. coli* M15 under the control of *lacI*^{q} T5 RNA polymerase. PuhC-C was not expressed at detectable levels in M15 and was not studied further due to promising results with PuhC-N.

For each expression experiment, the amount of 6xHis-tagged protein relative to other bands seen on polyacrylamide gels was best in 2xYT medium, although LB and Terrific Broth also gave similar yields. PuhC-N was soluble in the presence of 1% lauryldimethylamine oxide (LDAO), and PuhC-NS was soluble without detergent. During purification, the PuhC-N protein partially underwent proteolytic digestion, which amino acid analysis and the size of the N-terminal fragment suggested was due to the *E. coli* outer membrane protease OmpT, with proteolysis between Arg107 and Arg108. Both PuhC-N and PuhC-NS were purified, concentrated to about 20 mg/ml, sequenced from the N-terminus, and used to immunize rabbits. The expression, solubilization, and purification of PuhC-NS are shown in Figure 3.3.21.

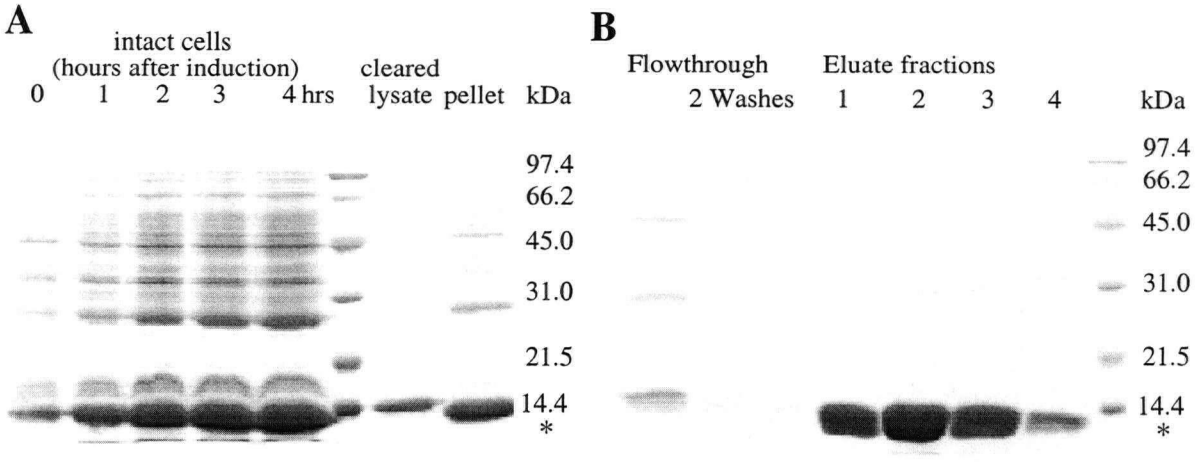

Figure 3.3.21. SDSPAGE showing (**A**) expression of recombinant PuhC-NS and (**B**) purification from *E. coli* via a nickel resin. The asterisk marks the band that corresponds to the PuhC-NS protein (expected size 13.0 kDa).

The antiserum detected PuhC in unfractionated cells and in chromatophores of the wild type strain SB1003 (Figure 3.3.22), which demonstrated that PuhC co-purifies with the photosynthetic apparatus. This band was consistently much more intense in chromatophores of SBK1(pMA1), which co-transcribed *pufQ* and 6xHis-tagged *puhC-N*, as well as in the chromatophore-free supernatant of SBK1(pMA3), which co-transcribed *pufQ* and the TM segmentless 6xHis-tagged *puhC-NS*. I have not yet identified the cause of this apparent superabundance. Whereas translation with the 6xHis tag did not exclude PuhC from its proper intracellular location, the observation that only a trace of PuhC-NS was associated with chromatophores (possibly trapped inside vesicles), and almost all of this truncated protein was in the supernatant, indicates that the TM segment of PuhC is required to tether it to the membrane.

The amount of PuhC in chromatophores of the LH2$^-$ *puhB* deletion strain DW23 was at least as much as in its *puhB*$^+$ parent MW442 (Figure 3.3.23). Preliminary observations with the LH2$^+$ strain MA05 and its complemented derivatives also suggest that PuhC may be slightly upregulated in the absence of PuhB (not shown).

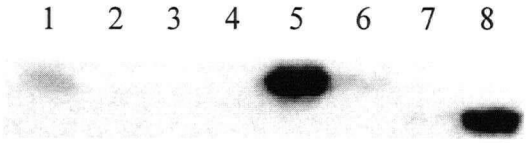

Figure 3.3.22. Immunodetection of PuhC's TM segment-dependent association with chromatophores. The antiserum detected PuhC in 50 μg of chromatophore protein from the wild type strain SB1003 (lane 1), but not in supernatant protein after chromatophores were removed by two rounds of ultracentrifugation (lane 2), in chromatophores of the *puhC* deletion strain SBK1 (lane 3), or in the supernatant protein of SBK1 (lane 4). Chromatophores of SBK1(pMA1), which co-expressed PufQ and the 6xHis-tagged protein PuhC-N from the *puf* promoter on a plasmid, contained much more of the protein (lane 5), of which only a trace amount was found in the supernatant (lane 6). Chromatophores of SBK1(pMA3), which co-expressed PufQ with the TM segmentless 6xHis-tagged PuhC-NS protein, contained no more than a trace amount of PuhC-NS (lane 7); a large amount of PuhC-NS was in the supernatant (lane 8).

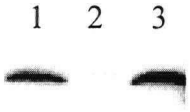

Figure 3.3.23. Immunodetection of PuhC in a *puhB* deletion strain. PuhC was detected in 50 μg of chromatophore protein from the LH2$^-$ strain MW442 (lane 1). This band was absent from chromatophores of the LH2$^-$ *puhC* deletion strain MWK1 (lane 2), but at least as intense in chromatophores of the LH2$^-$ *puhB* deletion strain DW23 (lane 3) as in MW442.

A TOXCAT hybrid with the predicted TM segment of PuhC (Figure 3.3.24) supported growth of *E. coli* MM39 on maltose minimal medium (not shown), indicating that this segment spans a bacterial inner membrane. No self-association of the PuhC TM segment was observed in a TOXCAT assay (not shown). The C-terminal, predicted periplasmic domain of PuhC (C118), expressed as a CyaA hybrid, did not exhibit any interaction with itself or with domains of PuhB (for specifics, see Section 3.2.6).

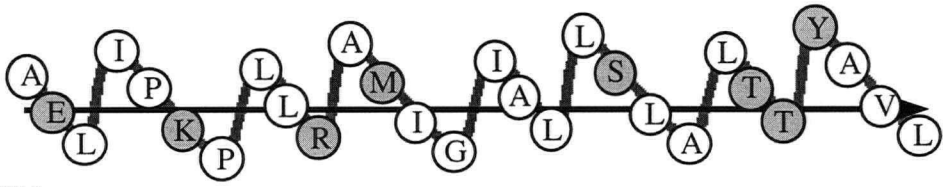

PuhC TM

Figure 3.3.24. The putative TM segment of PuhC. Grey circles mark potential electrostatic, hydrogen bonding, dipole-dipole, and aromatic ring stacking interactions. The arrow, pointing toward the C-terminus, indicates a face of the helix where I propose that it may interact with another helix based on the locations of residues capable of participation in interactions.

3.3.7. Attempt to purify 6xHis-tagged PuhC and associated proteins from *R. capsulatus*

Preliminary attempts to solubilize the RC-LH1 core complex from chromatophores of the LH2$^-$ *puhC-N*-complemented *puhC* deletion strain MWK1(pMA1) by use of the detergent diheptanoylphosphatidylcholine (DHPC) revealed that both the core complex and PuhC-N were solubilized by 15 mM DHPC. The PuhC-N protein, unfortunately, was not retained by a nickel column, indicating that the 6xHis tag may be either proteolytically removed or buried in an inaccessible environment (Figure 3.3.25).

When the concentration of DHPC was increased to 20 mM, the amount of LH1 in the soluble fraction was greatly reduced, apparently without release of much BChl (Figure 3.3.25), suggesting that removal of LH1 from the RC-LH1 complex may result in aggregation of LH1, which is pelleted by ultracentrifugation. The BPhe and voyeur BChl peaks of the RC were visible, but the special pair BChl was obscured by some residual LH1-like absorbance at 880 nm, apparently a portion of LH1 that remained soluble with the RC. PuhC-N remained soluble. It is not yet known whether the PufX protein remained associated with the RC or was pelleted with LH1.

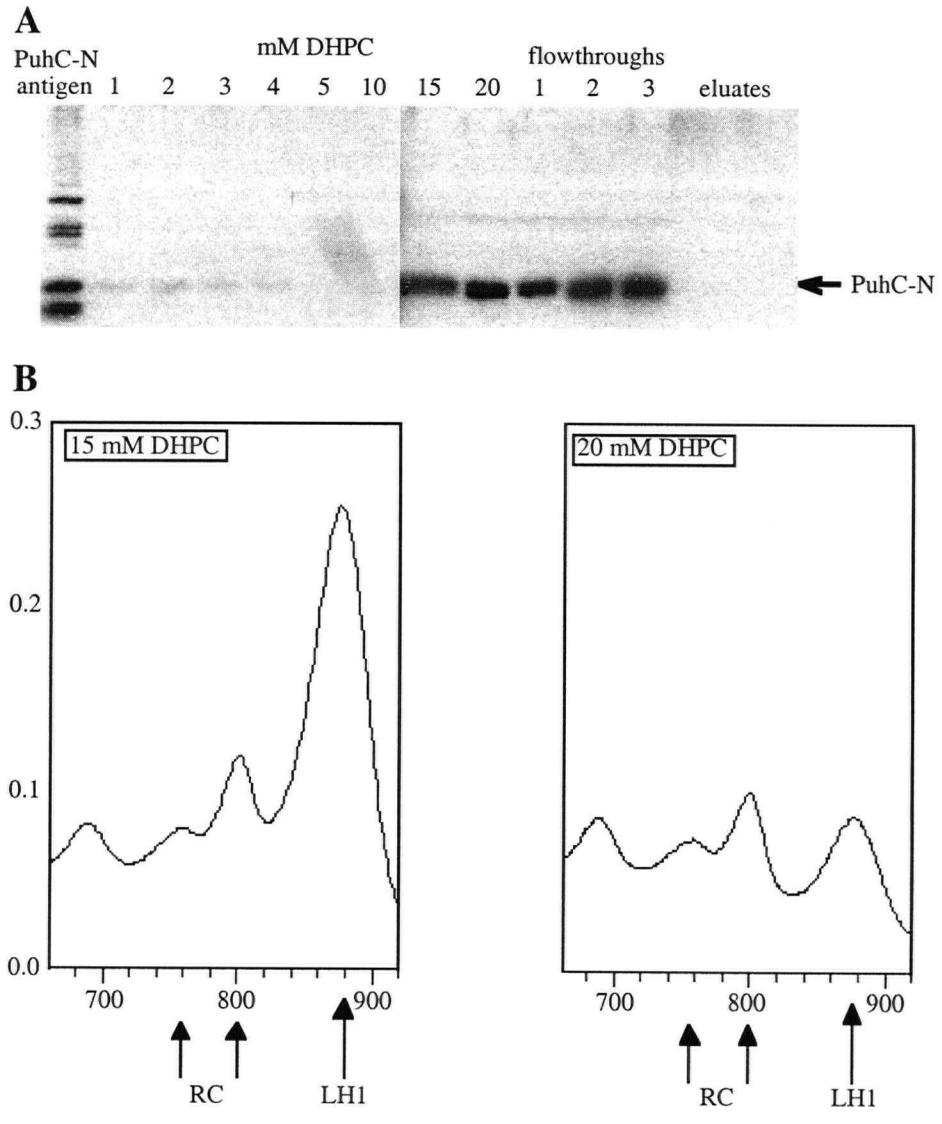

Figure 3.3.25. Solubilization of the RC-LH1 complex and PuhC-N from chromatophores of *R. capsulatus* strain MWK1(pMA1). (**A**) Immunoblot for PuhC in 16 μl of fractions solubilized from chromatophores with DHPC, and in early, middle, and late fractions of the flowthrough that did not bind to a nickel agarose resin. (**B**) Absorption spectra (room temperature, pathlength 1 cm) to detect the RC and LH1 in the fractions of soluble protein.

To summarize the results of this subchapter, several factors contribute to the phototrophic growth defect of *puhC*$^-$ strains: insufficient PufQ, insufficient adaptation time under semiaerobic conditions, and inhibitory effects of PuhE and LH2. The individual effects of PuhC on RC and LH1 assembly are subtle. Together, these factors result in an RC-LH1 deficiency but do not impair electron transport. It seems appropriate to categorize PuhC as an membrane-localized organization factor of the RC-LH1 core complex as a whole. Interestingly, *puhC* gene homologues complement the *puhC*$^-$ mutant phenotypes fully, partially, or not at all.

3.4. Characterization of PuhE as an RC-LH1 assembly control factor

3.4.1. The growth defect of the *puhE* deletion strains MA06 and MA07

The involvement of *puhE* in phototrophic growth was first discovered by construction of a deletion mutation of *puhC* with insertion of the Ω cartridge to abolish transcription of the 3' gene *puhE* in strains SBSpec ($LH2^+$) and MWSpec ($LH2^-$) (56). The observation that this polar mutation mitigated the $LH2^+$ *puhC* deletion phenotype of SBK1 was confirmed and further investigated by restoring *puhE* to both SBK1 and SBSpec in *trans* on plasmid pMA19 (see Section 3.3.1). I also confirmed that the polar effect on *puhE* did not improve phototrophic growth in the $LH2^-$ background by comparing MWSpec to the *puhC* deletion nonpolar mutant strain MWK1 (Table 3.4.1). In addition to this *puhC*-antagonistic role of *puhE*, the observation that plasmid pAH8, encoding a *pufQ-puhC* co-transcript, fully complemented the growth defects of SBK1 and MWK1, but not those of SBSpec and MWSpec, indicated a positive role of *puhE* in phototrophic growth (56). I confirmed this observation by use of plasmid pMA12, which carries only the *puhC-N* gene and not *pufQ*, to evaluate the effect of restoration of 6xHis-tagged *puhC* alone to SBSpec and MWSpec (Table 3.4.1). However, the definitive experiment would be to use a plasmid carrying untagged *puhC* without *pufQ*.

For a more thorough investigation of the role of *puhE*, I deleted the *puhE* gene and inserted a transcriptionally congruent KIXX cartridge in both $LH2^+$ and $LH2^-$ backgrounds (strains SB1003 and MW442) to produce strains MA06 and MA08, respectively. This cartridge generally does not terminate transcription (as evidenced by *puhC* mRNA in SBK1 in Figure 3.3.1, and PufX protein in MA01(pTL2) in Figure 3.5.9). The same deletion in SB1003 and MW442 with insertion of an Ω cartridge, expected to terminate transcription, produced strains MA07 and MA10, respectively.

There was considerable variability in the phototrophic growth of strains MA06 and MA07 compared to SB1003, and of MA08 and MA10 compared to MW442 (Figure 3.4.1, Tables 3.4.2 and 3.4.3). Generally, actively growing aerobic inocula showed the greatest difference; semiaerobic and densely grown aerobic inocula of the $puhE^-$ strains sometimes showed no phototrophic growth defect at all. There was no reproducible difference between $puhE^-$ strains bearing the KIXX and Ω

cartridges, and so termination of transcription made no difference to the phenotype. Therefore, *puhE* is likely to be the last photosynthesis gene of the *puh* operon (depicted in Figure 1.3).

Table 3.4.1. The phototrophic growth defects of the *puhC* deletion polar mutants SBSpec ($LH2^+$) and MWSpec ($LH2^-$) after 24 hours of semiaerobic growth were not fully compensated by restoration of *puhC-N* on pMA12.

$LH2^+$ strains	Genotype	Relative specific growth rate ± standard deviation of 3 cultures
SB1003	*pucC⁺pufQ⁺puhC⁺E⁺*	100% ± 1%
SBK1	*pucC⁺pufQ⁺puhC⁻E⁺*	13% ± 1%
SBK1(pMA20)	*pucC⁺pufQ⁺puhC⁻E⁺*(empty)	12% ± 1%
SBK1(pMA12)	*pucC⁺pufQ⁺puhC⁻E⁺(puhC-N)*	99% ± 1%
SBSpec	*pucC⁺pufQ⁺puhC⁻ΩE⁻*	59% ± 2%
SBSpec(pMA12)	*pucC⁺pufQ⁺puhC⁻ΩE⁻(puhC-N)*	92% ± 2%
$LH2^-$ strains		
MW442	*pucC⁻pufQ⁺puhC⁺E⁺*	100% ± 5%
MWK1	*pucC⁻pufQ⁺puhC⁻E⁺*	68% ± 5%
MWK1(pMA12)	*pucC⁻pufQ⁺puhC⁻E⁺(puhC-N)*	106% ± 4%
MWSpec	*pucC⁻pufQ⁺puhC⁻ΩE⁻*	70% ± 3%
MWSpec(pMA12)	*pucC⁻pufQ⁺puhC⁻ΩE⁻(puhC-N)*	80% ± 3%

Plasmid pMA19, which carries the *puhE* gene under control of the *puf* promoter, and plasmid pMA11, which encodes a *pufQ-puhE* transcriptional fusion, occasionally had apparent restorative effects on the growth of MA06 and MA07 (Figure 3.4.1, Table 3.4.2), but complementation with the *puhE* gene in *trans* was partial at best and sometimes insignificant (Table 3.4.2). The data in Sections 3.3.1 and 3.3.2 reaffirmed the difficulty of *trans*-complementation for *puhE*: the phototrophic growth defect and RC-LH1 deficiency of SBSpec(pMA19), with PuhE expressed from the plasmid, were more severe than those of SBK1, which had no transcription termination signal 5' of the chromosomal *puhE* gene. Thus, either the copy number of *puhE* or its transcription from the plasmid-borne *puf* promoter rather than the chromosomal *puh* promoter (with transcriptional readthrough from the *bchF* promoter) may interfere with phototrophic growth.

An extra copy of *pufQ* on plasmid pRR5C did not improve the growth of MA06 and MA07, but was observed to improve the growth of the $LH2^-$ strains MA08 and MA10. Examples of both failed and successful complementations are shown (Tables 3.4.2 and 3.4.3, Figure 3.4.1).

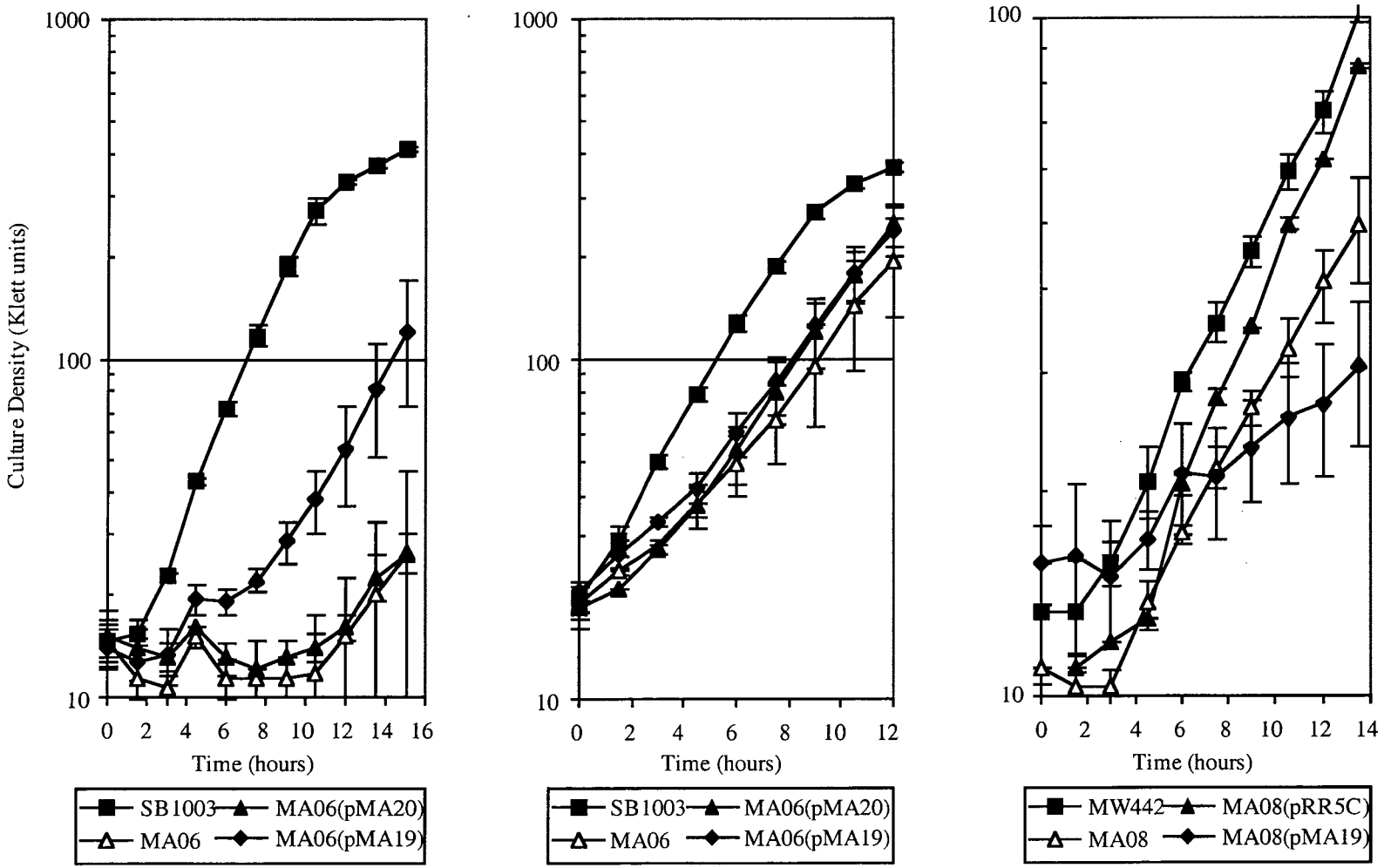

Figure 3.4.1. *Trans*-complementation of the phototrophic growth defect of *puhE* deletion strains MA06 and MA08 with *puhE* (plasmid pMA19) was variable. pMA20 is the empty vector. Extra *pufQ* (plasmid pRR5C) improved the growth of the LH2$^-$ *puhE* deletion strain MA08. Phototrophic cultures were inoculated from actively growing aerobic cultures (left and right), and from briefly semiaerobic cultures (centre).

Table 3.4.2. The phototrophic growth defects of the *puhE* deletion strains MA06 and MA07 were not remedied by *trans*-complementation with pMA19. pMA20 is the empty vector. Anaerobic phototrophic cultures were inoculated from actively growing aerobic cultures and then from the same cultures incubated semiaerobically for 3 hours.

aerobic inocula	Genotype chromosome (plasmid)	Relative specific growth rate ± standard deviation of 2-3 cultures
SB1003	*puhE*$^+$	100% ± 4%
MA06	*puhE*$^-$	38% ± 34%
MA06(pMA20)	*puhE*$^-$(empty)	44% ± 3%
MA06(pMA19)	*puhE*$^-$(*puhE*)	50% ± 17%
MA07	*puhE*$^-$Ω	38% ± 28%
MA07(pMA20)	*puhE*$^-$Ω(empty)	1% ± 1%
MA07(pMA19)	*puhE*$^-$Ω(*puhE*)	71% ± 6%
semiaerobic inocula		
SB1003	*puhE*$^+$	100% ± 6%
MA06	*puhE*$^-$	63% ± 15%
MA06(pMA20)	*puhE*$^-$(empty)	74% ± 6%
MA06(pMA19)	*puhE*$^-$(*puhE*)	68% ± 8%
MA07	*puhE*$^-$Ω	41% ± 26%
MA07(pMA20)	*puhE*$^-$Ω(empty)	70% ± 9%
MA07(pMA19)	*puhE*$^-$Ω(*puhE*)	64% ± 9%

Table 3.4.3. The phototrophic growth defects of the *puhE* deletion strains MA06 and MA07, grown from aerobic inocula, could be remedied by *trans*-complementation with *pufQ-puhE* (pMA11), but not *pufQ* alone (pRR5C).

LH2$^+$ strains	Genotype chromosome (plasmid)	Relative specific growth rate ± standard deviation of 2-3 cultures
SB1003	*pucC*$^+$*puhE*$^+$	100% ± 10%
MA06	*pucC*$^+$*puhE*$^-$	23% ± 14%
MA06(pRR5C)	*pucC*$^+$*puhE*$^-$(*pufQ*)	22% ± 13%
MA06(pMA11)	*pucC*$^+$*puhE*$^-$(*pufQpuhE*)	64% ± 17%
MA07	*pucC*$^+$*puhE*$^-$Ω	16% ± 10%
MA07(pRR5C)	*pucC*$^+$*puhE*$^-$Ω(*pufQ*)	36% ± 2%
MA07(pMA11)	*pucC*$^+$*puhE*$^-$Ω(*pufQpuhE*)	69% ± 4%
LH2$^+$ strains		
MW442	*pucC*$^-$*puhE*$^+$	100% ± 6%
MA08	*pucC*$^-$*puhE*$^-$	85% ± 8%
MA08(pRR5C)	*pucC*$^-$*puhE*$^-$(*pufQ*)	116% ± 0%
MA08(pMA19)	*pucC*$^-$*puhE*$^-$(*pufQpuhE*)	36% ± 9%
MA10	*pucC*$^-$*puhE*$^-$Ω	52% ± 10%
MA10(pRR5C)	*pucC*$^-$*puhE*$^-$Ω(*pufQ*)	94% ± 5%
MA10(pMA19)	*pucC*$^-$*puhE*$^-$Ω(*pufQpuhE*)	62% ± 18%

3.4.2. The RC-LH1 deficiency of the *puhE* deletion strain MA06

The absorption spectrum of intact cells of the LH2$^-$ *puhE*$^-$ strain MA08 had less absorption due to LH1 (and, perhaps, the RC) and increased absorbance at 780 nm, next to the RC peak at 800 nm, compared to the parental strain MW442 (Figure 3.4.2). The altered LH1 absorption and the 780 nm absorbance were also discerned in an LH2$^+$ background (not shown). The absorbance at 780 nm could be attributed to unbound BChl because it was observed only in intact cells, not in chromatophores (see Figure 3.4.4), indicating that the pigment absorbing at 780 nm was not bound to integral membrane proteins of the photosynthetic apparatus.

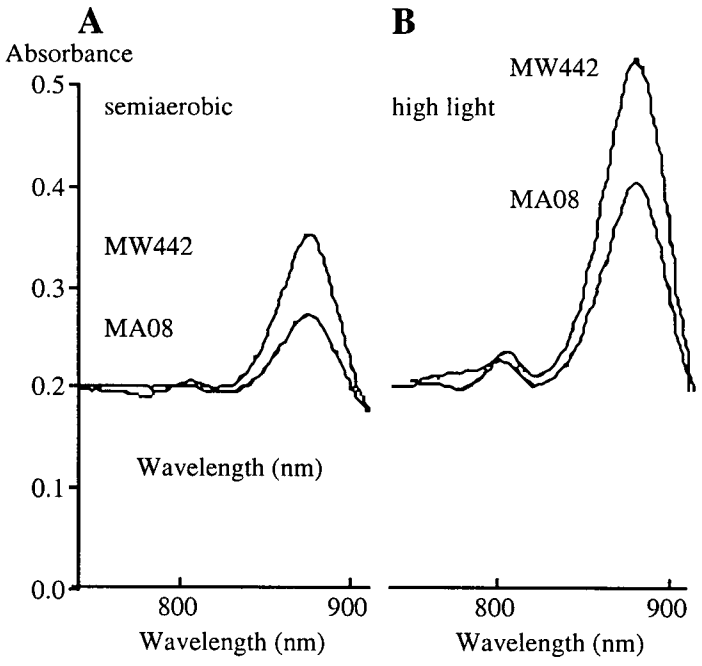

Figure 3.4.2. Absorption spectra (room temperature, pathlength 1 cm) of intact cells of the LH2$^-$ strains MW442 (*puhE*$^+$) and MA08 (*puhE*$^-$), normalized for light scattering at 650 nm. Note the absorption by unbound BChl at 780 nm, which distorted the RC peak at 800 nm, and the smaller size of the LH1 peak at 880 nm in MA08.

SDSPAGE of chromatophores from MA06 revealed that the amounts of LH1 polypeptides (and, perhaps, the RC polypeptides) per total protein were somewhat reduced due to the *puhE* deletion under high light intensity (Figure 3.4.3).

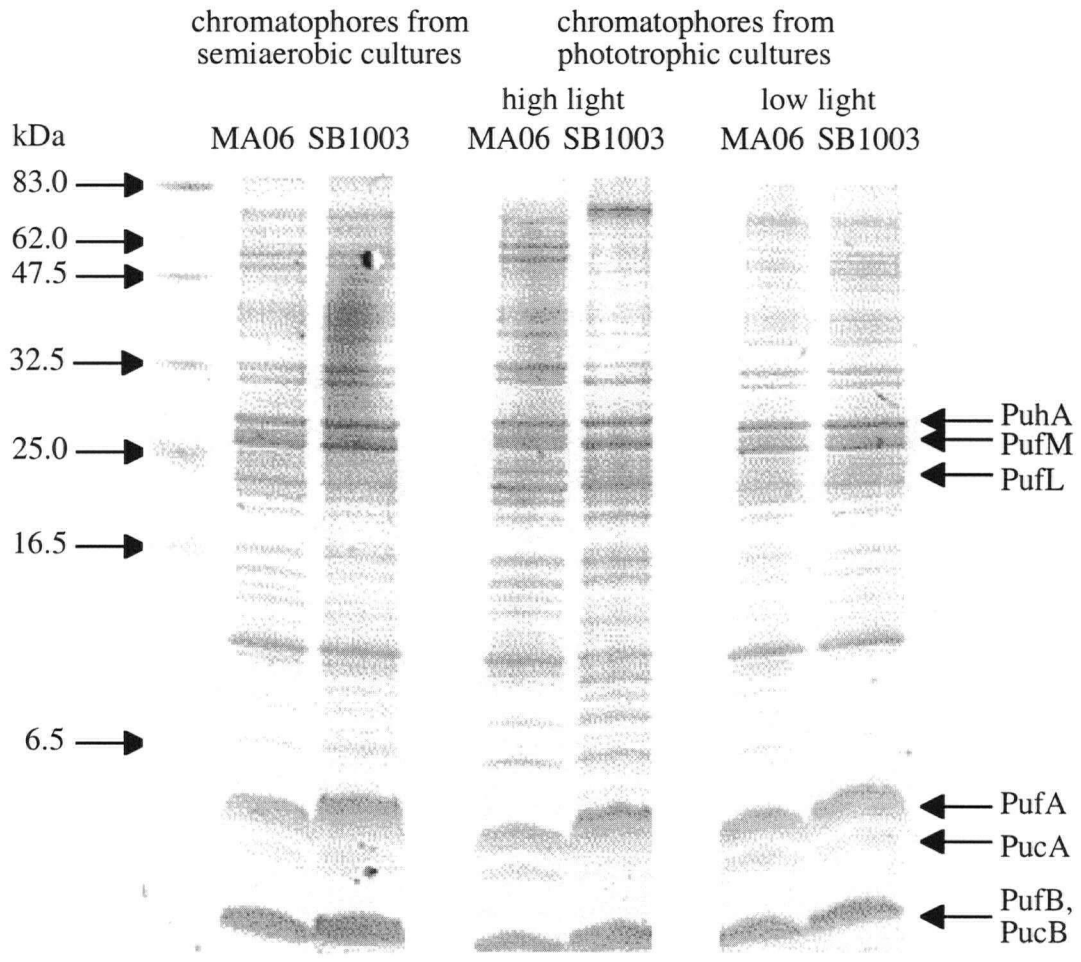

Figure 3.4.3. SDSPAGE of 50 μg of chromatophore protein from the *puhE*$^+$ strain SB1003 and the *puhE*$^-$ strain MA06. All three RC polypeptides (PuhA, PufM, PufL) and both LH1 polypeptides (PufA, PufB) were less abundant in MA06, most noticeably under high light intensity, while the amounts of LH2 polypeptides (PucA, PucB) were unaffected.

The LH1 deficiency was confirmed by low temperature absorption spectroscopy (Figure 3.4.4), and a slight RC deficiency was indicated by measurements of RC photobleaching with a train of eight flashes of light (Figure 3.4.5, Table 3.4.4). The carotenoid bandshift (explained in Section 2.14) after a single flash of light was almost the same as in the parental strain. In MA06, as in the *puhE*$^+$ parent SB1003, it consisted of a rapid initial shift, attributed to the reduction of quinones in the RC, followed by a more gradual further shift due to the generation of a sustained proton gradient coupled to oxidation of quinols by cyt *b/c*1, indicating that these reactions are not abolished by deletion of *puhE* (Figure 3.4.6). However, the slightly smaller carotenoid bandshift indicated that MA06 forms a lesser proton gradient, consistent with a lower RC content than SB1003 (Table 3.4.4). The carotenoid bandshift of MA06 accumulated over successive flashes, indicating that the

RC is properly connected to cyt *b/c*1 (Figure 3.4.7). These effects were similarly small when cells were grown either semiaerobically or phototrophically with low light intensity (30 $\mu E/m^2/s$), but in cells grown phototrophically with high light intensity (150 $\mu E/m^2/s$) there was a twofold reduction in RC function due to the *puhE* deletion.

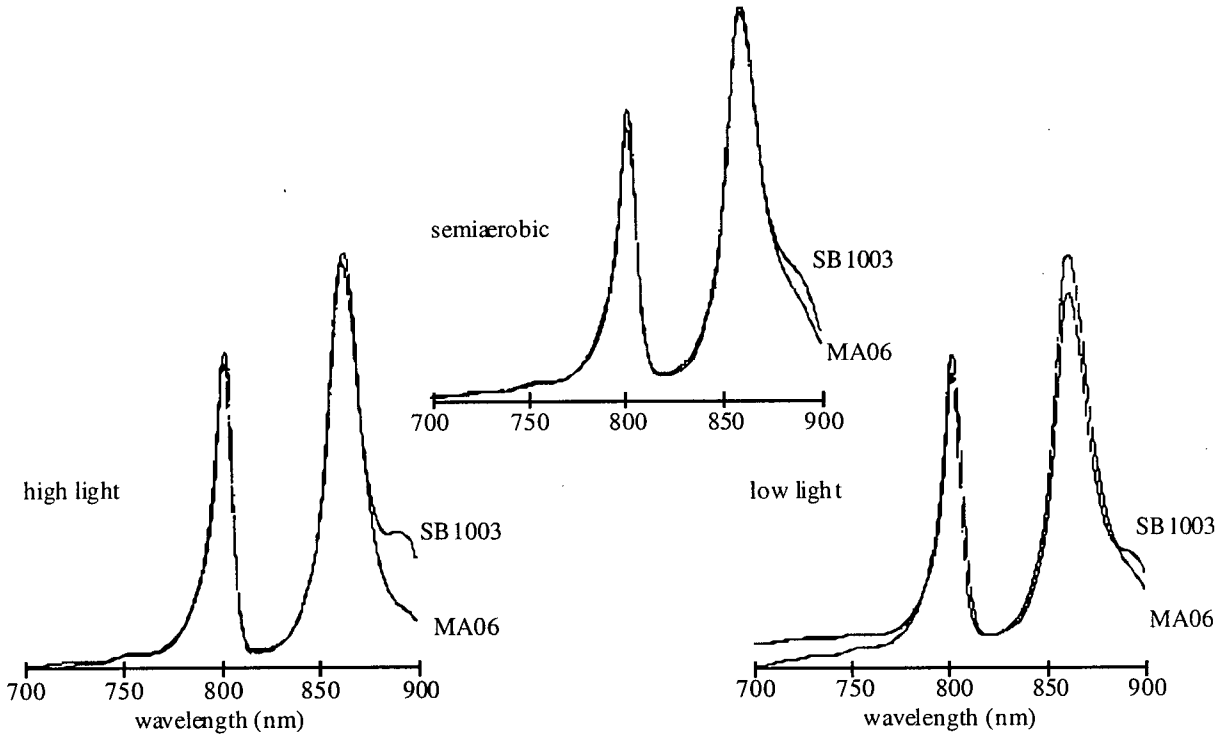

Figure 3.4.4. Low-temperature absorption spectra (77 K, pathlength 1 cm) of chromatophores from SB1003 and MA06. SB1003 had more LH1 absorption at 880 nm that appeared as a shoulder on the LH2 peak. This difference was not remarkable except when cultures were grown phototrophically with high light intensity. Data collected by R. C. Prince.

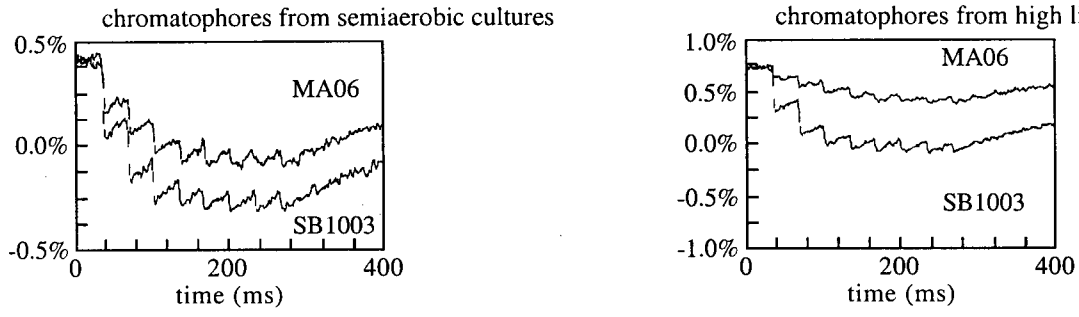

Figure 3.4.5. Photobleaching of the RC (room temperature, pathlength 1 cm) in chromatophores from SB1003 and MA06. The downward deflection with each flash indicates a decrease in absorption at 605 nm due to photooxidation of the RC special pair. Data collected by R. C. Prince.

Figure 3.4.6. Single-flash carotenoid bandshifts (room temperature, pathlength 1 cm) in chromatophores from phototrophically grown SB1003 and MA06. A slightly smaller bandshift was observed for MA06, indicating that a smaller proton gradient was produced (left), and the production of this proton gradient was sensitive to antimycin (right). Data collected by R. C. Prince.

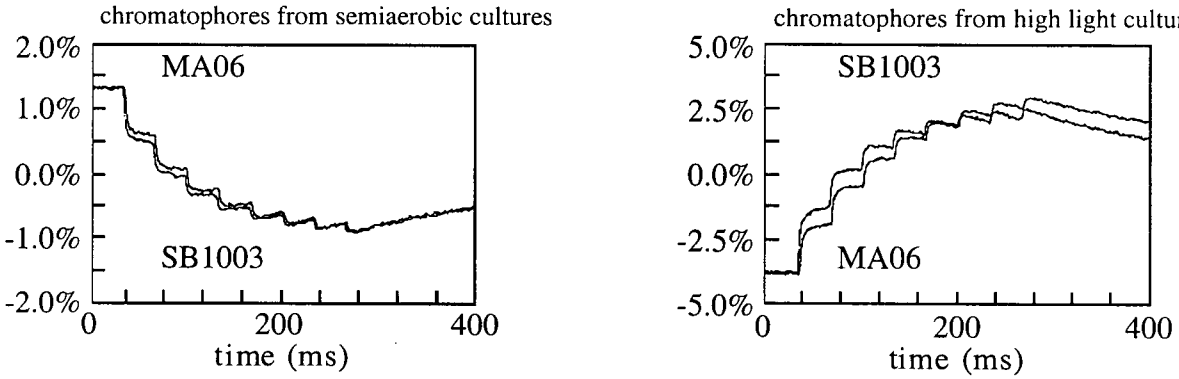

Figure 3.4.7. Eight-flash carotenoid bandshifts (room temperature, pathlength 1 cm) in chromatophores from SB1003 and MA06. Saturation was achieved in both strains despite the RC deficiency due to the *puhE*⁻ genotype. A shift to the red was observed for both semiaerobic conditions (decreased absorption at 510 nm vs. 540 nm) and phototrophic conditions (increased absorption at 490 nm vs. 475 nm). Data collected by R. C. Prince.

Table 3.4.4. Flash spectroscopic measurements (room temperature, pathlength 1 cm) of the effect of the *puhE* deletion on RC content and function in isolated chromatophores. Data collected by R. C. Prince.

Chromatophore sample	Amount of RC (RC photobleaching, relative to SB1003)	Proton gradient (single-flash carotenoid bandshift, relative to SB1003)
MA06 semiaerobic	67%	86%
MA06 high light	47%	76%
MA06 low light	74%	93%

3.4.3. RC-LH1 gene transcription and translation in *puhE* deletion strains

The cause of the RC-LH1 deficiency of the *puhE* deletion strain MA06 under high light intensity was studied initially by evaluating transcription of the *puf* operon, which encodes all of the RC-LH1 polypeptides except PuhA. The results of a β-galactosidase assay of MA06 and MA07 and their *puhE*$^+$ parent SB1003, in which a PufB::LacZ fusion protein was expressed from the *puf* promoter on plasmid pXCA6::935, indicate that transcription and translation of the *puf* genes is not significantly impaired in the absence of PuhE (Table 3.4.5), and so the effect of PuhE may be post-translational.

Because the *puhE* deletion increased production of the RC and LH1 when these complexes were expressed separately (see Sections 3.4.4 and 3.4.5), and enhanced phototrophic growth of RC$^+$LH1$^-$LH2$^-$ strains due to the *puhE* deletion was occasionally observed (not shown), the *pufQBALM* deletion strains MA01 (*puhE*$^+$) and MA04 (*puhE*$^-$) used for those experiments were also tested. No significant decrease or increase in activity was observed (Table 3.4.5).

Table 3.4.5. Similar β-galactosidase activity (nmol of *o*-nitrophenol per minute per 10^8 cells) was expressed from the *puf* promoter in *puhE*$^+$ (SB1003, MA01) and *puhE*$^-$ (MA06, MA07, MA04) strains.

semiaerobic cultures	Mean activity ± standard deviation of 3 samples
MA01(pXCA6::935)	5.1 ± 1.7
MA04(pXCA6::935)	4.7 ± 1.1
SB1003(pXCA6::935)	5.0 ± 1.6
MA06(pXCA6::935)	4.3 ± 1.5
MA07(pXCA6::935)	4.8 ± 0.4
phototrophic cultures - low light	
SB1003(pXCA6::935)	7.2 ± 1.2
MA06(pXCA6::935)	5.4 ± 0.5
MA07(pXCA6::935)	5.5 ± 1.4
phototrophic cultures - high light	
SB1003(pXCA6::935)	7.3 ± 0.9
MA06(pXCA6::935)	7.2 ± 1.1
MA07(pXCA6::935)	6.7 ± 1.1

A possible effect of *puhE* deletion on expression of the RC and LH1 polypeptides was also investigated by an RNA blot for *puf* mRNA. The amounts of *pufLMX* mRNA for the RC in MA01(pMA10) and MA04(pMA10) were equal, as were the amounts of *pufBAX* and *pufBA* mRNA for LH1 in MA01(p*Stu* I) and MA04(p*Stu* I) (Figure 3.4.8). Therefore, the enhanced production of the RC and of LH1, expressed separately in the *puhE*⁻ MA04 strains, is not due to a superabundance of *puf* mRNA, and I conclude that PuhE plays a post-translational inhibitory role in assembly of the RC and of LH1 separately.

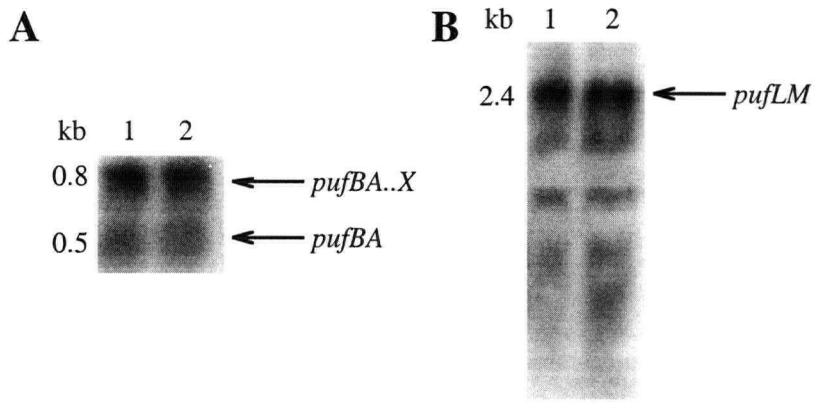

Figure 3.4.8. RNA blots of *puf* transcripts in *puhE*⁺ (MA01) and *puhE*⁻ (MA04) backgrounds. (**A**) LH1-specific transcripts in (1) MA01(p*Stu* I) and (2) MA04(p*Stu* I). (**B**) RC-specific transcripts in (1) MA01(pMA10) and (2) MA04(pMA10). The probe was an *Apa* I fragment extending from the middle of *pufQ* to the 3' region of *pufX*.

3.4.4. Effect of PuhE on assembly of the RC

The kinetics of assembly and decay of the RC, in the absence of one or both LH1 polypeptides, PufB and PufA, were measured in *puhE*⁺ (MA01) and *puhE*⁻ (MA04) backgrounds, which contained a deletion of the chromosomal *pufQBALM* genes and were complemented with plasmids carrying partial *puf* operons with deletions of either *pufB* or *pufA*, or both. The absence of LH1 was necessary in order to evaluate the amplitudes of RC peaks in absorption spectra, which are normally obscured by the LH1 peak at 880 nm. For a typical spectrum of a pure RC, see Figure 1.2.

The *puhE*⁺ and *puhE*⁻ strains were at similar culture densities throughout the experiments (Figure 3.4.9) and should have progressed similarly into semiaerobic growth conditions. A

comparison of absorption spectra over time of the *puhE*⁻ strains MA04(pTPR9) (lacking PufB), MA04(pTPR8) (lacking PufA), and MA04(pMA10) (lacking both LH1 polypeptides) and the corresponding *puhE*⁺ strains MA01(pTPR9), MA01(pTPR8), and MA01(pMA10) is shown in Figure 3.4.10. After 9 hours of semiaerobic growth, the MA04 (*puhE*⁻) strains had a large amount of absorption at 780 nm attributed to unbound BChl, which obscured the BPhe and voyeur BChl peaks of the RC; however, the *puhE*⁻ MA04 strains appeared to contain more nascent RCs than the corresponding *puhE*⁺ MA01 strains, as evidenced by the area of the special pair BChl peak at 865 nm. After 15 hours, when the RC voyeur BChl peak at 800 nm began to separate from the BPhe peak at 760 nm in MA01(pTPR9) and to a lesser extent in MA01(pTPR8), their *puhE*⁻ counterparts MA04(pTPR9) and MA04(pTPR8) still contained an excess of unbound BChl that obscured the voyeur BChl peaks. In these two *puhE*⁻ strains, the special pair BChl peak was now smaller in area but sharper than in the *puhE*⁺ strains. The special pair BChl peak in MA04(pMA10) was still larger than in MA01(pMA10), indicating that although very little RC was assembled in the absence of both PufB and PufA, the *puhE*⁻ mutation increased RC production. The situation was similar after 19.5 hours: there remained a large amount of unbound BChl in the *puhE*⁻ strains.

Quantitative analysis suggested that production of the RC, measured as the RC voyeur BChl peak area between 800 nm and 830 nm, was initially greater in the MA04 (*puhE*⁻) strains (Figure 3.4.11); however, the RC level did not remain higher than in the MA01 (*puhE*⁺) strains after 19.5 hours, except in the case of MA04(pMA10). The rates of production computed from these data (Table 3.4.6) suggested that RC assembly may be more rapid in the absence of PuhE; however, the large standard deviations preclude a compelling argument. Because there was always an excess of unbound BChl, it was difficult to evaluate the "structural order" of the RC (defined in Section 2.15) as either the height ratio of the voyeur BChl peak at 800 nm and the BPhe peak at 760 nm (Figure 3.4.12), or the ratio of RC voyeur BChl peak-specific area (800 nm to 830 nm) to the total RC voyeur BChl peak area, which was inflated by BPhe and unbound BChl absorption (780 nm to 830 nm) (Figure 3.4.13). Measurements of RC decay were not of sufficient quality to implicate or exclude the involvement of PuhE (Figure 3.4.14, Table 3.4.6).

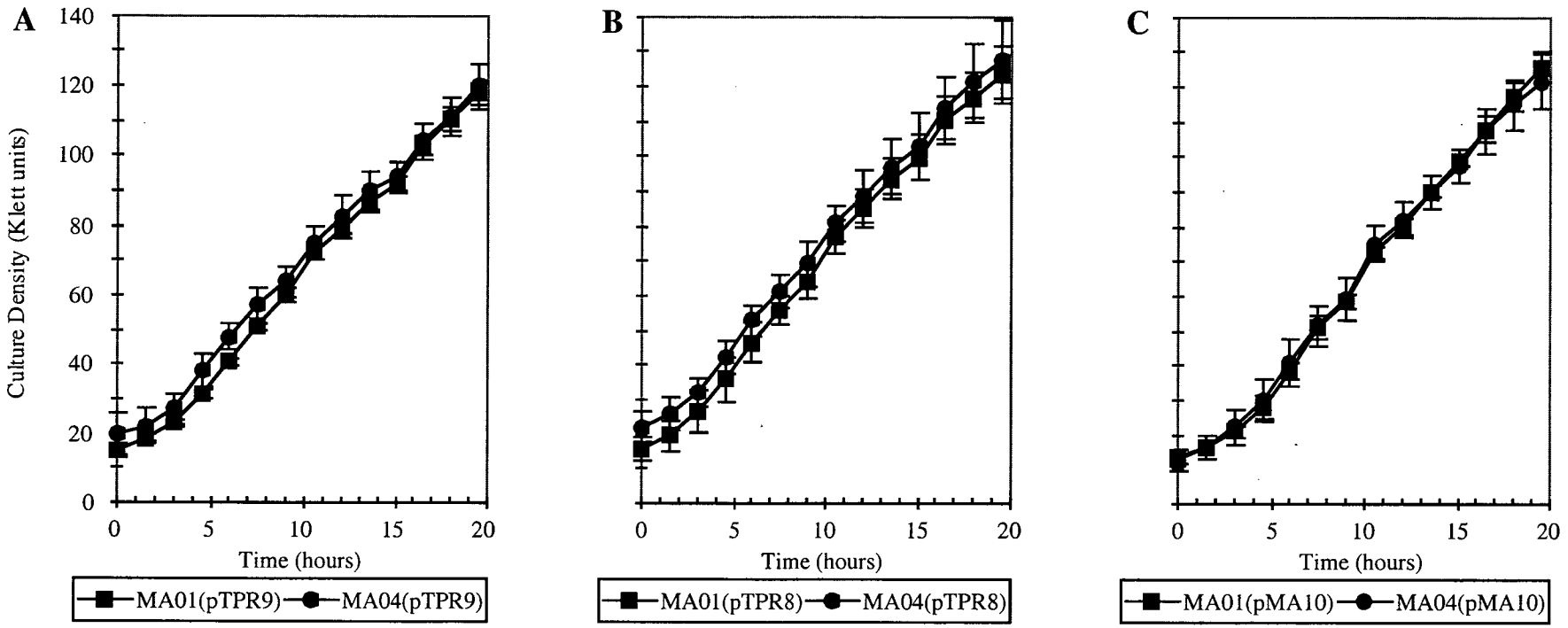

Figure 3.4.9. Semiaerobic growth of *puhE*$^+$ (MA01) and *puhE*$^-$ (MA04) strains expressing the RC (**A**) in the absence of PufB - plasmid pTPR9, (**B**) in the absence of PufA - plasmid pTPR8, and (**C**) in the absence of both LH1 polypeptides - plasmid pMA10.

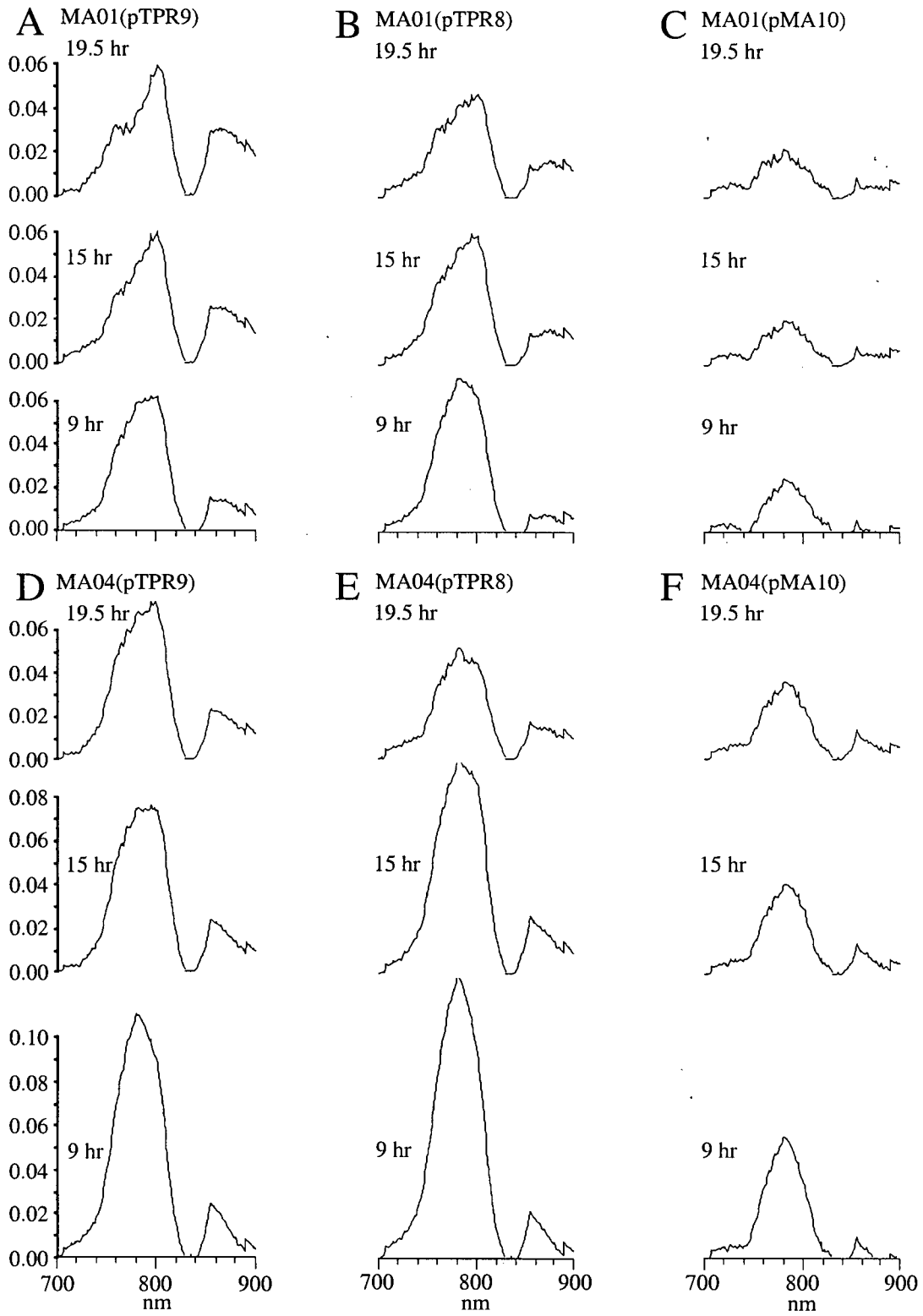

Figure 3.4.10. Absorption spectra (room temperature, pathlength 1 cm) of the nascent RC in the *puhE*$^+$ (MA01) and *puhE*$^-$ (MA04) backgrounds, in the absence of the LH1 polypeptides PufB - plasmid pTPR9 (**A**, **D**), PufA - plasmid pTPR8 (**B**, **E**), or both - plasmid pMA10 (**C**, **F**), after 9 hours, 15 hours, and 19.5 hours of semiaerobic growth. Spectra were normalized and a baseline was drawn as described in Section 2.15. In addition to RC absorption at 760 nm, 800 nm, and 865 nm, there is a peak at 780 nm, attributed to unbound BChl.

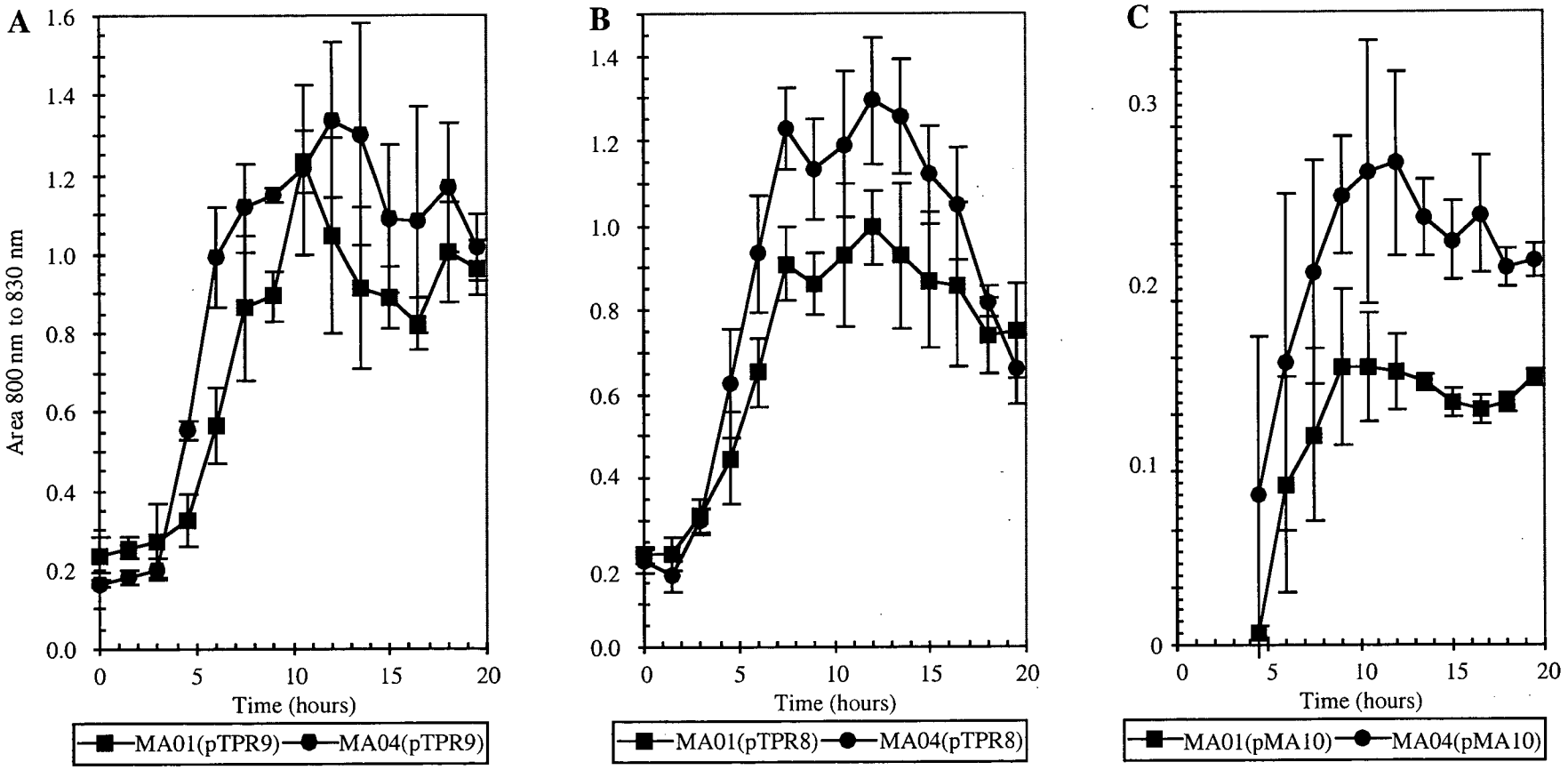

Figure 3.4.11. Production of the RC (**A**) in the absence of PufB - plasmid pTPR9, (**B**) in the absence of PufA - plasmid pTPR8, and (**C**) in the absence of both LH1 polypeptides - plasmid pMA10, in the *puhE*$^+$ (MA01) and *puhE*$^-$ (MA04) backgrounds. A portion of the RC voyeur BChl peak area was measured from 800 nm to 830 nm to minimize the contribution of absorption by BPhe and unbound BChl. The *puhE* deletion clearly increased RC production.

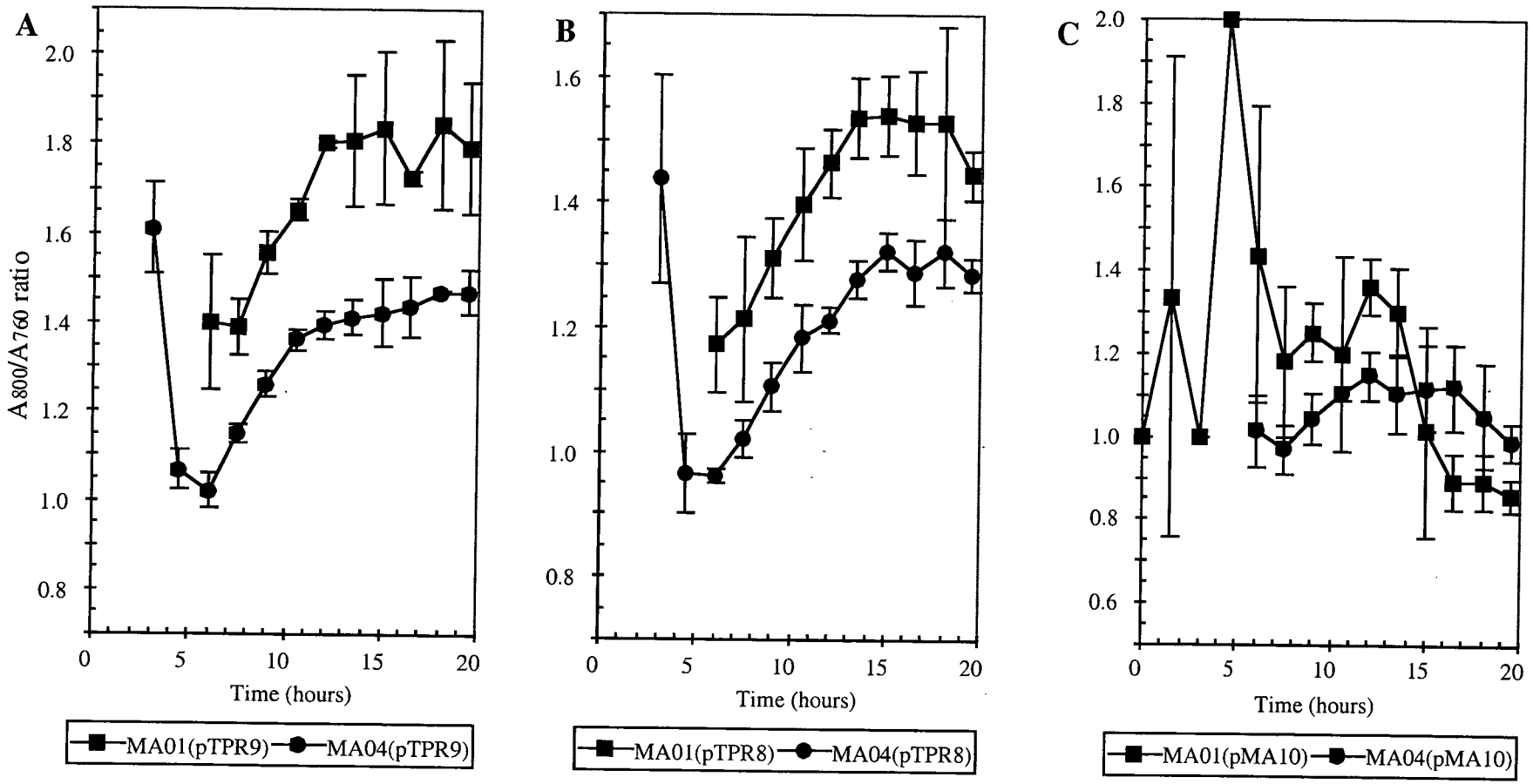

Figure 3.4.12. Peak height ratio of the RC (**A**) in the absence of PufB - plasmid pTPR9, (**B**) in the absence of PufA - plasmid pTPR8, and (**C**) in the absence of both LH1 polypeptides - plasmid pMA10, in the *puhE*$^+$ (MA01) and *puhE*$^-$ (MA04) backgrounds. The height of the voyeur BChl peak at 800 nm was divided by that of the BPhe peak at 760 nm, as a measure of RC "structural order," the proper binding of pigments to polypeptides. Increased unbound BChl production due to the *puhE* deletion made it difficult to interpret the reduced peak height ratio as poor RC structural order.

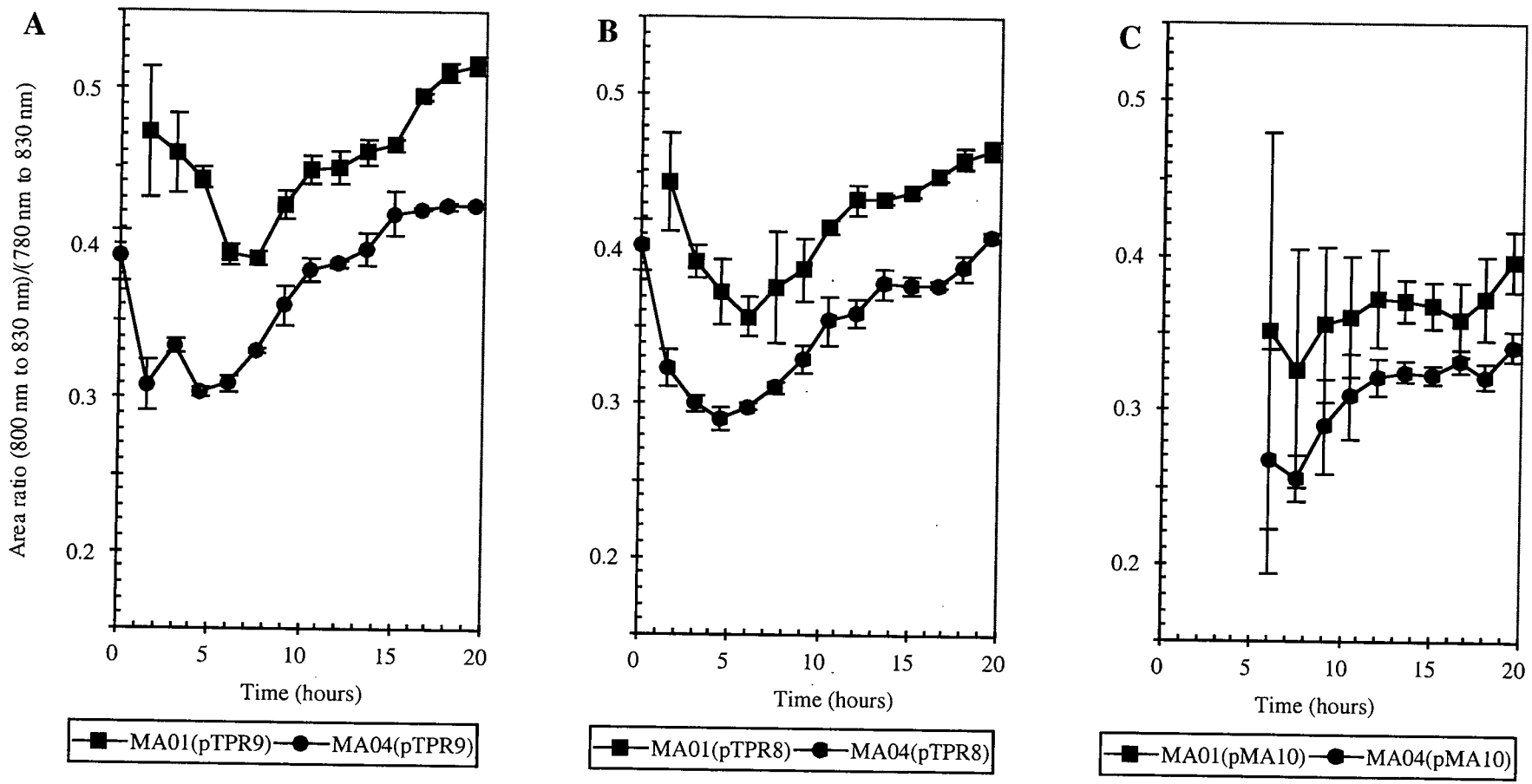

Figure 3.4.13. Voyeur BChl-specific peak area ratio of the RC (**A**) in the absence of PufB - plasmid pTPR9, (**B**) in the absence of PufA - plasmid pTPR8, and (**C**) in the absence of both LH1 polypeptides - plasmid pMA10, in the *puhE*$^+$ (MA01) and *puhE*$^-$ (MA04) backgrounds. The area of a portion of the voyeur BChl peak from 800 nm to 830 nm was divided by the area from 780 nm to 830 nm (which was inflated by absorption from the BPhe peak at 760 nm and the unbound BChl peak at 780 nm), as a measure of RC "structural order," the proper binding of pigments to polypeptides. Increased unbound BChl production due to the *puhE* deletion made it difficult to interpret the reduced peak height ratio as poor RC structural order.

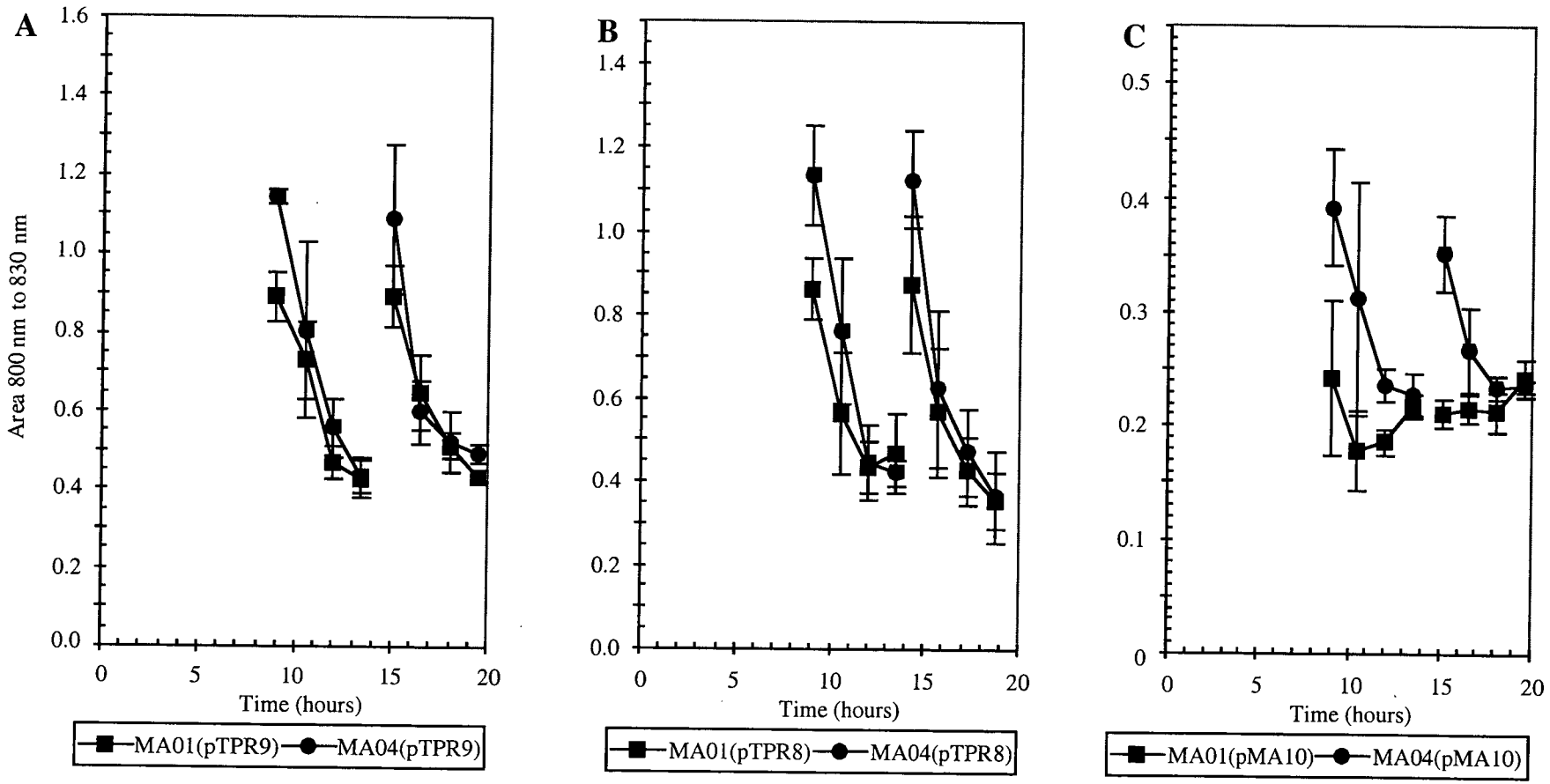

Figure 3.4.14. Decay of the RC (**A**) in the absence of PufB - plasmid pTPR9, (**B**) in the absence of PufA - plasmid pTPR8, and (**C**) in the absence of both LH1 polypeptides - plasmid pMA10, in the *puhE*$^+$ (MA01) and *puhE*$^-$ (MA04) backgrounds. Decay was initiated at 9 hr and at 15 hr by switching cultures to aerobic conditions. A portion of the RC voyeur BChl peak area was measured from 800 nm to 830 nm to minimize the contribution of absorption by BPhe and unbound BChl.

Table 3.4.6. Linear production rates (area units per hour) and exponential decay rate constants (per hour) for the RC in *puhE*$^+$ (MA01) and *puhE*$^-$ (MA04) backgrounds, determined from triplicate cultures. A portion of the RC voyeur BChl peak area was measured from 800 nm to 830 nm. Note: post-assembly RC decay in pMA10 strains (after 15 hours of semiaerobic growth) was a transient and insignificant phenomenon.

Strain	Genotype chromosome (plasmid)	RC production	Mid-assembly RC decay	Post-assembly RC decay
MA01(pTPR9)	*pufQBALM*$^-$*X*$^+$*puhE*$^+$(*pufQALMX*)	161 ± 32	234 ± 89	239 ± 91
MA04(pTPR9)	*pufQBALM*$^-$*X*$^+$*puhE*$^-$(*pufQALMX*)	222 ± 35	284 ± 158	440 ± 174
MA01(pTPR8)	*pufQBALM*$^-$*X*$^+$*puhE*$^+$(*pufQBLMX*)	156 ± 35	396 ± 192	327 ± 268
MA04(pTPR8)	*pufQBALM*$^-$*X*$^+$*puhE*$^-$(*pufQBLMX*)	232 ± 42	416 ± 146	424 ± 240
MA01(pMA10)	*pufQBALM*$^-$*X*$^+$*puhE*$^+$(*pufQLMX*)	35 ± 7	235 ± 139	28 ± 22
MA04(pMA10)	*pufQBALM*$^-$*X*$^+$*puhE*$^-$(*pufQLMX*)	56 ± 9	236 ± 139	229 ± 135

RC production in these experiments was near the limit of detection, and the changes in absorbance over time were small and varied depending on which LH1 polypeptide was present. Nevertheless, I suggest that the *puhE* deletion enhances RC assembly, as is most clearly shown by the difference in RC special pair BChl peak amplitude between MA01(pMA10) and MA04(pMA10), which are the *puhE*$^+$ and *puhE*$^-$ strains, respectively, lacking both LH1 polypeptides.

3.4.5. Effect of PuhE on assembly of LH1

Kinetics of assembly and decay of LH1 were measured in *puhE*$^+$ (MA01) and *puhE*$^-$ (MA04) backgrounds, which contained a deletion of the chromosomal *pufQBALM* genes and were complemented with only the *pufQBAX* genes on plasmid p*Stu* I. Such removal of genes encoding two RC polypeptides, PufL and PufM, leaving only PuhA, allowed the evaluation of LH1-specific absorption at 880 nm without the minor contribution of the RC special pair BChl peak at 865 nm. The strains MA01(p*Stu* I) (*puhE*$^+$) and MA04(p*Stu* I) (*puhE*$^-$) were at similar culture densities throughout the experiments (Figure 3.4.15) and should have progressed similarly into semiaerobic growth conditions. The mean amount of LH1 was higher in MA04(p*Stu* I) than in MA01(p*Stu* I) after 9 hours of semiaerobic growth, and remained somewhat higher after 15 hours and 19.5 hours, although there was substantial variation among the triplicate cultures (Figure 3.4.15). Such an

augmented level of LH1 was observed consistently with MA04(p*Stu* I) and also with MA13(p*Stu* I and MA14(p*Stu* I), which have deletions of *puhBE* and *puhCE*, respectively (not shown). The mean production rates computed from these data (Table 3.4.7) suggested more rapid LH1 assembly in the *puhE* deletion strain; however, this interpretation is compromised by the large standard deviation. Measurements of LH1 decay (Figure 3.4.15, Table 3.4.7) were not of sufficient quality to implicate or exclude the involvement of PuhE. Absorption at 780 nm (unbound BChl) was consistently higher in spectra of MA04(p*Stu* I) compared to MA01(p*Stu* I) (Figure 3.4.16).

These results indicate that the reduced levels of the RC and LH1 in *puhE* deletion strains such as MA06 may not be due to reduced production of either the RC or LH1 individually. Rather, the effect of PuhE could be to maintain optimal levels of the RC-LH1 core complex as a whole.

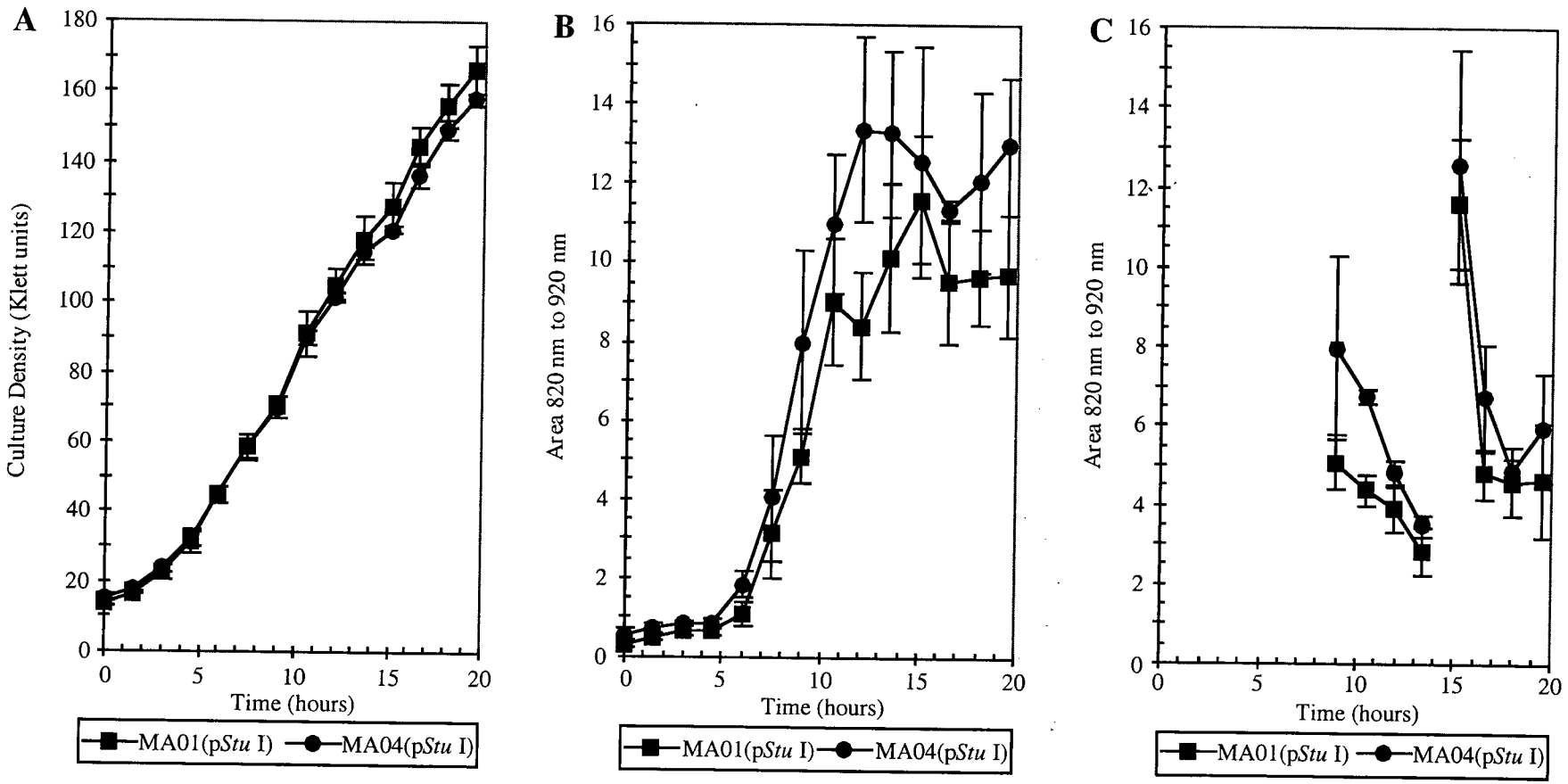

Figure 3.4.15. Assembly and decay of LH1 in the absence of PufL and PufM - plasmid p*Stu* I, in the *puhE*$^+$ (MA01) and *puhE*$^-$ (MA04) backgrounds. (**A**) Semiaerobic growth. (**B**) Production of LH1, measured as the peak area from 820 nm to 920 nm. (**C**) Decay of LH1, initiated at 9 hr and at 15 hr by switching cultures to aerobic conditions.

Table 3.4.7. Linear production rates (area units per hour) and exponential decay rate constants (per hour) for LH1 in *puhE*$^+$ (MA01) and *puhE*$^-$ (MA04) backgrounds, determined from triplicate cultures. The LH1 peak area was measured from 820 nm to 920 nm.

	Genotype chromosome (plasmid)	LH1 production	Mid-assembly LH1 decay	Post-assembly LH1 decay
MA01(p*Stu* I)	*pufQBALM*$^-$*X*$^+$*puhE*$^+$(*pufQBA...X?*)	525 ± 12	37 ± 185	628 ± 35
MA04(p*Stu* I)	*pufQBALM*$^-$*X*$^+$*puhE*$^-$(*pufQBA...X?*)	706 ± 184	91 ± 213	570 ± 246

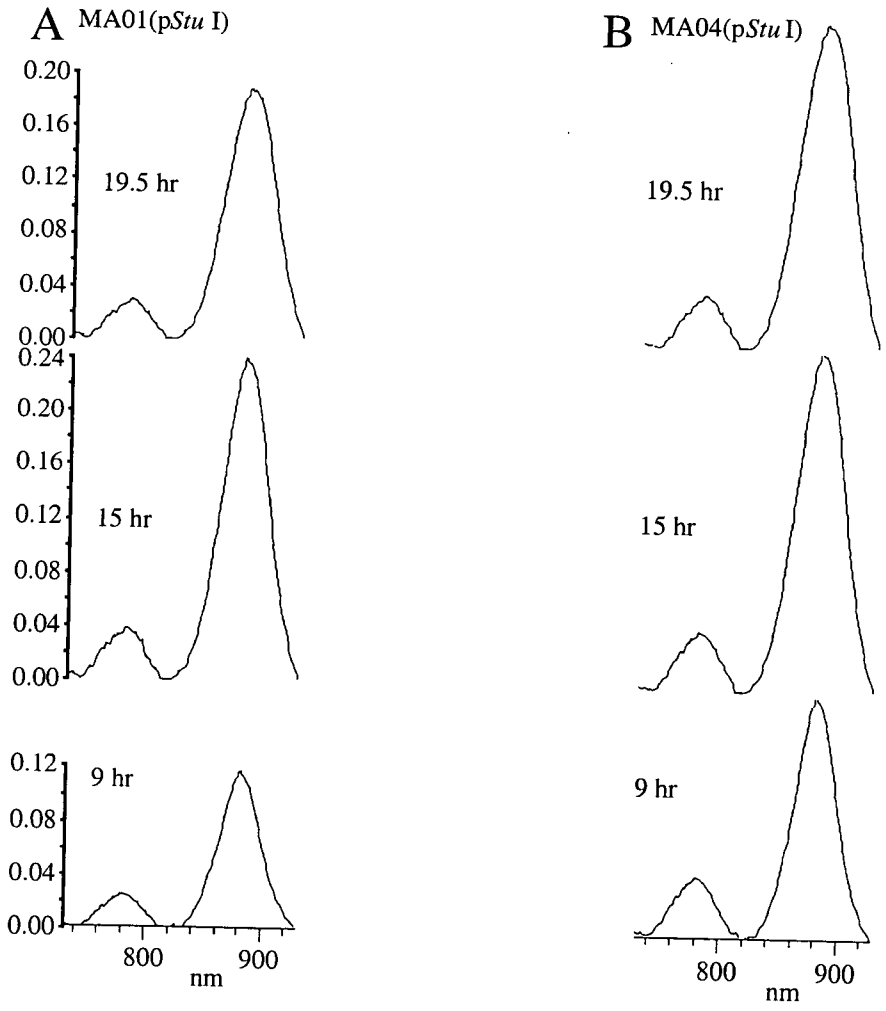

Figure 3.4.16. Absorption spectra (room temperature, pathlength 1 cm) of nascent LH1 in (**A**) *puhE*$^+$ (MA01) and (**B**) *puhE*$^-$ (MA04) backgrounds, in the absence of the RC polypeptides PufL and PufM - plasmid p*Stu* I, after 9 hours, 15 hours, and 19.5 hours of semiaerobic growth. Spectra were normalized and a baseline was drawn as described in Section 2.15. In addition to LH1 absorption at 880 nm, there is a small peak at 780 nm, attributed to unbound BChl.

3.4.6. Effects of PuhE and PufQ on production of unbound BChl

In derivatives of the *puhE* deletion strain MA04, absorbance at 780 nm was unusually high, obscuring the BPhe and voyeur BChl peaks of the RC (if present). Similar absorbance was detectable in the spectra of intact cells of the LH2$^-$ *puhE*$^-$ strain MA08 (see Figure 3.4.2), indicating that the *puhE* mutation is responsible for the phenomenon. This absorbance was attributed to unbound (soluble) BChl because it was not observed in the spectra of chromatophores (see Figure 3.4.4).

The production of unbound BChl was quantified in all five strains that expressed only LH1 from plasmid p*Stu* I (in the absence of the RC polypeptides PufL and PufM but not PuhA). Deletions of *puhB*, *puhC*, and the chromosomal copy of *pufX* had little or no effect on the patterns of BChl production (Figure 3.4.17) and decay (not shown) during or after LH1 assembly; however, deletion of *puhE* increased the amount of unbound BChl and accelerated its production, and possibly also accelerated decay of BChl induced after 9 hours but not 15 hours (Table 3.4.8).

The production of unbound BChl could be due to the RC and LH1 polypeptides, or due to *pufQ*, the only gene present on all four plasmids. Further investigation revealed that deletion of *puhE* was sufficient for a significant increase in BChl in MA04 compared to its *pufQ*$^-$*puhE*$^+$ parent MA01; however, when *pufQ* was restored on plasmid pRR5C, production of BChl increased further (Figure 3.4.18, Table 3.4.9). Plasmid pMA20, which is identical to pRR5C except that the *pufQ* gene has been deleted, did not affect unbound BChl production in either MA01 or MA04 (not shown). pMA20 and pRR5C are IncQ plasmids; augmented BChl production due to *pufQ* was also seen with pXCA6::935, which is an IncP plasmid like those used to restore the RC and LH1 genes, but carries a *pufB-lacZ* fusion in addition to *pufQ* (not shown).

I conclude that the effects of PuhE and PufQ on BChl biosynthesis are opposite, independent, and of comparable magnitude (Table 3.4.9).

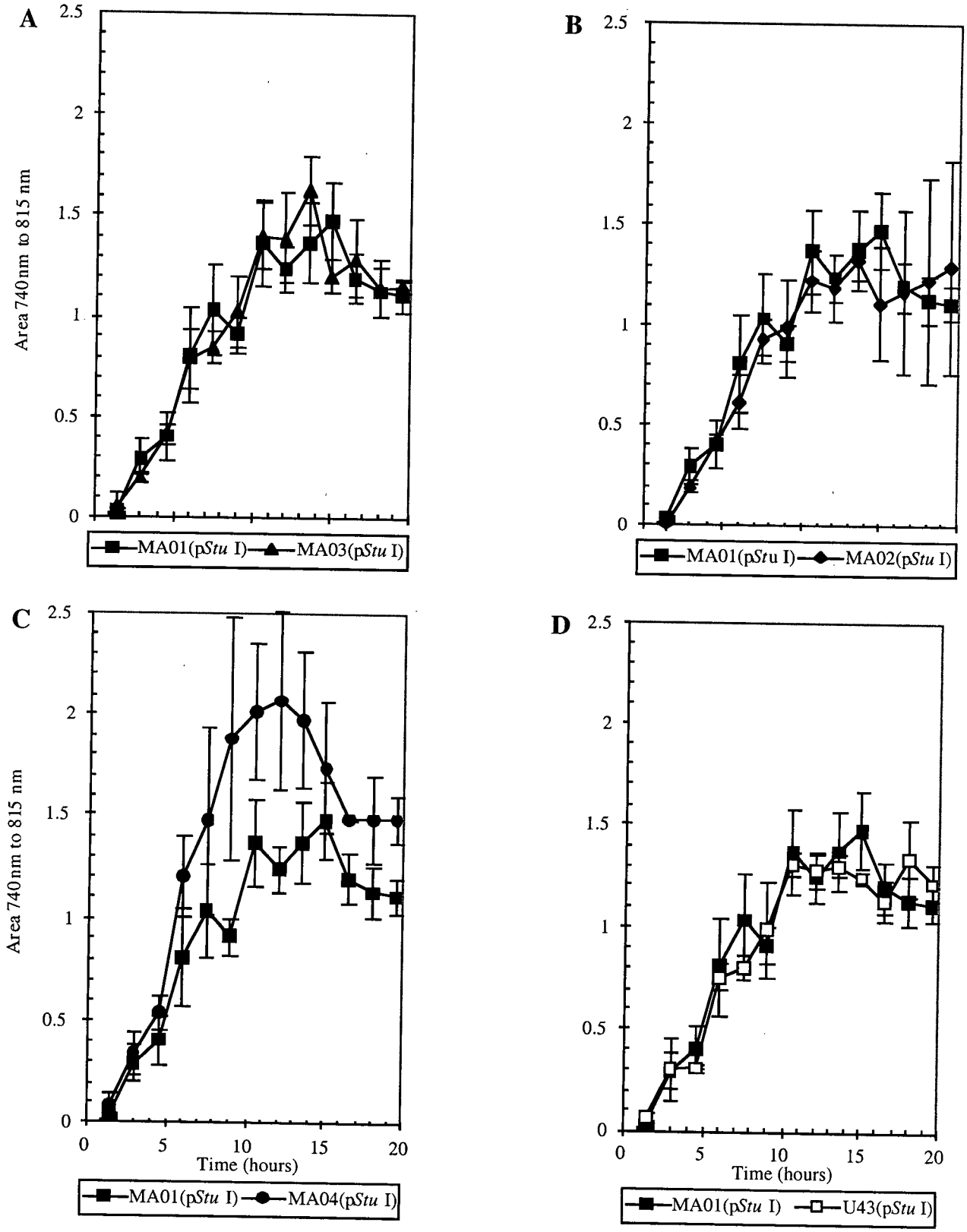

Figure 3.4.17. Production of unbound BChl in the presence of LH1 in the *pufX* merodiploid *puhB*$^{+}$*C*$^{+}$*E*$^{+}$ strain MA01(p*Stu* I) and (**A**) the *puhB*$^{-}$ strain MA03(p*Stu* I), (**B**) the *puhC*$^{-}$ strain MA02(p*Stu* I), (**C**) the *puhE*$^{-}$ strain MA04(p*Stu* I), and (**D**) U43(p*Stu* I), which has no chromosomal *pufX* gene. The unbound BChl peak area was measured from 740 nm to 815 nm.

Table 3.4.8. Linear production rates (area units per hour) and exponential decay rate constants (per hour) for unbound BChl in *puhB*$^+$*C*$^+$*E*$^+$ *pufX* merodiploid (MA01), *puhB*$^-$ (MA03), *puhC*$^-$ (MA02), *puhE*$^-$ (MA04) and chromosomal *pufX*$^-$ (U43) RC$^-$LH1$^+$LH2$^-$ backgrounds - plasmid p*Stu* I, determined from triplicate cultures. The unbound BChl peak area was measured from 740 nm to 815 nm.

Strain	Genotype chromosome (plasmid)	BChl production	BChl decay after 9 hours	BChl decay after 15 hours
MA01(p*Stu* I)	*pufQBALM*$^-$*X*$^+$(*pufQBA...X?*)	221 ± 9	76 ± 84	392 ± 185
MA03(p*Stu* I)	*pufQBALM*$^-$*X*$^+$*puhB*$^-$(*pufQBA...X?*)	227 ± 27	149 ± 84	329 ± 22
MA02(p*Stu* I)	*pufQBALM*$^-$*X*$^+$*puhC*$^-$(*pufQBA...X?*)	191 ± 8	224 ± 111	339 ± 141
MA04(p*Stu* I)	*pufQBALM*$^-$*X*$^+$*puhE*$^-$(*pufQBA...X?*)	346 ± 75	396 ± 189	527 ± 75
U43(p*Stu* I)	*pufQBALMX*$^-$(*pufQBA...X?*)	189 ± 17	125 ± 148	361 ± 78

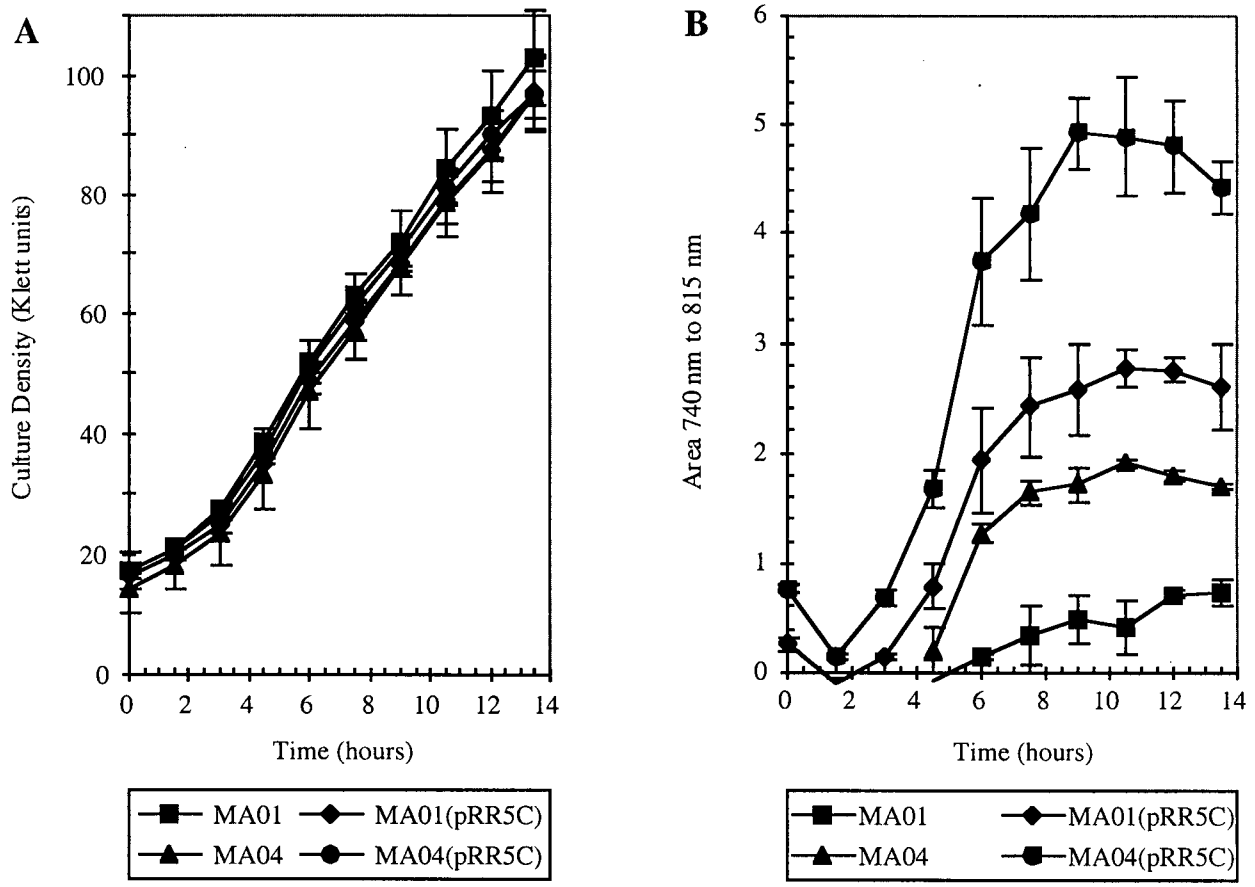

Figure 3.4.18. Production of unbound BChl in the absence of all pigment-binding proteins of the RC and LH1. (**A**) Semiaerobic growth and (**B**) unbound BChl production of *puhE*$^+$ (MA01) and *puhE*$^-$ (MA04) strains with and without *pufQ* (restored on plasmid pRR5C). The unbound BChl peak area was measured from 740 nm to 815 nm.

Table 3.4.9. Linear production rates (area units per hour) of unbound BChl in *puhE*$^+$ (MA01) and *puhE*$^-$ (MA04) strains with and without restoration of *pufQ* on plasmid pRR5C. The unbound BChl peak area was measured from 740 nm to 815 nm.

Strain and genotype		mean BChl production ± standard deviation of 3 cultures
MA01	*pufQBALM*$^-$*X*$^+$*puhE*$^+$(*pufQ*$^-$)	240 ± 94
MA01(pRR5C)	*pufQBALM*$^-$*X*$^+$*puhE*$^+$(*pufQ*$^+$)	951 ± 107
MA04	*pufQBALM*$^-$*X*$^+$*puhE*$^-$(*pufQ*$^-$)	836 ± 72
MA04(pRR5C)	*pufQBALM*$^-$*X*$^+$*puhE*$^-$(*pufQ*$^+$)	1636 ± 361

To summarize the results of this subchapter, the *puhE* deletion is responsible for a difficult transition from aerobic respiratory growth to anaerobic phototrophy, but does not cause a long-term growth defect. This difficulty may be due to impaired assembly of the RC-LH1 core complex, which is somewhat less abundant in *puhE*$^-$ strains grown semiaerobically and phototrophically; however, the assembly processes of the RC and LH1 are individually inhibited by PuhE, and so the reason why PuhE exists remains elusive. Nevertheless, the inefficiency of complementation in *trans* suggests that either the location or copy number of the *puhE* gene is important. Any conjecture regarding the function of PuhE must take into account the observation that it reduces the production of "unbound BChl" - possibly a pigment that PuhE must distribute to the assembly processes of the RC, LH1, and presumably LH2 as well. In this role, PuhE counterbalances PufQ.

3.5. Characterization of the effects of elevated and ectopic PufX expression

3.5.1. Effect of PufX on assembly of the RC

The chromosomal *pufX*$^+$ background MA01 was the control in studies of the *puhB*, *puhC*, and *puhE* deletions' effects on assembly and decay of plasmid-encoded RC (in the absence of one or both LH1 polypeptides, PufB and PufA) and LH1 (in the absence of the RC polypeptides PufL and PufM, leaving only PuhA). Because this background, with the chromosomal *pufQBALM* genes deleted and the *pufX* gene intact, was unprecedented, the more familiar U43 background, with the entire *pufQBALMX* operon deleted, was included as a second control.

The chromosomal *pufX*$^+$ and *pufX*$^-$ strains were at similar culture densities throughout the experiments (Figure 3.5.1) and should have progressed similarly into semiaerobic growth conditions. The absorption spectra of the RC in U43(pTPR9) (lacking PufB) and U43(pMA10) (lacking both LH1 polypeptides) resembled those of MA01(pTPR9), and MA01(pMA10), respectively, throughout assembly (Figure 3.5.2). However, U43(pTPR8) (lacking PufA) was deficient in terms of both RC production and BPhe-voyeur BChl peak differentiation, a surprise because its absorption spectrum was reported as "almost identical" to that of U43(pTPR9) (128).

Quantitative analysis showed that RC production was indeed compromised in U43(pTPR8) and much improved in MA01(pTPR8) (Figure 3.5.3). However, the rates of RC production computed from these data (Table 3.5.1) indicated no significant effect of *pufX* merodiploidy on the rate of RC production despite the higher peak amplitude reached in the presence of PufB and absence of PufA. A difference in RC "structural order" (defined in Section 2.15) between MA01(pTPR8) and U43(pTPR8) was obvious only when measured as the height ratio of the voyeur BChl peak at 800 nm and the BPhe peak at 760 nm (Figure 3.5.4) and not as the ratio of RC voyeur BChl peak-specific area (800 nm to 830 nm) to the total RC voyeur BChl peak area, which was inflated by absorption by BPhe and unbound BChl (780 nm to 830 nm) (Figure 3.5.5).

Measurements of RC decay were not of sufficient quality to implicate or exclude the involvement of PufX (Figure 3.5.6, Table 3.5.1).

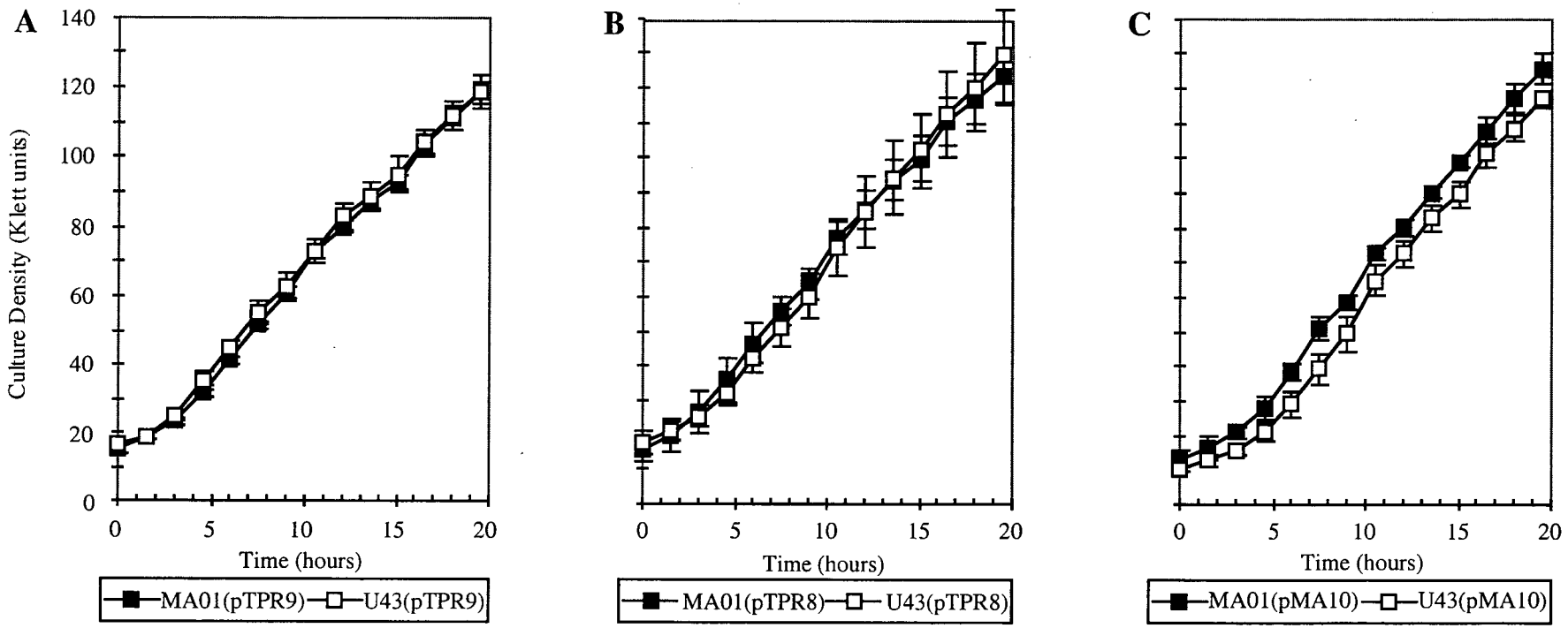

Figure 3.5.1. Semiaerobic growth of chromosomal *pufX*$^+$ (MA01) and *pufX*$^-$ (U43) strains expressing the RC (**A**) in the absence of PufB - plasmid pTPR9, (**B**) in the absence of PufA - plasmid pTPR8, and (**C**) in the absence of both LH1 polypeptides - plasmid pMA10. (Note: PufX is expressed together with two RC polypeptides from each plasmid.)

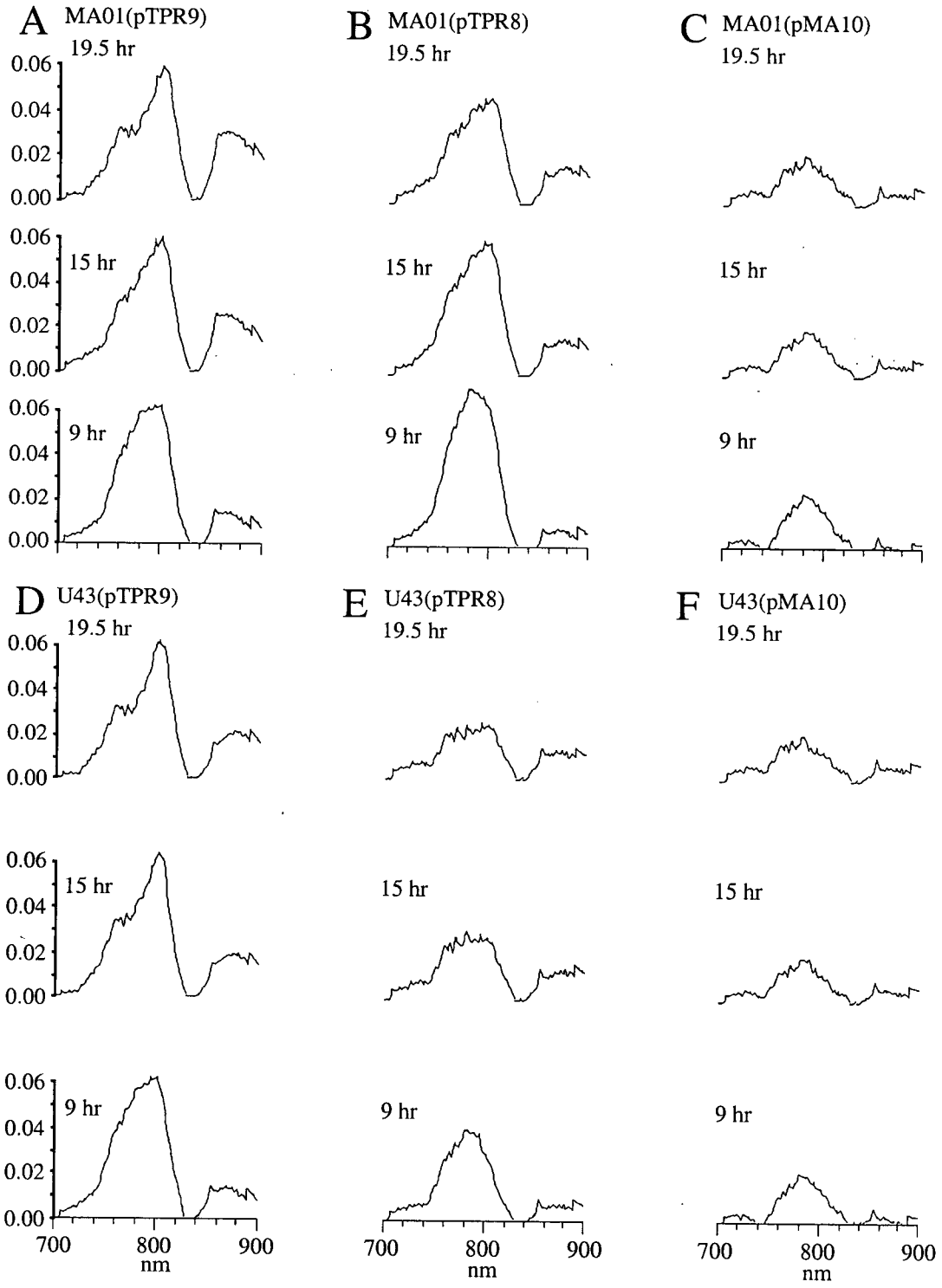

Figure 3.5.2. Absorption spectra (room temperature, pathlength 1 cm) of the nascent RC in the chromosomal *pufX*$^+$ (MA01) and *pufX*$^-$ (U43) backgrounds, in the absence of the LH1 polypeptides PufB - plasmid pTPR9 (**A**, **D**), PufA - plasmid pTPR8 (**B**, **E**), or both - plasmid pMA10 (**C**, **F**), after 9 hours, 15 hours, and 19.5 hours of semiaerobic growth. (Note: PufX is expressed together with two RC polypeptides from each plasmid.) Spectra were normalized and a baseline was drawn as described in Section 2.15. In addition to RC absorption at 760 nm, 800 nm, and 865 nm, there is a peak at 780 nm, attributed to unbound BChl.

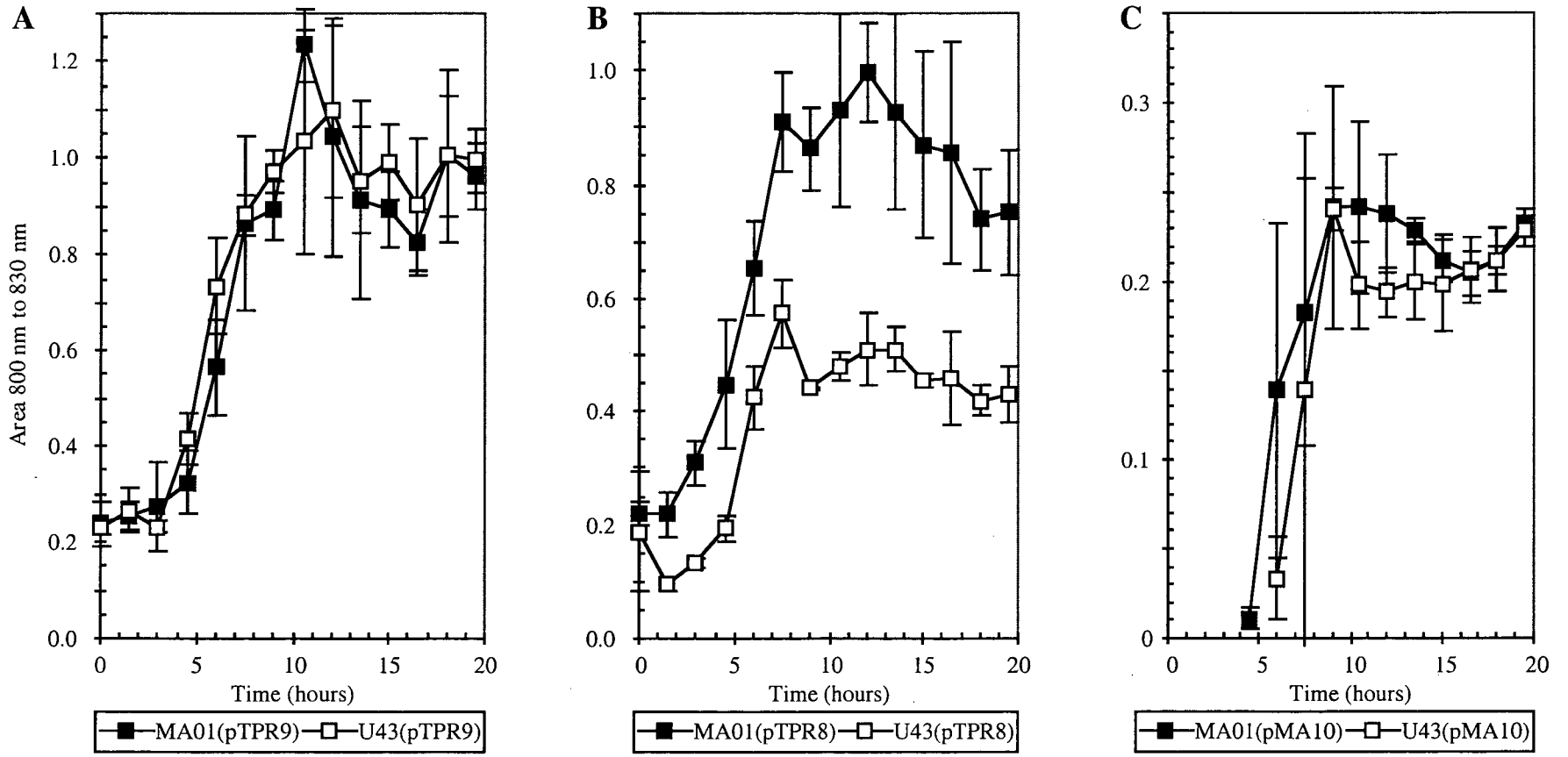

Figure 3.5.3. Production of the RC (**A**) in the absence of PufB - plasmid pTPR9, (**B**) in the absence of PufA - plasmid pTPR8, and (**C**) in the absence of both LH1 polypeptides - plasmid pMA10, in the chromosomal *pufX*$^{+}$ (MA01) and *pufX*$^{-}$ (U43) backgrounds. A portion of the RC voyeur BChl peak area was measured from 800 nm to 830 nm to minimize the contribution of absorption by BPhe and unbound BChl. In the presence of PufB and absence of PufA, *pufX* merodiploidy clearly increased RC production.

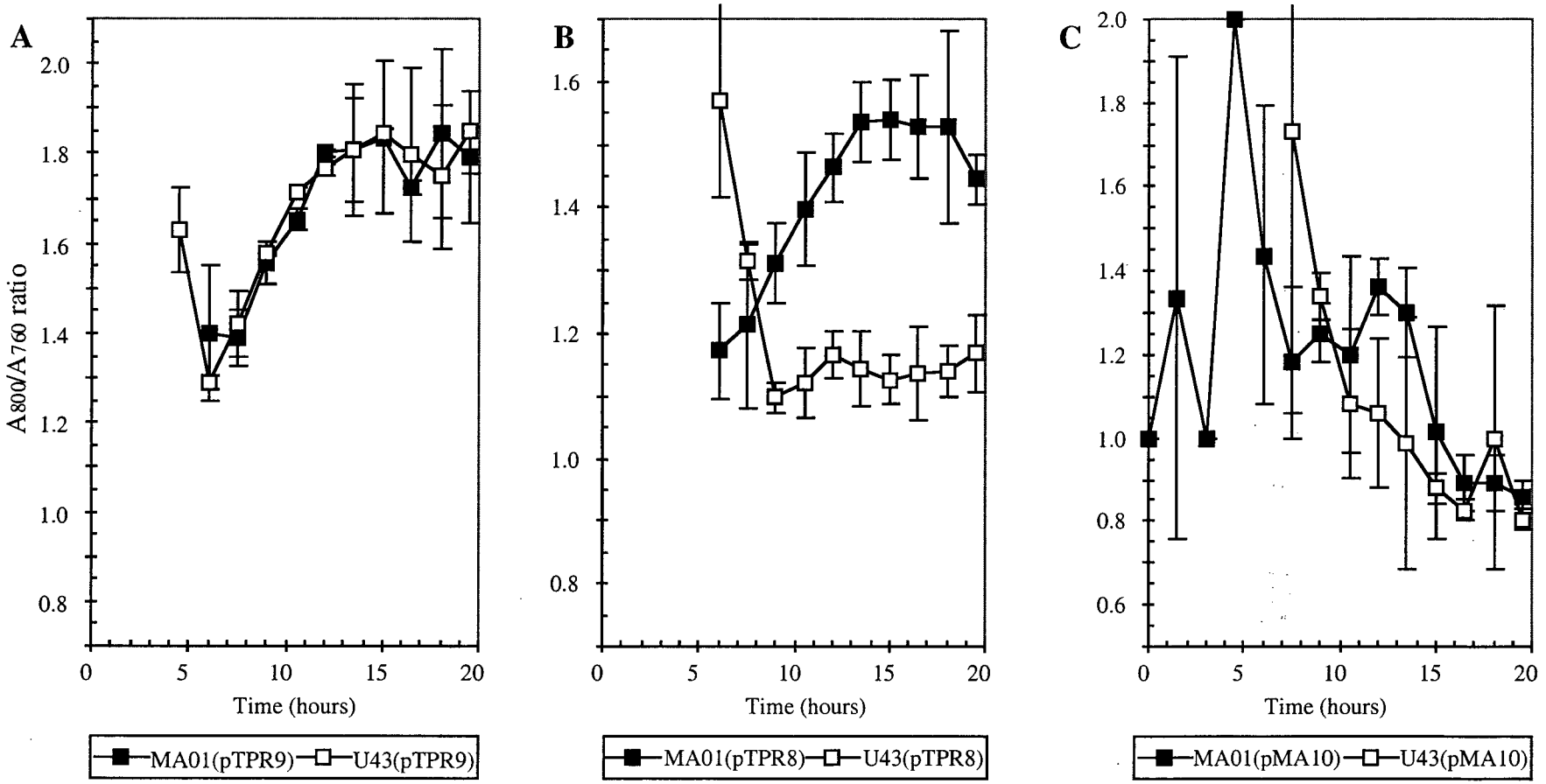

Figure 3.5.4. Peak height ratio of the RC (**A**) in the absence of PufB - plasmid pTPR9, (**B**) in the absence of PufA - plasmid pTPR8, and (**C**) in the absence of both LH1 polypeptides - plasmid pMA10, in the chromosomal *pufX*$^+$ (MA01) and *pufX*$^-$ (U43) backgrounds. (Note: PufX is expressed together with two RC polypeptides from each plasmid.) The height of the voyeur BChl peak at 800 nm was divided by that of the BPhe peak at 760 nm, as a measure of RC "structural order," the proper binding of pigments to polypeptides. In the presence of PufB and absence of PufA, *pufX* merodiploidy clearly increased RC structural order by this measurement.

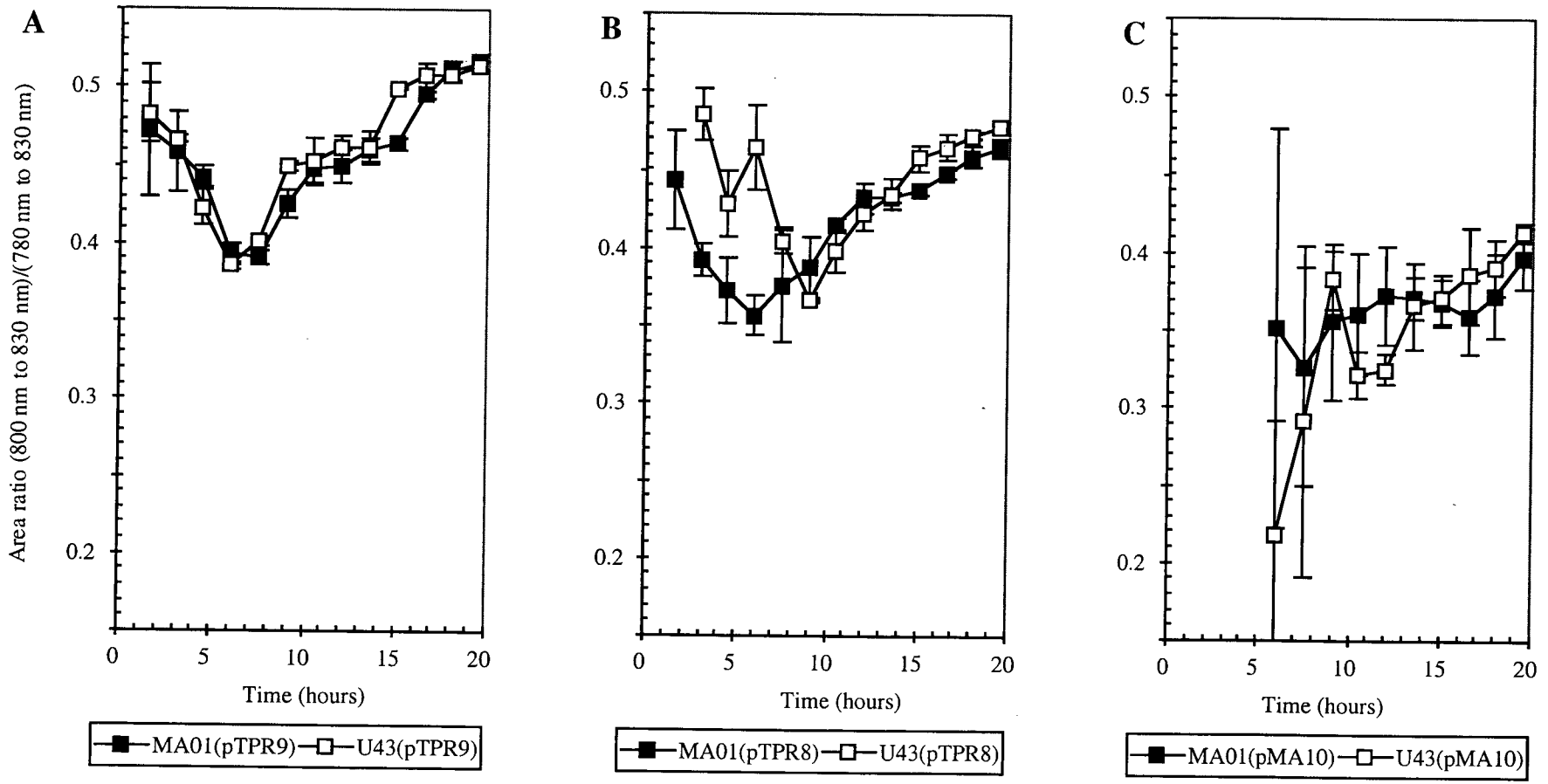

Figure 3.5.5. Voyeur BChl-specific peak area ratio of the RC (**A**) in the absence of PufB - plasmid pTPR9, (**B**) in the absence of PufA - plasmid pTPR8, and (**C**) in the absence of both LH1 polypeptides - plasmid pMA10, in the chromosomal *pufX*$^{+}$ (MA01) and *pufX*$^{-}$ (U43) backgrounds. (Note: PufX is expressed together with two RC polypeptides from each plasmid.) The area of a portion of the voyeur BChl peak from 800 nm to 830 nm was divided by the area from 780 nm to 830 nm (which was inflated by absorption from the BPhe peak at 760 nm and the unbound BChl peak at 780 nm), as a measure of RC "structural order," the proper binding of pigments to polypeptides. No difference in RC structural order was observed using this measurement.

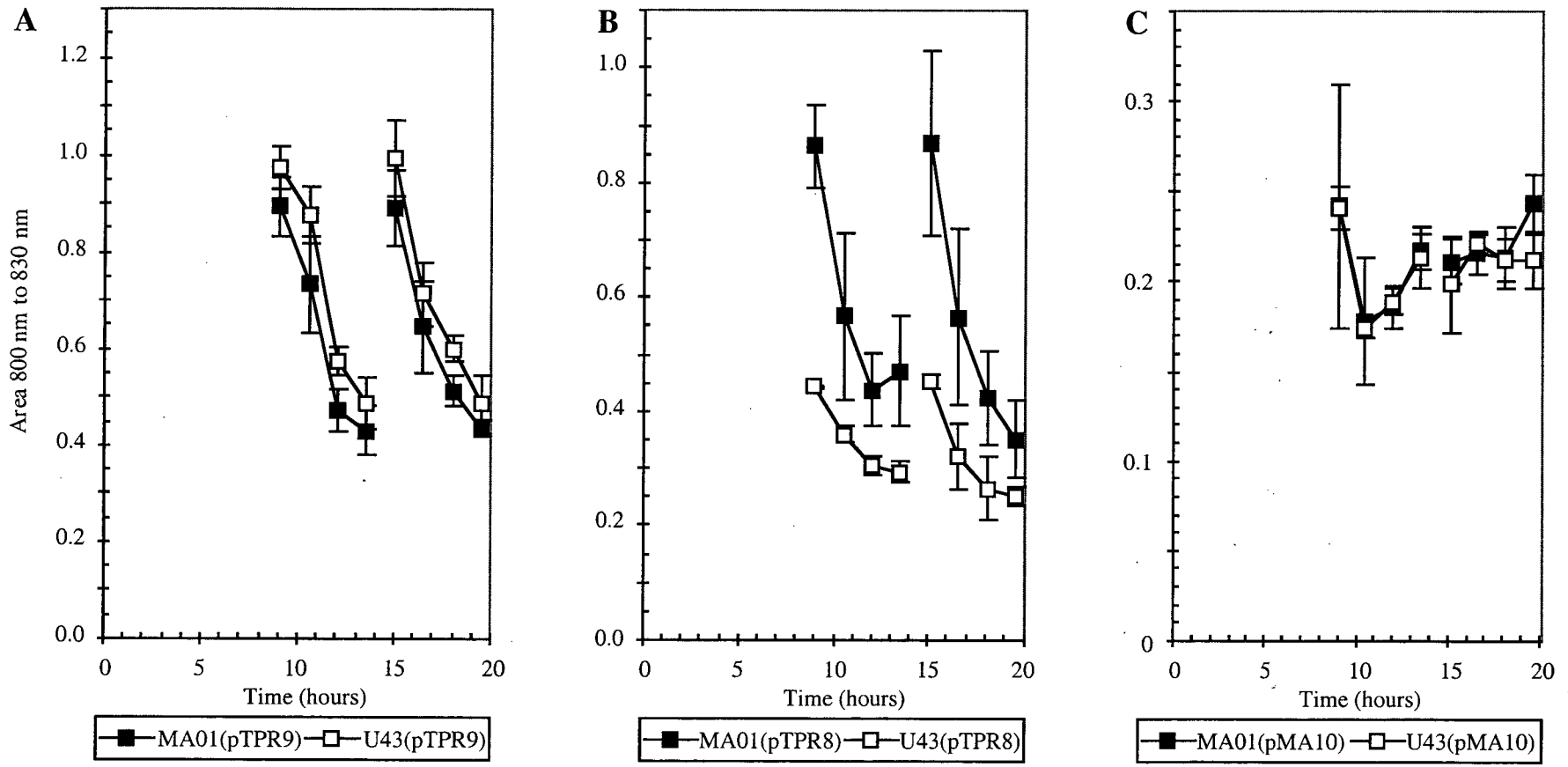

Figure 3.5.6. Decay of the RC (**A**) in the absence of PufB - plasmid pTPR9, (**B**) in the absence of PufA - plasmid pTPR8, and (**C**) in the absence of both LH1 polypeptides - plasmid pMA10, in the chromosomal *pufX*$^+$ (MA01) and *pufX*$^-$ (U43) backgrounds. Decay was initiated at 9 hr and at 15 hr by switching cultures to aerobic conditions. A portion of the RC voyeur BChl peak area was measured from 800 nm to 830 nm to minimize the contribution of absorption by BPhe and unbound BChl.

RC production in these experiments was near the limit of detection, and the changes in absorbance over time were small and varied depending on which LH1 polypeptide was present. Nevertheless, the consistent observation of an aberrant RC absorption spectrum in U43(pTPR8) compared to MA01(pTPR8), together with the RNA blot showing plentiful *pufLM* mRNA transcription for RC polypeptides from pTPR8 (see Figure 3.1.2), suggests a model in which the *pufX* merodiploid strain MA01(pTPR8) produces more PufX protein, which co-operates with PufB to direct RC assembly, possibly by substituting for PufA. Experiments that support this hypothesis are described in Sections 3.5.3 and 3.5.4.

Surprisingly, the enhanced RC assembly in MA01(pTPR8) compared to U43(pTPR8) did not result in improved phototrophic growth (see Figure 3.1.3), and on some occasions, growth appeared to be impaired in the *pufX* merodiploid strains, including MA01(pTPR8) (not shown).

Table 3.5.1. Linear production rates (area units per hour) and exponential decay rate constants (per hour) for the RC in chromosomal *pufX*$^+$ (MA01) and *pufX*$^-$ (U43) backgrounds, determined from triplicate cultures. PufX is expressed together with two RC polypeptides from each plasmid. A portion of the RC voyeur BChl peak area was measured from 800 nm to 830 nm. Note: post-assembly RC decay in pMA10 strains (after 15 hours of semiaerobic growth) was a transient and insignificant phenomenon. When U43(pMA10) was switched to aerobic conditions post-assembly, the average trend was an increase in RC peak size, hence the negative value of the decay rate constant.

Strain	Genotype chromosome (plasmid)	RC production	Mid-assembly RC decay	Post-assembly RC decay
U43(pTPR9)	*pufQBALMX*$^-$(*pufQALMX*)	163 ± 4	92 ± 92	210 ± 80
MA01(pTPR9)	*pufQBALMX*$^+$(*pufQALMX*)	161 ± 32	234 ± 89	239 ± 91
U43(pTPR8)	*pufQBALMX*$^-$(*pufQBLMX*)	128 ± 18	181 ± 17	286 ± 159
MA01(pTPR8)	*pufQBALMX*$^+$(*pufQBLMX*)	156 ± 35	396 ± 192	327 ± 268
U43(pMA10)	*pufQBALMX*$^-$(*pufQLMX*)	33 ± 7	243 ± 35	-67 ± 103
MA01(pMA10)	*pufQBALMX*$^+$(*pufQLMX*)	35 ± 7	235 ± 139	28 ± 22

3.5.2. PufX does not directly affect LH1 assembly

Kinetics of assembly and decay of LH1 were measured in chromosomal *pufX*$^+$ (MA01) and *pufX*$^-$ (U43) backgrounds, which were complemented with the *pufQBAX* genes on plasmid p*Stu* I (lacking *pufLM* and the putative ribosome-binding site of *pufX*). Such removal of genes encoding two RC polypeptides, PufL and PufM, leaving only PuhA, allowed the evaluation of LH1-specific absorption at 880 nm without the minor contribution of the RC special pair BChl peak at 865 nm. The strains MA01(p*Stu* I) and U43(p*Stu* I) were at similar culture densities throughout the experiments (Figure 3.5.7) and should have progressed similarly into semiaerobic growth conditions. LH1 assembly was not different between U43(p*Stu* I) and MA01(p*Stu* I) (Figure 3.5.7, Table 3.5.2), even though an earlier study found that the PufX protein inhibited *in vitro* LH1 reconstitution by 50% when present at a ratio of 1:2 with PufA (125). This discrepancy may be due to a low ratio of PufX to PufA even in the *pufX* merodiploid strain, as well as the presence of LH1 assembly factors such as LhaA *in vivo* (170).

It is well-documented that deletion of *pufX* results in increased LH1 absorption in *R. capsulatus* and *R. sphaeroides* (34, 74, 87, 94), and I describe a similar effect of *pufX* copy number in Section 3.5.3. The *puf* operon on plasmid p*Stu* I lacks the RC genes *pufLM* and the putative ribosome-binding site of *pufX*, so that the only active *pufX* gene should be on the chromosome of MA01(p*Stu* I) and absent from U43(p*Stu* I). Although leaky expression of PufX can be detected in U43(p*Stu* I) (see Figure 3.5.10), an effect of *pufX* copy number should still be observed (see Figure 3.5.11). Therefore, I suggest that PufX simply does not affect LH1 absorption in the absence of the RC.

Measurements of LH1 decay (Figure 3.5.7, Table 3.5.2) were not of sufficient quality to indicate a destabilizing effect of PufX on LH1, analogous to that observed *in vitro* (125).

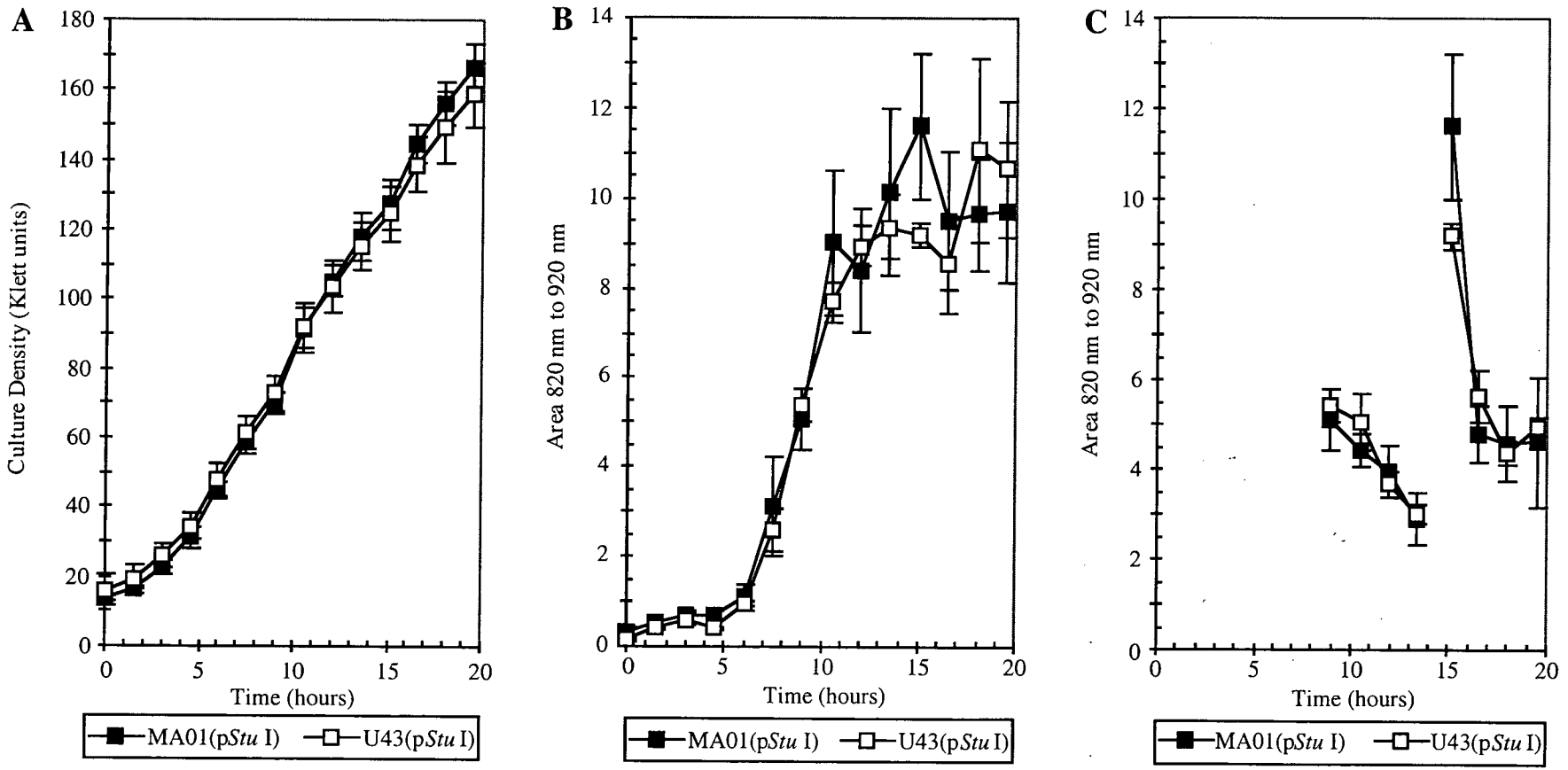

Figure 3.5.7. Assembly and decay of LH1 in the absence of PufL and PufM - plasmid p*Stu* I (carrying *pufX* without the putative ribosome-binding site), in the chromosomal *pufX*$^+$ (MA01) and *pufX*$^-$ (U43) backgrounds. (**A**) Semiaerobic growth. (**B**) Production of LH1, measured as the peak area from 820 nm to 920 nm. (**C**) Decay of LH1, initiated at 9 hr and at 15 hr by switching cultures to aerobic conditions.

Table 3.5.2. Linear production rates (area units per hour) and exponential decay rate constants (per hour) for LH1 in chromosomal *pufX*$^+$ (MA01) and *pufX*$^-$ (U43) backgrounds, determined from triplicate cultures. Plasmid p*Stu* I, which restores the LH1 polypeptides without the RC polypeptides PufL and PufM, carries *pufX* without the putative ribosome-binding site. The LH1 peak area was measured from 820 nm to 920 nm.

	Genotype chromosome (plasmid)	LH1 production	Mid-assembly LH1 decay	Post-assembly LH1 decay
U43(p*Stu* I)	*pufQBALMX*$^-$(*pufQBA...X?*)	494 ± 32	76 ± 138	450 ± 72
MA01(p*Stu* I)	*pufQBALM*$^-$*X*$^+$(*pufQBA...X?*)	525 ± 12	37 ± 185	628 ± 35

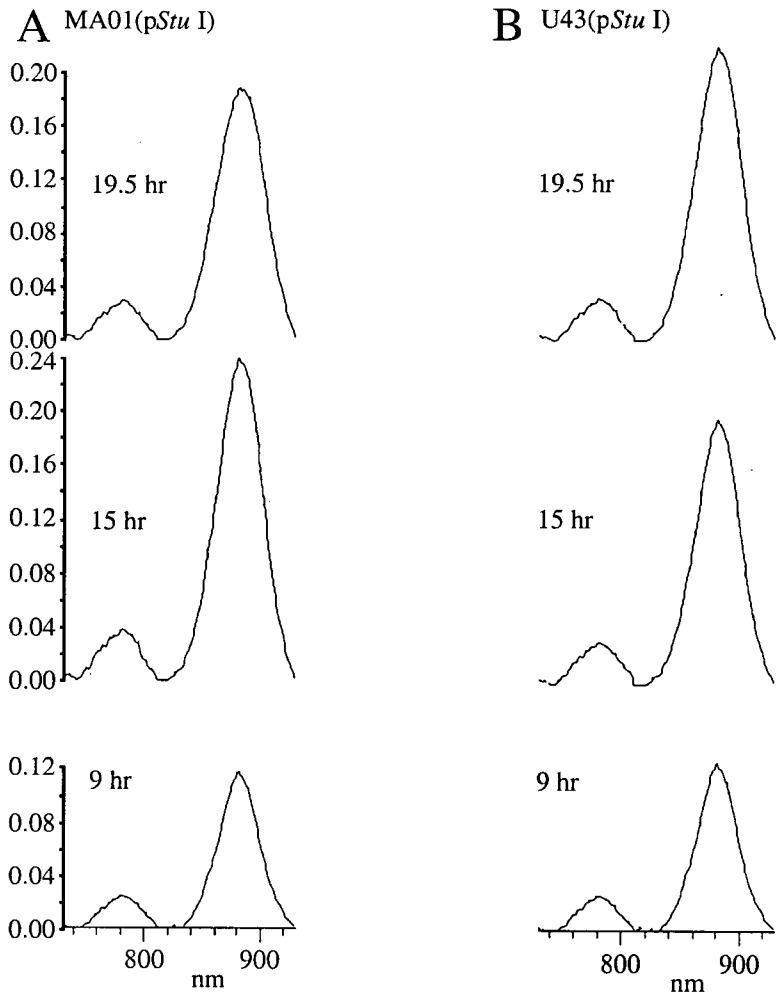

Figure 3.5.8. Absorption spectra (room temperature, pathlength 1 cm) of nascent LH1 in chromosomal (**A**) *pufX*$^+$ (MA01) and (**B**) *pufX*$^-$ (U43) backgrounds, in the absence of the RC polypeptides PufL and PufM - plasmid p*Stu* I (carrying *pufX* without the putative ribosome-binding site), after 9 hours, 15 hours, and 19.5 hours of semiaerobic growth. Spectra were normalized and a baseline was drawn as described in Section 2.15. In addition to LH1 absorption at 880 nm, there is a small peak at 780 nm, attributed to unbound BChl.

3.5.3. Immunodetection of *R. capsulatus* PufX; effects of PufX on RC-LH1 absorption spectra and phototrophic growth

An antiserum generated against synthetic, KLH-conjugated peptides of the cytoplasmic and periplasmic segments of *R. capsulatus* PufX recognized the protein in unfractionated cells of U43(pTB999), which had the entire *pufQBALMX* operon deleted from the chromosome and restored on a plasmid, but not in U43(pTL2), which had a deletion of *pufX* on the plasmid (Figure 3.5.9). The PufX-specific band in MA01(pTL2), which has *pufX* intact on the chromosome and under control of the natural promoters and a KIXX cartridge promoter, was more intense than that in U43(pTB999). This indicates that the chromosomal *pufX* gene produced a significant amount of PufX in the MA01 background, in contrast to U43(pTL2), which lacked the chromosomal *pufX* gene. In MA01(pTB999), which had *pufX* on both chromosome and plasmid, more PufX was present than in MA01(pTL2). Surprisingly, although the amount of PufX in the *puhC*$^-$ strain MA02(pTB999) was comparable to that in MA01(pTB999), the amount in MA02(pTL2), the *puhC*$^-$ strain expressing PufX only from the chromosome, was quite low, suggesting that accumulation of chromosome-derived PufX may depend on PuhC as well as on plasmid-derived PufX. SB1003, the wild type (LH2$^+$*puf*$^+$) parent of all these strains, had abundant PufX, but its *puhB*$^-$ derivative, MA05, had only a trace amount. Complementation of MA05 with the 6xHis-tagged *puhB-N* gene co-transcribed with *pufQ* from plasmid pMA7 restored PufX; plasmid pMA17, carrying *puhB-N* alone, did not.

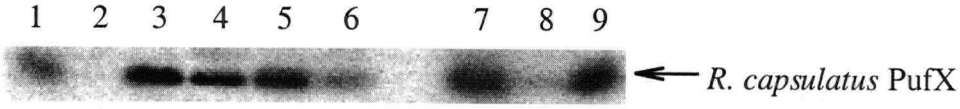

Figure 3.5.9. Immunoblot of *R. capsulatus* PufX in unfractionated cells (50 μg of protein) of *pufX*$^-$, *pufX*$^+$, and *pufX* merodiploid strains: (1) U43(pTB999), (2) U43(pTL2), (3) MA01(pTB999), (4) MA01(pTL2), (5) MA02(pTB999), (6) MA02(pTL2), (7) the wild type strain SB1003, (8) the *puhB* deletion strain MA05, and (9) MA05(pMA7), in which *pufQ* and *puhB-N* were co-transcribed. Restoration of *puhB-N* alone to MA05(pMA17) did not increase the level of PufX (not shown).

PufX was not detected well in U43, MA01, and MA02 strains carrying *puf* operons with deletions of *pufB* and *pufA* on plasmids pTPR9, pTPR8, and pMA10, and only a trace amount was detected in the strains carrying a *puf* operon deleted for *pufLM* on p*Stu* I (Figure 3.5.10). The presence of a faint band in U43(p*Stu* I) suggested that some expression of PufX still occured when the putative ribosome-binding site of *pufX* was deleted. I propose that although the *Stu* I-*Tth*111 I deletion in p*Stu* I removed the sequence 5' of the *pufX* initiation codon Met1 (AGGAGAAGAGACC**ATG** - the putative ribosome-binding site is underlined and Met1 is in boldface) (74), fusion of a sequence between *pufA* and *pufL* with the first two codons of *pufX* (CTGAGG**ATG**TCCATG) allowed initiation of translation at Met3.

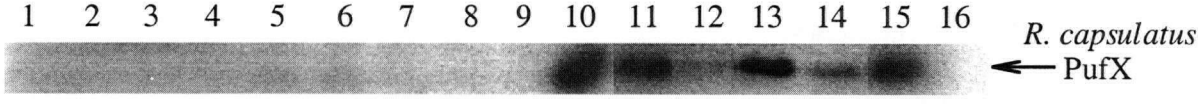

Figure 3.5.10. Immunoblot of *R. capsulatus* PufX in unfractionated cells (50 μg of protein) lacking components of the RC-LH1 core complex. The U43 series of strains lacks the *pufQBALMX* genes on the chromosome whereas the MA01 and MA02 series have *pufX* intact; the MA02 series is *puhC*⁻. PufX is not detected well in strains complemented with plasmids carrying *pufQALMX*: (1) U43(pTPR9), (2) MA01(pTPR9), (3) MA02(pTPR9); or *pufQBLMX*: (4) U43(pTPR8), (5) MA01(pTPR8), (6) MA02(pTPR8); or *pufQLMX*: (7) U43(pMA10), (8) MA01(pMA10), (9) MA02(pMA10). PufX is abundant in the wild type strain SB1003 (lane 10) and observed in strains complemented with *pufQBALMX*: (11) U43(pTB999), (13) MA01(pTB999), (15) MA02(pTB999). A trace amount of PufX is detected in U43(p*Stu* I) (lane 12), which is complemented with *pufQBAX* lacking the putative ribosome-binding site of *pufX*. The amount of PufX in MA01(p*Stu* I) (lane 14) is only slightly increased due to the chromosomal *pufX* gene, and PufX was not detected in the *puhC*⁻ strain MA02(p*Stu* I) (lane 16).

The absence of PufX has been observed to cause increased LH1 absorption in both *R. capsulatus* (74, 87) and *R. sphaeroides* (34, 94). The *R. sphaeroides* studies indicate that the amount of antenna BChl per RC is higher (34, 94). In *R. capsulatus*, the *pufX* deletion increased the amounts of both RC and LH1 polypeptides in chromatophores (86), whereas an increase in LH1 polypeptides due to the *pufX* deletion was reported in *pufBA* merodiploid *R. sphaeroides* without quantification of RC polypeptides (7). Therefore, there are several possible reasons for the increase in LH1 absorption. It may represent either extra LH1 complexes without RCs, or an extended LH1 oligomer around the RC, or increased absorption by the pigments bound by LH1 polypeptides. In

Section 4.7 of the Discussion, I will summarize the evidence that indicates that PufX modulates the binding of pigment cofactors by LH1.

As expected, the *pufX*⁻ strain U43(pTL2) had more LH1 absorption than U43(pTB999), which had a complete *puf* operon on the plasmid (Figure 3.5.11, Table 3.5.3). Strains MA01(pTB999) and MA02(pTB999), with an extra copy of *pufX* on the chromosome and more PufX protein, had less LH1 absorption, indicating that excess PufX can reduce LH1 absorption below normal in the presence of the RC. MA01(pTL2), which contained more PufX protein than U43(pTB999), and MA02(pTL2), which contained less (Figure 3.5.9), both had LH1 peak heights intermediate between those of U43(pTB999) and U43(pTL2) (Table 3.5.3). This surprising observation suggests that the PufX protein produced from the chromosome and accumulating in the presence of PuhC may not be functionally equivalent to that produced from the plasmid in U43(pTB999) in terms of RC-LH1 organization.

Notably, the absence of *pufX* from the plasmid increased LH1 absorption regardless of the *pufX* gene's presence on the chromosome (Table 3.5.3).

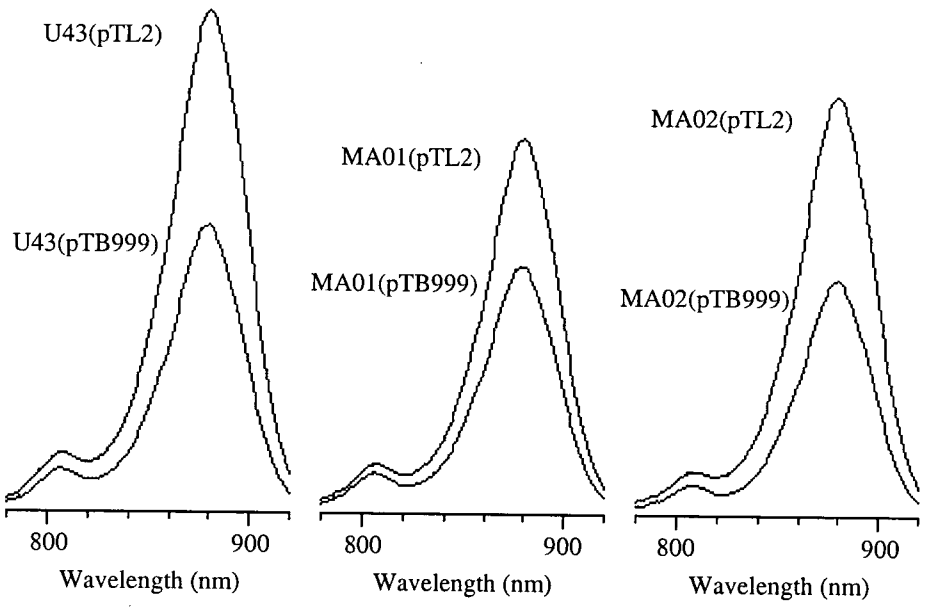

Figure 3.5.11. Absorption spectra (room temperature, pathlength 1 cm) of the RC and LH1 in intact cells of *pufX*⁻, *pufX*⁺, and *pufX* merodiploid strains (200 μg protein). A baseline was drawn from 700 nm to 930 nm. LH1 absorption was measured at 880 nm.

Table 3.5.3. The amount of LH1-specific absorption depends on the location of the *pufX* gene.

Strain (with lane number from Figure 3.5.9)		LH1 peak height at 880 nm (relative to U43(pTB999))	LH1 peak height at 880 nm (pTL2 strains relative to isogenic pTB999 strains)
U43(pTL2)	2	175%	175%
MA01(pTB999)	3	86%	
MA01(pTL2)	4	131%	152%
MA02(pTB999)	5	82%	
MA02(pTL2)	6	146%	178%

Earlier studies described PufX as essential for phototrophic growth of an LH2$^+$ strain of *R. capsulatus* grown on RCV minimal medium under high light intensity (87). U43(pTL2), an unpublished LH2$^-$ *pufX*$^-$ strain constructed in that study, was reported to have the same phenotype (85). However, in my hands U43(pTL2) could grow phototrophically at a slow rate without any apparent lag (Figure 3.5.12, Table 3.5.4) when the inocula were grown semiaerobically for 24 hours. When the inocula were incubated semiaerobically for 48 hours, growth of U43(pTL2) was insignificant until well into the experiment, at which point growth may be due to secondary mutations as observed previously in both *R. capsulatus* and *R. sphaeroides* (7, 86, 88). Growth was significantly better when the intact *puf* operon was present on the plasmid in strain U43(pTB999), when *pufX* alone was intact on the chromosome and the remaining *puf* genes were on the plasmid in MA01(pTL2), and when both *pufX* genes were present in MA01(pTB999) (Figure 3.5.12, Table 3.5.4). The growth rates of MA01(pTB999) and MA01(pTL2) were occasionally slower than that of U43(pTB999) (not shown), suggesting that the excess PufX produced from the chromosomal gene (see Figure 3.5.9) might be inhibitory to phototrophic growth. I have not been able to determine the cause of this variability.

The *puhC*$^-$ strain MA02(pTL2), which expresses a low level of PufX from the chromosome (Figure 3.5.9), always exhibited poor phototrophic growth compared to the *pufX* merodiploid *puhC*$^-$ strain MA02(pTB999), whereas the *puhC*$^+$ strains MA01(pTL2) and MA01(pTB999) grew equally well regardless of different *pufX* copy numbers (Figure 3.5.12, Table 3.5.4). Therefore, the PuhC protein may be important for PufX derived from the chromosome (but not the plasmid) to associate stably with the RC-LH1 proteins expressed from the plasmid and function in phototrophic growth.

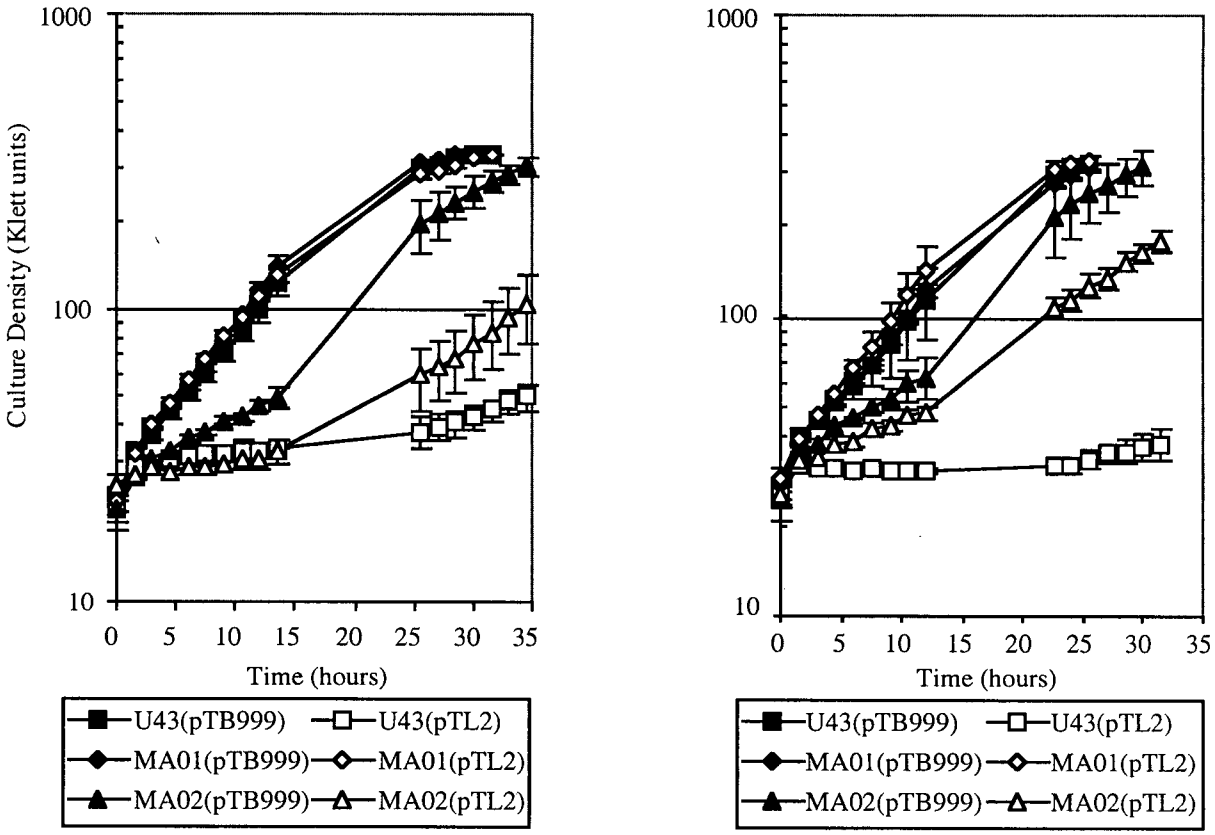

Figure 3.5.12. Phototrophic growth of strains that are *pufX*$^+$ on the chromosome or on a plasmid, *pufX* merodiploid, and *pufX*$^-$, after 24 hours (left) and 48 hours (right) of semiaerobic growth.

Table 3.5.4. Effects of ectopic expression of PufX and *pufX* merodiploidy upon phototrophic growth after semiaerobic growth for 24 hours and 48 hours. These strains correspond, in order, to lanes 1 to 6 of Figure 3.5.9.

Strain **24 hours**	Genotype chromosome (plasmid)	Relative specific growth rate ± standard deviation of 3 cultures
U43(pTB999)	*puhC*$^+$*pufQBALMX*$^-$(*pufQBALMX*)	100% ± 3%
U43(pTL2)	*puhC*$^+$*pufQBALMX*$^-$(*pufQBALM*)	13% ± 1%
MA01(pTB999)	*puhC*$^+$*pufQBALM*$^-$*X*$^+$(*pufQBALMX*)	107% ± 7%
MA01(pTL2)	*puhC*$^+$*pufQBALM*$^-$*X*$^+$(*pufQBALM*)	103% ± 4%
MA02(pTB999)	*puhC*$^-$*pufQBALM*$^-$*X*$^+$(*pufQBALMX*)	47% ± 8%
MA02(pTL2)	*puhC*$^-$*pufQBALM*$^-$*X*$^+$(*pufQBALM*)	12% ± 8%
48 hours		
U43(pTB999)	*puhC*$^+$*pufQBALMX*$^-$(*pufQBALMX*)	100% ± 21%
U43(pTL2)	*puhC*$^+$*pufQBALMX*$^-$(*pufQBALM*)	6% ± 3%
MA01(pTB999)	*puhC*$^+$*pufQBALM*$^-$*X*$^+$(*pufQBALMX*)	100% ± 6%
MA01(pTL2)	*puhC*$^+$*pufQBALM*$^-$*X*$^+$(*pufQBALM*)	109% ± 18%
MA02(pTB999)	*puhC*$^-$*pufQBALM*$^-$*X*$^+$(*pufQBALMX*)	57% ± 14%
MA02(pTL2)	*puhC*$^-$*pufQBALM*$^-$*X*$^+$(*pufQBALM*)	39% ± 3%

3.5.4. TOXCAT analysis of PufX transmembrane segments of *R. capsulatus* and *R. sphaeroides*

TOXCAT hybrids with the single predicted TM segment of PufX from *R. capsulatus* and that from *R. sphaeroides* (Figure 3.5.13) both supported growth of *E. coli* MM39 on maltose minimal medium, confirming their transmembrane nature. In this simulation of the photosynthetic membrane environment, both TM segments were able to self-associate as indicated by moderate CAT activity in cell lysates (Figure 3.5.14). This result is consistent with the hypothesis that PufX forms the axis of twofold symmetry in dimeric RC-LH1 complexes of *R. sphaeroides* (43, 44, 136). Moreover, the ability of PufX to self-associate means that the excess PufX predicted to support RC assembly in the absence of PufA in strain MA01(pTPR8) may be dimeric or possibly even oligomeric.

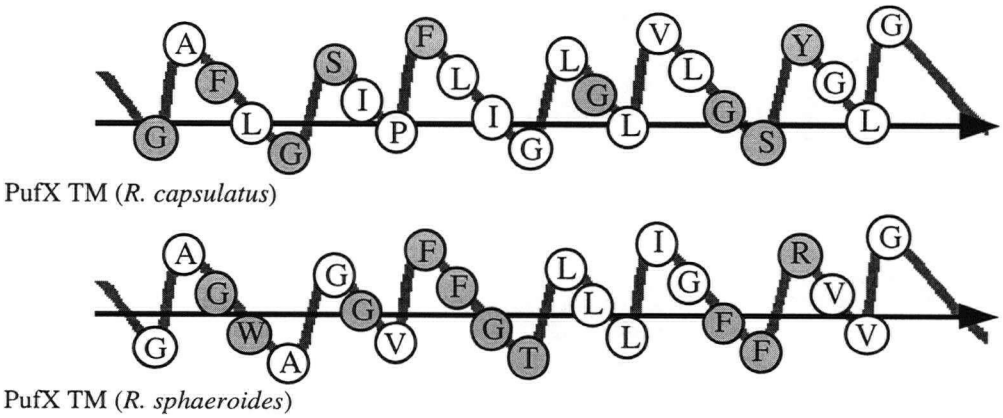

Figure 3.5.13. The putative TM segments of *R. capsulatus* PufX and *R. sphaeroides* PufX. Grey circles mark potential electrostatic, hydrogen bonding, dipole-dipole, and aromatic ring stacking interactions, and the GxxxG motifs. The arrows, pointing toward the C-terminus of each protein, indicate a face of each helix where I propose that it may interact with another helix based on either the GxxxG motifs or the locations of residues capable of participation in interactions.

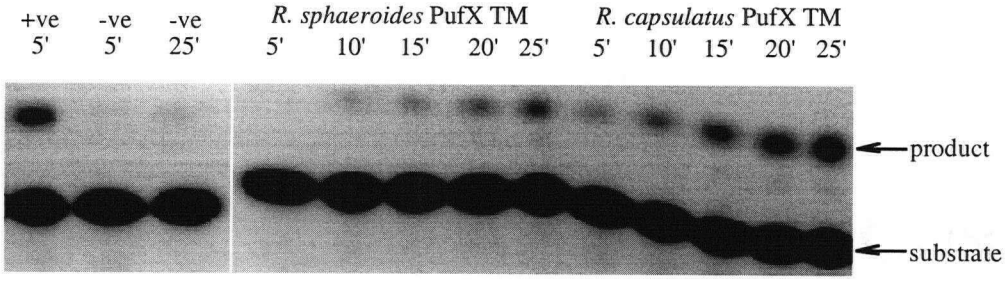

Figure 3.5.14. Thin layer chromatogram showing CAT activity in lysates of *E. coli* MM39 expressing TOXCAT hybrids of the TM segment of PufX of *R. capsulatus* and of *R. sphaeroides*: acetylation of fluorescently labelled 1-deoxychloramphenicol over time. The positive control is a hybrid of the glycophorin A TM segment; the negative control is the same TM segment with a G83I substitution.

To summarize the results of this subchapter, excess PufX promotes RC assembly in an LH1 polypeptide-specific manner: only in the absence of PufA and presence of PufB. PufX is undetectable in LH1$^-$ strains, and at low levels in the absence of either PufL and PufM or PuhB. PuhC also affects PufX and function. LH1 absorption and phototrophic growth are affected not only by the amount of PufX protein and RC absorption, but by the location of the *pufX* gene. PufX is capable of homodimerization through its TM segment, which suggests its location in RC-LH1 complexes at the axis of twofold symmetry as well as the ability of excess PufX to resemble oligomeric PufA.

3.6. *In silico* analyses of PuhB, PuhC, PuhD, PuhE, PufQ, and PufX

3.6.1. Sequence features, evolution, and topology of predicted PuhB proteins

In a phylogenetic tree of PuhB sequences from eleven species (Figure 3.6.1), the α3-Proteobacteria (genera *Rhodobacter* and *Roseobacter*) clustered together, but the β-proteobacterium *R. gelatinosus* was positioned amidst other α-proteobacteria, and the third major branch included two uncultured marine proteobacteria as well as the γ-proteobacterium *T. roseopersicina*. This unexpected pattern suggests the possibility of lateral exchange of *puhB* sequences.

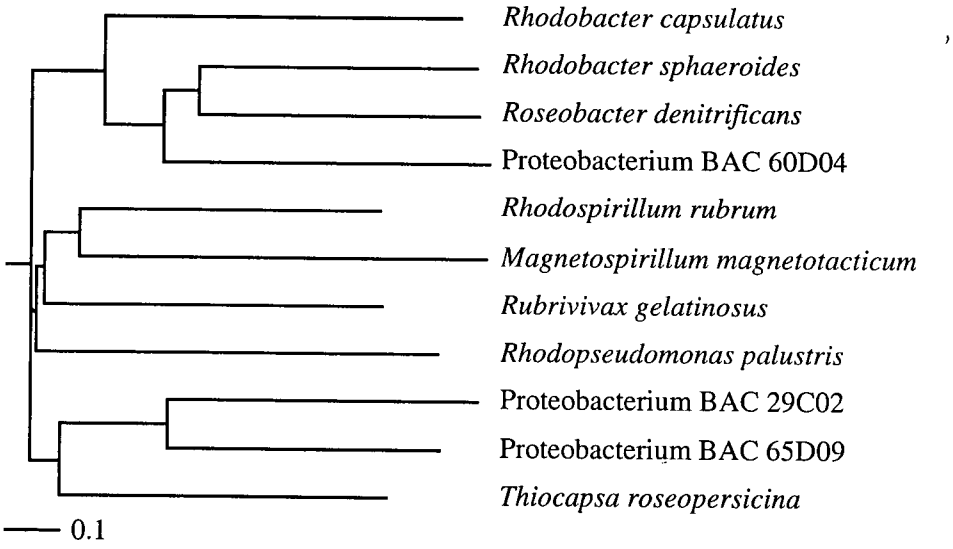

Figure 3.6.1. Phylogenetic tree of PuhB proteins, plotted with ClustalW software (http://www.es.embnet.org). The length of the bar represents a corrected mean distance of 0.1 substitutions per residue.

An alignment of predicted PuhB protein sequences revealed some conserved features, such as alternating acidic and aromatic residues near the N-terminus (Figure 3.6.2). In contrast with the negative effect of an N-terminal 6xHis tag in *R. capsulatus*, the *R. gelatinosus* PuhB N-terminal region is extended and contains several His residues. The second TM segment of PuhB, which may homodimerize in *R. capsulatus*, is not conserved in sequence.

Figure 3.6.2. Sequence alignment of predicted PuhB proteins. Sequence identity and similarity are indicated in boldface, and the TM segments are overlined.

Hydropathy analyses together with the positive inside rule (157) suggested a conserved topology of the PuhB protein: a cytoplasmic N-terminal domain, three TM segments, and a periplasmic C-terminal domain (Figure 3.6.3).

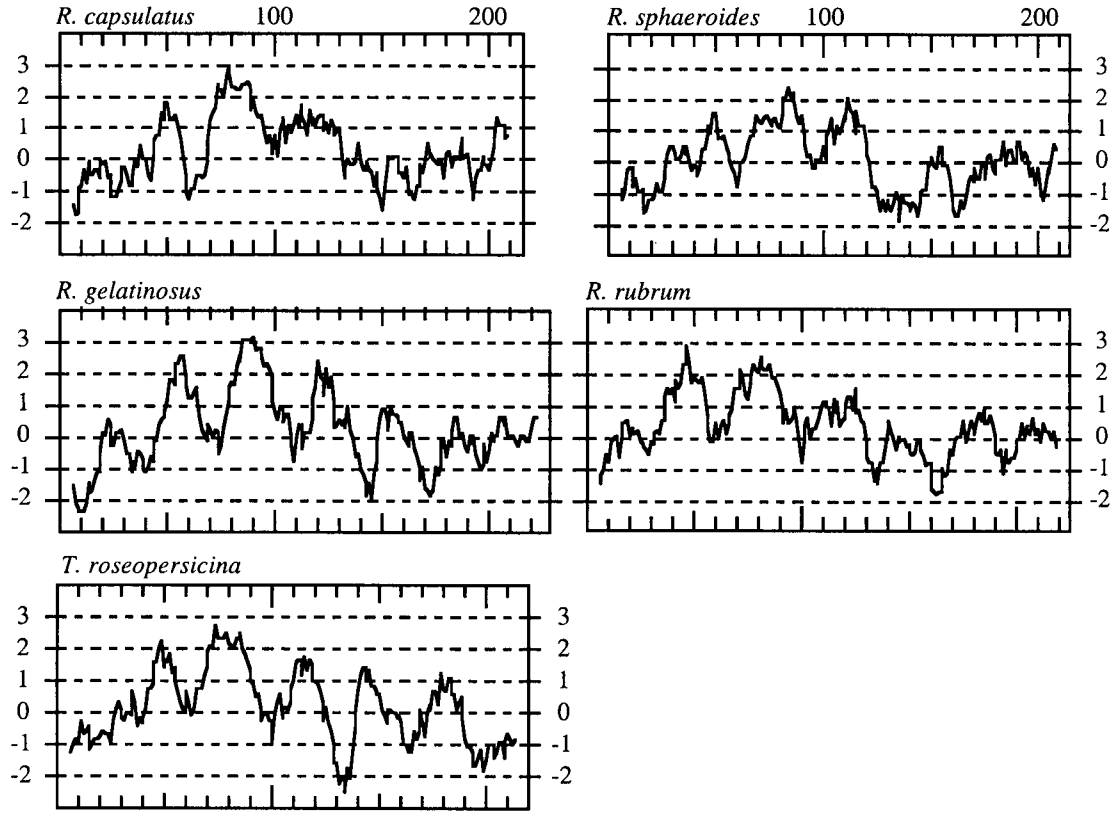

Figure 3.6.3. Hydropathy plots of selected PuhB proteins, done with DNA Strider software (91), using the Kyte-Doolittle algorithm (78). Positive values on the vertical axis indicate hydrophobic segments, and the horizontal axis indicates the number of amino acid residues from the N-terminus.

3.6.2. The highly divergent predicted PuhC proteins and the Puc2A polypeptide of *R. sphaeroides*

Phylogenetic analysis positioned the *R. capsulatus* PuhC protein sequence closest to that of *R. sphaeroides*, its best substitute out of the three tested (Figure 3.6.4). Surprisingly, the very poor substitute from *R. gelatinosus*, a β-proteobacterium, was a closer sequence match than the moderately good substitute from *R. rubrum*, an α-proteobacterium. Lateral exchange of *puhC*

sequences is a possible explanation for this result. Consistent with an underlying pattern of vertical inheritance, PuhC of the γ-proteobacterium *T. roseopersicina* occupied a unique branch of the tree.

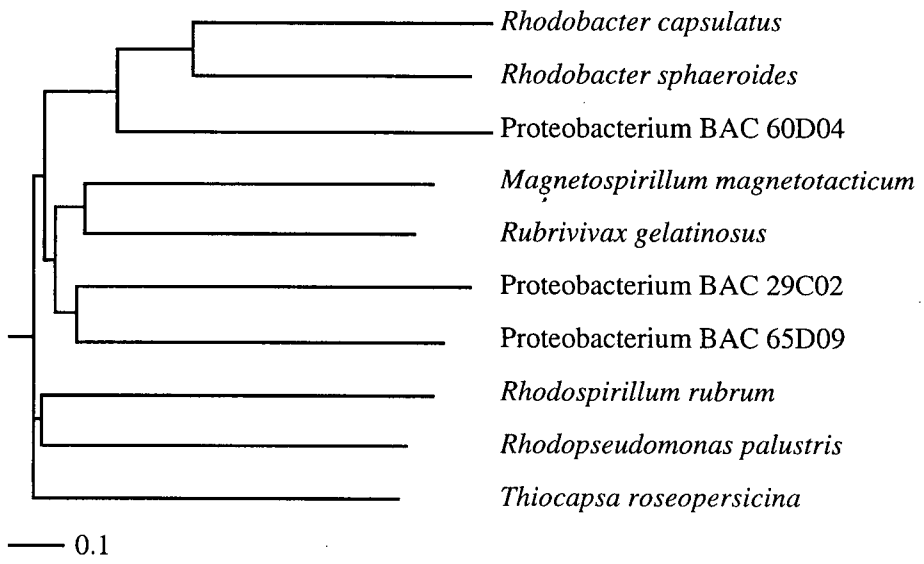

Figure 3.6.4. Phylogenetic tree of PuhC proteins, plotted with ClustalW software (http://www.es.embnet.org). The length of the bar represents a corrected mean distance of 0.1 substitutions per residue.

In addition to the *puh* operon, *R. sphaeroides* has a sequence weakly similar to *puhC* within the *puc2A* gene. This gene encodes a C-terminally extended PucA (LH2α) polypeptide that is co-expressed with Puc2B, a typical LH2β polypeptide, but appears to form a protein complex that is not LH2 (172). The C-terminal extension of Puc2A, located entirely in the periplasm, consists of twenty-odd repeats of a $P(A/V)_{1\text{-}2}E_{1\text{-}2}A_{2\text{-}3}$ motif followed by sequence motifs weakly similar to conserved sequences in the predicted periplasmic C-terminal domain of PuhC. This weak similarity to PuhC has gone unnoticed so far (172). I aligned the most C-terminal sequence of Puc2A with the predicted PuhC proteins of ten species of purple bacteria (Figure 3.6.5).

There are very few conserved amino acids in the sequences of PuhC proteins; the most obvious, scattered near the C-terminus, are E95, F98, R108, R110, N128, G129, D135, T138, G139, F147, G148, and F155 of *R. capsulatus* (Figure 3.6.5). The spacing of these residues is invariant in all PuhC sequences, but the Puc2A sequence, if related to PuhC, has undergone significant deletions. The most PuhC-like features of Puc2A are the motifs EGGYV and DPVTG.

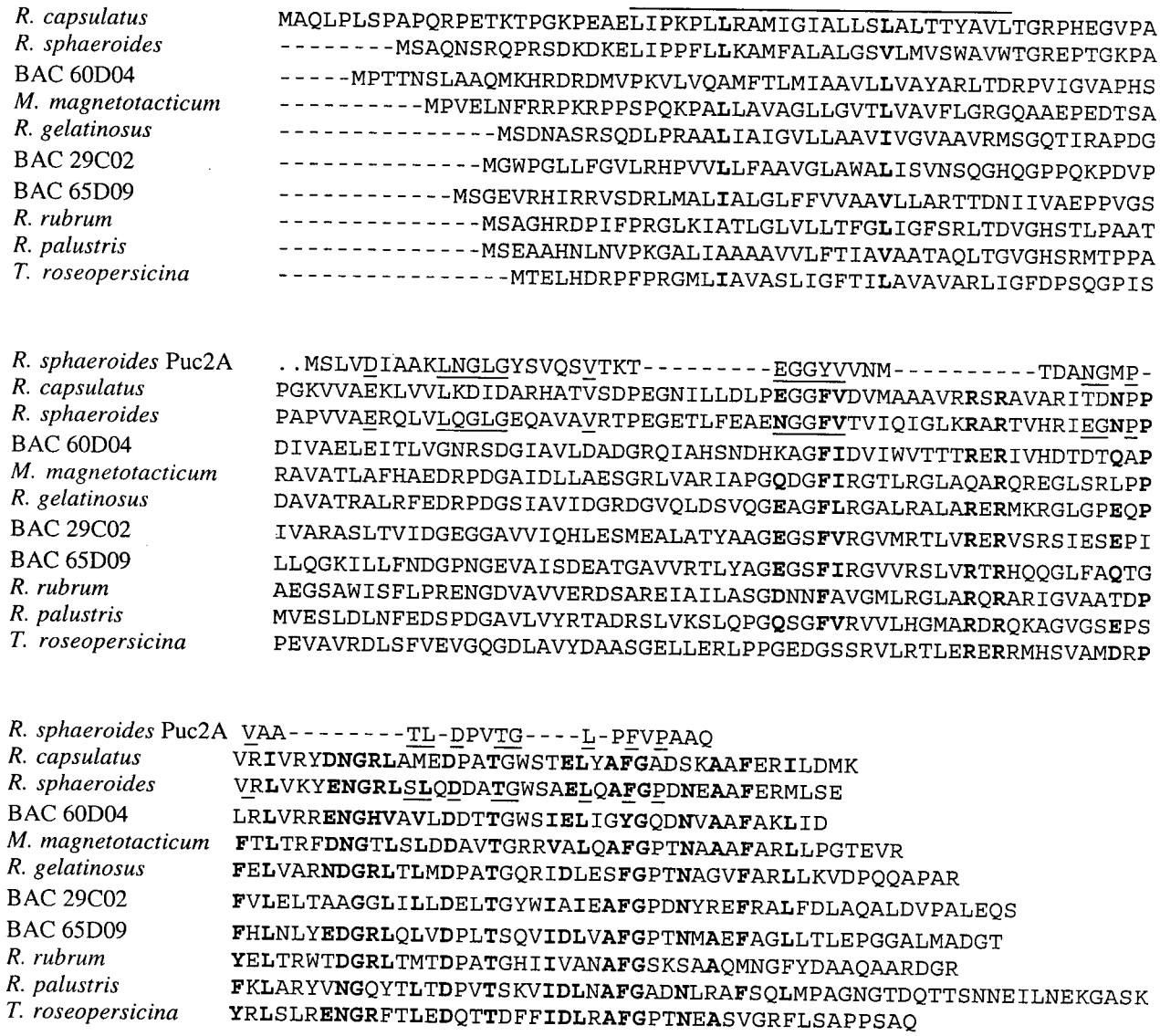

Figure 3.6.5. Sequence alignment of predicted PuhC proteins. Sequence identity and similarity are indicated in boldface, sequence identity or similarity of *R. sphaeroides* Puc2A to *R. sphaeroides* PuhC is underlined, and the TM segment is overlined.

Hydropathy analyses together with the positive inside rule (157) suggest a conserved topology of PuhC with a short cytoplasmic N-terminal region, a single TM segment, and a fairly large periplasmic C-terminal domain (Figure 3.6.6).

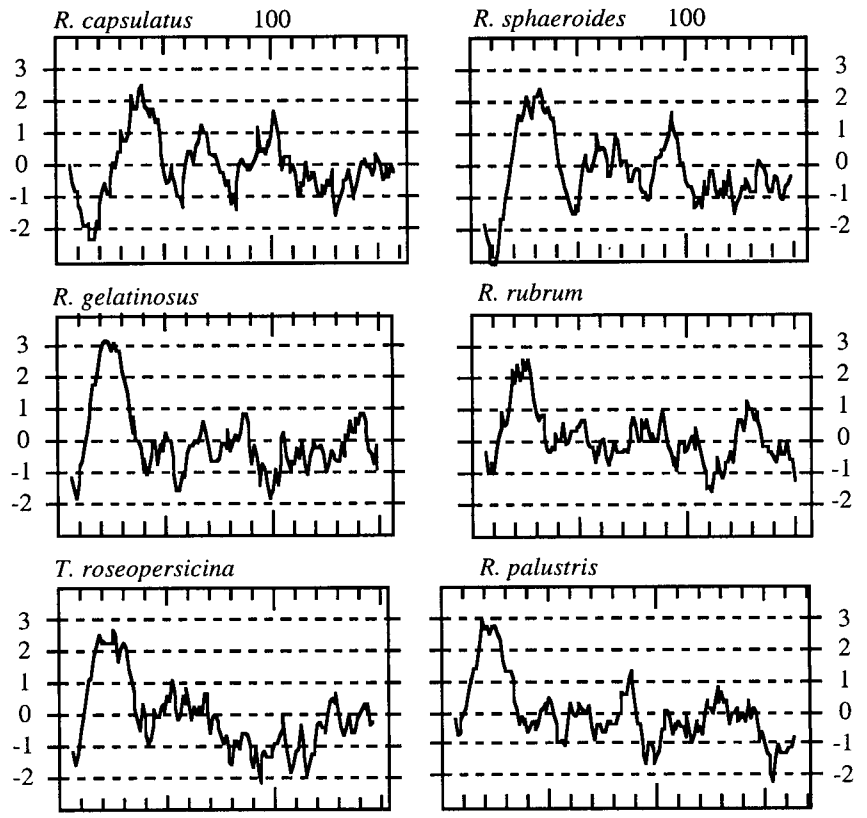

Figure 3.6.6. Hydropathy plots of selected PuhC proteins, done with DNA Strider software (91), using the Kyte-Doolittle algorithm (78). Positive values on the vertical axis indicate hydrophobic segments, and the horizontal axis indicates the number of amino acid residues from the N-terminus.

3.6.3. The variable region of the *puh* operon and the eventful history of *puhD*

Phylogenetic trees suggest that the *puhBCE* gene products of *R. capsulatus* have remained most similar to those of *R. sphaeroides* and Proteobacterium BAC 60D04 (Figures 3.6.1, 3.6.4, and 3.6.10). It is surprising, therefore, that *R. capsulatus* lacks the genes *puhD* and *acsF*, which are located between *puhC* and *puhE* in *R. sphaeroides* and BAC 60D04. Together with *R. sulfidophilum* (for which the 5' region of *puhE* is incompletely sequenced but appears to contain *acsF*), these are the four species of α3-proteobacteria for which *puh* sequences are available. The *puhD* and *acsF* genes are also present in more distant α-proteobacterial relatives of *R. capsulatus*, namely *R. palustris* and *M. magnetotacticum*, and absent from *R. rubrum* and two uncultured marine proteobacteria, BAC29C02 and BAC65D09. The absence of *puhD* from the β-

proteobacterium *R. gelatinosus* (which has *acsF*) and the γ-proteobacterium *T. roseopersicina* (which lacks *acsF*) suggests that the ancestral *puh* operon may have consisted of only *puhABCE*. The *acsF* gene, encoding an aerobic oxidative cyclase of the BChl biosynthetic pathway, could have been transferred laterally from the cyanobacteria to an ancestor of certain α-Proteobacteria, and integrated in the 5' region of *puhE*. The *puhD* sequence may have appeared or been acquired earlier or later than *acsF*. The position of *R. gelatinosus* in the phylogenetic tree of PuhC sequences suggests that it acquired *puhC* laterally from an α-proteobacterial *puhABCE* operon similar to those of BAC29C02 and BAC65D09, and the 3' sequence *puhD* could have been lost from an ancestor of *R. gelatinosus* subsequently. The most recent event is almost certainly the loss of *puhD-acsF* from *R. capsulatus* at the species level.

A phylogenetic tree indicates that PuhD is most similar between *R. sphaeroides* and Proteobacterium BAC60D04 (Figure 3.6.7), consistent with results for the other Puh proteins.

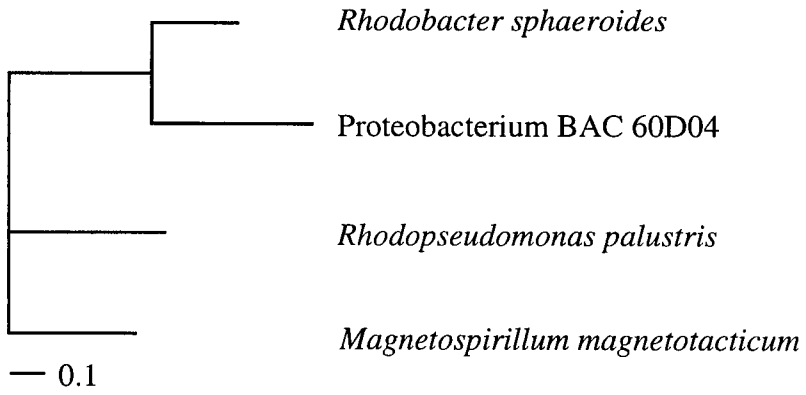

Figure 3.6.7. Phylogenetic tree of PuhD proteins, plotted with ClustalW software (http://www.es.embnet.org). The length of the bar represents a corrected mean distance of 0.1 substitutions per residue.

The *puhD* sequences are the smallest of the *puh* genes (98 to 103 codons) and have not been investigated by mutational analysis. The sequences of predicted PuhD polypeptides are highly conserved (Figure 3.6.8), and bear no homology to any other protein in the databases. Surprisingly, the hydropathy plots of three sequences indicate no TM segments, whereas that of *R. sphaeroides* PuhD suggests the possibility of a central TM segment (Figure 3.6.9).

R. sphaeroides -----MGLFTKQAEEVPCTVEVSHQFESLHAHVRFDNGAIVHPGDEVLVHGAPVLAAFGE
BAC 60D04 -----MGLFTRSKETAPCTVTISHRFEELSAHVKFNNGAVVHPGDSVQVEGPEIMAPYGV
R. palustris ----MFGLGKRTSFDVPCTVEIEQTSETLHAHVVLDGDIEIGPGDEVLVHDAPTHVDFGE
M. magnetotacticum MGREAWPGSGRTVVEVPCTVEIEQTPESLHAHVTLDAGFEIEPGDEVRVNDAPTEVPYGE

R. sphaeroides VVVEERTATITRASGLERLWTRLTGDLGAMELCEFSFSEQVTL
BAC 60D04 CVEEQRMATITRASKIERLWTRSTGDFEFMELCEFSFSEGVLS
R. palustris RLVVRRTATVVRAGLLDKIRARFEGYRELTELYEVSFSTGRVQ
M. magnetotacticum RLTVRRTATVTRAGRLERAWTKLIAHLELTELYEVSFSERRKL

Figure 3.6.8. Sequence alignment of predicted PuhD proteins. Sequence identity and similarity are indicated in boldface.

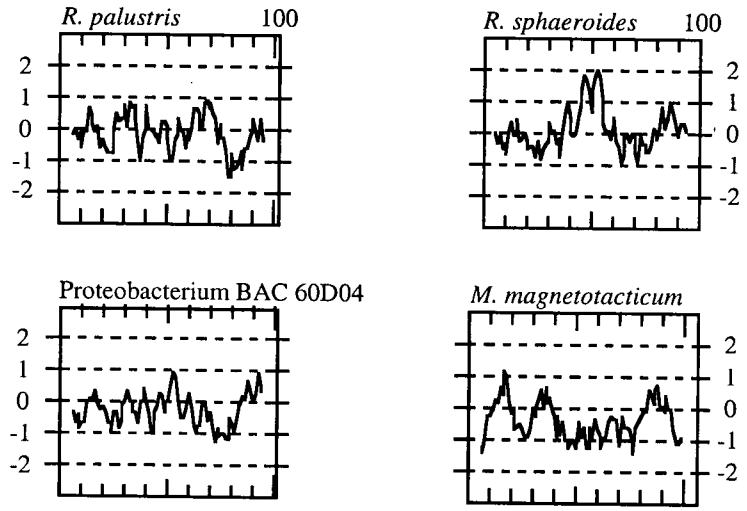

Figure 3.6.9. Hydropathy plots of PuhD proteins, done with DNA Strider software (91), using the Kyte-Doolittle algorithm (78). Positive values on the vertical axis indicate hydrophobic segments, and the horizontal axis indicates the number of amino acid residues from the N-terminus.

3.6.4. Predicted PuhE proteins of purple bacteria and *Chloroflexus*

The discovery of an incomplete putative *puhE* sequence in the green filamentous anoxygenic phototroph *C. aurantiacus* suggests that it may contain a *puh* operon even though its RC lacks a PuhA polypeptide. In a phylogenetic tree of twelve PuhE sequences (Figure 3.6.10), *C. aurantiacus* was positioned closest to the cluster of four PufQ-containing species of the α3-Proteobacteria. This suggests that the *puhE* gene may have been laterally transferred to *C. aurantiacus* from the α-

Proteobacteria. As expected, there was a separate branch for the PuhE sequence of the γ-proteobacterium *T. roseopersicina*, but that of the β-proteobacterium *R. gelatinosus*, surprisingly, was related to that of *R. rubrum*, an α-proteobacterium.

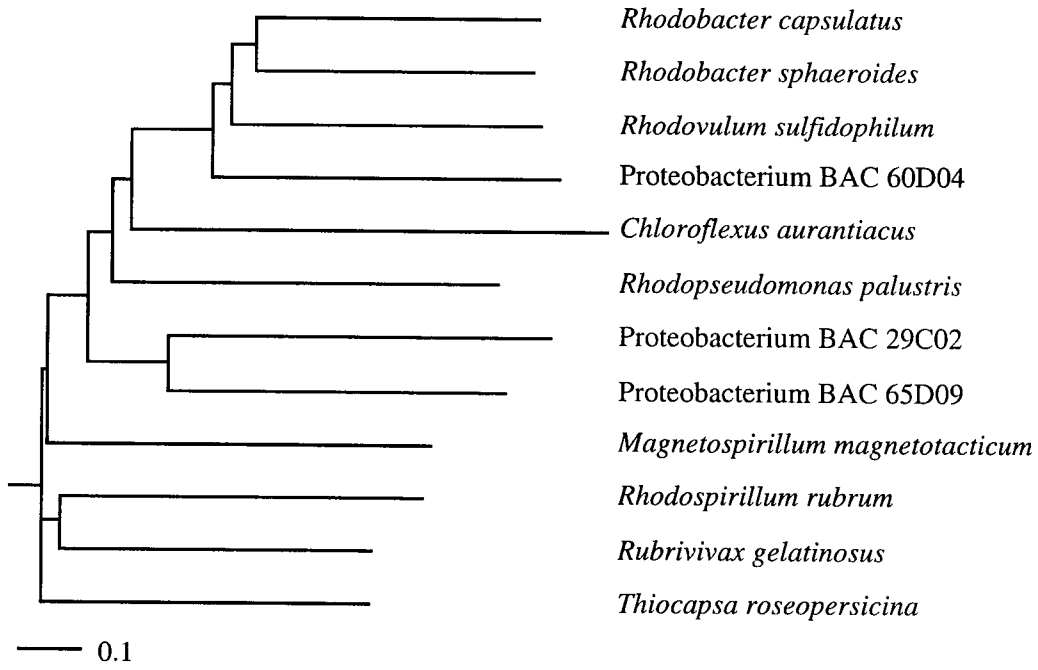

Figure 3.6.10. Phylogenetic tree of PuhE proteins, plotted with ClustalW software (http://www.es.embnet.org). The length of the bar represents a corrected mean distance of 0.1 substitutions per residue.

Several conserved sequences, often containing one or more aromatic residues (e.g. WWF, WGW, WHE, WTF, EHW, WXW), were apparent in an alignment of the predicted PuhE proteins (Figure 3.6.11).

Hydropathy plots indicated the presence of an extremely short N-terminal region in all PuhE proteins, seven TM segments, and a C-terminal domain of variable length (Figure 3.6.12). The fifth predicted TM segment is not very hydrophobic, but the prediction is consistent with the positive inside rule (157), which suggests a periplasmic N-terminus and cytoplasmic C-terminus. The *C. aurantiacus* PuhE sequence has the shortest C-terminal domain, and the largest, that of *R. palustris* PuhE, is 105 amino acid residues longer, although *C. aurantiacus* and *R. palustris* occupy adjacent positions in the PuhE phylogenetic tree.


R. capsulatus -MNNPWLVALTTIFVWWFSTGAILWRIRRADLSGRAAHMRSVVGGLPLLIGGYIAMANSADDTSVRGAHVAFLSAVSVWGWFELAFLSGVVAGPNR
R. sphaeroides MLTSPWVVALSAIFVWWFSTGILLWRVRHADNRGPEAHLTSVILGLPMLFAGAWGYVHTLHDETVGGVYVAFLSALGVWGWIELSFLSGVITGPNT
R. sulfidophilum MIATAWFAALAAFFIWWFSTGAILIVVRRAEHRGRLAHLRATVMALPLLGGGVWLFEVTRHVETVATAYLAFLSAIAIWGWVELAFLTGVITGPNT
BAC 60D04 MLGSPWIAALIAIFSWWFFTGIILLIVRRKDVAGATAHGASVVLGVPLLALGIFGAVISAASLSVANIYLAFFSVLLIWGWIELAFLSGVITGPLR
C. aurantiacus XXXRSTVVSWPGPRR
R. palustris -MVSYLGPPIFAAFVWWFSTGAVLL-L--VGSVGRSELLRAVCAG-GMLTIALCGLSVTAHDVSVGAAYMAFSCIIFLWGAQEIAFLSGWLTGPRA
BAC 29C02 ---MLFPALVIAVSSWWLLTGLALL-L--VHQSHDRVRLGFLALS-ILALVAWALVPFTVSSSEPLAAALGFILGLLIWGWLEVSYLLGYVNGPNH
BAC 65D09 -MSEFALALLVALTGWWFSTGVILW-L--VHRNERHHRTIFVLAT-ATMLLAYYGVGTSVHQSTPQSVVLAFCLALLLWGWLEMGYLMGFVTGPRK
M. magnetotacticum -MSGPVAPALYAILLWWSATGLVLV-L--QHLPRRTHARSMIAAS-AALAGALWAIRAVADDDSEAGAYIGFTAAIVVWGWQEMSYYMGFVSGPKP
R. rubrum -MSDIGVPMLYTLFVWWFGTGAVLF-L--DGLPRHTFKWTMLGAT-VLFGAGLWGLHATADNTSVGATYSAFTCGFLIWAWQEVSFYTGWVTGPRK
R. gelatinosus -MLSVAIPVLFAVFVWWFSTGLILL-L--DGLPRKTFRWSLVIST-ALAATAFAALVHTAGNTTPADAYCAFTCALLVWGWHELAFLTGWITGPRK
T. roseopersicina -MLEYGYPVLFALGLWWFSTGLVLY-L--DNLPGRTFGWTMLGGA-AVLAFAVFALVVSSTSTSLSATYIAFTSGVIVWGVLEMSYFTGLLTGPRK
R. capsulatus DHCPPFASMTERFLRSVGTLLWHEIGLISALILCAVLVWTGENHFGLWTFATLFFARVSAKLNLFLGVPRINTQFLPKPLAHLASHFRHARMNFLF
R. sphaeroides DPCPLHARAPERFLRAVGTVLWHEIVLLTVLIAMAVHAADAPNRFGLWTFLVLFVARVSAKLNLYLGVPYINVEFLPSTLAHLSSYFRHTRMNRFF
R. sulfidophilum TRCHPHARGWERFMRAYGTIAYHETLLVVILFAMLVTSHGSANGVGVWTFIVLFFARISAKLNLFLGVPKINIEFLPTPLSHLPSHFKISRLNWLF
BAC 60D04 DPCPKSLRGWARFRRAWQTVSHHEALLLCGLVLMAVIALDAANPLGFWAYFILFAARISAKLNLFFGVPRINLEFIPQPLLHLSSYFKQGPVTGVF
C. aurantiacus KPCPPDARGFQRFYYALGTHFYHQLSCLLELGLLVWLLQDASHWLGPLTFGLSWALQQSAKLNVLYGVRSLQVDLFPAHLAFLASYWQPGPPSAFF
R. palustris EPCPPGAKGFARFSYALQAIIYHEICLLACGGVVLVVTLGAENQVGLWTYVALWVLRQSAKINLFLGVPVTNDELMPDAVQFLKTYFARKPVSAFF
BAC 29C02 EVCDKNATMWQRFKGGVATTIYHEVCVLLSVGLLAVMSLGQVNPTAFYTLTVLWLMRWSAKLNLFLGVRSFNDRWLPDHLHYLASYLKTDRLNPFL
BAC 65D09 EACPLGASTASRMRLGLRTCLWHELTLLLMVAVLAWLSWQQPNQTALWTFTVLWLMRWSSKLNLVLGVRNYNQSWLPDRLAYVHSYIPRRLINPLF
M. magnetotacticum AACAPNLRGFDRFLAALATSLWHDFAILAGGLAILCLSWGQRNRVALWTYALLVLMNASARLNLFLGVRNLKRRVXXX
R. rubrum VCCPPGCRGWKHFLHALHANLWHELSMALSAALVVWLTWGAPNQVGTWTFMVLWWMHESARLNVLFGVRNLNAEFLPEHLAHMKGFLTQKPINLLF
R. gelatinosus TATPAGASTWTRFVHAIQAILWHEIAIISVGVAIVAVTWGEPNQVGTWTYIVLWTMRASAKLNLFLGVRNLSEEFLPEHLKYLVSFFRRRAMNLLF
T. roseopersicina APCPPGCPAWKRFGLAILTSLYHEFAVLSAVAFLVVISWGEPNQVGTWTFVVLWLMRWSAKLNLFLGVPNLN-DWLPEHLAYLKSYMPKRSMNLLF
R. capsulatus PVSITVLTFATGCWMERAA-DAQTDGIFIGFVLLTVLTALALLEHWFMVLPLPDQKLWTWMLPSVEDPAETVAEPVPGRIPVGE
R. sphaeroides PLSVTLLTFATGCWIERALSAGGANHREVGFWLLAALTALAVLEHWFMVVNLQDRKLWKWMMPERRRPVRGGRVP-PSHLPDTVRRGEAKLLKEKA
R. sulfidophilum PISISALTFAVACFMERLF-AVGAPHDKVGFGLLTTITALALLEHWLMVLPLPDERLWRWMLPERKASAE--KDKIPSNDLSRT
BAC 60D04 GLGVTGLSLVTAALGLALF-SASTVEAQIGHALLFALCALATLEHWLMVIPLPDAKLWRWMLPTLSTNTKTGQSHEL
C. aurantiacus RPSVSVSTLLALMLWLSIG-AHIGDPAAIRLALLASLLTLGALEHWLLLIPAPATVPAPATD
R. palustris PISVTMATAVLVVMIQRIVEVADTPFEVVGLTLVSTLFALGVVEHWFMLLPLPAITLWSWGIRPGFSPENIVMEQKPSAPIAAASAQGSPAQLSEA
BAC 29C02 PLSTLIGFYATYSLFGSAS-AAAEITQQLSLNLIATLMLLASIEHLFLMFPLNDAALWSWARENVTPLRAVRDDKDDL
BAC 65D09 PVSVILGVFVTYSLIDSAM-QAADMGPMIALTLAGTIAALGTLEHLFLMAPLRDAALWDWAAPDRGPGVSKSGSQP
R. rubrum PISVTASTVALVVMVMQASDPATSGHHTAGLAMLGALLGLAIIEHWFLILPLPFAELWGWYMRSRERWRTTGPTPPAAPPPSSFAGAAAPVTPGPR
R. gelatinosus PISVTVPTIVAGLMVNEALLPGTAPAMHVGLLLVATMLGMAVIEHWMMVLPLPVAALWRWALRSREPGEPHDPPPLLVPPSDNNLLHAR
T. roseopersicina PISVTVPTLVVVLMVSRALSPGASEFEVVSLILVASLLALGILEHWFLVLPLPDEALWAWALPSRDADGKPGGEPSRQPGQGETRSDGPKRAMAAT

R. sphaeroides	GRL
R. palustris	PTAAEARPAAPQLVVVPTARAEEAQPKARQLCARQRLEDQFRQTFLEQHPRSGLATARVAEPAATLNGRTS
R. rubrum	AAAKCQVSSVES
T. roseopersicina	RKVLRPQTTSPSPGRCVGKARSGAPIAELP

Figure 3.6.11. Sequence alignment of predicted PuhE proteins. Sequence identity and similarity are indicated in boldface, and the TM segments are overlined. (Continued from previous page.)

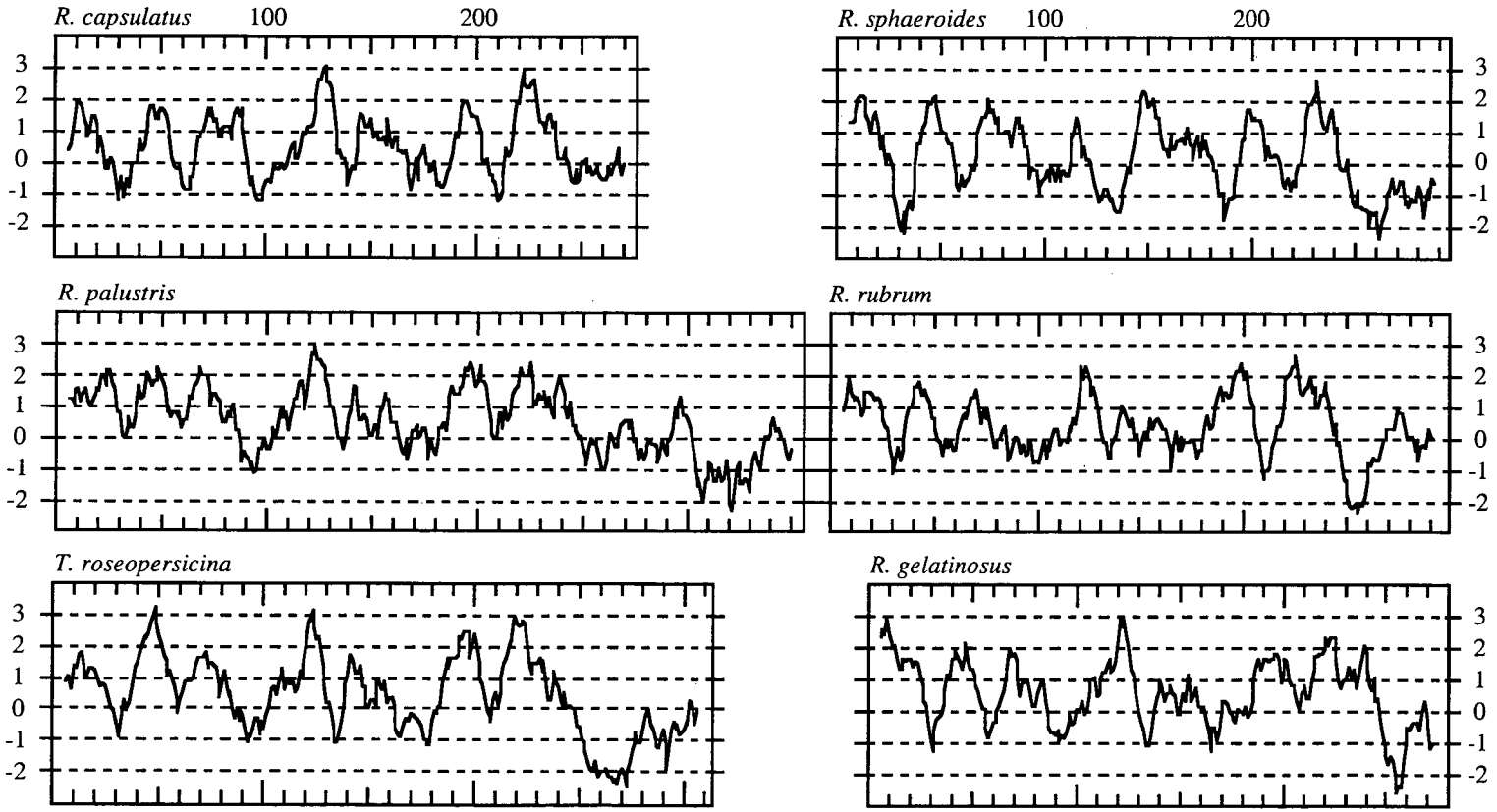

Figure 3.6.12. Hydropathy plots of selected PuhE proteins, done with DNA Strider software (91), using the Kyte-Doolittle algorithm (78). Positive values on the vertical axis indicate hydrophobic segments, and the horizontal axis indicates the number of amino acid residues from the N-terminus. Note the C-terminal extensions in *R. palustris* and *T. roseopersicina*.

3.6.5. The predicted PufQ and PufX proteins

The *pufQ* gene is found only in the α3-Proteobacteria: *R. capsulatus*; *R. sphaeroides*; and *R. sulfidophilum*, and in Proteobacterium BAC60D04, which clusters with them in all phylogenetic trees of Puh proteins. An alignment of the four predicted PufQ proteins is shown in Figure 3.6.13. Hydropathy plots indicate that all PufQ proteins contain a single TM segment (Figure 3.6.14), and the positive inside rule (157) predicts a cytoplasmic N-terminus.

```
R. capsulatus       M-Q--SQRLRAHGVQHVDRVPRPEFALYFSLILIVAVPFALVGWVMALVRERRIPECGPF
R. sphaeroides      MSDHAVNTPVHAARAHGHRAPRAEFYVYFAVILLGAFPVAFVSWIVSTIRHRRLPKRGPF
R. sulfidophilum    MTDQTSD--VHMV--RGHRPPKAEFMVYFTIIFIAALPLAFIASFLAMVRQGDLKTKGPI
BAC 60D04           MTDFANEMSGLSKQPRSLRHSKNEYRVYLALIFLAALPFCTVIWAYRLIRHMTLPTLGPI
                                                                             1

R. capsulatus       ARAWREAGEITPEIFRP
R. sphaeroides      ASAWFDAKAITPLIFRA
R. sulfidophilum    ARAWSQARIITPMIFSA
BAC 60D04           QSAISEARTITPRIFQT
                      2     3       4  5
```

Figure 3.6.13. Sequence alignment of predicted PufQ proteins. Sequence identity or similarity among all four PufQ proteins is indicated in boldface, and the TM segment is overlined. The numbers indicate the sites of point mutations of *pufQ* in *R. sphaeroides* (52) cited in Section 1.3: (1) G58P; (2) A63S; (3) A69S; (4) deletion of termination codon and 3' loop; and (5) mutation of 3' end of *pufQ* mRNA.

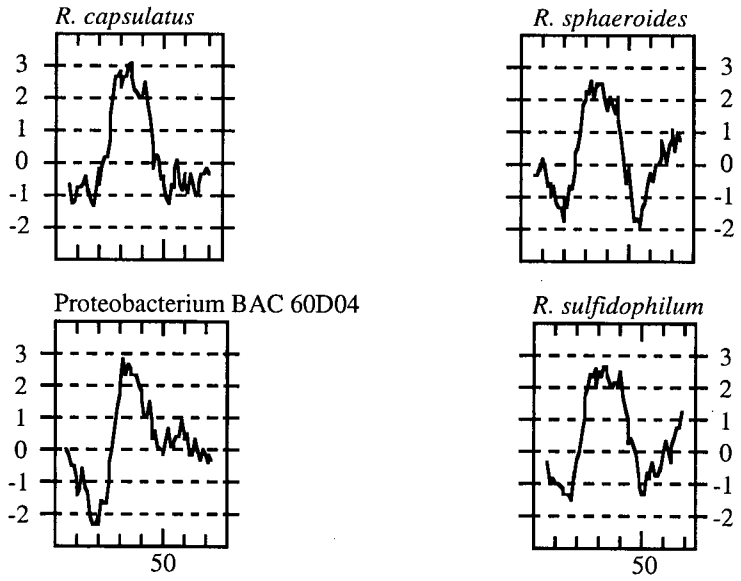

Figure 3.6.14. Hydropathy plots of PufQ proteins, done with DNA Strider software (91), using the Kyte-Doolittle algorithm (78). Positive values on the vertical axis indicate hydrophobic segments, and the horizontal axis indicates the number of amino acid residues from the N-terminus.

The *pufX* gene is found only within the genus *Rhodobacter*. Like the polypeptides of LH1 and LH2 (Figure 3.6.15), PufX polypeptides (Figure 3.6.16) contain a single TM segment as evident from hydropathy plots (Figure 3.6.17), and have a cytoplasmic N-terminus (124). Although there is insufficient sequence similarity to suggest a common origin, the (D/N/E/Q)X(K/R)IW sequence near the N-terminus of PucA polypeptides is also found in the PufX polypeptides. Most PufA polypeptides have the sequence MX(K/R)IW instead, with the initial Met replacing the acidic/amide residue typical of PucA.

R. capsulatus PufB ---------MADKNDLSFTGLTDEQAQELHAVYMSGLSAFIAVAVLAHLAVMIWRPWF
R. capsulatus PucB ----------MTDDKAGPSGLSLKEAEEIHSYLIDGTRVFGAMALVAHILSAIATPWLG

R. capsulatus PufA --------------MSKFYKIWLVFDPRRVFVAQGVFLFLLAVLIHLILLSTPAFNWLTV
R. capsulatus PucA ---------------MNNAKIWTVVKPSTGIPLILGAVAVAALIVHAGLLTNTTWFANYW

R. capsulatus PufA ATAKHGYVAAAQ
R. capsulatus PucA NGNPMATVVAVAPAQ

Figure 3.6.15. Sequences of the LH1 and LH2 polypeptides of *R. capsulatus*. PufB and PucB are paralogous, as are PufA and PucA. The TM segments are overlined. The conserved histidines (underlined) near the ends of the TM segments ligate BChl, while that near the beginning of the PucB TM segment may be connected to a BChl ligand by hydrogen bonding as in other species (75, 111). The sequence NXKIW (underlined) is a conserved feature of PucA.

R. blasticus **MAE**---YNYSH**E**PNAVI**N**LR**V**W**A**LG**QM**V**W**G**A**FLAAVGVVVVICLL**V**GTYLA**G**LLL**P**EQSK
R. capsulatus **M**S-MFDKPFDY**E**NGS**K**F**E**MGI**I**WIGR**QM**AY**GA**FLGSIP**F**LLGL**G**L**V**LGSYG**LG**LM**LP**ERAH
R. veldkampii **MAEK**----HYL**D**GAT**K**VGMATMGAAA**M**GK**G**MGITAVV**FF**GT**V**FF**V**VALAFI**G**QF**LP**DRSR
R. sphaeroides **MADK**TIFNDHL**N**TNPKT**N**LRL**W**VAF**QM**MK**GA**GWAGGV**FF**GTLLLIGFFRV**V**GRML**P**IQEN
R. azotoformans **MADK**TIFDDHLKTNP**K**T**N**LRL**W**VAF**QM**MK**GA**GWAGAV**FF**GTLLMIGFFRV**LG**RAL**P**IDEN

R. blasticus **QAPSP**YGALE**I**VQTIDVA
R. capsulatus **QAPSP**YTTEV**V**VQHATEVV
R. veldkampii **EAPYP**NTIFQ**V**NDIDGTVDGKYTRFAN
R. sphaeroides **QAPAP**NITGALETGIELIKHLV
R. azotoformans **PAPAP**NLTGALETGIELIKHLV

Figure 3.6.16. Sequence alignment of predicted PufX proteins. Sequence identity and similarity among PufX proteins are indicated in boldface, the putative TM segment is overlined, the GxxxG motifs are underlined, and the terminal regions proteolytically removed are doubly underlined. Note the NXRLW sequence (underlined) similar to PucA above.

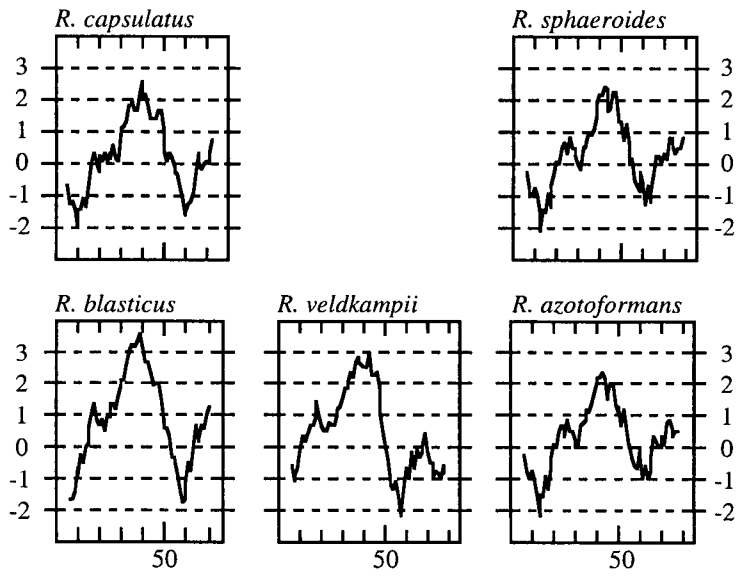

Figure 3.6.17. Hydropathy plots of PufX proteins from five *Rhodobacter* species, done with DNA Strider software (91), using the Kyte-Doolittle algorithm (78). Positive values on the vertical axis indicate hydrophobic segments, and the horizontal axis indicates the number of amino acid residues from the N-terminus.

4. DISCUSSION

4.1. Prologue

A recurring theme in my work has been the discovery of multiple effects of a single protein, from which the most obvious effect does not necessarily indicate the protein's primary function. Within a hierarchical structure of multi-polypeptide proteins and complexes such as the photosynthetic apparatus, my results indicate that a protein such as PuhB has a direct effect on RC assembly, an indirect effect on the level of LH1, and a pronounced effect on PufX; altogether, it facilitates the transition from aerobic to semiaerobic to anaerobic conditions prior to phototrophic growth. Networks of protein-protein interactions have become apparent through this study: the balance between PufQ and PuhE and their connection to PuhC; the dependence of PufX on PuhB and PuhC; a possible PuhB-PufQ co-operation; a role of PufX in RC assembly; and a requirement for the RC in the effect of PufX on LH1 absorption.

Throughout this work, earlier observations and assumptions have been challenged, modified, and even rejected. These developments have necessitated the formulation of new concepts; for example, when speaking of "RC assembly" I have had to differentiate among "RC production," "RC structural order," and the detection of pulse-labelled RC polypeptides in chromatophores over time (155). The dichotomous classification of photosynthesis proteins as "essential" and "non-essential" for phototrophic growth in earlier studies (2, 87, 167) is no longer adequate: for example, PuhC and PufX are conditionally essential; PuhB is *not* essential but indisputably important; and PuhE appears to have both positive and negative roles. Moreover, the photosynthetic apparatus is surprisingly resilient: *R. capsulatus* can grow phototrophically despite drastically reduced RC assembly and the total absence of antenna complexes; LH2 supports growth without LH1; and excess PufX may co-operate with PufB to enhance RC assembly.

With the ongoing characterization of these five enigmatic proteins: PuhB, PuhC, PuhE, PufQ, and PufX, the puzzle of purple bacterial photosynthesis is coming together in unexpected patterns.

4.2. The LH1 polypeptides as RC assembly factors

This study shows that the RC of *R. capsulatus* is much more dependent upon LH1 for assembly than that of *R. sphaeroides*, which had a well-defined, characteristic three-peak spectrum in the total absence of LH1 polypeptides (68). The reason for this difference is unclear; perhaps RC assembly in *R. sphaeroides* benefits from expression of its second set of LH2 polypeptides (172), or is simply more robust. In *R. capsulatus*, there was not only an effect of deletions of *pufB* and *pufA* upon the *pufLM* transcript (Figure 3.1.2) but a clear difference in the shape of the RC absorption spectrum. The BPhe, voyeur BChl, and special pair BChl peaks were all smaller and less distinct without PufA, and even more so without both LH1 polypeptides (Figure 3.1.1).

The absorption spectra of the *pufB*$^-$*pufA*$^+$ *R. capsulatus* strain U43(pTPR9) and the *pufB*$^+$*pufA*$^-$ strain U43(pTPR8) were first recorded by Richter and Drews (128), and it is surprising that they did not report a difference in RC amount and structural order between the two, which is evidence of the much greater role of PufA over PufB in RC assembly. Differences between the earlier experiments and these are possible because I obtained U43 and the plasmids separately and recreated the two strains. However, the sizes of *puf* DNA fragments were entirely as expected when I digested the two plasmids to create pMA10 (not shown). Therefore, I assume that the dependence of the RC spectrum on PufA and not PufB was simply overlooked by the earlier investigators.

Richter and Drews reported the ability of their strains to grow phototrophically with only the RC, unassisted by LH1 or LH2 (127, 128), but did not report differences in growth rate between the two strains due to the different LH1 polypeptides present. To the best of my knowledge, I am the first to observe phototrophic growth of *R. capsulatus* strains with near-total deletions of both LH1 polypeptide genes, which is surprising because much work was done with LH1 deletion and missense mutations to address the issue of whether the RC is functional without LH1. In the year 1985, an uncharacterized mutation in *R. sphaeroides* was reported to permit phototrophic growth without LH1 (96). Subsequently, *R. capsulatus* was found not to grow when LH1 was abolished (66) due to the T38P substitution in PufA (65). This discrepancy was attributed to dissimilar dependence on LH1 of the two *Rhodobacter* species (64, 120). Thereafter, *R. capsulatus* was

reported to grow phototrophically despite substitutions in the BChl-binding site of PufA (20), multiple charge reversals of ionizable amino acid residues in the N-terminal cytoplasmic regions of PufA (K3E, K6E, R14E, R15D) (47, 147) and PufB (D2K, D5R, D13R, E14R) (31), which abolished LH1, and even substitutions in PufA and PufB that apparently increased the number of BChl and carotenoid molecules bound to LH1 (4, 127). From those results, it should have been clear that RC function and phototrophic growth are sensitive to specific changes in the LH1 polypeptides even when LH1 cannot be detected, and that a truly LH1$^-$ phenotype with respect to RC assembly would require the unambiguous absence of both LH1 polypeptides. A definitive phototrophic growth experiment with deletions of both *pufB* and *pufA* in *R. capsulatus* should have been anticipated with the publication of strains U43(pTPR9) and U43(pTPR8) in 1991 (128), but such an experiment was reported in 1992 with deletion of *pufBA* in *R. sphaeroides* instead (68). Another *R. sphaeroides* strain, in which only *pufA* had been deleted and the first 35 codons of *pufB* had the potential to be translated with a long C-terminal extension, was also studied in the years 1992-1996 (69, 94, 95).

I believe my work to be the first investigation of phototrophic growth by *R. capsulatus* with only an RC and no LH1 polypeptides. The uniqueness of *R. capsulatus* compared to *R. sphaeroides* (68) is that even with no obvious RC peaks under semiaerobic growth conditions, *R. capsulatus* strains U43(pMA10) and MA01(pMA10) were capable of phototrophic growth (Figure 3.1.3). Even more surprising is the fact that the *pufX* merodiploid *pufB*$^+$*A*$^-$ strain MA01(pTPR8) did not grow phototrophically any faster than the *pufB*$^+$*A*$^-$ strain U43(pTPR8) (Figure 3.1.3), despite its enhanced RC production and improved RC structural order (Figures 3.5.2-3.5.4). Unless the measures of RC assembly used here are irrelevant to RC function, this suggests that excess PufX, as much as it stimulates RC assembly, interferes with RC function in a *pufB*$^+$*A*$^-$ background.

4.3. The PuhB protein and a concerted assembly model for the RC

The PuhB protein was at one time thought to be essential for phototrophic growth (167). This is incorrect; growth is delayed, rarely abolished, in *puhB* deletion strains. A re-examination of data collected for the earlier study (26) confirms that this phenotype was incorrectly interpreted. My results indicate that the function of PuhB is clearly to assemble the RC with BChl properly bound, and *puhB* deletion strains cannot grow phototrophically with an aberrant RC immediately after a switch from semiaerobic respiratory growth. What is remarkable is that phototrophic capability develops as cultures progress into anaerobic growth conditions. The nature of this adaptation is a mystery, although the PufX deficiency of semiaerobically grown cells of the *puhB* deletion strain MA05 (Figure 3.5.9) suggests that stable insertion of PufX into the RC-LH1 core complex may be part of the adaptation, and that this can occur only under anaerobic conditions in the absence of PuhB. Electron microscopy of MA05 cells and immunoblots for PufX at different times after transfer to phototrophic conditions might be informative.

Although the *puhB* deletion reduces the levels of both the RC and LH1 (Figures 3.2.2, 3.2.3, and 3.2.7), LH1 assembly is unaffected by PuhB in the absence of the RC (Figure 3.2.14, Table 3.2.7). It appears that the major direct effect of the *puhB* deletion is on RC assembly (Figures 3.2.9-3.2.12), and that the indirect effect on LH1 brought about by this poorly assembled RC is worse than if there were no RC at all.

The slightly less severe LH1 deficiency of the *puhB*$^-$*E*$^-$ strain MA12 compared to the *puhB*$^-$ strain MA05 under phototrophic growth conditions (Figures 3.2.2 and 3.2.3) is reminiscent of the *puhE* deletion's augmentation of LH1 assembly in the absence of the RC polypeptides PufL and PufM (Figures 3.4.15-3.4.16). In other words, because deletion of *puhB* interferes with the incorporation of BChl into the RC, additional deletion of *puhE*, which modulates RC-LH1 assembly, may increase the flux of available BChl towards LH1 assembly instead.

The discovery of homodimerization of the second TM segment of PuhB (Figure 3.2.17) necessitates an inquiry into its functional significance. Could symmetry be required for PuhB's RC assembly function? There is twofold symmetry of the pigments bound by PufL and PufM within

each RC, but it is imperfect. The RC-LH1 structure can dimerize in the presence of PufX, but the relevance of dimerization to RC assembly is unknown, and a PuhB protein has been detected in *R. palustris* (38), a species that may exclusively contain a monomeric RC-LH1 core complex (129). As one possibility, I propose a model of concerted RC assembly in which one face of PuhB associates with a fully formed RC and conveys structural information to direct the efficient assembly of a second RC on the opposite face (Figure 4.1). The observation that PufX is poorly immunodetected when the RC-LH1 core complex is not intact (Figure 3.5.10) suggests that PufX is stabilized by association with the core complex, and assembly of the core complex by dimeric PuhB may be a prerequisite for this association.

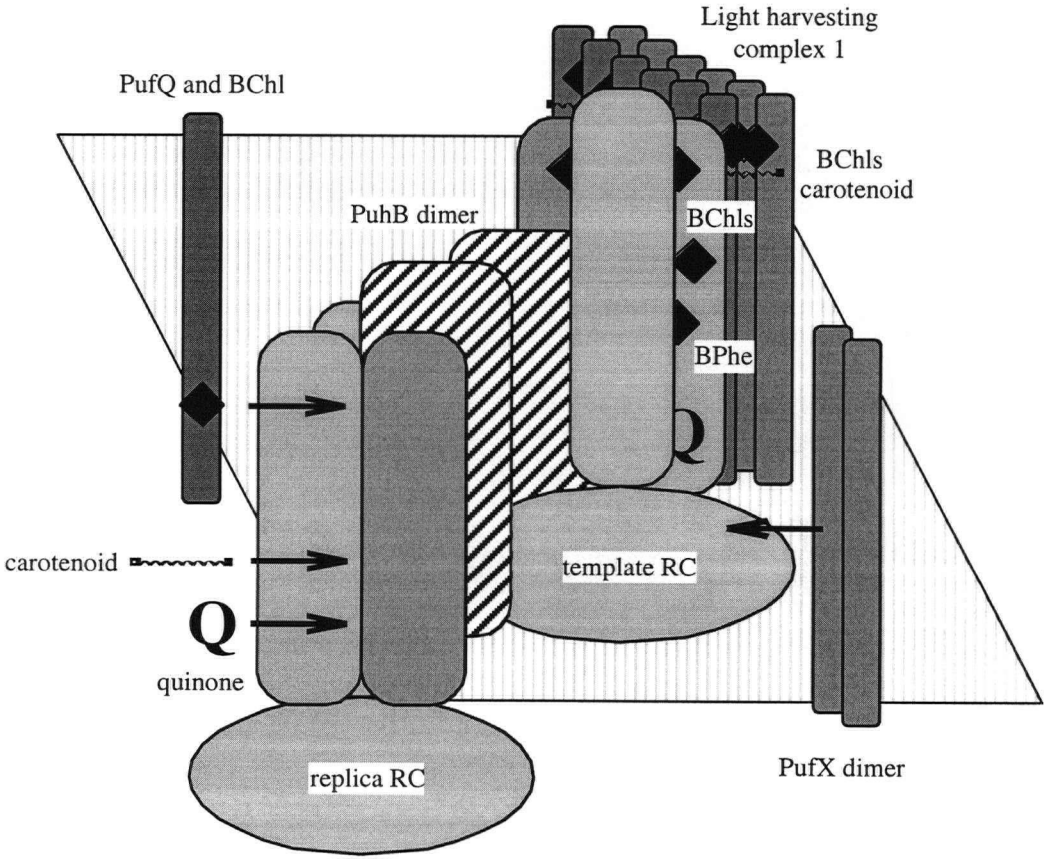

Figure 4.1. A model of concerted RC assembly by PuhB. As an RC assembly factor, PuhB may participate in the insertion of cofactors such as BChl (and BPhe), carotenoid, and quinones. PufQ, which is implicated in BChl biosynthesis and LH complex assembly, may also be present during RC assembly and interact with PuhB. The homodimerization of PuhB's second TM segment suggests that PuhB may function as a dimer, perhaps using one RC as a template for the assembly of another. Subsequently, the two RCs may remain connected through a dimer of PufX. The PufX deficiency of *puhB*$^-$ cells may reflect the instability of PufX unable to associate with the RC-LH1 core complex without PuhB's prior involvement in RC assembly.

The functional relationship of PuhB to PufQ is unknown, but a guess is possible based on the observation that co-transcription of *pufQ* and *puhB-N* allows complementation of a *puhB* deletion, whereas a *trans* combination of *puhB-N* and extra *pufQ* is insufficient. (Experiments with an anti-PufQ antiserum generated by J. Smart and obtained from W. Richards are in progress to determine whether PufQ levels are similar in both merodiploid strains.) Stabilization of *puhB-N* mRNA by *pufQ* is possible but unlikely, as none of the other *puhB* genes or 6xHis-tagged *puhC* genes is ineffective when transcribed alone. Instead, chaperonage of newly translated PuhB-N by PufQ translated nearby may be taking place. I speculate that in wild type cells, a more casual interaction may take place between PufQ and PuhB during RC assembly, perhaps to promote transfer of BChl from PufQ to the RC.

4.4. The PuhC protein and a semiconservative replication model for LH1 around the RC

My observations of the *puhC* deletion's small effects on assembly of the RC and LH1 were carried out using strains that are not isogenic. The *puhC*$^+$ strain MA01 has a KIXX cartridge inserted into the *pufQBALM* deletion, and the *puhC*$^-$ strain MA02 instead has a gentamicin resistance cartridge inserted into the same deletion. Expression of PufX from the chromosome might be different in the two strains. I discount this possibility because the amounts of PufX are similar in MA01(pTB999) and MA02(pTB999) (Figure 3.5.9). Moreover, MA02(pTPR8) resembles MA01(pTPR8) in that both exhibit improved RC assembly compared to the chromosomal *pufX*$^-$ strain U43(pTPR8) (Figures 3.3.14-3.3.17 and 3.5.2-3.5.4), suggesting that PufX is similarly abundant in MA01(pTPR8) and MA02(pTPR8). Therefore, the slight reduction of RC structural order in MA02(pTPR9) (the PufB$^-$A$^+$ strain) and MA02(pTPR8) (the PufB$^+$A$^-$ strain) compared to MA01(pTPR9) and MA01(pTPR8) can be attributed to deletion of *puhC*. Because LH1 assembly is similar in MA01(p*Stu* I), a *pufX* merodiploid strain, and U43(p*Stu* I), in which the only copy of *pufX* is that with the putative ribosome-binding site deleted, there is no doubt that the somewhat reduced steady-state level of LH1 in the *pufX* merodiploid strain MA02(p*Stu* I) is due to the *puhC* deletion. An excess of PufX is known to inhibit LH1

reconstitution *in vitro* (125), but PufX is not even detected in MA02(p*Stu* I) (Figure 3.5.10) and is not in such excess in MA02(pTB999) (Figure 3.5.9), which may reflect the amount of PufX expressed but not stable in MA02(p*Stu* I). To reiterate, the small differences in RC and LH1 assembly between MA01 and MA02 strains are due to the *puhC* deletion, not *pufX* transcription.

The small effects of PuhC on the individual processes of RC and LH1 assembly suggest that PuhC acts on the core complex as a whole. Consistent with this idea, the amount of PufX expressed from the chromosome in the *puhC*$^-$ strain MA02(pTL2) is surprisingly low compared to that expressed from both the chromosome and the plasmid in MA02(pTB999) (Figure 3.5.9), and phototrophic growth of MA02(pTL2) is similarly poor (Figure 3.5.12). Because these differences are not seen between the *puhC*$^+$ strains MA01(pTL2) and MA01(pTB999), I suggest that PuhC may be required for PufX expressed from the chromosome to accumulate in the absence of plasmid-encoded PufX, and for it to contribute to phototrophic growth. In other words, PuhC may reorganize RC-LH1-PufX core complexes, allowing PufX to associate stably.

As one possible model, I propose that PuhC is required to reorganize and expand the LH1 structure around each RC, adding more PufA-PufB dimers so that a second, newly formed RC can be incorporated into the structure, whereupon the LH1 antenna could be apportioned between the two RCs (Figure 4.2). In this capacity, PuhC would facilitate the entry of PufX, translated separately from the RC-LH1 polypeptides, into the core complex. I imagine that such semiconservative, organized, perpetual RC-LH1 biogenesis would be more efficient than *de novo* biogenesis of individual complexes. In the absence of PuhC, the cell would rely entirely on *de novo* biogenesis processes insufficient to sustain the production of core complexes in rapidly dividing cells. In this model, addition of PufQ and removal of PuhE from the system would result in increased BChl availability and improved *de novo* biogenesis, mitigating the growth defect as observed (Table 3.3.4, Figure 3.3.5). Furthermore, prolonged semiaerobic growth would allow more core complexes to accumulate and sustain phototrophic growth for one or two generations more, consistent with my observations (Table 3.3.1, Figure 3.3.2).

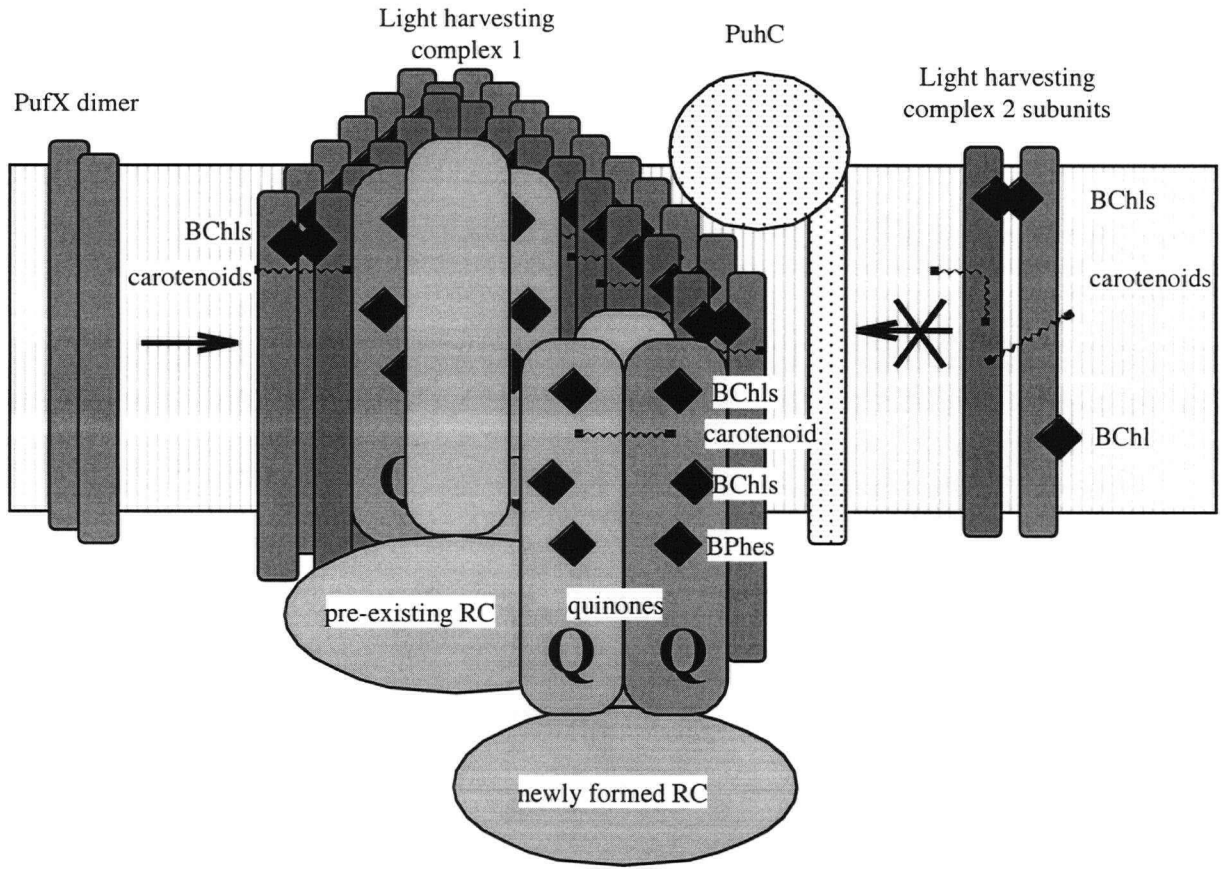

Figure 4.2. A semiconservative replication model for LH1 around the RC, with PuhC as the organizing factor. The *puhC* deletion has minor effects at most on assembly of the RC and LH1, and yet is required for optimal levels of the RC-LH1 core complex. I suggest that PuhC is required to expand the LH1 structure around a pre-existing RC to incorporate a newly formed RC. In this capacity, PuhC could allow PufX expressed separately from the RC-LH1 polypeptides to take its place within the core complex, and could exclude LH2 polypeptides, consistent with the apparent growth advantage of LH2-deficient mutants in the absence of PuhC.

The high frequency (estimated as 1.5 x 10^{-4} of the population) of secondary mutants of the *puhC*⁻ strain SBK1 that have an alleviated growth defect (Section 3.3.1) suggests that the mutations are of many kinds. Some of the secondary mutations that reduce the level of LH2 may be in the *puc* operon, which encodes the LH2 structural genes and the assembly factor PucC. My results indicate that *puhC* deletion has a lesser effect in the absence of LH2 (Table 3.3.3). Other mutations may be in *pufQ*, because such point mutations affect assembly of LH1 and LH2 in *R. sphaeroides* (52); this possibility is supported by the observation that phototrophic growth of SBK1 benefits from *pufQ* merodiploidy (Table 3.3.4, Figure 3.3.5), although the amount of LH2 per cell is not reduced thereby (Figure 3.3.12). Other mutations may be in *puhE*, as suggested by the similar growth of the *puhC*⁻ secondary mutant strain SBK18 and the *puhC* deletion polar mutant strain SBSpec (Figure

3.3.3); however, loss of LH2 in a *puhC*⁻ background makes the presence of PuhE irrelevant (Table 3.4.1). The eleven secondary mutant strains that I isolated were not genotyped. The technique of denaturing gradient formaldehyde gel electrophoresis could be applied to digested chromosomal DNA from these strains to identify fragments that differ from SBK1 in even one base pair (41).

As part of the LH1 reorganization function I have proposed for PuhC, I suggest that PuhC serves to exclude LH2 polypeptides that might interfere with the association of the RC and LH1. The proximity of the RC and LH2 is evident from the observation that the RC polypeptide PuhA and the LH2 polypeptide PucA can be chemically cross-linked in *R. capsulatus* (115), and from the ability of LH2 to transfer energy directly to the RC in the absence of LH1 in *R. sphaeroides* (57). Earlier investigations failed to observe LH2-assisted phototrophic growth without LH1 in an *R. capsulatus* strain that was thought to have an improperly oriented RC (66), and led to the conclusion that the two *Rhodobacter* species are different in this fundamental aspect (64, 120). The mutation responsible for the proposed RC disorientation was identified as a T38P substitution in PufA (65). This threonyl residue is conserved in *R. sphaeroides*, and perhaps such a substitution would abolish direct LH2-to-RC energy transfer in that species too. Therefore, disregarding earlier studies, I constructed the MA15 series of $RC^{+}LH1^{-}LH2^{+}$ strains and tested them for phototrophic growth capability.

The equal growth rates of the $RC^{+}LH1^{-}LH2^{+}$ strain MA15(pTPR9) and the $RC^{+}LH1^{+}LH2^{-}$ strain MA01(pTB999) (Table 3.1.1) support the hypothesis that the RC in *R. capsulatus* can efficiently obtain light energy from both LH2 and LH1 directly. In this experiment, the amount of the RC and LH1 in MA01(pTB999) may be less than in the parental strain MW442 because the superoperonal structure (11, 162, 163) is lost by placing the *puf* operon on a plasmid, while the amount of LH2 should be high in MA15(pTPR9). Nevertheless, the RC and LH2 appear to function well together in the absence of LH1. Interference by the LH2 structural polypeptides in RC-LH1 assembly was proposed to explain the RC-LH1 deficiency of *R. capsulatus* cells that lack PucC, a factor essential for LH2 production, and possess the structural polypeptides of LH2; a "shepherding" role was hypothesized for PucC (83). I have suggested a similar role for PuhC in the organization of RC-LH1 core complexes, and I speculate that in *R. capsulatus* and similar purple

bacterial species that possess LH2, the PuhC protein excludes LH2 polypeptides from the core complex.

The discovery of a putative natural fusion protein of an LH2 polypeptide with weakly PuhC-like sequences, namely Puc2A of *R. sphaeroides* (172) (Figure 3.6.5), invites speculation about the functional relationship of LH2 and PuhC and the potential outcome of the Puc2A evolutionary event. Puc2A is not a part of LH2, and the C-terminal extension of Puc2A, fused to the functional LH2α polypeptide Puc1A instead, can prevent Puc1A from incorporating into an LH2 complex (172). However, it is not known whether the salient feature of the extension is the terminal region that resembles a vestigial PuhC periplasmic domain or the bulk of the extension consisting of the repeating motif $P(A/V)_{1\text{-}2}E_{1\text{-}2}A_{2\text{-}3}$. The repeating motif is similar in composition to the C-terminal extensions of two PucA polypeptides of *R. palustris* (79), PucA of *Rhodocyclus tenuis* (59), and PucA of *R. gelatinosus*, of which the last forms an LH2 complex with the extension (AAAAAAAVAPAPVAAPQAPAQ) protruding into the periplasm (137). Either the extraordinary length of *R. sphaeroides* Puc2A's C-terminal extension, all of which is in the periplasm (172), or its PuhC-like sequences may be responsible for its inability to form LH2. Future characterization of the non-LH2 complex formed by Puc2A (172) may contribute to our understanding of PuhC.

Several reasons are conceivable for the increased PuhC band intensity of strains SBK1(pMA1) and SBK1(pMA3), which express 6xHis-tagged PuhC proteins from a $pufQ^+$ plasmid, compared to the wild type strain SB1003 (Figure 3.3.22). These include: (1) preferential recognition of 6xHis-tagged proteins by the antiserum, (2) increased expression of the proteins from the *puf* promoter on the plasmid compared to the *puh* promoter on the chromosome, and (3) increased stability of PuhC due to either the 6xHis tag or co-translation with PufQ. Repetition of the experiment, including the recently constructed strains SBK1(pMA12) and SBK1(pMA13), which express the 6xHis-tagged PuhC proteins from $pufQ^-$ plasmids, will determine whether co-translation with PufQ determines the steady-state level of PuhC. I am also constructing a plasmid to express PuhC without the 6xHis tag and PufQ, with which I will be able to determine whether the *puhC* gene's location and the 6xHis tag contributed to the dramatic difference in PuhC protein levels. Notably, there was no corresponding difference in phototrophic growth or chromatophore protein bands (not shown).

The ability of *R. sphaeroides* PuhC to substitute almost perfectly in *R. capsulatus* shows that in the PuhC proteins of the two species, with 43% sequence identity (Figure 3.6.5), critical aspects of structure and function are conserved. This is to be expected because PuhC is an RC-LH1 core complex assembly factor and *R. capsulatus-R. sphaeroides* hybrid core complexes are functional *in vivo* (46, 173). On the other hand, it is remarkable that *R. rubrum* PuhC, with 15% sequence identity, is a moderately good substitute in *R. capsulatus*, whereas *R. gelatinosus* PuhC, with 16% sequence identity, has a minimal effect. I speculate that the structural and/or catalytic core of the PuhC periplasmic domain may consist of the very few residues that are conserved (Figure 3.6.5), folded into a characteristic shape with variable surface features recognized by other photosynthesis factors in each species. It may be that the surface of PuhC of *R. capsulatus* is matched more closely by that of *R. rubrum* than that of *R. gelatinosus*.

With the availability of the recombinant 6xHis-tagged PuhC-N and PuhC-NS proteins, which are easily purified, it should be possible to study the structure of PuhC or of its C-terminal domain by X-ray crystallography, nuclear magnetic resonance spectroscopy, and so forth. Thereafter, *in silico* threading of the *R. sphaeroides*, *R. rubrum*, and *R. gelatinosus* PuhC polypeptides onto the *R. capsulatus* structure could lead to tentative identifications of the structural differences likely to interfere with function in *R. capsulatus*, and assist in the design of domain-swapping experiments. Hybrid PuhC proteins could be tested as substitutes in *R. capsulatus*, and evaluated as described in this thesis (Sections 3.3.1 and 3.3.2), to determine the structural basis of PuhC's species-specificity.

4.5. The PuhE protein: a co-ordinator of BChl biosynthesis and RC-LH1 assembly?

PuhE appears to play a role in the assembly of both the RC and LH1, but it is not yet clear whether it participates in assembly or modulates the BChl biosynthetic pathway. Models of both kinds must be considered, and the possibilities are not mutually exclusive.

As one possibility, I suggest that PuhE, a predicted integral membrane protein with seven TM segments, may function as a transporter that partitions BChl into two or more routes: one specific for the RC; and the others for the LH complexes (Figure 4.3). If such is its role, PuhE should also

be able to control BChl biosynthesis by monitoring the availability of BChl and the activity of various integral membrane proteins that serve as assembly factors: PuhB for the RC; LhaA for LH1; and PucC for LH2.

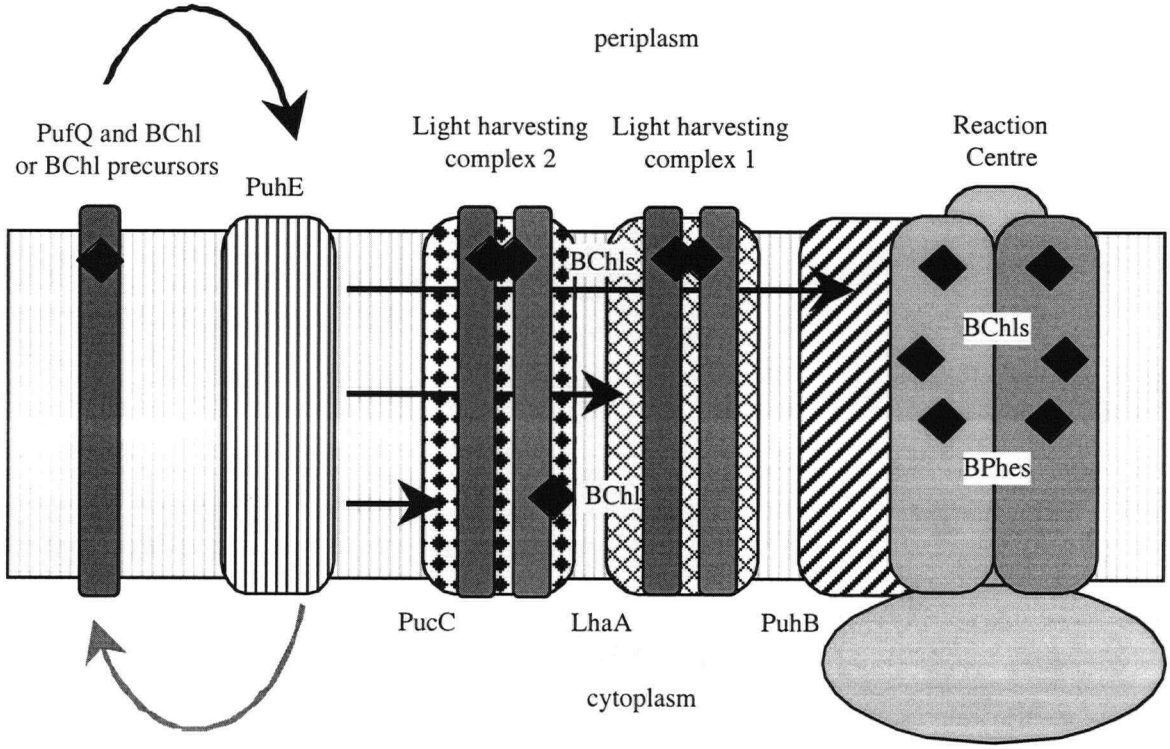

Figure 4.3. Hypothetical role of PuhE as a co-ordinator of RC and LH complex assembly and BChl biosynthesis. The opposite effects of PufQ and PuhE on "unbound BChl" production suggest that whereas PufQ stimulates BChl biosynthesis and may bind the BChl precursor protochlorophyllide, PuhE may generate a signal to inhibit BChl biosynthesis according to the availability of BChl and PufQ. Deletion of *puhE* slightly augments assembly of both the RC and LH1 individually, but results in a small RC-LH1 deficiency. Therefore, PuhE may co-ordinate the assembly of the RC and LH complexes by apportioning BChl (and possibly BPhe) to distinct pathways within the membrane and possibly the periplasm, involving assembly factors such as PuhB for the RC, LhaA for LH1, and PucC for LH2. PuhE may achieve this range of involvement by serving as a transporter through which BChl, synthesized in the periplasm and still associated with PufQ, passes to various assembly factors.

In the year 1970, Peters reported that weakening of the *R. sphaeroides* cell wall with agents such as lysozyme and EDTA during early semiaerobic growth led to diminished BChl biosynthesis, and most of the "unbound BChl" produced was not retained by the cell. He argued that the final steps in BChl biosynthesis probably took place in the periplasm, such that both the enzymes and their products could be released easily (114). More than twenty years later, excreted BChl

precursors in *R. capsulatus* were found associated with a porin from the outer membrane (16). I speculate that late intermediates in the BChl biosynthetic pathway (from protochlorophyllide to BChl) originate in the periplasm, and the final product passes through PuhE, which controls its distribution to RC and LH complex assembly factors in the membrane. Alternatively, PuhE might determine whether BChl (or a BChl precursor) is directed to an assembly pathway that operates in the membrane or one that operates in the periplasm. By intercepting BChl, PuhE could ensure that LH complex assembly, which requires only two to three BChl molecules per unit and can even occur *in vitro* without any assembly factors (151), does not outcompete the more complicated process of RC assembly that requires six BChl/BPhe molecules and four other cofactors per unit.

My experiments support the hypothesis that LH1 assembly can outcompete RC assembly. In the *puhE*$^-$*pufQ*$^+$ background, the amount of unbound BChl produced is higher in the absence of all RC-LH1 pigment-binding polypeptides (Figure 3.4.18) than when LH1 is present (Figure 3.4.17), and the difference correlates with augmented LH1 assembly and a slightly higher level of LH1 (Figure 3.4.15). In contrast, when the RC alone is present, its assembly is enhanced only in the early stages of semiaerobic growth, when there is a surge of production of apparently unbound BChl that exceeds the RC-bound BChl (Figure 3.4.10). Unlike LH1, the RC tends to reach the same level after 19.5 hours regardless of the presence of PuhE (Figure 3.4.11). This difference implies that the two processes require a co-ordinator, which I suggest is PuhE.

PuhE may also perform a sensory function within the cell: to control the biosynthesis of BChl in proportion with the availability of RC-LH1 polypeptides. My observations of what I call "unbound BChl" in RC$^+$LH1$^-$LH2$^-$ and RC$^-$LH1$^+$LH2$^-$ strains (both *puhE*$^+$ and *puhE*$^-$) during assembly are rather unusual because unbound BChl is not observed in *R. capsulatus* strains at steady state, even when the ratio of BChl to pigment-binding polypeptides is abnormally high (4), suggesting that BChl biosynthesis is tightly regulated. However, a similar peak at 780 nm, attributed to unbound BChl, has been observed during early semiaerobic growth of *R. sphaeroides* (114), *in vitro* during LH1 assembly in isolated *R. capsulatus* membranes (97), and in a chromatographically distinct fraction of *R. capsulatus* membranes thought to be the site of LH1 polypeptide insertion (123). It will be interesting to characterize the compound that accumulates in the *puhE*$^-$ strains even

in steady state, to determine whether it is BChl or BPhe (lacking the central Mg atom), whether the hydrophobic tail is present, and whether it can be identified as an intermediate in BChl biosynthesis or in the relatively uncharacterized process of BChl degradation (15).

If there exists a carrier polypeptide for BChl precursors in the membrane (80, 81), and that carrier is PufQ (10, 40), then PuhE could gauge the amount of BChl available by interacting with PufQ, then direct the BChl bound by PufQ toward the RC or LH1 or LH2. An interaction of PufQ with PuhE could account for the manifold roles indicated for PufQ in biogenesis of the photosynthetic apparatus and could explain the apparent copy number effect of the *pufQ* and *puhE* genes on phototrophic growth of the *puhC* deletion strains SBK1 and SBSpec (Figure 3.3.5, Table 3.3.4): an excess of plasmid-expressed PuhE proteins from pMA19 would generate a stronger inhibitory signal from the same stimulus, whereas an excess of plasmid-expressed PufQ proteins from pRR5C would prompt PuhE to allow more BChl biosynthesis.

Related to the issue of *pufQ/puhE* copy number is the counterintuitive observation that expression of PuhE from both the chromosomal gene of SBK1 and the unnatural *pufQ-puhE* transcript of pMA11 does not inhibit phototrophic growth as much as expression of PufQ and PuhE from pMA11 only in SBSpec (Figure 3.3.5, Table 3.3.4). The significance of *puhE* co-transcription with *puhABC* and the possibility of self-inhibition of PuhE through the formation of higher-order complexes remain to be investigated. As the last apparent photosynthesis gene of a superoperon that begins with *bchF* (Figure 1.3) (9, 11), *puhE* is ideally positioned for negative feedback to the BChl biosynthetic pathway because the appearance of PuhE indicates that several BChl biosynthesis genes, *lhaA*, and the other *puh* genes encoding RC-LH1 assembly and organization factors have been transcribed. I was unable to reverse PuhE$^-$ phenotypes by restoration of *puhE* in *trans* under control of the *puf* promoter (Tables 3.3.4 and 3.4.2). Therefore, I suggest that the terminal location of the *puhE* gene may be important.

A noteworthy feature of PuhE is the large number of conserved aromatic amino acyl side chains, many of them located within transmembrane helices (Figure 3.6.8). I suggest that a network of aromatic ring stacking interactions, possibly forming binding sites for BChl, could be an important structural and functional feature of PuhE.

4.6. Can *R. capsulatus* grow phototrophically without PufX?

There is a widespread belief that PufX is conditionally essential for phototrophic growth of *R. capsulatus*, based on publications of Lilburn *et al.* (86-88) that described the LH2$^+$ *pufX*$^-$ strain ΔRC6(pTL2) as unable to grow phototrophically on RCV minimal medium whereas the LH2$^+$ *pufX*$^+$ strain ΔRC6(pTB999) grew. Lilburn also constructed the LH2$^-$ *pufX*$^-$ strain U43(pTL2) and reported a similar growth defect without showing data (85). On the other hand, in an earlier study of phototrophic growth on RCV medium supplemented with 0.1% yeast extract, Klug and Cohen concluded that deletion of *pufX* from a plasmid-borne *puf* operon used to complement ΔRC6 and U43 had a slight negative effect in the LH2$^+$ background and a slight positive effect in the LH2$^-$ background (74). These differences could be attributed to the inclusion of yeast extract in an otherwise minimal medium, because Lilburn also reported that ΔRC6(pTL2) grew similarly to ΔRC6(pTB999) in YPS, a complex medium, under high light intensity (87). However, in my phototrophic growth experiments with RCV and YPS media in parallel, the *pufX* deletion strains ΔRC6(pTL2) and U43(pTL2) grew much more poorly than the control strains ΔRC6(pTB999) and U43(pTB999) in both media (not shown). I am unable to account for all of these discrepancies, but I suggest that some variation may be due to the duration of semiaerobic incubation preceding a phototrophic growth experiment, because the phototrophic growth rate of the *pufX*$^-$ strain U43(pTL2) in RCV medium was 13% of that of the *pufX*$^+$ strain U43(pTB999) after 24 hours of semiaerobic incubation and only 6% after 48 hours (Table 3.5.4).

Lilburn stated that he considered the ΔRC6 background similar to the wild type strain B10 (160) except for deletion of the *puf* operon, whereas the then-uncharacterized mutation responsible for the LH2$^-$ phenotype of MW442, the parent of U43, might interfere with analysis of *pufX* (85). In fact, the 3315 bp deletion in ΔRC6 extends from the *Sal* I site in *pufQ* to an *Xho* II site 488 bp after the 3' end of *pufX* (22), not the 5' end as stated in Lilburn's work. The consequence is that ΔRC6, unlike U43, has a deletion of part of the coding sequence of *dxsA* (Figure 4.4), a gene that encodes one of two 1-deoxy-D-xylulose-5-phosphate synthase (DXS) isoenzymes of *R. capsulatus* (55). DXS is the first enzyme of the isoprenoid biosynthesis pathway, by which quinones are made,

and is produced from two genes, *dxsA* within the photosynthesis gene cluster and *dxsB* outside it. DxsA has a fivefold higher affinity than DxsB for pyruvate, one of its substrates (55). One should expect quinones to be less abundant in ΔRC6 than in a wild type strain, perhaps making the role of PufX in quinone movement appear more important than it is. By analogy with mutation of another redundant gene of the isoprenoid biosynthesis pathway, *idiA*, which encodes one of two isopentenyl diphosphate isomerase enzymes in *R. capsulatus*, a DxsA-null strain might experience an energy shortage and exhibit increased transcription from the *bch*, *crt*, *puc*, *puf*, and *puh* promoters (104). Unfortunately, some studies of *pufX* in *R. sphaeroides* have also been carried out in *dxsA*⁻ strains (6-8, 34).

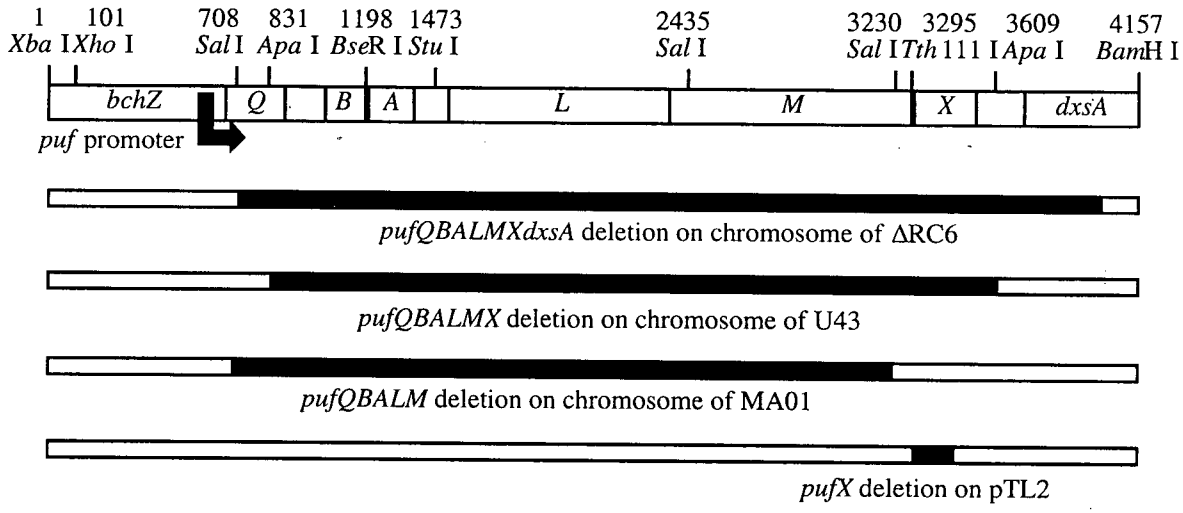

Figure 4.4. The *pufQBALMXdxsA* deletion in strain ΔRC6. The restriction sites used to make the mutations for the present study are included for reference. It is not known whether the promoter for *dxsA* is deleted or transcription of *dxsA* is disrupted in U43, which contains a transcription termination signal, and MA01, which does not. Restoration of the *puf* operon without *pufX* on plasmid pTL2 would not restore expression of *dxsA* to any strain due to the transcription termination signal inserted at the site of a deletion in the *pufX* gene.

Although deletion of *dxsA* might explain the differences between ΔRC6(pTL2) and U43(pTL2) observed by others, the *dxsA* promoter has not been identified and it is not known whether DxsA affects phototrophic growth. The *dxsA* promoter may be within the *pufQBALMX* deletion of U43, or in the *pufQBALM* deletion of my strains such as MA01, or may even be the *puf* promoter itself.

My observations of similar phototrophic growth of ΔRC6(pTL2) and U43(pTL2) (not shown), and of U43(pTB999) and MA01(pTB999) (Figure 3.1.3 and Table 3.1.1, Figure 3.5.12 and Table 3.5.4) suggest that *dxsA* is either relatively unimportant for phototrophic growth under these laboratory conditions or inactive in all three backgrounds. I consider it unlikely that LH1 polypeptide-specific enhanced RC assembly in MA01(pTPR8) compared to U43(pTPR8) (Figures 3.5.3 and 3.5.4) could be due to DxsA rather than PufX.

4.7. The PufX protein's multiple roles in organization of the RC-LH1 core complex

The simplest model of how increased expression of PufX improves RC assembly is that PufX normally interacts with the RC at a unique site to assist assembly. With a larger pool of transient PufX polypeptides, this site would be occupied more often. I reject this model on the grounds that improved RC assembly due to a normal interaction with PufX should result in improved phototrophic growth of *pufX* merodiploid strains, which I did not observe (Figure 3.1.3). Instead, I suggest that the excess PufX polypeptides, possibly complexed with BChl (82), occupy multiple sites in lieu of PufA-BChl around the RC. Random motions may permit each PufX polypeptide to homodimerize briefly with its neighbours, alternating sides to create a transient structure that resembles oligomeric PufA and enhances RC assembly. These multiple PufX proteins might interfere with the long-range orientation of the RC described for *R. sphaeroides* (45, 143), or occlude the quinone exchange site, resulting in no net improvement in phototrophic growth.

The role of PufX is notable: only in the absence of PufA and in the presence of PufB did increased expression of PufX increase the area of half the voyeur BChl peak to ~0.9 from ~0.5 (Figure 3.5.3) and the RC peak height ratio to ~1.5 from ~1.1 (Figure 3.5.4). In the presence of PufA, the RC had a characteristic spectrum, and in the absence of both LH1 polypeptides its assembly was poor, regardless of the extra *pufX* gene. In other words, despite a higher level of expression (Figure 3.5.9) and the ability to self-associate (Figure 3.5.14), PufX did not enhance RC assembly in the presence of PufA, or without the co-operation of PufB. Although *R. capsulatus* PufX is thought not to interact with PufB because it does not inhibit the formation of PufB-PufB

dimers associated with BChl *in vitro* (125), it is possible that in the presence of the RC, PufX is able to interact with PufB. The isolated PufB protein of *R. sphaeroides* has a solution structure, determined by nuclear magnetic resonance spectroscopy, that suggested that its N-terminal cytoplasmic helix could interact with PufA and reach inward to contact the RC polypeptide PuhA (27). It is possible that the N-terminal helix of PufB contacting PuhA forms part of the site occupied by PufX, and a PufB-PufX-PuhA interaction allows improved RC assembly.

The discovery that the effect attributable to PufX was exerted without the protein accumulating to a level detectable by immunoblot is truly remarkable. Although PufX was readily detected when plasmids carrying intact *puf* operons (pTB999) or the remaining *puf* genes without *pufX* (pTL2) were introduced into the *pufQBALM* deletion strain MA01 (Figure 3.5.9), its amount was vanishingly low in the absence of either PufA or PufB, or without PufL and PufM (Figure 3.5.10). I speculate that, like the individually produced PufA and PufB proteins (128), PufX inserts into the membrane transiently, supports RC assembly, and is degraded rapidly in the absence of an intact RC-LH1 complex. This is a noteworthy difference from *R. sphaeroides*, in which PufX can be detected in purified protein fractions from strains that lack either the RC or LH1 (124).

Another unexpected observation was that while deletion of *pufX* resulted in an enlarged LH1 peak in U43(pTL2) compared to the *pufX*$^+$ strain U43(pTB999) (Figure 3.5.11), there was no such difference in LH1 peak size between the chromosomal *pufQBALMX* deletion strain U43(p*Stu* I) and *pufQBALM* deletion strain MA01(p*Stu* I), in which the LH1 polypeptides were expressed from a plasmid-borne *puf* operon lacking the RC genes *pufLM* and the putative ribosome-binding site of *pufX* (Figure 2.1) (Figures 3.5.7 and 3.5.8). Although some PufX was expressed from plasmid p*Stu* I in both strains (Figure 3.5.10), it is unlikely that this would interfere with the *pufX* copy number effect on LH1, because this effect was apparent even when strains MA01(pTB999) and U43(pTB999), with an intact *pufX* ribosome-binding site on the plasmid and much higher levels of PufX (Figure 3.5.9), were compared (Figure 3.5.11). Reduction of the LH1 absorption peak area, therefore, appears to be an RC-dependent effect of PufX.

The LH1 absorption peak was 75% higher in U43(pTL2) than in U43(pTB999) (Table 3.5.3), whereas measurements of LH1 BChl per RC in *R. sphaeroides* indicated only a difference of about

16% due to PufX (6, 94). This discrepancy may be due to several genotypic differences between the strains tested: the *R. capsulatus* strains had an LH2 assembly defect (point mutation in *pucC*) whereas the *R. sphaeroides* strains were LH2$^-$ due to deletions of structural genes (*puc1BA*) (6, 94), and either were merodiploid for *pufQ*, the BChl biosynthesis gene *bchA*, and the isoprenoid biosynthesis gene *dxsA* (94), or had a deletion extending into *dxsA* (6). Protein-swapping experiments with LH1 and PufX of *R. capsulatus* in *R. sphaeroides* suggested species-specific pleiotropic effects as well (46). The increase in LH1 absorption has been correlated with higher levels of LH1 polypeptides (7, 86). However, it is also possible that the absence of PufX results in a conformational change in LH1 that affects light absorption by LH1-bound BChl such that a large increase in peak height reflects a small increase in the number of BChl molecules bound to LH1.

Although more PufX was expressed from the chromosome in strain MA01(pTL2) than from the plasmid in U43(pTB999) (Figure 3.5.9), MA01(pTL2) did not have the normal low level of LH1 absorption (Table 3.5.3, Figure 3.5.11) and occasionally exhibited slower phototrophic growth (not shown). Indeed, the absence of *pufX* from the plasmid increased LH1 absorption at 880 nm by 52% despite the presence of *pufX* on the chromosome, even though the chromosomal *pufX* gene appeared to reduce LH1 absorption by 14% in MA01(pTB999) relative to U43(pTB999) in the presence of the plasmid-borne gene (Table 3.5.3). The chromosomal copy of *pufX* differed only in that it was "ectopic," translated from a different transcript than the RC-LH1 polypeptides.

A model of RC-LH1 assembly in which co-translation of PufX in spatial proximity with the RC-LH1 polypeptides plays a role is a novel idea that, if proven correct with further *in vitro* and *in vivo* experiments, would add a new dimension to our understanding of the factors that affect the photosynthetic apparatus. There is a recent parallel to this situation that may not be widely recognized: the assembly of LH2 in *R. sphaeroides* (172). The Puc1A polypeptide was found associated with both co-translated Puc1B and ectopically expressed Puc2B, which are 94% identical and contributed 70% and 30%, respectively, to the total LH2. However, no LH2 was observed when *puc1B* was deleted, despite normal transcription and translation of LacZ fusions of Puc1A, Puc2B, and the assembly factor Puc1C. Only when *puc2B* was substituted for *puc1B* on a plasmid-borne *puc1BA* operon did a cell lacking both *pucB* and both *pucA* chromosomal genes regain 100% of the

normal amount of LH2 (172), indicating that co-translation of *pucBA* was critical for LH2 assembly and that interactions between separately translated PucB and PucA proteins probably occur only subsequently through reorganization of LH2. I suggest that Puc1A in *R. sphaeroides* may be highly unstable unless it can pair with a nearby PucB polypeptide even as they are being synthesized by adjacent ribosomes. Similar stabilization of *R. capsulatus* PufA by PufB prior to membrane insertion has been proposed (97, 128), and *in vitro* tests suggest that PucB of *P. molischianum* might form LH1 instead of LH2 if it were co-translated with PufA instead of PucA (151), but the significance of co-translation was not actually evaluated in those studies.

The earlier observation that the requirement for PufX was partially suppressed by transition mutations of the fifth and sixth bases of the *pufA* gene (the TCC codon for Ser2 being changed to CCC or TTC, Pro or Phe) (86, 88) suggested that either PufX influences the shape of the PufA ring or the two proteins are so similar (Figures 3.6.15 and 3.6.16) that a slight modification allowed PufA to substitute for PufX and facilitate quinone exchange. The former possibility was favoured by the observation that PufX co-purifies with PufA (125), whereas my observations of superior RC assembly in MA01(pTPR8) compared to U43(pTPR8) (Figures 3.5.2-3.5.4), attributable to increased PufX expression (Figure 3.5.9), and self-association of the PufX TM segment (Figure 3.5.14) are consistent with the possibility that PufX expressed at a high level may oligomerize and resemble PufA enough to substitute for it in RC assembly.

A potentially significant observation concerning the role of PufX in quinone exchange is that the PufX-PufA association reduced the binding of BChl by LH1 (125). Other evidence that PufX displaces BChl from LH1 comes from observations in *R. sphaeroides*: that secondary mutations that suppressed a *pufX* deletion strain's growth defect were almost always those that reduced BChl binding (7); and that deletion of *pufX* compensated for the reduced amount of LH1-specific BChl per RC due to binding of the carotenoid neurosporene rather than the usual sphaeroidene (94). I suggest that allosteric association with PufX reduces the binding of pigment cofactors at the cytoplasmic face of LH1 (where Ser2 of PufA is located) so that quinones are able to enter the RC, become reduced, leave the RC and reach cyt *b/c*1 (Figure 4.5). In other words, the aperture that allows quinone exchange may not be very large, and PufX itself need not be located there. Indeed,

my observation of homodimerization of the PufX TM segment (Figure 3.5.14) is consistent with the tentative location of PufX at the axis of twofold symmetry in RC-LH1 dimers (43, 44, 136), and does not support speculation that the two PufX molecules in a dimeric core complex are located apart, each opposite a gap in the PufB ring of LH1 where quinone exchange might occur (143).

Phosphorylation of the Ser2 residue of *R. capsulatus* PufA occurs when newly synthesized PufA is membrane-associated and tightly bound to phospholipids, but not stably inserted (18, 122, 123). Dephosphorylation is concurrent with formation of the intracytoplasmic membrane and the onset of phototrophic growth (73, 123). Phosphorylation of PufA is dependent on electron transport and the proton-translocating ATP synthase even in the presence of exogenous ATP (28, 122) and is downregulated under high light intensity (18, 48). I suggest that, like the carboxylated N-terminus of PucA that ligates the B800 BChl near the cytoplasmic side of LH2 in the purple bacterium *Rhodoblastus acidophilus* (111), the negatively charged phosphate group so near to the N-terminus of PufA could participate in binding of a cytoplasmic-side porphyrin cofactor such as BChl, and this cofactor would obstruct quinone exchange. A B800 BChl appears to be present in the core antenna (LH1) of *Halorhodospira halochloris* and *Halorhodospira abdelmalekii* (146), *C. aurantiacus* (161), an unnamed thermophilic filamentous bacterium (117), *R. tenuis* (59), and *Roseospirillum parvum* (113), but has never been observed in *R. capsulatus*. I suggest that in *R. capsulatus*, an extra pigment bound to phosphorylated Ser2 might escape detection because phosphorylation appears to be transient,. Only a very small fraction of PufA molecules are in the phosphorylated state. If phosphorylated Ser2 can bind a B800 BChl or perhaps a carotenoid, substitution of Ser2 with Pro or Phe would abolish this binding and widen the spaces near the cytoplasmic side of the LH1 arc, allowing quinone exchange and resulting in improved phototrophic growth, as observed in secondary mutants of a *pufX*$^-$ strain (86, 88).

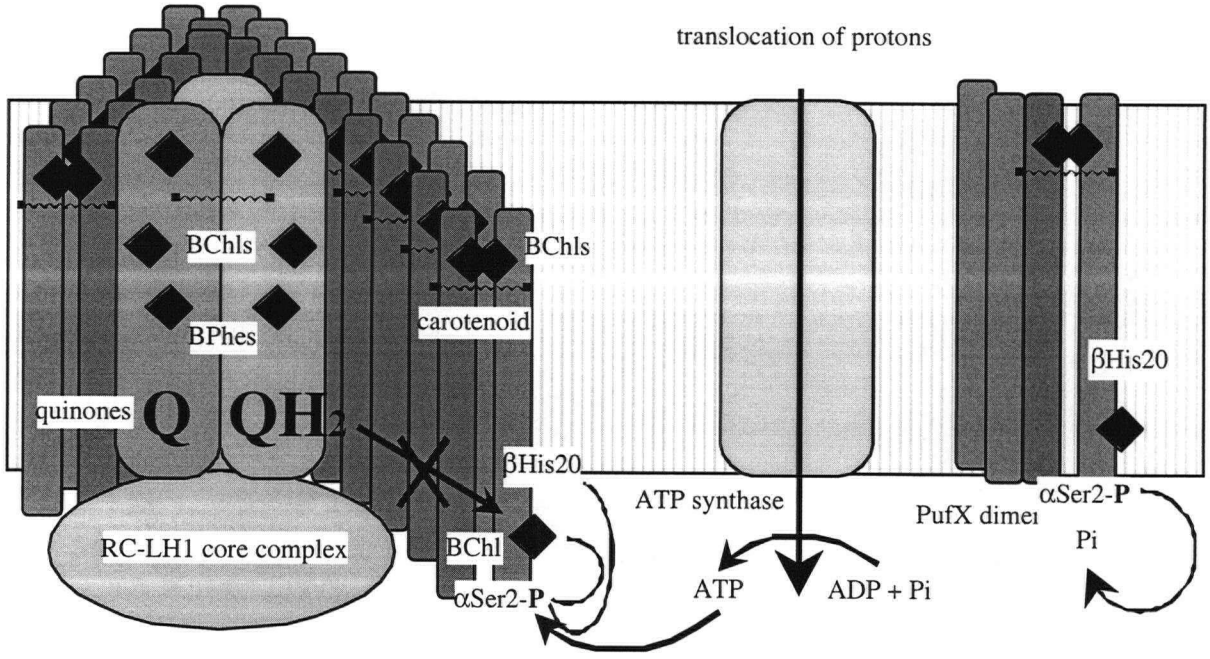

Figure 4.5. An alternative model of how PufX creates a gate for quinone exchange. PufX has been suggested to form the gate by replacing one PufA molecule and creating a gap in the PufB ring (143). I speculate instead that a conformational change brought about by association with PufX stimulates the dephosphorylation of Ser2 of PufA, disrupting a hydrogen bond to His20 of PufB and removing the barrier to quinone exchange. Substitutions of these two amino acyl residues suppress the phototrophic growth defect of *pufX*⁻ strains (7, 86, 88), and His20 is known to stabilize the ligation of a BChl cofactor near the cytoplasmic side of the membrane by carboxyl groups in similar structures ((75, 111)). In wild type *R. capsulatus*, only a small fraction of PufA molecules are phosphorylated by an ATP synthase-dependent process. These appear to be newly synthesized proteins, tightly bound to phospholipids but not stably integrated in the membrane (18, 28, 48, 73, 122, 123). I hypothesize that in the absence of PufX, dephosphorylation of PufA is slower, and therefore quinone exchange is blocked.

The histidyl residue of the LH2 polypeptide PucB that donates a hydrogen bond to the N-terminal carboxyl group of PucA in *R. acidophilus*, stabilizing the ligation of the B800 BChl (111), is present also in the paralogous sequences of PufB polypeptides, and is numbered as His20 of *R. capsulatus* PufB (174) (Figure 3.6.15). The idea that this residue is capable of a similar role in PufB as in PucB is supported by observations in *P. molischianum*, a species in which the PucA and PucB sequences are unusually similar to those of PufA and PufB polypeptides, respectively, and PucB is capable of pairing with PufA to form an LH1 complex *in vitro* (151). In the *P. molischianum* LH2 complex, the B800 BChl is ligated by the carboxyl side chain of Asp6 of PucA, and this carboxyl group is hydrogen bonded to the same water molecule as the His residue analogous to His20 of PufB (75). Thus, in a PucB polypeptide that resembles PufB and can even assume the role of PufB in LH1, this His residue stabilizes the ligation of a B800 BChl in LH2.

PucA (and PufX) proteins conserve the *P. molischianum* Asp6 residue as an amino acyl residue with an acidic or amide side chain, and this position aligns with the initial Met residues of most PufA sequences (Figures 3.6.15-3.6.16), which are typically formylated or otherwise modified at the N-terminus (174). This might, in theory, allow ligation of a B800 BChl by PucA polypeptides after the fashion of *P. molischianum* PucA, and by PufA polypeptides after the fashion of *R. acidophilus* PucA, with "His20" residues stabilizing the ligands with hydrogen bonds. However, the *R. capsulatus* and *R. sphaeroides* PufA sequences are exceptional in that the initial Met is replaced with Met-Ser-Lys-Phe (Figure 3.6.15), and so I have imagined PufA phospho-Ser2, as an alternative to PufA N-formyl-Met1, connected to PufB His20 by hydrogen bonding and binding a B800 BChl or carotenoid pigment.

Binding of an extra BChl due to His20 of PufB in a subset of PufA-PufB dimers has been proposed as an explanation for the observed increased ratio of 2.5 BChl molecules per PufA-PufB dimer when either an Phe23Ala substitution was made in PufA or a Gly10Val substitution was made in PufB of *R. capsulatus* (4). Notably, in *R. sphaeroides*, mutation of this PufB His20 residue to Arg suppressed the growth defect due to deletion of *pufX* (7), suggesting that this residue does something to inhibit quinone exchange in the absence of PufX. This and the two PufA Ser2 substitutions in *R. capsulatus* are three out of the four known mutations that suppress the growth defects of *pufX*⁻ mutant strains without relying on extra copies of LH1 genes or diminution of the LH1 structure (7, 88, 94, 95). It is possible that PufA Ser2 and PufB His20 together form the primary barrier to quinone exchange in the absence of PufX.

I speculate that even without an extra pigment cofactor, a hydrogen bond between PufA Ser2 and PufB His20 could prevent quinone exchange across LH1, if not for a conformational change, and possibly the stimulation of Ser2 dephosphorylation, brought about by association of PufA with PufX. Mutation of *R. sphaeroides* PufB His20 to Val reduced *in vitro* association of PufB with PufA fivefold and also inhibited reconstitution of LH1 from dimeric subunits of PufA-$(BChl)_2$-PufB (152), consistent with a hydrogen bonding role. Consistent with stronger hydrogen bonding interactions within LH1 in the absence of PufX, the LH1 complex of a *pufX*⁻ strain of *R. sphaeroides* was resistant to the removal of PufA-PufB dimer subunits with the detergent lithium

dodecyl sulfate, whereas LH1 from the *pufX*$^+$ strain was not (164). This observation agrees with a closed circular structure for LH1 in the *pufX*$^-$ strain as well as with my idea. It is not known whether *R. sphaeroides* PufA Ser2 is phosphorylated, or how this might affect hydrogen bonding.

Structural analysis of RC-LH1 core complexes from *pufX*$^+$ and *pufX*$^-$ *R. capsulatus* and *R. sphaeroides* strains under conditions of high and low phosphorylation of Ser2 of PufA, as well as from the mutant strains in which 2.5 molecules of BChl were present per PufA-PufB dimer without any apparent unbound BChl (4), could determine whether my speculation is correct.

Efforts to determine the structure of the *R. sphaeroides* RC-LH1 complex are ongoing (70, 136, 143). Of particular interest is the recent discovery that large tubular photosynthetic membrane structures in an LH2$^-$ mutant strain of *R. sphaeroides* contain only a helical paracrystalline array of RC-LH1 core complexes and no detectable cyt *b/c1* (143). Assuming that all of these core complexes contribute to phototrophic growth, this indicates that escape of quinols from the RC to reach cyt *b/c1* in a distant location may be much more efficient than anticipated. I suggest that quinone exchange may not require lateral diffusion through the hydrophobic environment of the membrane; instead, release near the cytoplasmic face of the photosynthetic membrane may allow quinols to travel through the cytoplasm, either as micelles or in association with a carrier protein.

PufX of *R. capsulatus* and PufX of *R. sphaeroides* each self-associated through their TM segments (Figure 3.5.14). Recent structural studies have suggested a location of PufX either at the axis of twofold symmetry in the dimeric RC-LH1 core complex (136) or within the inner ring of PufA around each RC, opposite a gap in the outer ring of PufB that is thought to allow quinone exchange (143). My experiment suggests that in both *Rhodobacter* species, PufX may be at the axis of twofold symmetry, which would account for its essential role in the dimerization and paracrystalline organization of RC-LH1 core complexes (43-45, 143). This observation leads to the question of how self-association of each PufX TM segment is brought about. Each PufX TM segment has two GxxxG motifs (Figures 3.5.13 and 3.6.16), which have been implicated in self-association of TM helices (130); however, in *R. sphaeroides*, the motifs are located in tandem near the cytoplasmic side of the segment, and in *R. capsulatus* they are separate. It is interesting that this motif has been conserved even though its position has shifted, and that consequently, the face of the

PufX helix that points toward the RC may be different in the two species. The predicted PufX TM segments of three other *Rhodobacter* species do not have these GxxxG motifs (153) (Figure 3.6.16), and may or may not be dimeric. The GxxxG motifs might well be what allows PufX of *R. capsulatus* to substitute in *R. sphaeroides* despite low sequence homology (46). Mutational analysis of the PufX TM sequences is an important future experiment.

The self-association of the PufX TM segments was apparently much weaker than that of the positive control, the TM segment of glycophorin A, as evidenced by lower CAT activity (Figure 3.5.14). This is consistent with the fact that PufX-containing RC-LH1 core complexes exist as both monomers and dimers, dimerization being PufX-dependent (43). However, it is also possible that dimerization of PufX in the photosynthetic membrane of *Rhodobacter* species is strengthened by binding of a cofactor not present in the *E. coli* membrane of the TOXCAT system: for example, BChl, with which PufX interacts *in vitro* (82). Law *et al.* have speculated that BChl binds to either His59 or Gln60 of *R. capsulatus* PufX (Asn60-Gln61 in *R. sphaeroides*) at the level of the B880 pair bound by LH1 near the periplasmic side of the membrane (82). However, these sites are not present in my PufX TM segment constructs, which were designed based on the observation that truncation of *R. sphaeroides* PufX at Arg53 does not prevent its insertion into the RC-LH1 core complex (44), and because my PufX TM segments spanned the membrane of *E. coli*, supporting growth on maltose minimal medium (not shown), I suggest that the BChl-binding sites proposed by Law *et al.* could be located in the periplasm and therefore unprecedented as BChl ligands.

There are no recognizable BChl-binding amino acyl residues (His, Asn, Gln, Asp, Glu) in my PufX TM segment constructs (Figure 3.5.13). However, it has been proposed that a Gly residue in place of His may allow a water molecule to ligate BChl in the RC special pair binding pocket (51). With its single TM segment, PufX may be expected to resemble LH1 and LH2 polypeptides in its tolerance for this substitution (Figure 3.6.16). Directed substitutions of the BChl-ligating His residues of LH1 have not included Gly (20, 108), but in *R. tenuis*, Gly is naturally found in place of PufB His20 of *R. capsulatus*, and nevertheless a B800 BChl may be present in LH1 of *R. tenuis* (59). If PufX does bind BChl *in vivo*, I suggest that the binding pocket may be at one of the conserved Gly residues at either end of the TM segments I identified (Figure 3.6.16). Near the

cytoplasmic side of the membrane, Gly29 of one molecule in a PufX dimer of *R. capsulatus* (Gly30 in *R. sphaeroides*) could position a water molecule for hydrogen bonding to the ligand of a B800 BChl cofactor. This ligand, provided by the opposite PufX molecule, could be Glu17 in *R. capsulatus* (Asn18 in *R. sphaeroides*), which corresponds to Asp6 of *P. molischianum* PucA, the ligand of B800 BChl in LH2 (75) (Figure 3.6.16). Alternatively, near the periplasmic side, it is conceivable that Gly51 of *R. capsulatus* PufX (Gly52 in *R. sphaeroides*) allows ligation of BChl by water. Other possibilities are that the conserved Met26 of *R. capsulatus* PufX (Met27 in *R. sphaeroides*) ligates BChl (as Met residues sometimes ligate heme), or that the natural cofactor of PufX is not BChl but BPhe, in which case the binding pocket could even be Phe/Leu (21). Unfortunately, it was difficult to study the ability of LH1 polypeptides to interact with BPhe *in vitro* due to the formation of BPhe aggregates (29), and so it may also be difficult to study the cofactor specificity of PufX by an *in vitro* approach. Substitutions of key residues in PufX, together with an investigation of its structure, may be more informative.

A recent paper reported that the RC-associated PufC cytochrome of *R. denitrificans* has an N-terminal TM segment and may be distantly related to PufX (60). Similar PufC proteins lacking a conserved Cys residue for covalent attachment of a fatty acid anchor to the membrane are predicted for other purple phototrophic bacterial species, including *R. sulfidophilum* (92), *P. molischianum* (101), *Acidiphilum rubrum* (102), and others (13, 153), and for the green filamentous anoxygenic phototrophic bacterium *C. aurantiacus* (32). The PufC TM segments of *R. sulfidophilum* and most other *Rhodovulum* species studied have tandem GxxxG motifs (153). The other species do not have GxxxG motifs. However, variations such as SxxxG also correlate with homodimerization (130), and therefore the PufC TM segments of *P. molischianum* (SAIIG) and *C. aurantiacus* (SVAVG) may also homodimerize. Future TOXCAT studies may indicate whether the species in which PufC has a TM segment have monomeric or dimeric RC-LH1 complexes. To date, the species in which only RC-LH1 monomers have been observed are *Blastochloris viridis* (139), which has a lipid-anchored PufC (165), and *R. rubrum* (67) and *R. palustris* (129), which lack PufC altogether. It may be that some RC-LH1 structures dimerize through their PufC cytochrome polypeptides. The implications of PufC dimerization for electron transfer are unclear.

4.8. The *puh* operon as a whole

The focus of my work is on three of the four co-expressed Puh proteins of *R. capsulatus*. Having identified them as factors in the assembly of the photosynthetic apparatus, I would like to address the fundamental question of why these four genes are co-transcribed in *R. capsulatus* (Sections 3.3.1 and 3.4.1) and found in a similar organization in all purple bacteria so far (Section 1.4). It is not at all obvious why five of the RC-LH1 core complex proteins (the pigment-binding polypeptides PufB, PufA, PufL, PufM, and either the cytochrome PufC or its putative remnant PufX) are co-expressed, while the RC H polypeptide PuhA is co-expressed with three or more proteins that are not known components of the photosynthetic apparatus. As an initial conjecture, I propose that the proteins PuhA, PuhB, and PuhC operate in economical pathways of RC-LH1 biogenesis.

Recent work in this laboratory indicates that PuhA does not only participate in proton uptake by the RC (106); its presence in the membrane was required for the accumulation of full-length PufL and PufM polypeptides in the *R. sphaeroides* membrane-free fraction during extended semiaerobic growth (150). PufL and PufM were each required for the other to accumulate in the membrane-free fraction, and PuhA was not detected there (149). This phenomenon could reflect the recycling of PufL and PufM from the membrane to cytoplasmic assembly factors and back, and suggests that PuhA may participate in a salvage pathway of RC-LH1 biogenesis in purple bacteria. Indeed, the apparent absence of PuhA from the similar photosynthetic apparatus of the green filamentous bacterium *C. aurantiacus* (37) suggests to me that PuhA may have appeared after the rest of the core photosynthetic apparatus, and its present role in proton uptake may have evolved in addition to some other role. I propose that the entire *puhABCE* operon consists of genes that make RC-LH1 assembly more efficient than what undirected biogenesis could accomplish (Figure 4.6).

Although the functional importance of homodimerization by the second TM segment of PuhB remains to be established, it is tempting to speculate that PuhB functions in RC assembly as a dimer. In Section 4.3, I suggested that the PuhB dimer could assemble a new RC on one side by transmitting structural information from a previously assembled RC on the other side.

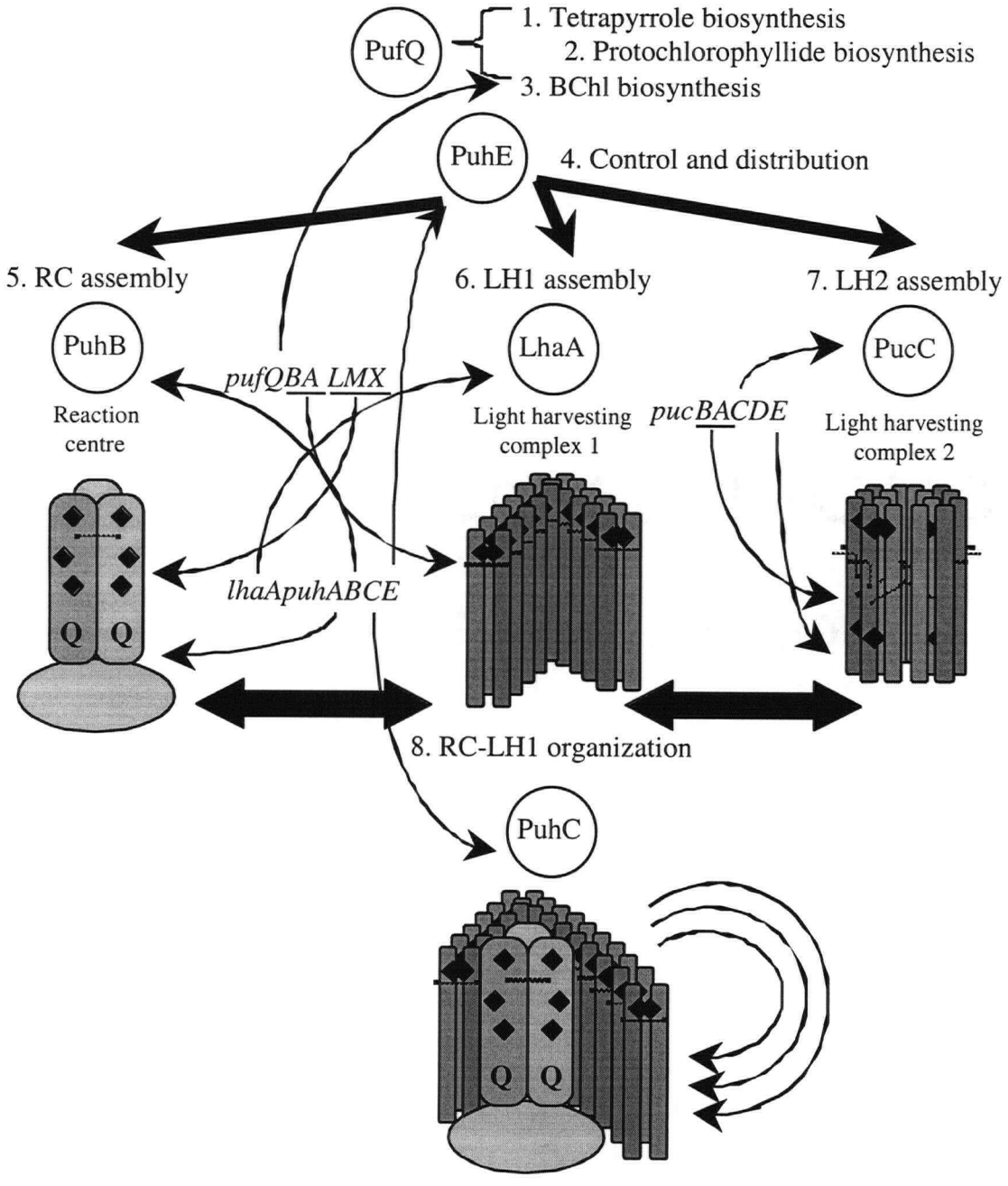

Figure 4.6. An integrated scheme of photosynthetic apparatus production in *R. capsulatus*. (1) PufQ stimulates early steps in BChl biosynthesis prior to chelation of magnesium. (2) PufQ has not been implicated in the biosynthesis of protochlorophyllide, but (3) may be associated with subsequent BChl precursors until pigment-protein complexes are assembled. (4) I hypothesize that PuhE controls the production of BChl and distributes it optimally to three pathways: (5) RC-PufX assembly by PuhB; (6) LH1 assembly by LhaA; and (7) LH2 assembly by PucC. (8) The role of PuhC may be to allow efficient expansion and reorganization of the RC-LH1 core complex. All of the known assembly factors and structural polypeptides of the *R. capsulatus* photosynthetic apparatus are encoded by three sets of genes: the *puf* operon, the *puh* operon (together with its 5' gene *lhaA*), and the *puc* operon. Several details have been omitted from this sketch: the roles of PufX in the organization of LH1 around the RC, the dimerization of RC-LH1 core complexes, and the alignment of core complexes; the accumulation of PufL-PufM in the cytoplasm due to PuhA; the dependence of RC assembly on LH1 and PufX; the effect of PuhB on LH1 assembly through the RC; possible PuhB-PufQ and PuhC-PufX interactions; and the LH1/LH2 shepherding roles proposed for PuhC and PucC. The double arrows should be taken as inclusive of all of these phenomena.

I observed that the phototrophic growth defect due to a *puhC* deletion is mitigated by several factors that would enhance *de novo* RC-LH1 biogenesis: prolonged semiaerobic incubation, reduced potential interference by LH2, and increased BChl availability due to a shifted balance of PufQ *versus* PuhE. Therefore, in Section 4.4, I suggested that PuhC is required for a more efficient process than *de novo* RC-LH1 biogenesis, namely expansion of the LH1 structure around one RC until it is large enough to associate with two RCs.

My observations suggest that PuhE co-ordinates the individual assembly processes of the RC and LH1 to achieve optimal levels of the core complex, and that PuhE is especially important under high light intensity, when degradation of BChl is more active (15). In Section 4.5, I suggested that PuhE is a sensor that regulates BChl biosynthesis and/or degradation as well as a transporter that directs BChl into specific assembly pathways.

Our understanding of the *puh* operon will be incomplete until we can account for the inclusion of *puhD* and *acsF* in other purple bacterial species, and only *acsF* in *R. gelatinosus*. Nothing is yet known about the function of the predicted PuhD polypeptides of *R. sphaeroides* and *R. palustris*. On the other hand, both *acsF* (under aerobic conditions) and *bchE* (under anaerobic conditions) are implicated in the same step of BChl biosynthesis, namely cyclization of the fifth ring attached to the porphyrin macrocycle (109), and whereas *acsF* is present on the 5' side of *puhE* in six purple bacterial photosynthesis gene clusters, two others have *bchE* on the 3' side of *puhE* (see Section 1.4 for details). Cyclization of the fifth ring is the step that produces protochlorophyllide, the BChl precursor for which association with PufQ has been reported (40). It is possible that there is an evolutionary advantage to co-regulation of the fifth ring cyclization enzymes with PuhE, the functional antagonist of PufQ in *R. capsulatus*.

The temporal sequence of Puf and Puh protein expression in *R. capsulatus* needs to be established, as has been done for the Puf proteins and PuhA in *R. sphaeroides* (124). Furthermore, the diversity of organisms that make use of the PuhB, PuhC, and PuhE proteins should be investigated through similar mutational analyses in other purple bacterial species, along with 5' sequence analysis of *puhE* in *C. aurantiacus* and probing for related sequences in other species of the anoxygenic phototrophic bacteria.

The subcellular locations of PuhB, PuhC, and PuhE relative to the RC-LH1 complex remain to be determined, perhaps by analysis of fractions of solubilized chromatophores separated on a sucrose gradient. In the case of PuhC, immunodetection is possible, whereas different techniques such as mass spectrometry of proteins separated by SDS-PAGE (142) may be required to identify PuhB and PuhE. Mass spectrometry of all five proteins: PuhB, PuhC, PuhE, PufQ, and PufX would reveal any post-translational processing undergone by them, which is particularly apropos in the case of PufX, to determine whether the protein expressed from the chromosomal and plasmid-borne genes, translated alone or together with the RC-LH1 proteins, is subject to differential modification that determines its utility. For example, proteolytic removal of 9 residues from the C-terminus (112) may affect association of *R. capsulatus* PufX with the RC-LH1 core complex as does deletion of a similar number of codons from the C-terminus of the *R. sphaeroides pufX* gene (44). Further efforts to obtain antisera that recognize PuhB and PuhE may make use of KLH-conjugated synthetic peptides, as I did for PufX, or another host species suitable for 6xHis-tagged membrane protein overexpression, such as *Lactococcus lactis* (77).

It should be determined if there are proteins with which PuhB, PuhC, and PuhE interact, and, if so, they should be identified. The RC and LH1 polypeptides including PufX are obvious candidates, as are PufQ, LhaA, and PucC. The development of better bacterial two-hybrid systems would facilitate this task. Currently, the CyaA system (71), which in theory can be applied to integral membrane proteins due to the diffusible cAMP signal (see Section 1.6), lacks an indicator of recombinant protein expression. The available anti-CyaA serum (58) did not recognize my hybrid proteins. The TOXCAT system (131) has such an indicator, the maltose test (see Section 1.6), but this test does not extend to certain classes of proteins that could be expressed as TOXCAT hybrids: cytoplasmic proteins and integral membrane proteins with cytoplasmic C-termini. Moreover, the TOXCAT system could not be expanded to a two-hybrid system easily in my hands (not shown).

The most promising two-hybrid system at present is the GALLEX system (140), which could be used to test *R. capsulatus* protein TM segments against each other within two classes: those that are known or predicted to run from cytoplasm to periplasm (PufA, PufB, PufX, PufQ, PuhB-TM1,

PuhB-TM3, PuhC, etc.), and those that are known or predicted to run from periplasm to cytoplasm (PuhA, PuhB-TM2, etc.). Because PuhE consists of seven putative TM segments oriented parallel and antiparallel to each other, a more versatile system will be required to study all of its potential interactions. If the results of my thesis are any indication, these experiments should provide an entirely new dimension of information about the structural networks of the photosynthetic apparatus and its assembly factors.

5. CONCLUSIONS

The significance of my research to the field of purple bacterial photosynthesis is apparent from the numerous effects and interconnections identified for the proteins studied, from which I have speculated as to the fundamental function of each protein.

I propose that the function of PuhB is to assemble BChl into the RC, and that this is particularly important under semiaerobic conditions. In the absence of PuhB, PufX is poorly immunodetected, and the RC is spectrally aberrant, poorly assembled, and unable to sustain growth, resulting in delayed adaptation to phototrophic growth conditions. The possibly dimeric structure of PuhB suggests that it may interact with two RCs, one on either side. PuhB may also interact with PufQ.

PuhC may be a reorganizing factor for LH1 that permits the addition of new PufA-PufB dimers and PufX during the biogenesis of core complexes, while excluding LH2 polypeptides. Several lines of evidence, notably the effects of PufQ and PuhE on *puhC* deletion strains, support the hypothesis that PuhC is essential for a preferred route of RC-LH1 biogenesis in *R. capsulatus*.

PuhE is the least essential and most enigmatic of the proteins studied here. It appears to be a control factor that downregulates BChl production and therefore plays an antagonistic role towards PufQ. The regulation and copy number of *puhE* seem to be important. The multitransmembrane structure of PuhE suggests a role in transport, perhaps to apportion BChl into RC-specific and LH complex-specific pathways for optimal assembly of the RC-LH1 core complex.

My results are consistent with a model of dimeric RC-LH1 core complex structure in which PufX is the axis of twofold symmetry. Increased expression of PufX in *R. capsulatus* revealed that this protein, without accumulating, significantly enhanced RC assembly in the absence of PufA, and that the function of PufX may depend on co-translation with the RC-LH1 polypeptides.

By building on my discoveries of these proteins' manifold effects and their connections to each other, a coherent picture of photosynthetic apparatus assembly should eventually emerge.

6. REFERENCES

1. **Adams, C. W., M. E. Forrest, S. N. Cohen, and J. T. Beatty.** 1989. Structural and functional analysis of transcriptional control of the *Rhodobacter capsulatus puf* operon. J. Bacteriol. **171:**473-482.
2. **Aklujkar, M., A. L. Harmer, R. C. Prince, and J. T. Beatty.** 2000. The *orf162b* sequence of *Rhodobacter capsulatus* encodes a protein required for optimal levels of photosynthetic pigment-protein complexes. J. Bacteriol. **182:**5440-5447.
3. **Alberti, M., D. E. Burke, and J. E. Hearst.** 1995. Structure and sequence of the photosynthetic gene cluster. *In* R. E. Blankenship, M. T. Madigan, and C. E. Bauer (ed.), Anoxygenic photosynthetic bacteria. Kluwer Academic Publishers, Dordrecht, The Netherlands.
4. **Babst, M., H. Albrecht, I. Wegmann, R. Brunisholz, and H. Zuber.** 1991. Single amino acid substitutions in the B870 α and β light-harvesting polypeptides of *Rhodobacter capsulatus*: Structural and spectral effects. Eur. J. Biochem. **202:**277-284.
5. **Barany, F.** 1985. Single-stranded hexameric linkers: a system for in-phase insertion mutagenesis and protein engineering. Gene **37:**111-123.
6. **Barz, W. P., F. Francia, G. Venturoli, B. A. Melandri, A. Verméglio, and D. Oesterhelt.** 1995. Role of PufX protein in photosynthetic growth of *Rhodobacter sphaeroides*. 1. PufX is required for efficient light-driven electron transfer and photophosphorylation under anaerobic conditions. Biochemistry **34:**15235-15247.
7. **Barz, W. P., and D. Oesterhelt.** 1994. Photosynthetic deficiency of a *pufX* deletion mutant of *Rhodobacter sphaeroides* is suppressed by point mutations in the light-harvesting complex genes *pufB* or *pufA*. Biochemistry **33:**9741-9752.
8. **Barz, W. P., A. Verméglio, F. Francia, G. Venturoli, B. A. Melandri, and D. Oesterhelt.** 1995. Role of PufX protein in photosynthetic growth of *Rhodobacter sphaeroides*. 2. PufX is required for efficient ubiquinone/ubiquinol exchange between the reaction center Q_B site and the cytochrome bc_1 complex. Biochemistry **34:**15248-15258.
9. **Bauer, C. E., J. J. Buggy, Z. Yang, and B. L. Marrs.** 1991. The superoperonal organization of genes for pigment biosynthesis and reaction center proteins is a conserved feature in *Rhodobacter capsulatus*: analysis of overlapping *bchB* and *puhA* transcripts. Mol. Gen. Genet. **228:**438-444.
10. **Bauer, C. E., and B. L. Marrs.** 1988. *Rhodobacter capsulatus puf* operon encodes a regulatory protein (PufQ) for bacteriochlorophyll biosynthesis. Proceedings of the National Academy of Sciences, USA **85:**7074-7078.
11. **Beatty, J. T.** 1995. Organization of photosynthesis gene transcripts., p. 1209-1219. *In* R. E. Blankenship, M. T. Madigan, and C. E. Bauer (ed.), Anoxygenic photosynthetic bacteria. Kluwer Academic Publishers, Dordrecht, The Netherlands.
12. **Beatty, J. T., and H. Gest.** 1981. Generation of succinyl-coenzyme A in photosynthetic bacteria. Arch. Microbiol. **129:**335-340.
13. **Béjà, O., M. T. Suzuki, J. F. Heidelberg, W. C. Nelson, C. M. Preston, T. Hamada, J. A. Eisen, C. M. Fraser, and E. F. DeLong.** 2002. Unsuspected diversity among marine aerobic anoxygenic phototrophs. Nature **415:**630-633.
14. **Bibb, M. J., and S. N. Cohen.** 1982. Gene expression in *Streptomyces*: construction and application of promoter-probe plasmid vectors in *Streptomyces lividans*. Mol. Gen. Genet. **187:**265-277.
15. **Biel, A. J.** 1995. Genetic analysis and regulation of bacteriochlorophyll biosynthesis., p. 1125-1134. *In* R. E. Blankenship, M. T. Madigan, and C. E. Bauer (ed.), Anoxygenic photosynthetic bacteria. Kluwer Academic Publishers, Dordrecht, The Netherlands.
16. **Bollivar, D. W., and C. E. Bauer.** 1992. Association of tetrapyrrole intermediates in the bacteriochlorophyll *a* biosynthetic pathway with the major outer-membrane porin protein of *Rhodobacter capsulatus*. Biochem. J. **282:**471-476.

17. **Bollivar, D. W., J. Y. Suzuki, J. T. Beatty, J. M. Dobrowski, and C. E. Bauer.** 1994. Directed mutational analysis of bacteriochlorophyll *a* biosynthesis in *Rhodobacter capsulatus*. J. Mol. Biol. **237:**622-640.
18. **Brand, M., A. F. García, N. Pucheu, A. Meryandini, N. Kerber, M. H. Tadros, and G. Drews.** 1995. Phosphorylation of the light-harvesting polypeptide LHIα of *Rhodobacter capsulatus* at serine after membrane insertion under chemotrophic and phototrophic growth conditions. Biochim. Biophys. Acta **1231:**169-175.
19. **Brent, R., and M. Ptashne.** 1980. The *lexA* gene product represses its own promoter. Proc. Natl. Acad. Sci. USA **77:**1932-1936.
20. **Bylina, E. J., S. J. Robles, and D. C. Youvan.** 1988. Directed mutations affecting the putative bacteriochlorophyll-binding sites in the light-harvesting I antenna of *Rhodobacter capsulatus*. Israel J. Chem. **28:**73-78.
21. **Bylina, E. J., and D. C. Youvan.** 1988. Directed mutations affecting spectroscopic and electron transfer properties of the primary donor in the photosynthetic reaction center. Proc. Natl. Acad. Sci. USA **85:**7226-7230.
22. **Chen, C.-Y. A., J. T. Beatty, S. N. Cohen, and J. G. Belasco.** 1988. An intercistronic stem-loop structure functions as an mRNA decay terminator necessary but insufficient for *puf* mRNA stability. Cell **52:**609-619.
23. **Cheng, Y. S., C. A. Brantner, A. Tsapin, and M. L. P. Collins.** 2000. Role of the H protein in assembly of the photochemical reaction center and intracytoplasmic membrane in *Rhodospirillum rubrum*. J. Bacteriol. **182:**1200-1207.
24. **Choudhary, M., and S. Kaplan.** 2000. DNA sequence analysis of the photosynthesis region of *Rhodobacter sphaeroides* 2.4.1^T. Nucleic Acids Res. **28:**862-867.
25. **Cohen-Bazire, G., S. Sistrom, and R. Y. Stanier.** 1957. Kinetic studies of pigment synthesis by non-sulphur purple bacteria. J. Cell. Comp. Physiol. **49:**25-68.
26. **Collins, W. J.** 1995. Polar and non-polar directed mutagenesis of *Rhodobacter capsulatus orf*214. Undergraduate research project report. University of British Columbia, Vancouver, B.C., Canada.
27. **Conroy, M. J., W. H. J. Westerhuis, P. S. Parkes-Loach, P. A. Loach, C. N. Hunter, and M. P. Williamson.** 2000. The solution structure of *Rhodobacter sphaeroides* LH1β reveals two helical domains separated by a more flexible region: Structural consequences for the LH1 complex. J. Mol. Biol. **298:**83-94.
28. **Cortez, N., A. F. García, M. H. Tadros, N. Gad'on, E. Schiltz, and G. Drews.** 1992. Redox-controlled, *in vivo* and *in vitro* phosphorylation of the α subunit of the light-harvesting complex I in *Rhodobacter capsulatus*. Arch. Microbiol. **158:**315-319.
29. **Davis, C. M., P. S. Parkes-Loach, C. K. Cook, K. A. Meadows, M. Bandilla, H. Scheer, and P. A. Loach.** 1996. Comparison of the structural requirements for bacteriochlorophyll binding in the core light-harvesting complexes of *Rhodospirillum rubrum* and *Rhodobacter sphaeroides* using reconstitution methodology with bacteriochlorophyll analogs. Biochemistry **35:**3072-3084.
30. **Ditta, G., T. Schmidhauser, E. Yakobsen, P. Lu, X.-W. Liang, D. R. Finlay, D. Guiney, and D. R. Helinski.** 1985. Plasmids related to the broad host range vector, pRK290, useful for gene cloning and for monitoring gene expression. Plasmid **13:**149-153.
31. **Dörge, B., G. Klug, N. Gad'on, S. N. Cohen, and G. Drews.** 1990. Effects on the formation of antenna complex B870 of *Rhodobacter capsulatus* by exchange of charged amino acids in the N-terminal domain of the *a* and *ß* pigment-binding proteins. Biochemistry **29:**7754-7758.
32. **Dracheva, S., J. A. Williams, G. V. Driessche, J. J. V. Beeumen, and R. E. Blankenship.** 1991. The primary structure of cytochrome *c*-554 from the green photosynthetic bacterium *Chloroflexus aurantiacus*. Biochemistry **30:**11451-11458.
33. **Drews, G., and J. R. Golecki.** 1995. Structure, molecular organization, and biosynthesis of membranes of purple bacteria., p. 231-257. *In* R. E. Blankenship, M. T. Madigan, and C. E. Bauer (ed.), Anoxygenic photosynthetic bacteria. Kluwer Academic Publishers, Dordrecht, The Netherlands.

34. **Farchaus, J. W., W. P. Barz, H. Grünberg, and D. Oesterhelt.** 1992. Studies on the expression of the *pufX* polypeptide and its requirement for photoheterotrophic growth in *Rhodobacter sphaeroides*. EMBO J. **11:**2779-2788.
35. **Fathir, I., T. Mori, T. Nogi, M. Kobayashi, K. Miki, and T. Nozawa.** 2001. Structure of the H subunit of the photosynthetic reaction center from the thermophilic purple sulfur bacterium, *Thermochromatium tepidum*. Eur. J. Biochem. **268:**2652-2657.
36. **Feick, R., R. v. Grondelle, C. P. Rijgersberg, and G. Drews.** 1980. Fluorescence emission by wild-type and mutant strains of *Rhodopseudomonas capsulata*. Biochim. Biophys. Acta **593:**241-253.
37. **Feick, R., J. A. Shiozawa, and A. Ertlmaier.** 1995. Biochemical and spectroscopic properties of the reaction center of the green filamentous bacterium, *Chloroflexus aurantiacus*., p. 699-708. *In* R. E. Blankenship, M. T. Madigan, and C. E. Bauer (ed.), Anoxygenic photosynthetic bacteria. Kluwer Academic Publishers, Dordrecht, The Netherlands.
38. **Fejes, A., E. C. Yi, D. R. Goodlett, and J. T. Beatty.** 2003. Shotgun proteomic analysis of chromatophores from the purple phototrophic bacterium *Rhodopseudomonas palustris*. Photosynth. Res. **78:**195-203.
39. **Fidai, S., J. A. Dahl, and W. R. Richards.** 1995. Effect of the PufQ protein on early steps in the pathway of bacteriochlorophyll biosynthesis in *Rhodobacter capsulatus*. FEBS Lett. **372:**264-268.
40. **Fidai, S., S. B. Hinchigeri, and W. R. Richards.** 1994. Association of protochlorophyllide with the PufQ protein of *Rhodobacter capsulatus*. Biochem. Biophys. Res. Comm. **200:**1679-1684.
41. **Fischer, S. G., and L. S. Lerman.** 1983. DNA fragments differing by single base-pair substitutions are separated in denaturing gradient gels: correspondence with melting theory. Proc. Natl. Acad. Sci. USA **80:**1579-1583.
42. **Fotiadis, D., P. Qian, A. Philippsen, P. A. Bullough, A. Engel, and C. N. Hunter.** 2004. Structural analysis of the reaction center light-harvesting complex I photosynthetic core complex of *Rhodospirillum rubrum* using atomic force microscopy. J. Biol. Chem. **279:**2063-2068.
43. **Francia, F., J. Wang, G. Venturoli, B. A. Melandri, W. P. Barz, and D. Oesterhelt.** 1999. The reaction center-LH1 antenna complex of *Rhodobacter sphaeroides* contains one PufX molecule which is involved in dimerization of this complex. Biochemistry **38:**6834-6845.
44. **Francia, F., J. Wang, H. Zischka, G. Venturoli, and D. Oesterhelt.** 2002. Role of the N- and C-terminal regions of the PufX protein in the structural organization of the photosynthetic core complex of *Rhodobacter sphaeroides*. Eur. J. Biochem. **269:**1877-1885.
45. **Frese, R. N., J. D. Olsen, R. Branvall, W. H. J. Westerhuis, C. N. Hunter, and R. v. Grondelle.** 2000. The long-range supraorganization of the bacterial photosynthetic unit: A key role for PufX. Proc. Natl. Acad. Sci. USA **97:**5197–5202.
46. **Fulcher, T. K., J. T. Beatty, and M. R. Jones.** 1998. Demonstration of the key role played by the PufX protein in the functional and structural organization of native and hybrid bacterial photosynthetic core complexes. J. Bacteriol. **180:**642–646.
47. **García, A. F., W. Mantele, N. Gad'on, M. H. Tadros, and G. Drews.** 1991. Growth and photosynthetic activities of wild-type and antenna-deficient mutant strains of *Rhodobacter capsulatus*. Arch. Microbiol. **155:**205-209.
48. **García, A. F., A. Meryandini, M. Brand, M. H. Tadros, and G. Drews.** 1994. Phosphorylation of the α and β polypeptides of the light-harvesting complex I (B870) of *Rhodobacter capsulatus* in an *in vitro* translation system. FEMS Microbiol. Lett. **124:**87-92.
49. **Germeroth, L., H. Reilander, and H. Michel.** 1996. Molecular cloning, DNA sequence and transcriptional analysis of the *Rhodospirillum molischianum* B800/850 light-harvesting genes. Biochim. Biophys. Acta **1275:**145:150.

50. **Ghosh, R., S. Ghosh-Eicher, M. DiBerardino, and R. Bachofen.** 1994. Protein phosphorylation in *Rhodospirillum rubrum*: purification and characterization of a water-soluble B873 protein kinase and a new component of the B873 complex, Ω, which can be phosphorylated. Biochim. Biophys. Acta **1184:**28-36.
51. **Goldsmith, J. O., B. King, and S. G. Boxer.** 1996. Mg coordination by amino acid side chains is not required for assembly and function of the special pair in bacterial photosynthetic reaction centers. Biochemistry **35:**2421-2428.
52. **Gong, L., J. K. Lee, and S. Kaplan.** 1994. The Q gene of *Rhodobacter sphaeroides*: its role in *puf* operon expression and spectral complex assembly. J. Bacteriol. **176:**2946-2961.
53. **Gopta, O. A., B. A. Feniouk, W. Junge, and A. Y. Mulkidjanian.** 1998. The cytochrome *bc*1 complex of *Rhodobacter capsulatus*: ubiquinol oxidation in a dimeric Q-cycle? FEBS Lett. **431:**291-296.
54. **Gromet-Elhanan, Z.** 1995. The proton-translocating F0F1 ATP synthase-ATPase complex., p. 807–830. *In* R. E. Blankenship, M. T. Madigan, and C. E. Bauer (ed.), Anoxygenic photosynthetic bacteria. Kluwer Academic Publishers, Dordrecht, The Netherlands.
55. **Hahn, F. M., L. M. Eubanks, C. A. Testa, B. S. J. Blagg, J. A. Baker, and C. D. Poulter.** 2001. 1-Deoxy-D-xylulose 5-phosphate synthase, the gene product of open reading frame (ORF) 2816 and ORF 2895 in *Rhodobacter capsulatus*. J. Bacteriol. **183:**1-11.
56. **Harmer, A.** 1998. Mutational analysis of the *Rhodobacter capsulatus orf162b* gene. M.Sc. thesis. University of British Columbia, Vancouver, B.C., Canada.
57. **Hess, S., K. Visscher, J. Ulander, T. Pullerits, M. R. Jones, C. N. Hunter, and V. Sundström.** 1993. Direct energy transfer from the peripheral LH2 antenna to the reaction center in a mutant of *Rhodobacter sphaeroides* that lacks the core LH1 antenna. Biochemistry **32:**10314-10322.
58. **Hormozi, K., R. Parton, and J. Coote.** 1999. Adjuvant and protective properties of native and recombinant *Bordetella pertussis* adenylate cyclase toxin preparations in mice. FEMS Immunol. Med. Microbiol. **23:**273-282.
59. **Hu, Q., R. A. Brunisholz, G. Frank, and H. Zuber.** 1996. The antenna complexes of the purple non-sulfur photosynthetic bacterium Rhodocyclus tenuis. Structural and spectral characterization. Eur. J. Biochem. **238:**381-390.
60. **Hucke, O., E. Schiltz, G. Drews, and A. Labahn.** 2003. Sequence analysis reveals new membrane anchor of reaction centre-bound cytochromes possibly related to PufX. FEBS Lett. **535:**166-170.
61. **Igarashi, N., J. Harada, S. Nagashima, K. Matsuura, K. Shimada, and K. V. P. Nagashima.** 2001. Horizontal transfer of the photosynthesis gene cluster and operon rearrangement in purple bacteria. J. Mol. Evol. **52:**333-341.
62. **Imhoff, J. F.** 1995. Taxonomy and physiology of phototrophic purple bacteria and green sulfur bacteria., p. 1-15. *In* R. E. Blankenship, M. T. Madigan, and C. E. Bauer (ed.), Anoxygenic photosynthetic bacteria. Kluwer Academic Publishers, Dordrecht, The Netherlands.
63. **Jackson, J. B., and P. L. Dutton.** 1973. The kinetic and redox potentiometric resolution of the carotenoid shifts in *Rhodopseudomonas sphaeroides* chromatophores: their relationship to electric field alterations in electron transport and energy coupling. Biochim. Biophys. Acta **325:**102-115.
64. **Jackson, W. J., P. J. Kiley, C. E. Haith, S. Kaplan, and R. C. Prince.** 1987. On the role of the light-harvesting B880 in the correct insertion of the reaction center of *Rhodobacter capsulatus* and *Rhodobacter sphaeroides*. FEBS Lett. **215:**171-174.
65. **Jackson, W. J., and R. C. Prince.** 1987. Genetic and DNA sequence analysis of a R. capsulatus mutant unable to properly insert photochemical reaction centers into the membrane., p. 725-728. *In* J. Biggins (ed.), Progress in Photosynthesis Research, vol. 4. Marinus Nijhoff, Dordrecht, The Netherlands.

66. **Jackson, W. J., R. C. Prince, G. J. Stewart, and B. L. Marrs.** 1986. Energetic and topographic properties of a *Rhodopseudomonas capsulata* mutant deficient in the B870 complex. Biochem. **25:**8440-8446.

67. **Jamieson, S. J., P. Wang, P. Qian, J. Y. Kirkland, M. J. Conroy, C. N. Hunter, and P. A. Bullough.** 2002. Projection structure of the photosynthetic reaction centre-antenna complex of *Rhodospirillum rubrum* at 8.5 Å resolution. EMBO J. **21:**3927-3935.

68. **Jones, M. R., G. J. S. Fowler, L. C. D. Gibson, G. G. Grief, J. D. Olsen, W. Crielaard, and C. N. Hunter.** 1992. Mutants of *Rhodobacter sphaeroides* lacking one or more pigment-protein complexes and complementation with reaction-centre, LH1, and LH2 genes. Mol. Microbiol. **6:**1173-1184.

69. **Jones, M. R., R. W. Visschers, R. v. Grondelle, and C. N. Hunter.** 1992. Construction and characterization of a mutant of *Rhodobacter sphaeroides* with the reaction center as the sole pigment-protein complex. Biochemistry **31:**4458-4465.

70. **Jungas, C., J. L. Ranck, J. L. Rigaud, P. Joliot, and A. Verméglio.** 1999. Supramolecular organization of the photosynthetic apparatus of *Rhodobacter sphaeroides*. EMBO J. **18:**534-542.

71. **Karimova, G., J. Pidoux, A. Ullmann, and D. Ladant.** 1998. A bacterial two-hybrid system based on a reconstituted signal transduction pathway. Proc. Natl. Acad. Sci. USA **95:**5752-5756.

72. **Keen, N. T., S. Tamaki, D. Kobayashi, and D. Trollinger.** 1988. Improved broad-host range plasmids for DNA cloning in Gram-negative bacteria. Gene **70:**191-197.

73. **Kerber, N., N. Pucheu, M. Tadros, G. Drews, and A. García.** 1998. The phosphorylation of light-harvesting polypeptides LHIα (B870) and LHIIα (B800-850) of *Rhodobacter capsulatus* B10 was higher under chemotrophic oxic than under phototrophic anoxic growth conditions. Curr. Microbiol. **37:**32-38.

74. **Klug, G., and S. N. Cohen.** 1988. Pleiotropic effects of localized *Rhodobacter capsulatus puf* operon deletions on production of light-absorbing pigment-protein complexes. J. Bacteriol. **170:**5814-5821.

75. **Koepke, J., X. Hu, C. Muenke, K. Schulten, and H. Michel.** 1996. The crystal structure of the light-harvesting complex II (B800-850) from *Rhodospirillum molischianum*. Structure **4:**581-597.

76. **Kovács, Á. T., G. Rákhely, and K. L. Kovács.** 2003. Genes involved in the biosynthesis of photosynthetic pigments in the purple sulfur photosynthetic bacterium *Thiocapsa roseopersicina*. Appl. Env. Microbiol. **69:**3093-3102.

77. **Kunji, E. R. S., D.-J. Slotboom, and B. Poolman.** 2003. *Lactococcus lactis* as host for overproduction of functional membrane proteins. Biochim. Biophys. Acta **1610:**97-108.

78. **Kyte, J., and R. F. Doolittle.** 1982. A simple method for displaying the hydropathic character of a protein. J. Mol. Biol. **157:**105-132.

79. **Larimer, F. W., P. Chain, L. Hauser, J. Lamerdin, S. Malfatti, L. Do, M. L. Land, D. A. Pelletier, J. T. Beatty, A. S. Lang, F. R. Tabita, J. L. Gibson, T. E. Hanson, C. Bobst, J. L. T. y. Torres, C. Peres, F. H. Harrison, J. Gibson, and C. S. Harwood.** 2004. The genome sequence of the metabolically versatile photosynthetic bacterium *Rhodopseudomonas palustris*. Nature Biotech. **22:**55-61.

80. **Lascelles, J.** 1966. The accumulation of bacteriochlorophyll precursors by mutant and wild-type strains of *Rhodopseudomonas sphaeroides*. Biochem. J. **100:**175-183.

81. **Lascelles, J.** 1968. The bacterial photosynthetic apparatus. Adv. Microbial Physiol. **2:**1-42.

82. **Law, C. J., J. Chen, P. S. Parkes-Loach, and P. A. Loach.** 2003. Interaction of bacteriochlorophyll with the LH1 and PufX polypeptides of photosynthetic bacteria: use of chemically synthesized analogs and covalently attached fluorescent probes. Photosynth. Res. **75:**193-210.

83. **LeBlanc, H.** 1995. Directed mutagenesis and gene fusion analysis of the *Rhodobacter capsulatus puc* operon. Ph.D. thesis. University of British Columbia, Vancouver, B.C., Canada.

84. **LeBlanc, H., A. S. Lang, and J. T. Beatty.** 1999. Transcript cleavage, attenuation and an internal promoter in the *Rhodobacter capsulatus puc* operon. J. Bacteriol. **181:**4955-4960.
85. **Lilburn, T. G.** 1990. The role of the *pufX* gene product of *Rhodobacter capsulatus*. M.Sc. thesis. University of British Columbia, Vancouver, B.C., Canada.
86. **Lilburn, T. G., and J. T. Beatty.** 1992. Suppressor mutants of the photosynthetically incompetent *pufX* deletion mutant *Rhodobacter capsulatus* ΔRC6(pTL2). FEMS Microbiol. Lett. **100:**155-160.
87. **Lilburn, T. G., C. E. Haith, R. C. Prince, and J. T. Beatty.** 1992. Pleiotropic effects of *pufX* gene deletion on the structure and function of the photosynthetic apparatus of *Rhodobacter capsulatus*. Biochim. Biophys. Acta **1100:**160-170.
88. **Lilburn, T. G., R. C. Prince, and J. T. Beatty.** 1995. Mutation of the Ser2 codon of the light-harvesting B870 α polypeptide of *Rhodobacter capsulatus* partially suppresses the *pufX* phenotype. J. Bacteriol. **177:**4593-4600.
89. **Loach, P. A., and P. S. Parkes-Loach.** 1995. Structure-function relationships in core light-harvesting complexes (LHI) as determined by characterization of the structural subunit and by reconstitution experiments. *In* R. E. Blankenship, M. T. Madigan, and C. E. Bauer (ed.), Anoxygenic photosynthetic bacteria. Kluwer Academic Publishers, Dordrecht, The Netherlands.
90. **Manoil, C.** 1991. Analysis of membrane protein topology using alkaline phosphatase and β-galactosidase. Methods Cell Biol. **34:**61-75.
91. **Marck, C.** 1991. DNA Strider™ 1.2. A C program for DNA and protein sequences analysis., Centre d'Etudes de Saclay, 91191 Gif-sur-Yvette Cedex France.
92. **Masuda, S., M. Yoshida, K. V. P. Nagashima, K. Shimada, and K. Matsuura.** 1999. A new cytochrome subunit bound to the photosynthetic reaction center in the purple bacterium, *Rhodovulum sulfidophilum*. J. Biol. Chem. **274:**10795-10801.
93. **McDermott, G., S. M. Prince, A. A. Freer, A. M. Hawthornthwaite-Lawless, M. Z. Papiz, R. J. Cogdell, and N. W. Isaacs.** 1995. Crystal structure of an integral membrane light-harvesting complex from photosynthetic bacteria. Nature **374:**517-521.
94. **McGlynn, P., C. N. Hunter, and M. R. Jones.** 1994. The *Rhodobacter sphaeroides* PufX protein is not required for photosynthetic competence in the absence of a light harvesting system. FEBS Lett. **349:**349-353.
95. **McGlynn, P., W. H. J. Westerhuis, M. R. Jones, and C. N. Hunter.** 1996. Consequences for the organization of reaction center-light harvesting antenna 1 (LH1) core complexes of *Rhodobacter sphaeroides* arising from deletion of amino acid residues from the C terminus of the LH1 α polypeptide. J. Biol. Chem. **271:**3285-3292.
96. **Meinhardt, S. W., P. J. Kiley, S. Kaplan, A. R. Crofts, and S. Harayama.** 1985. Characterization of light-harvesting mutants of *Rhodopseudomonas sphaeroides*. I. Measurement of the efficiency of energy transfer from light-harvesting complexes to the reaction center. Arch. Biochem. Biophys. **236:**130-139.
97. **Meryandini, A., and G. Drews.** 1996. Import and assembly of the a and b-polypeptides of the light-harvesting complex I (B870) in the membrane system of *Rhodobacter capsulatus* investigated in an *in vitro* translation system. Photosynth. Res. **47:**21-31.
98. **Meyer, T. E., and T. J. Donohue.** 1995. Cytochromes, iron-sulfur, and copper proteins mediating electron transfer from the cyt *b/c*1 complex to photosynthetic reaction center complexes., p. 725–745. *In* R. E. Blankenship, M. T. Madigan, and C. E. Bauer (ed.), Anoxygenic photosynthetic bacteria. Kluwer Academic Publishers, Dordrecht, The Netherlands.
99. **Miller, J. H.** 1972. Experiments in molecular genetics. Cold Spring Harbor Laboratory, Cold Spring Harbor, New York.
100. **Mitchell, P.** 1976. Possible molecular mechanisms of the protonmotive function of cytochrome systems. J. Theor. Biol. **62:**327-367.
101. **Nagashima, K. V. P., K. Matsuura, and K. Shimada.** 1996. The nucleotide sequence of the *puf* operon from the purple photosynthetic bacterium, *Rhodospirillum molischianum*:

comparative analyses of light-harvesting proteins and the cytochrome subunits associated with the reaction centers. Photosynth. Res. **50:**61–70.

102. **Nagashima, K. V. P., K. Matsuura, N. Wakao, A. Hiraishi, and K. Shimada.** 1997. Nucleotide sequences of genes coding for photosynthetic reaction center and light-harvesting proteins of *Acidiphilum rubrum* and related aerobic acidophilic bacteria. Plant Cell Physiol. **38:**1249-1258.
103. **Nagashima, S., K. Shimada, K. Matsuura, and K. V. P. Nagashima.** 2002. Transcription of three sets of genes coding for the core light-harvesting proteins in the purple sulfur bacterium, *Allochromatium vinosum*. Photosynth. Res. **74:**269-280.
104. **Nickens, D., J. J. Buggy, and C. E. Bauer.** 1999. A mutation that affects isoprenoid biosynthesis results in altered expression of photosynthesis genes and synthesis of the photosynthetic apparatus in *Rhodobacter capsulatus*., p. 149-157. *In* G. A. Peschek, W. Löffelhardt, and G. Schmetterer (ed.), The phototrophic prokaryotes. Kluwer Academic Publishers, Dordrecht, The Netherlands.
105. **Norrander, J., T. Kempe, and J. Messing.** 1983. Construction of improved M13 vectors using oligodeoxynucleotide-directed mutagenesis. Gene **26:**101-106.
106. **Okamura, M. Y., and G. Feher.** 1995. Proton-coupled electron transfer reactions of Q_B in reaction centers from photosynthetic bacteria. *In* R. E. Blankenship, M. T. Madigan, and C. E. Bauer (ed.), Anoxygenic photosynthetic bacteria. Kluwer Academic Publishers, Dordrecht, The Netherlands.
107. **Okamura, M. Y., M. L. Paddock, M. S. Graige, and G. Feher.** 2000. Proton and electron transfer in bacterial reaction centers. Biochim. Biophys. Acta **1458:**148-163.
108. **Olsen, J. D., J. N. Sturgis, W. H. J. Westerhuis, G. J. S. Fowler, C. N. Hunter, and B. Robert.** 1997. Site-directed modification of the ligands to the bacteriochlorophylls of the light-harvesting LH1 and LH2 complexes of *Rhodobacter sphaeroides*. Biochemistry **36:**12625-12632.
109. **Ouchane, S., A.-S. Steunou, M. Picaud, and C. Astier.** 2004. Aerobic and anaerobic Mg-protoporphyrin monomethylester cyclases in purple bacteria: a strategy adopted to bypass the repressive oxygen control system. J. Biol. Chem. **279:**6385-6394.
110. **Papiz, M. Z., S. M. Prince, A. M. Hawthornthwaite-Lawless, G. McDermott, A. A. Freer, N. W. Isaacs, and R. J. Cogdell.** 1996. A model for the photosynthetic apparatus of purple bacteria. Trends Plant Sci. **1:**198-206.
111. **Papiz, M. Z., S. M. Prince, T. Howard, R. J. Cogdell, and N. W. Isaacs.** 2003. The structure and thermal motion of the B800–850 LH2 complex from Rps. acidophila at 2.0 Å resolution and 100 K: new structural features and functionally relevant motions. J. Mol. Biol. 326:1523–1538.
112. **Parkes-Loach, P. S., C. J. Law, P. A. Recchia, J. Kehoe, S.Nehrlich, J. Chen, and P. A. Loach.** 2001. Role of the core region of the PufX protein in inhibition of reconstitution of the core light-harvesting complexes of *Rhodobacter sphaeroides* and *Rhodobacter capsulatus*. Biochemistry **40:**5593-5601.
113. **Permentier, H. P., S. Neerken, K. A. Schmidt, J. Overmann, and J. Amesz.** 2000. Energy transfer and charge separation in the purple non-sulfur bacterium *Roseospirillum parvum*. Biochim. Biophys. Acta **1460:**338-345.
114. **Peters, G. A.** 1970. Morphological and spectral aspects of pigment development and related studies in the non-sulfur, purple photosynthetic bacterium, *Rhodopseudomonas spheroides*. Ph. D. thesis. University of Michigan, Ann Arbor, MI, USA.
115. **Peters, J., J. Takemoto, and G. Drews.** 1983. Spatial relationships between the photochemical reaction center and the light-harvesting complexes in the membrane of *Rhodopseudomonas capsulata*. Biochemistry **22:**5660-5667.
116. **Peterson, G.** 1983. Determination of total protein. Meth. Enzymol. **91:**95-119.
117. **Pierson, B. K., and R. W. Castenholz.** 1995. Taxonomy and physiology of filamentous anoxygenic phototrophs., p. 31-47. *In* R. E. Blankenship, M. T. Madigan, and C. E. Bauer (ed.), Anoxygenic photosynthetic bacteria. Kluwer Academic Publishers, Dordrecht, The Netherlands.

118. **Pinta, V., M. Picaud, F. Reiss-Husson, and C. Astier.** 2002. *Rubrivivax gelatinosus acsF* (previously *orf358*) codes for a conserved, putative binuclear-iron-cluster-containing protein involved in aerobic oxidative cyclization of Mg-protoporphyrin IX monomethylester. J. Bacteriol. **184:**746-753.
119. **Prentki, P., and H. M. Krisch.** 1984. *In vitro* insertional mutagenesis with a selectable DNA fragment. Gene **29:**303-313.
120. **Prince, R. C., and W. J. Jackson.** 1987. The role of light-harvesting I antenna proteins in the correct insertion of the photochemical reaction center of *Rhodobacter capsulatus* and *Rhodobacter sphaeroides*., p. 721-724. *In* J. Biggins (ed.), Progress in Photosynthesis Research, vol. 4. Marinus Nijhoff, Dordrecht, The Netherlands.
121. **Prince, S. M., M. Z. Papiz, A. A. Freer, G. McDermott, A. M. Hawthornthwaite-Lawless, R. J. Cogdell, and N. W. Isaacs.** 1997. Apoprotein structure in the LH2 complex from *Rhodopseudomonas acidophila* strain 10050: modular assembly and protein pigment interactions. J. Mol. Biol. **268:**412-423.
122. **Pucheu, N. L., N. L. Kerber, P. Pardo, M. Brand, G. Drews, and A. F. García.** 1996. Bioenergetic factors controlling *in vitro* phosphorylation of LHIα (B870) polypeptides in membranes isolated from *Rhodobacter capsulatus*. Arch. Microbiol. **165:**119-125.
123. **Pucheu, N. L., N. L. Kerber, E. A. Rivas, N. Cortez, and A. F. García.** 1997. Association of LHIα (B870) polypeptide with phospholipids during insertion in the photosynthetic membrane of an LHII$^-$ mutant of *Rhodobacter capsulatus*. Curr. Microbiol. **34:**155-161.
124. **Pugh, R. J., P. McGlynn, M. R. Jones, and C. N. Hunter.** 1998. The LH1-RC core complex of *Rhodobacter sphaeroides*: interaction between components, time-dependent assembly, and topology of the PufX protein. Biochim. Biophys. Acta **1366:**301-316.
125. **Recchia, P. A., C. M. Davis, T. G. Lilburn, J. T. Beatty, P. S. Parkes-Loach, C. N. Hunter, and P. A. Loach.** 1998. Isolation of the PufX protein from *Rhodobacter capsulatus* and *Rhodobacter sphaeroides*: Evidence for its interaction with the α-polypeptide of the core light harvesting complex. Biochemistry **37:**11055-11063.
126. **Richards, W. R., R. B. Wallace, M. S. Tsao, and E. Ho.** 1975. The nature of a pigment-protein complex excreted from mutants of *Rhodopseudomonas sphaeroides*. Biochemistry **14:**5554-5561.
127. **Richter, P., M. Brand, and G. Drews.** 1992. Characterization of LHI$^-$ and LHI$^+$ *Rhodobacter capsulatus pufA* mutants. J. Bacteriol. **174:**3030-3041.
128. **Richter, P., and G. Drews.** 1991. Incorporation of light-harvesting complex I α and β polypeptides into the intracytoplasmic membrane of *Rhodobacter capsulatus*. J. Bacteriol. **173:**5336-5345.
129. **Roszak, A. W., T. D. Howard, J. Southall, A. T. Gardiner, C. J. Law, N. W. Isaacs, and R. J. Cogdell.** 2003. Crystal structure of the RC-LH1 core complex from *Rhodopseudomonas palustris*. Science **302:**1969-1972.
130. **Russ, W. P., and D. M. Engelman.** 2000. The GxxxG motif: A framework for transmembrane helix-helix association. J. Mol. Biol. **296:**911-919.
131. **Russ, W. P., and D. M. Engelman.** 1999. TOXCAT: a measure of transmembrane helix association in a biological membrane. Proc. Natl. Acad. Sci. USA **96:**863-868.
132. **Sambrook, J., E. F. Fritsch, and T. Maniatis.** 1989. Molecular Cloning: A Laboratory Manual, 2nd ed. Cold Spring Harbor Laboratory Press, Cold Spring Harbor, N.Y.
133. **Sauer, P. R. R., F. Lottspeich, E. Unger, R. Mentele, and H. Michel.** 1996. Deletion of a B800-850 light-harvesting complex in *Rhodospirillum molischianum* DSM119 leads to "Revertants" expressing a B800-820 complex: insights into pigment binding. Biochemistry **35:**6500-6507.
134. **Savage, H., M. Cyrklaff, G. Montoya, W. Kühlbrandt, and I. Sinning.** 1996. Two-dimensional structure of light harvesting complex II (LHII) from the purple bacterium *Rhodovulum sulfidophilum* and comparison with LHII from *Rhodopseudomonas acidophila*. Structure **4:**243-252.

135. **Schägger, H., and G. von Jagow.** 1987. Tricine-sodium dodecyl sulfate-polyacrylamide gel electrophoresis for the separation of proteins in the range from 1 to 100 kDa. Analyt. Biochem. **166:**368-379.
136. **Scheuring, S., F. Francia, J. Busselez, B. A. Melandri, J. Rigaud, and D. Levy.** 2004. Structural role of PufX in the dimerization of the photosynthetic core complex of *Rhodobacter sphaeroides.* J. Biol. Chem. **279:**3620–3626.
137. **Scheuring, S., F. Reiss-Husson, A. Engel, J.-L. Rigaud, and J.-L. Ranck.** 2001. High-resolution AFM topographs of *Rubrivivax gelatinosus* light harvesting complex LH2. EMBO J. **20:**3029-3035.
138. **Scheuring, S., J. Seguin, S. Marco, D. Lévy, C. Breyton, B. Robert, and J.-L. Rigaud.** 2003. AFM characterization of tilt and intrinsic flexibility of *Rhodobacter sphaeroides* light harvesting complex 2 (LH2). J. Mol. Biol. **325:**569-580.
139. **Scheuring, S., J. Seguin, S. Marco, D. Levy, B. Robert, and J. Rigaud.** 2003. Nanodissection and high-resolution imaging of the *Rhodopseudomonas viridis* photosynthetic core complex in native membranes by AFM. Proc. Natl. Acad. Sci. USA **100:**1690-1693.
140. **Schneider, D., and D. M. Engelman.** 2003. GALLEX, a measurement of heterologous association of transmembrane helices in a biological membrane. J. Biol. Chem. **278:**3105-3111.
141. **Scolnik, P. A., and B. L. Marrs.** 1987. Genetic research with photosynthetic bacteria. Annu. Rev. of Microbiol. **41:**703-726.
142. **Shevchenko, A., M. Wilm, O. Vorm, and M. Mann.** 1996. Mass spectrometric sequencing of proteins silver-stained polyacrylamide gels. Anal. Chem. **68:**850-858.
143. **Siebert, C. A., P. Quian, D. Fotiadis, A. Engel, C. N. Hunter, and P. A. Bullough.** 2004. Molecular architecture of photosynthetic membranes in *Rhodobacter sphaeroides*: the role of PufX. EMBO J. **23:**690-700.
144. **Simon, R., U. Priefer, and A. Pühler.** 1983. A broad host range mobilization system for *in vivo* genetic engineering: transposon mutagenesis in Gram-negative bacteria. Bio/Technology **1:**37-45.
145. **Solioz, M., and B. Marrs.** 1977. The gene transfer agent of *Rhodopseudomonas capsulata.* Arch. Biochem. Biophys. **181:**300-307.
146. **Steiner, R., and H. Scheer.** 1985. Characterisation of a B800/1020 antenna from the photosynthetic bacteria *Ectothiorhodospira halochloris* and *Ectothiorhodospira abdelmalekii.* Biochim. Biophys. Acta **807:**278-284.
147. **Stiehle, H., N. Cortez, G. Klug, and G. Drews.** 1990. A negatively charged N terminus in the α polypeptide inhibits formation of light-harvesting complex I in *Rhodobacter capsulatus.* J. Bacteriol. **172:**7131-7137.
148. **Taylor, D. P., S. N. Cohen, W. G. Clark, and B. L. Marrs.** 1983. Alignment of genetic and restriction maps of the photosynthesis region of the *Rhodopseudomonas capsulata* chromosome by a conjugation-mediated marker rescue technique. J. of Bacteriol. **154:**580-590.
149. **Tehrani, A., and J. T. Beatty.** 2004. Effects of precise deletions in *Rhodobacter sphaeroides* reaction center genes on steady-state levels of reaction center proteins: A revised model for reaction center assembly. Photosynth. Res. **79:**101–108.
150. **Tehrani, A., R. C. Prince, and J. T. Beatty.** 2003. Effects of photosynthetic reaction center H protein domain mutations on photosynthetic properties and reaction center assembly in *Rhodobacter sphaeroides.* Biochemistry **42:**8919-8928.
151. **Todd, J. B., P. S. Parkes-Loach, J. F. Leykam, and P. A. Loach.** 1998. *In vitro* reconstitution of the core and peripheral light-harvesting complexes of *Rhodospirillum molischianum* from separately isolated components. Biochemistry **37:**17458-17468.
152. **Todd, J. B., P. A. Recchia, P. S. Parkes-Loach, J. D. Olsen, G. J. S. Fowler, P. McGlynn, C. N. Hunter, and P. A. Loach.** 1999. Minimal requirements for *in vitro* reconstitution of the structural subunit of light-harvesting complexes of photosynthetic bacteria. Photosynth. Res. **62:**85-98.

153. **Tsukatani, Y., K. Matsuura, S. Masuda, K. Shimada, A. Hiraishi, and K. V. P. Nagashima.** 2004. Phylogenetic distribution of unusual triheme to tetraheme cytochrome subunit in the reaction center complex of purple photosynthetic bacteria. Photosynth. Res. **79:**83-91.

154. **van den Berg, W. H., R. C. Prince, C. L. Bashford, K. Takamiya, W. D. Bonner, and P. L. Dutton.** 1979. Electron and proton transport in the ubiquinone-cytochrome *b-c*2 oxidoreductase of *Rps. sphaeroides*: Patterns of binding and inhibition by antimycin. J. Biol. Chem. **254:**8594-8604.

155. **Varga, A. R., and S. Kaplan.** 1993. Synthesis and stability of reaction center polypeptides and implications for reaction center assembly in *Rhodobacter sphaeroides.* J. Biol. Chem. **268:**19842-19850.

156. **Vieira, J., and J. Messing.** 1982. The pUC plasmids, and M13mp7-derived system for insertion mutagenesis and sequencing with synthetic universal primers. Gene **19:**259-268.

157. **von Heijne, G.** 1989. Control of topology and mode of assembly of a polytopic membrane protein by positively charged residues. Nature **341:**456-458.

158. **Walz, T., and R. Ghosh.** 1997. Two-dimensional crystallization of the light-harvesting I-reaction centre photounit from *Rhodospirillum rubrum.* J. Mol. Biol. **265:**107-111.

159. **Walz, T., S. J. Jamieson, C. M. Bowers, P. A. Bullough, and C. N. Hunter.** 1998. Projection structures of three photosynthetic complexes from *Rhodobacter sphaeroides*: LH2 at 6Å, LH1 and RC-LH1 at 25Å. J. Mol. Biol. **282:**833-845.

160. **Weaver, P. F., J. D. Wall, and H. Gest.** 1975. Characterization of *Rhodopseudomonas capsulata.* Arch. Microbiol. **105:**207-216.

161. **Wechsler, T. D., R. A. Brunisholz, G. Frank, F. Suter, and H. Zuber.** 1987. The complete amino acid sequence of the antenna polypeptide B806-866-β from the cytoplasmic membrane of the green bacterium *Chloroflexus aurantiacus.* FEBS Lett. **210:**189-194.

162. **Wellington, C. L., and J. T. Beatty.** 1991. Overlapping mRNA transcripts of photosynthesis gene operons in *Rhodobacter capsulatus.* J. Bacteriol. **173:**1432-1443.

163. **Wellington, C. L., A. K. P. Taggart, and J. T. Beatty.** 1991. Functional significance of overlapping transcripts of *crtEF, bchCA,* and *puf* photosynthesis gene operons in *Rhodobacter capsulatus.* J. Bacteriol. **173:**2954-2961.

164. **Westerhuis, W. H. J., J. N. Sturgis, E. C. Ratcliffe, C. N. Hunter, and R. A. Niederman.** 2002. Isolation, size estimates, and spectral heterogeneity of an oligomeric series of light-harvesting 1 complexes from *Rhodobacter sphaeroides.* Biochemistry **41:**8698-8707.

165. **Weyer, K. A., F. Lottspeich, H. Gruenberg, F. Lang, D. Oesterhelt, and H. Michel.** 1987. Amino acid sequence of the cytochrome subunit of the photosynthetic reaction centre from the purple bacterium *Rhodopseudomonas viridis.* EMBO J. **8:**2197–2202.

166. **Wong, D. K.-H.** 1994. Directed mutational analysis of the *Rhodobacter capsulatus puhA* gene and downstream open reading frames. M.Sc. thesis. University of British Columbia, Vancouver, B.C., Canada.

167. **Wong, D. K.-H., W. J. Collins, A. Harmer, T. G. Lilburn, and J. T. Beatty.** 1996. Directed mutagenesis of the *Rhodobacter capsulatus puhA* gene and pleiotropic effects on photosynthetic reaction center and light-harvesting I complexes. J. Bacteriol. **178:**2334-2342.

168. **Woodbury, N. W., and J. P. Allen.** 1995. The pathway, kinetics and thermodynamics of electron transfer in wild type and mutant reaction centers of purple nonsulfur bacteria. *In* R. E. Blankenship, M. T. Madigan, and C. E. Bauer (ed.), Anoxygenic photosynthetic bacteria. Kluwer Academic Publishers, Dordrecht, The Netherlands.

169. **Yen, H. C., N. T. Hu, and B. L. Marrs.** 1979. Characterization of the gene transfer agent made by an overproducer mutant of *Rhodopseudomonas capsulata.* J. Mol. Biol. **131:**157-168.

170. **Young, C. S., R. C. Reyes, and J. T. Beatty.** 1998. Genetic complementation and kinetic analyses of *Rhodobacter capsulatus ORF1696* mutants indicate that the ORF1696 protein enhances assembly of the light-harvesting I complex. J. Bacteriol. **180:**1759-1765.

171. **Youvan, D. C., S. Ismail, and E. J. Bylina.** 1985. Chromosomal deletion and plasmid complementation of the photosynthetic reaction center and light harvesting genes from *Rhodopseudomonas capsulata.* Gene **38:**19-30.

172. **Zeng, X., M. Choudhary, and S. Kaplan.** 2003. A second and unusual *pucBA* operon of *Rhodobacter sphaeroides* 2.4.1: genetics and function of the encoded polypeptides. J. Bacteriol. **185:**6171-6184.

173. **Zilsel, J., T. Lilburn, and J. T. Beatty.** 1989. Formation of functional inter-species hybrid photosynthetic complexes in *Rhodobacter capsulatus.* FEBS Lett. **253:**247-252.

174. **Zuber, H., and R. J. Cogdell.** 1995. Structure and organization of purple bacterial antenna complexes., p. 315-348. *In* R. E. Blankenship, M. T. Madigan, and C. E. Bauer (ed.), Anoxygenic photosynthetic bacteria. Kluwer Academic Publishers, Dordrecht, The Netherlands.